GEOLOŠKI ZAVOD SLOVENIJE
Dimičeva ulica 14, 1001 Ljubljana

Geotechnical, Geological, and Seismological (GG&S) Evaluations for the New Nuclear Power Plant at the Krško Site (NPP Krško II)

Geology – phase 1

Revision 1

LJUBLJANA, October 2010

Project	Geotechnical, Geological, and Seismological (GG&S) Evaluations for the New Nuclear Power Plant at the Krško Site (NPP Krško II)
Phase	1st
Contract:	Consortium agreement 1130-167/07
INVESTOR:	Gen-Energija, d.o.o.
Consortium Share of Supplies:	Tasks: 4.3.1.0, 4.3.1.0b, 4.3.1.c1, 4.3.1.c, 4.3.1.d, 4.3.1.e, 4.4.1.a, 4.4.1.b, 4.4.1 c, 4.4.1.d, 4.4.2.d/1
Consortium partners	BRGM, GeoZS, IRSN, ZAG
Responsible for Consortium leader: BRGM Project leader	dr. Behrooz Bazargan - Sabet
Responsible for Geološki zavod Slovenije director	dr. Marko Komac
Place	Ljubljana
Date	25.10.2010
Arch. No.	J-II-30d/b6b-3/6-c

Contributors

Atanackov Jure GeoZS
Baize Stéphane IRSN
Baumont David IRSN
Bavec Miloš GeoZS
Bitri Adnan BRGM
Celarc Bogomir GeoZS
Gelis Céline IRSN
Corboz Philippe Geoexpert Ltd.
Gosar Andrej ARSO
Jomard Hervé IRSN
Mathieu Francis BRGM
Mišič Miha GeoZS
Poljak Marijan, GeoZS
Rižnar Igor I. Rižnar s.p.
Scotti Oona IRSN
Skaberne Dragomir GeoZS
Šket - Motnikar Barbara ARSO
Trabelsi Selam CGGVERITAS
Trajanova Mirka GeoZS
Živčić Mladen ARSO

Responsible :	GeoZS	Miloš Bavec
Reviewer:	BRGM	Thiery Winter
Approbation;	IRSN	Behrooz Bazargan - Sabet

KEY WORDS: NPP Krško II, geology, tectonics, sesimotectonics, drilling, geophysics

List of contents

List of figures

List of tables

List of appendices

BACKGROUND

The consortium BRGM, GeoZS, IRSN, ZAG is executing the project Geological, geotechnical and seismological (GG&S) evaluations for the new nuclear power plant at Krško site (NPP Krško II). The project is governed by the Contract between GEN and BRGM and further by the Consortium agreement 1130-167/07 and the Addendum 1 to the Consortium agreement. The project is divided into two phases. This report presents the results of geological investigations (including the pre-existing ones) conducted within phase 1. It comprises the work tasks (defined by the Quality assurance document) 4.3.1.0, 4.3.1.0b, 4.3.1.c1, 4.3.1.c, 4.3.1.d, 4.3.1.e, 4.4.1.a, 4.4.1.b, 4.4.1 c, 4.4.1.d and 4.4.2.d/1. This report was compiled and edited by M. Bavec (GeoZS) and comprises workshop minutes, handouts and partial reports provided by IRSN, BRGM and GeoZS with their subcontractors.

1 INTRODUCTION

The project aim is evaluation of existing geological and seismological data based on pre-existing and newly acquired geological data. During phase 1 the main goal is confirmation or modification of the seismotectonic model and consequently modification of seismic source model(s) with special focus on:

1. potential activity of structures within 5 km radius (site vicinity) of the two proposed sites ("E" and "W"; Figure 1) for NPP Krško II and
2. potential for surface faulting at sites and immediate vicinity of sites.

During phase 1 of the project the following tasks were completed and are presented in this report (field investigations are indicated on Figure 1):

- existing geological data were studied,
- morphological analyses were performed,
- existing geophysical data were studied and partly reinterpreted,
- acquisition, processing and interpretation of 13 high resolution seismic lines was done,
- paleoseismological trench was made across the trace of the Libna fault,
- geophysical preliminaries and field mapping for trenching preparation on Mt. Libna were conducted,
- 6 boreholes were logged and samples were geologically analyzed,
- additional field mapping was done,
- fault plane solutions were calculated for selected earthquakes,
- stress field was evaluated based on fault plane solutions, borehole deformation measurement, and geodetic data,
- geological structures were analyzed as potential seismic sources,
- seismotectonic model was updated

The results are presented here in relation to the Revised Seismotectonic Model of the Krško Basin from revised PSHA study for NPP Krško (Swan et al., 2004). Based on results presented in this report, the seismic source model was built and is presented in a separate report named: *Seismotectonic summary of the data used to build the seismic source model* (Bavec, ed., 2010).

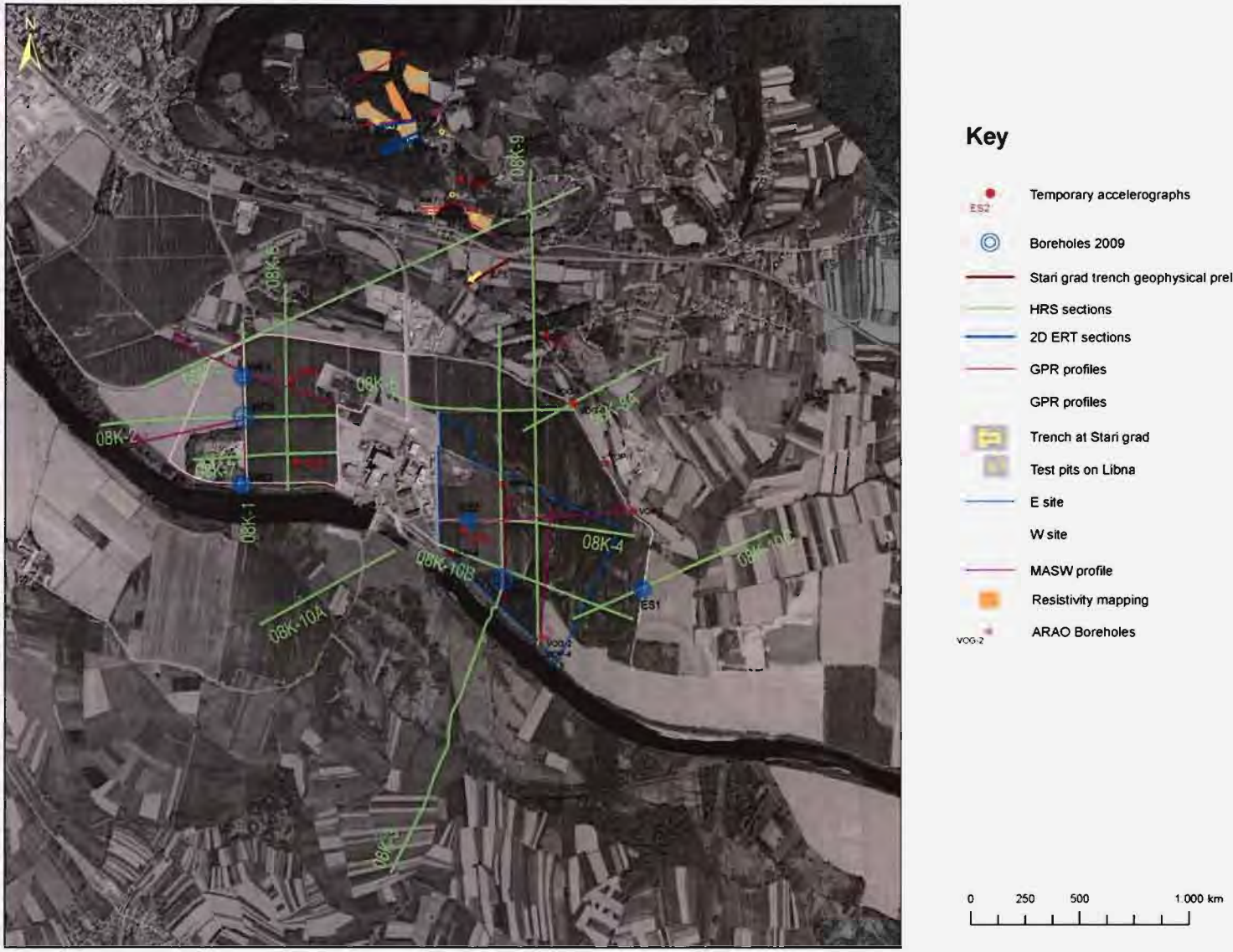

Figure 1. The near vicinity of the proposed sites. Investigations performed during the phase 1 of the project are indicated. Recent boreholes by ARAO (Brenčič, ed., 2006; Petkovšek, ed., 2010) are also marked. The potential NPP sites are referred to in this report as "E" (East) and "W" (West).

1.1 METHODOLOGY, DATING, REGULATORY GUIDELINES

1.1.1 REGULATORY GUIDELINES

Determining a structure as »active« has major further implications for evaluation of geological and seismological hazards at the site and near region (IAEA, 2002; NS-G-3.3).

1. Active structures in near- regional area may act as seismogenic sources (in addition to zones of diffuse seismicity) and have to be defined as such if data do not oppose such interpretation.
2. Active structures at the site need to be investigated for their capability (i.e. surface faulting / surface faulting potential). Here it is important to note that stable sliding, seismic fault ground rupture and seismogenic surface faulting are modes of fault displacement that characterize a fault as »capable«. Furthermore there are several cases in which a fault should be considered as capable in active areas (IAEA, 2002; NS-G-3.3, chapters 6.2 and 6.4):

    a. If it shows evidence of past movement or movements (such as significant deformation and/or dislocations) of a recurring nature within such a period that it is reasonable to infer that further movements at or near the surface may occur. In highly active areas, where both earthquake data and geological data consistently reveal short earthquake recurrence intervals, periods of the order of tens of thousands of years may be appropriate for the assessment of capable faults. In less active areas, it is likely that much longer periods are appropriate. The 10 CFR (NRC, 2007) code gives more specific age brackets for this determination: movement at or near surface once in 35.000 years or recurring movement within the past 500.000 years.

    b. If a structural relationship with a known capable fault has been demonstrated such that movement of the one fault may cause movement of the other at or near the surface.

    c. If the maximum potential earthquake associated with a seismogenic structure is sufficiently large and at such a depth that it is reasonable to infer that, in the geodynamic setting of the plant, movement at or near the surface may occur.

    d. It should be taken into consideration that surface faulting may also occur without being associated with significant releases of seismic energy. For instance, seismic fault creep may be important along some segments of major strike-slip faults — it is relatively common in volcano-tectonic environments and, for normal faults, it is sometimes induced by the extraction of underground fluids. Fault creep has typically been observed in areas characterized by high tectonic activity and seismicity. Stable sliding, seismic fault ground rupture and seismogenic surface faulting can be considered modes of fault displacement that may occur both in time and in space along capable faults (IAEA, 2002; NS-G-3.3, chapter 6.2)

1.1.2 DETERMINING AGE OF GEOLOGIC DEFORMATION

Following IAEA and NRC recommendations and requirements we consider Quaternary deposits to characterize active deformation and capable faults.

However, in the context of Krško basin geology, a problem arises from the fact that stratigraphy is poorly constrained for Quaternary sediments as well as from the fact that sedimentary succession near sites is unfavorable for determination of potential minor displacements. Namely at site and its near vicinity, historic Holocene fluvial sediments (app. 400 years; see the Stari Grad trench report) overlay the Pontian succession (between 5 Ma in the vicinity of NPP; Brenčič, ed., 2006 and 10.5 Ma at trench site). Beside, the Plio-Quaternary series (see description below) is present underneath the Holocene gravel at the Southernmost tip of the proposed E site and on the Libna Hill to the North.
According to Verbič (2004), a series of continental gravely/conglomeratic sediments (e.g. Globoko aloformation; referred here also as Plio-Quaternary deposits) is not chronologically characterized between the Brežice formation (150 ka) and the Pontian deposits (app. 5 Ma) (Figure 2). He estimates that the age of this series is between 1 and 2 Ma. Minimum age estimate was done by application of TL and OSL dating of Plio-Quaternary sediments from the Globoko open pit (Bavec, 2000). The minimum age of sediment was estimated at 306.000 years $\pm 2\sigma$, however this estimate was largely driven by properties of the sediment and capability of the dating method. Thus this is only the estimate of minimum possible age and by no means the estimate of age.

Thus this formation is actually a post-Pontian and pre-Middle-Pleistocene horizon and could be either entirely Pliocene, or entirely Pleistocene or really Pliocene and Pleistocene.

It should also be noted that Plio-Quaternary is a fluvial sedimentary succession and as such not really perfect for possible displacement calculations based solely on morphologic criteria. In Krško basin pronounced erosional relief is known at the series' lower boundary (e.g. Verbič, 2004). Moreover, also the upper boundary of the series was uneven after deposition. Although terraces were not observed in Krško basin, they have been reported in the area app. 20 km upstream Sava (Bavec, 2003).

Thus, at this stage of the project we have to consider faults showing deformation within the Plio-Quaternary or younger deposits as potentially active. This approach may be conservative and may exceed regulatory requirements. An attempt was made to date the upper layers of the "Plio-Quaternary" deposits from Globoko (best preserved section) by the Electro-Spin Resonance (ESR) which is a pertinent method to perform dating on quartz-rich deposits as old as Pliocene (Laurent et al., 1998). At the end of Phase 1 we were not able to obtain the laboratory results due to technical reasons (capacity of the only lab known to us).

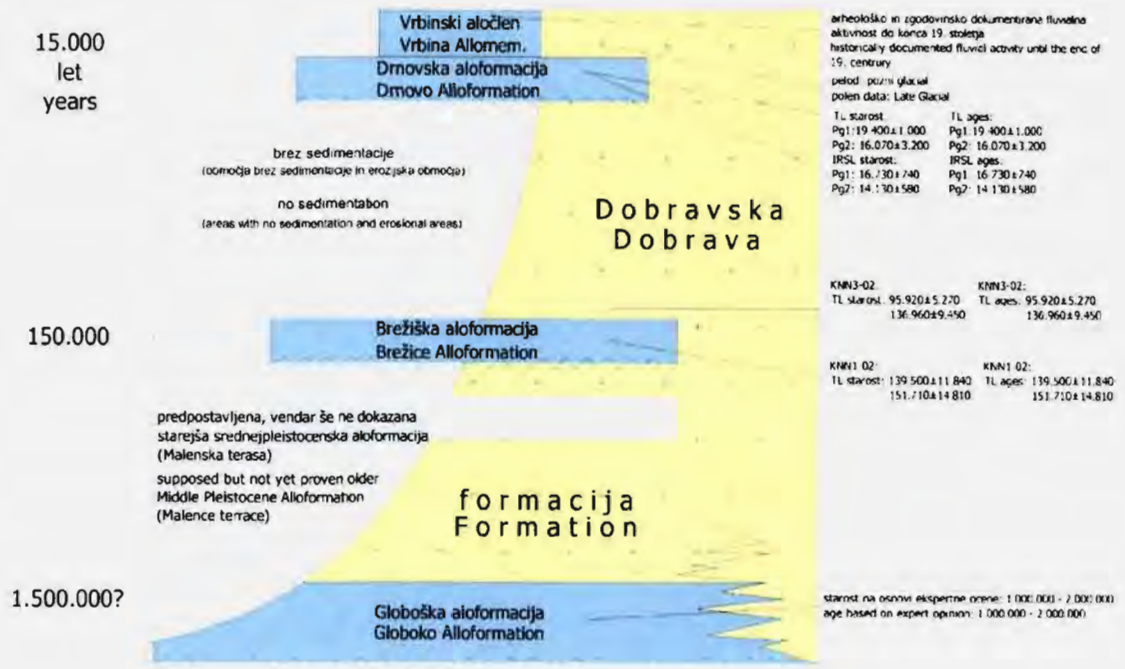

Figure 2. Morphostratigraphic division of Plio-Quaternary and Quaternary deposits in Krško Basin (Verbič, 2005).

1.1.3 DETERMINING ACTIVE FAULTS

The 2003 PSHA study (Swan et al., 2004) and the later investigations (e.g. Brenčič, ed., 2006) performed in the very vicinity of the locations in concern indicated existence of potentially active structures in the vicinity (radius < 5 km) of the proposed sites. Active faults according to 2003 PSHA in near regional area (25 km) were also revaluated taking into consideration post-PSHA seismicity data and revaluation of geophysical data.

The following actions were performed in the site vicinity area to address activity / capability of structures in the site vicinity area:

- Revaluation of existing geophysical data
- High resolution reflection seismic survey
- Morphometric analysis of the site vicinity
- Trenching across the trace of the Libna fault and additional structural mapping along the trace of the Libna fault
- Geodetic measurements

Following the dating approach described above, all faults in the tectonic model presented here are actually potentially active, however they are not treated as potential seismic sources. The criteria for determining one as seismic source were: sufficient length and structural

importance. i.e. having significant offset in (Plio-)Quaternary sediments and being involved in the first order deformations (Balaton faults, or Dinaric faults dissecting the Balaton ones).

2 GEOPHYSICAL DATA

First, the pre-existing geophysical data were analyzed, evaluated and in some cases reinterpreted. Secondly, 13 new HR reflection seismic profiles were acquired in field and interpreted. Position of the seismic lines is shown on Figures 1, 3 and 4 and the new lines are shown in more detail on Figure 6.

2.1 PRE-EXISTING SEISMIC REFLECTION DATA

A workshop was organized for re-evaluation of the existing seismic data at GeoZS in Jan 2008. Generally findings from previous studies (summarized in Rižnar, 2007) were confirmed, however some new interpretations were made that contributed to modifications of the tectonic model.

We focused primarily on the parts of regional lines and high resolution lines that are located at a maximum distance of 5 km from the Krško NPP (Nuclear Power Plant) (Figure 3).

2.1.1 RESOLUTION

2.1.1.1 SINGLE-FOLD ANALOGUE REFLECTION PROFILING IN 1959

The first seismic reflection investigation, composed of four profiles with single fold analogue recording was performed in 1959 for oil and gas storage prospecting. In comparison with modern digital profiles, the quality of these sections is rather poor (Figure 5b). In general, deeper parts of the basin are better imaged, whereas noise dominates in the shallow parts. It was possible to interpret only two horizons (Figure 5b): the top of Badenian limestone (horizon B) and the pre-Tertiary basement (horizon C). Possibilities for interpretation of faults are very limited on these profiles. We found these profiles applicable only for identification of the Krško syncline axis.

2.1.1.2 MULTI-FOLD REFLECTION PROFILING IN 1994/95

First modern digital high-resolution seismic reflection survey was performed in a profile P-3/94 and P-4/95 of intermediate depth penetration, using 15 m group spacing and 12-fold coverage (Gosar, 1998).
In this profile the most prominent reflections were obtained from near the top of the Badenian limestone (horizon B), while the Mesozoic basement (horizon C) was less pronounced (Figure. 5a). In the shallower part, a clear image of the boundary between Pontian sandy marl and Pannonian marl (horizon A) was also obtained. A folded structure is clearly visible in this profile, with a maximum depth to the pre-Tertiary basement of 1500 m. Theoretical vertical resolution of this profile is similar to the resolution of PHARE regional profiles.

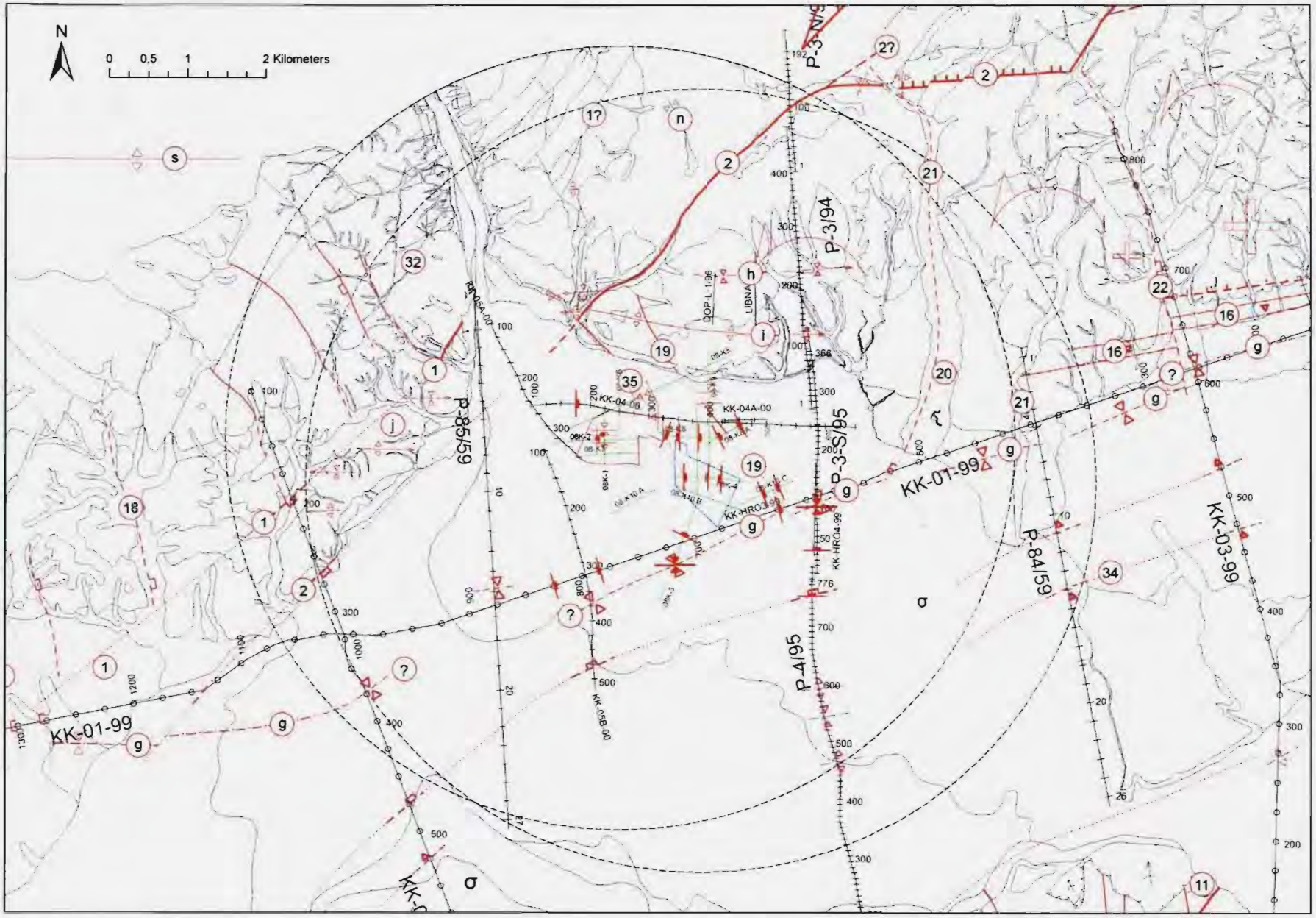

Figure 3. Site vicinity map with tectonic interpretation and position of pre-existing and newly acquired reflection seismic profiles. Observations of deformation on seismic profiles is indicated. See Figure 4 for explanation.

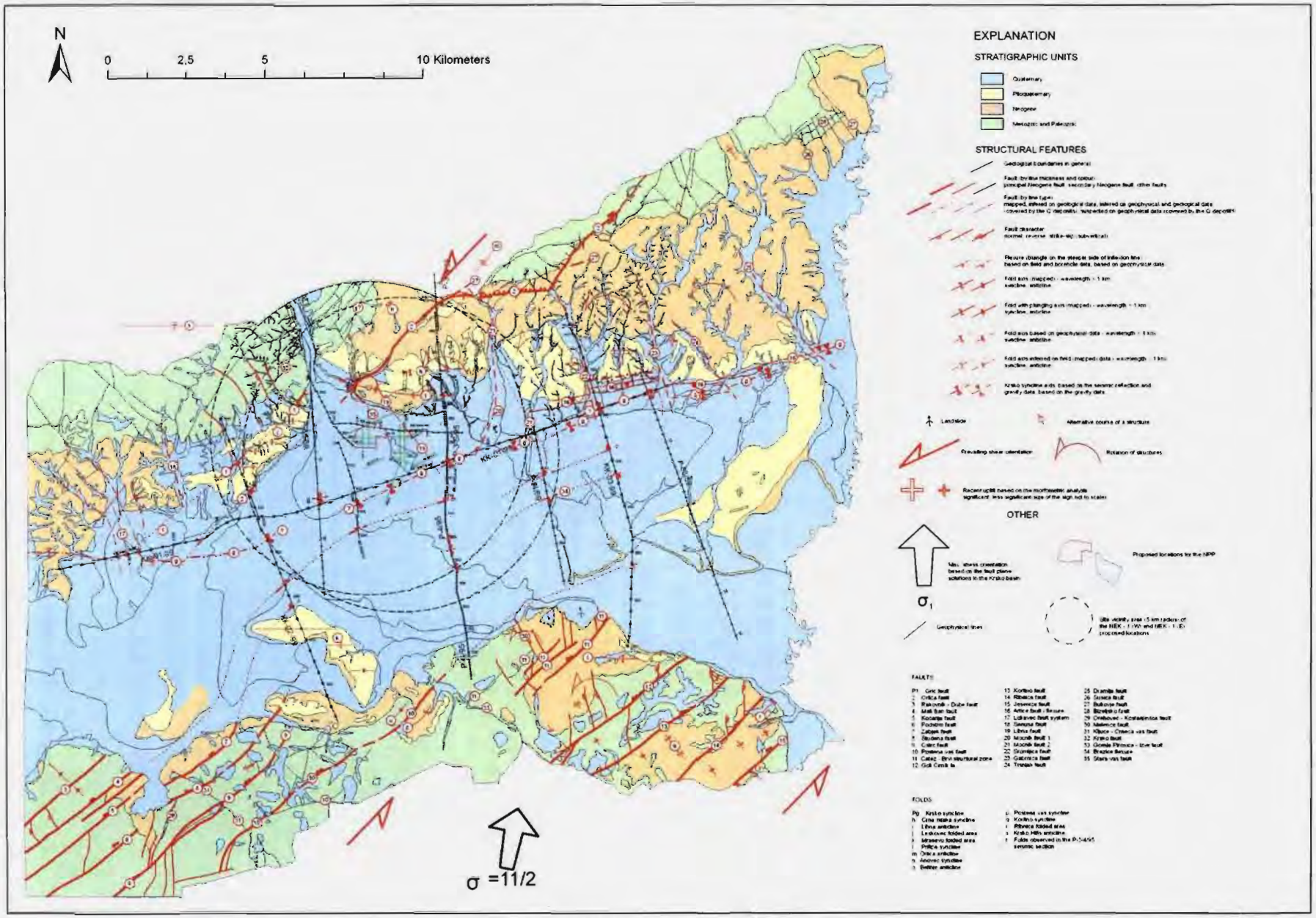

Figure 4 Tectonic map of Krško basin based on updated 1:25.000 geologic map

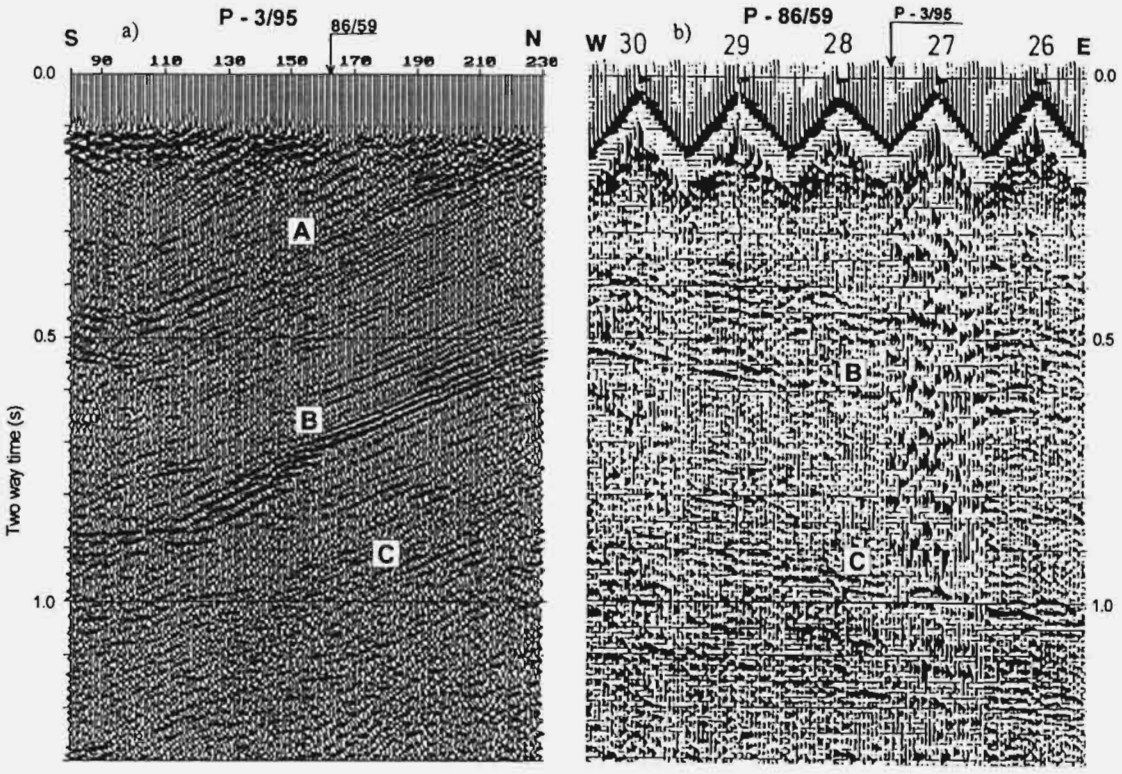

Figure 5. Comparison of 12-fold digital P3/95 profile (a) and the single-fold analogue P86/59 profile (b) at their crossing point.

In addition, very-high-resolution shallow reflection profiling was performed at two locations close to the NPP for the detection of eventual near-surface faults. Single geophones with 3 m spacing and small explosive charges were used. In the profile, recorded 0.5 km East of the NPP site, some discontinuities in reflectors were established that can be interpreted as faults. Theoretical vertical resolution of this profile is similar to the resolution of PHARE high-resolution profiles.

2.1.1.3 MULTI-FOLD REFLECTION PROFILING IN 1999/2000

Reflection profiling in the frame of EU PHARE project (Persoglia ed., 2000), comprises of three regional reflection profiles (KK-01/99, KK-02/99, KK-03/99) in a total length of 41 km. They were measured with an explosive source fired in 5-10 m deep boreholes, using 15 m group spacing and 18-fold coverage. Good penetration of the seismic signals was obtained within the basin down to the Mesozoic (pre-Badenian) basement at depths greater than 2 km. The primary objective of the seismic investigations was to differentiate Neogene and younger structures. The deepest horizon mapped was the top of Mesozoic rocks, i.e. the top of Cretaceous flysch or of Triassic dolomite (horizon C). The explosive used and the depth of charge, beneath the weathered zone, produced seismic signals having a wide frequency band, well suited for the required resolution and characterization of the different geological layers and for revealing the structural elements. In the shallow section, frequencies are around 80 to 90 Hz; at the base of the basin the signal frequencies are still between 40 and 60 Hz, giving a resolution of around 5 m in the shallower parts and 25 m near the base of the basin. Estimated theoretical vertical resolution ($\lambda/4$) of regional profiles is at 360 m depth 11-15 m and at 650

m depth 14-18 m. The seismic velocities range, from very low values in some parts of the near surface deposits, to more than 2500 m/s for the Neogene sequences and 3000 m/s or larger for the Mesozoic.
Further extension of the program was proposed to close the loop of seismic lines around the NPP location in order to resolve the structures in close proximity of the NPP site, to verify the structural trends of the area and the presence of potential active faults. The extended program (lines KK-04/00, KK-05A/00 and KK-05B/00) was completed using a mobile accelerated weight drop (Hydrapulse) source. This choice was required by the proximity of houses, factories and other constructions. The acquired data offer good images of the terminations of the Tertiary and Quaternary sedimentary units at the Northern flank of the basin (the anticline of the Libna-Orlica Mt. area). The line KK-05B/00 permits a good tie with the DRN-1/89 well and the stratigraphic correlation with the markers encountered by the well. Some profiles (line KK-05A/00) are rather noisy, but still provide some constraints on the location of the geological structures.
Six horizons were identified in all regional reflection profiles. They include the Mesozoic basement of the Krško basin and a sufficient number of horizons within the Neogene sequence to capture its internal structure.
In addition four shallow very-high-resolution profiles (KK-HR01/99, KK-HR02/99, KK-HR03/99 and KK-HR04/99) were measured at selected locations using 2 m geophone spacing, 100 Hz geophones, 12-fold coverage and seismic gun as a source. Estimated theoretical vertical resolution ($\lambda/4$) of these profiles is at 30 m depth 4-5 m and at 55 m depth 5-7 m. The high-resolution lines were useful for a qualitative differentiation of the near-surface Quaternary sediments, of their continuity and for the detection of eventual faults extending to the surface.

2.1.2 SEISMOHORIZONS

During the PHARE (2000) campaign, seismohorizons were identified in borehole Drnovo 1 (DRN-1) as the following geological units:
P1 - Pontian (quartz sand).
P2 - Pontian (marl).
A - Pontian; near the separation of layers with prevalently sands from marls.
M - Near-Pliocene - Miocene (Pannonian marls) transition.
B - Near top of Badenian (Lithothamnian limestone)
C - Near top of Mesozoic.

Seismohorizons **C, B, M, A, P1** and **P2** were used in the PHARE seismic sections. The horizons were correlated with the DRN1/89 reference borehole (1252 m) (Kranjc et al., 1990 [48]). The link established at the Southern end of KK 05B-00 seismic section was considered satisfactory although it has more of a qualitative nature because no time-depth relationship is available. The seismohorizons do not exactly represent the mapped formations boundaries.

C horizon represents the top of the Mesozoic and corresponds very well to the mapped Mesozoic/Neogene boundary. In the DRN 1/89 borehole, the C horizon it is found at 970 m.

B horizon represents the near top of Badenian limestone in the PHARE seismic sections. Badenian limestone is found at 690 to 647 m in the DRN 1/89 borehole. In the Southern part of the mapped area Badenian limestone relatively thin, up to 70 m. In the Northern part of the mapped area Badenian limestone is thicker, up to 300 m, but in the Northeastern part its thickness is drastically reduced to less than 50m on account of marly and sandy limestone and

marl of the same age. As only a few quite distinct reflectors are observed with various thickness and intensity, only the upper part of the limestone was taken into account as the most traceable one.

M horizon is described as near Pliocene / Miocene transition in PHARE report (Persoglia (ed.), 2000). Taking into account the estimated position of the horizon in the DRN-1/89 borehole, it corresponds to the transition from stratified Sarmatian marls to (massive or thick bedded) Pannonian marls at the depth of 561 m.
The correlation with the mapped boundary is quite accurate in the Southern part of the KK 02/99 seismic section. In the Northern part of the KK 02/99 section the correlation is poor due to absence of the Sarmatian deposits.

A horizon described as transition from Pannonian marls to Pontian sands. In correlation with the DRN 1/89 borehole it represents the transition from marl (carbonate silt/clay) to quartz sands and clay that has been drilled at the depth of 318 m. Such a transition (interchanging of sand and marl upon the Pannonian marl) is observed (mapped) in the N part of the mapped area, E of Močnik creek (fault), but not elsewhere.

P1 and P2 horizons were determined solely for their clarity and traceability and do not represent any of the mapped lithostratigraphic boundaries.

2.1.3 DESCRIPTION OF PRE-EXISTING SEISMIC REFLECTION DATA

Deformations described in the following chapter are listed according to their location (depth and horizontal position). Previous interpretation is described as well if the structure is reinterpreted or has already been noted in the previous PSHA. If the observed deformation is refered to a known structure, it is listed in bold at the end of each section and enumerated as in chapter 4.2.2.2 (e.g.**Gabrnica fault (23)**) where a complete description of these structures is described.

2.1.3.1 PROFILE KK-01-99

The line follows the longitudinal axis of the Krško basin fairly close to its deepest part, i.e. the axis of the Krško syncline, close to its core. On this seismic section, all Tertiary, including Plio-Quaternary, units could be recognized. In the seismic section one clearly distinguishes two large sub-basins as also identified by the Bouguer anomalies. The top of Mesozoic occurs at more than 2000 m in the eastern sub-basin, at about 1900 m in the western subbasin and at about 1000 m depth at the saddle, which separates the two sub-basins.

The lowermost Tertiary sequence between horizon C and B represents, most probably the Ottnangian sediments. These have relatively weak and diffuse seismic signals what could be caused by their heterogeneous lithological content that consists of loose gravel, sand and sandy clay. The average and almost uniform thickness of this sequence is about 300 meters, except in the eastern part of the profile, where these sediments in a distinct depression (the Raka depression) reach thickness up to 1000 meters. Such a great thickness is anomalous one even in relation to the entire Sava folds. Thus, the existence of older Tertiary units (Eggenburgian or even Egerian) should not be excluded. However, regardless of the exact age of sediments that fill up this depression, they show several distinct angular discordances with visible onlaping sequences what suggests a syn-sedimentary activity of the depression. It,

however, ceased to exist in Badenian time when the *Lithothamnium* limestone (horizon B) started to be deposited.

This last unit is expressed by several distinct seismic horizons that have relative uniform and constant thickness (100 m). Badenian lithostratigraphical sequence transits upward into sandy and marly limestone, and sandy marl with intercalations of calcarentites that are of Badenian to Sarmatian age. These could be distinguished as a separate unit between horizons B and M. This sequence have relative uniform thickness of 200 meters, except in another distinct depression in the eastern part of the profile (Globoko depression), where it shows a slight increase. This thickness increase is well expressed by overlapping of seismic horizon that corresponds to sandy marl that lies over the *Lithotamnium* limestone. That means that this depression started to be formed during, or after, Badenian time.

The next recognizable and relatively uniformly expressed sequence is the Pannonian marl that corresponds to the unit between horizon M and A. Its almost uniform thickness (about 100) is slightly increased only in the Globoko depression. Upwards, this marl transits into sandy marl of Lower Pontian age, and this could also be distinguished as a separate sequence (unit between horizon A and P_2). Its main characteristics is variable thickness, from 100 meters in the eastern part to 600 meters in the Globoko depression on the west. Here, this unit is represented by an alternation of sandy and marly layers, what is well also expressed in seismic horizons.

The Upper Pontian is represented by sand with rare lenses of gravel, except in the Globoko area, where a lateral lithological equivalent consisting of gravel, sand and clay with coal is developed. The beginning of this sequence is recognized as the P_2 seismic horizon. The whole unit has relative constant thickness (approx. 300 m) in the western part of the section, since in the Globoko depression, there is a distinct thickening expressed by different seismic reflectors. This situation corresponds to the lithology of the Globoko coal mine that is well documented by previously described drillings. Within the Upper Pontian sand, a layer of sandy marl has been mapped in the field. This layer, that consists of the two main marly layer 3-5 m thick, occurs in the uppermost part of the sand series. It might correspond to a distinct seismic horizon well expressed over the entire length of the seismic line that is labelled as the P_1 horizon.

The uppermost layer in the eastern part of the seismic section could be assigned to the Plio-Quaternary sediments that according to the borehole data reach here the thickness of 200 meters (Q horizons). This anomalous thickness of Plio-Quaternary sediments, as well as of the Neogene series in the Globoko depression, determines this one as an active deposition centre in the time span Badenian–Pontian, but also in Pliocene and Quaternary.

Structurally, both described depressions and a saddle between them may represent *Dinaric* structures that were re-activated during Neogene time. Tectonic control of the Neogene deposition could be supposed for the Globoko depression on the basis of a distinct normal faults situated at the eastern rim of the above mentioned saddle. They seem to be syn-sedimentary growth faults that originate from the pre-Tertiary basement, and form a half-graben type of structure. However, the Raka depression can not be explained on the same way yet, because it is not fully covered by seismic lines.

The whole Neogene lithostratigraphical sequence is, otherwise, dissected by a number of faults that propagate from the pre-Neogene basement, where the most of them are the listric

ones. They represent the most probably re-activated *Dinaric* faults of Palaeogene age. Neogene activity is expressed by growth- or blind - faulting. These faults exhibit generally normal character. A number of them crosscut the whole Neogene sequence, however, their propagation into Quaternary sediments can not be determined due to the lack of reliable seismic signals from upper several tens of meters. The most distinct fault or a set of faults with inferred horizontal displacement is a fault in the Raka depression that forms a flower-shape structure. It crosscuts the whole Neogene series. This fault may correspond to the south-western continuation of the Orlica fault, or to an N-S oriented fault along the Rokavec creek valley E of Raka.

Station points (s.p.) 125 - 150
A normal fault (Persoglia, (ed.), 2000 [60]) with subsided W block is observed. The fault is sub vertical, with listric western dip below the M seismohorizon (sh). The fault is observed between 0,9 (below the P2 sh) and 1,3 s TWT (two way travel time). The observation is referred to the **Gabrnica Fault (23)**

s.p. 275 - 300 (Persoglia, ed., 2000)
A West dipping sub vertical fault with subsided W block, is recognized below 0,85 s. The fault is listric below M sh, and observed above 1,65 s TWT. The observation is referred to the **Sromljica fault (22).**

s.p. 375 - 400
A poorly interpreted sub vertical fault (Persoglia, ed., 2000) observed between app. 0,4 and 1,0 s TWT. Younger strata are more deformed than older. The A horizon is subsided in the W block of the fault. Its propagation towards the surface is unreliable as the P1 horizon shows larger offset than the older ones. The observation is referred to the **Močnik fault 2 (21)**

s.p. 525
A subvertical, slightly W dipping fault, with subsided W block observed between 400 and 1600 m (0,43 - 1,47 s TWT) (WS, 2008; Persoglia, ed., 2000). The fault is not affecting the unconformity in Pontian.
The observation is referred to the **Močnik fault 1 (20)**

s.p. 625
An E dipping normal fault with subsided E block is observed from 1200 m up to the mute zone WS, 2008; Persoglia, ed., 2000). The fault is poorly interpreted in the upper app. 800 m (larger offset in younger than in older horizons). The observation is referred to the **Libna fault (19)**

s.p. 800
A vertical fault with subsided W block, interpreted only up to app. 400 m (0,45 - 0,83 s TWT)

s.p. 825 (850-825)
An East dipping fault with subsided E block. The fault is poorly interpreted in the upper app. 800 m (larger offset in younger than in older horizons). It is observed between 0,46 - 1,38 s TWT

s.p. 1000 - 1125.
A set of low angle normal, E dipping faults with subsided E block is interpreted (Persoglia (ed.), 2000 [60]), affecting only Ng/Mz boundary (between 0,88 - 1,26 s TWT). Except for

the one at **s.p.1125 - 1150** affecting the Badenian horizon at 0,70 - 0,82 s TWT. Others affect only the Mesozoic/Neogene boundary (C horizon).

s.p. 1275
A fault with subsided W block
Interpreted up to app. 400 m

s.p. 1300
A fault with subsided W block is interpreted up to the mute zone, but the high resolution section confirmed, that the fault doesn't penetrate the Quaternary deposits there.

s.p. 1325
A main branch of the flower structure, an East dipping fault with subsided E block is observed from the 1,2 s TWT and interpreted up to the mute zone (app. 400 m). The observation is referred to the **Lokavec fault (17)**.

2.1.3.2 PROFILE KK-02-99

This western most line cuts transversally the Krško basin, i.e. it lies perpendicularly to the Krško syncline axis, between Šutna on Mts. Gorjanci and NW of Leskovec village in the Krško hills.

All previously described Neogene units are well recognizable also in this line. The oldest Ottnangian sequence is transgressively deposited over the Mesozoic basement, what is clearly expressed by onlaping of seismic horizons. Its average thickness is 100-200 m, except in the central part of the section, where it is slightly increased. This anomaly could be caused by syn-sedimentary processes or by secondary folding of the Krško syncline core.

The following units, i.e. the Badenian–Sarmatian (between the B and M horizons); Pannonian (between the M and A); and Lower Pontian (between the A and P_2 horizons) have almost uniform thickness with well expressed parallel seismic reflectors. The exception is the Badenian limestone (horizon B) that is a transgressive unit over Ottnangian clastic series. The Upper Pontian sequence, consisting of sand (above the P_2 horizon), indicates a syn-sedimentary filling of the syncline core; same onlaping reflectors can be recognized here. The uppermost seismic horizon (P_1) that corresponds to a marl layer within the sand is also well expressed here, as well as the Plio-Quaternary to Quaternary unit above the Q horizon.

The line reveals well the real structural shape of the Krško syncline. It is asymmetric with steeper northern and gentler southern limb. The main folding took place after the deposition of the whole Neogene sequence, what is suggested by parallel position of above mentioned horizons.

In the northern limb, the pre-Tertiary basement is apparently also disturbed by a set of faults that have south verging reverse character. They do not propagate into Neogene units, however, Ottnangian sediments to the south of this structural anomaly have slightly increased thickness, so it can be supposed that their deposition was partially controlled by Neogene syn-sedimentary activity of these basement faults. Badenian limestone that overlie Ottnangian sediments are also disturbed, but in this case, by a set of south verging normal faults. Their eventual upward propagation, due to bad seismic signals, can not be determined. However, a

set of normal faults with some north verging antithetic ones suggests also a strike-slip character of the main fault, resulting in a flower–like structure in its upper part. Thus, this structural anomaly could also represent the Orlica fault.

The southern limb of the main syncline exhibits similar pattern. There are indications of north verging reverse faulting in the pre-Tertiary basement that here propagates into the Neogene, at last into Ottnangian, sediments. This faulting might have caused some gravity sliding that is well expressed in Ottnangian sediments. At least, one reverse fault apparently propagates upwards and crosscuts the whole Neogene sequence. On the other hand, this whole structural anomaly could be interpreted as a set of normal north verging faults. They all seem to be the blind ones disappearing within Badenian–Sarmatian sequence.

s.p. 200
A North dipping, reverse fault at 200 m depth is observed (WS, 2008) affecting the Badenian horizon (B). Probably Grič fault (1).

s.p. 250 - 275
A fault with probable North dip and reverse character was interpreted between 400 and 500 m depth. (WS, 2008). The fault is affecting the Badenian strata. The observation is referred to the Orlica fault. The same structure was interpreted as a South dipping listric fault with subsided S block in the PHARE project (Persoglia, (ed.), 2000 [60]).

s.p. 375 Krško Syncline axis
The axial plane is subvertical

s.p. 450 - 500
A possible flower structure with S and N dipping faults (at N side of the bulge) is observed. A N block is subsided. The structure is observed between 400 and 1000 m (WS, 2008). North dipping listric faults were interpreted in the PHARE project (Persoglia, (ed.), 2000 [60])

s.p. 525
A flexure in the Badenian and Sarmatian reflectors

2.1.3.3 PROFILE KK-03-99

This transversal cross the eastern part of the syncline axis, between the Čatež village in the south and Sromlje village in the north. It also crosscuts the Globoko depression.

On the profile, all the Neogene, as well as the Plio-Quaternary units, are well expressed and recognizable. The following lithostratigraphic units express relative uniform thickness: Ottnangian clastites (these are slightly thicker in the middle part of the syncline or depression), Badenian limestone, and Badenian to Sarmatian calcarenite and sandy marl. The distinct change is at the Sarmatian/Pannonian boundary (horizon M). Pannonian marl is transgressively deposited with visible onlaping horizons. Upwards, there is also a distinct increase of the Pannonian marl thickness towards the syncline axis. Pannonian marl is overlain by an alternation of Lower Pontian sand and marl and with Upper Pontian sand and Plio-Quaternary sediments. These express above the Q horizon a distinct discordance over the Upper Pontian sediments. All this means that the Globoko depression was an intensive syn-

sedimentary deposition centre specially active during Pannonian and Pontian time, but also during Quaternary.

Structurally, the Globoko depression, that coincide with the core of the Krško syncline, is a - symmetric with steeper northern side. This is caused by a distinct south verging reverse fault that has a root in the pre-Tertiary basement, and propagates upwards through the whole Neogene sequence into the Plio-Quaternary sediments. The amount of displacement diminishes from the depth to the surface, so the Badenian limestone are displaced the most, since the youngest ones (Pontian and Plio-Quaternary) express only flexuring. Indeed, this structure was also recognized during previous field mapping (Poljak et al, 1985; 1999) and drilling (Markič, 1999; Markič and Rokavec, 2003) as a structural flexure, and it was named the Artiče normal fault or flexure.

The southern side of the Globoko depression is practically not disturbed. Slight disturbances in some seismic horizons in the Pontian sand and marl, are probably caused by gravity sliding processes. At the southern end of the profile, one or two faults could be mapped. They propagate from the pre-Tertiary basement through the Ottnangian and Badenian sediments and apparently disappears in the Pannonian ones. Both are steeply-dipping south verging reverse faults. It should be mentioned that this back trusting within the Krško syncline is also expressed on the northern side of the Libna hill that was covered by the P-3-94 line, and interpreted as such (Gosar, 1998).

s.p. 675 - 625 Artče fault and flexure
A South verging reverse fault is observed between 1800 and 1000 m. Towards the surface, no reflectors could be traced to quantify a possible offset, but the flexure indicating a change of dip is clear (WS 2008).

s.p. 600 - 625 Krško Syncline axis
Sub vertical axial plane of the axis is observed.

s.p. 475 - 500
A flexure is observed between the s.p. 475 and 500 with a possible flower structure at the S side of the bulge. **Brežice flexure (34)?**

s.p. 575 and 550
Another bulge is recognized between s.p. 575 and 550 in the base of Badenian and diminishing upwards (WS II, 2008).

s.p. 310 and 240
An antiform (bulge) is recognized between s.p. 310 and 240 in the base of Badenian and diminishing upwards (WS II, 2008).

2.1.3.4 PROFILES P-3-4/95 (COMPLETE REGIONAL PROFILE)

A 13-km-long profile (P-3/95 and P-4/95) was recorded across the eastern part of the Krško basin (2 km east of the NPP) by using 15-m group spacing, arrays of 12 geophones, and 12-fold coverage. Because available funds did not allow drilling of shot-holes below the water table, the suppression of ground roll was a principle task of data processing. Along with processing parameters, they were optimized to improve the resolution.

In this profile the most prominent reflections were obtained from near the top of the Badenian limestone (horizon B), while the Mesozoic basement (horizon C) was less pronounced (Figure. 5a). In the shallower part, a clear image of the boundary between Pontian sandy marl and Pannonian marl (horizon A) was also obtained. A folded structure is clearly visible in this profile, with a maximum depth to the pre-Tertiary basement of 1500 m. Theoretical vertical resolution of this profile is similar to the resolution of PHARE regional profiles

In the Northern section (N of s.p. 340 of the P-3-S/95 line) no reflectors are interpretable.

At stations 250, 300 and 340 on P3S-95 the reflector is discontinuous. The vertical resolution is 10 to 15m. These discontinuities may be interpreted either as tectonic features that could fracture the reflector or as lateral changes of seismic reflector signature due to changes of silt/limestone content. No obvious reflector can be identified below this one.

s.p. 340 (P-3-S/95)
Discontinuous (M) reflector is observed, but it is not clear whether it a tectonic offset or a disturbance due to lithologic changes. A reverse, S verging fault may be interpreted. It is observed between 0,8 and 0,9 s TWT depth (WS 2008). The vertical resolution is app. 10 - 15 m. The Mz/Mg boundary is affected.

s.p. 260 - 320 (P-3-S/95)
Disturbance (offset) of Badenian reflector is observed between 0,2 and 0,3 s TWT (WS 2008) maybe due to static corrections.

Folds are observed at the following s.p.:

- **s.p. 500** (P-3 /95) Črna Mlaka syncline axis (h)
- **s.p. 375 - 400** (P-3 /95) Libna anticline axis (i)
- **s.p. ~100** (P-3-S/95) Krško syncline axis (g) with slightly N verging axial plane
- **s.p. 20 (P-3-S/95)**

s.p. 20 (P-3-S/95)
A normal fault with subsided Northern block is interpreted by Gosar (1998) and confirmed at the 2008 workshop (WS, 2008). The fault is interpreted up to the mute zone at app. 400 m, affecting the Pontian deposits.

s.p. 700 (P-4/95)
A normal fault with subsided Northern block is interpreted by Gosar (1998) and confirmed at the 2008 workshop. The fault is interpreted up to the mute zone at app. 300 m, affecting the Pannonian deposits.

Folds are observed at the following s.p.:

- **s.p. 590 Anticline**
- **s.p. 540 Syncline**
- **s.p. 590 Anticline**
- **s.p. 460 Anticline**

2.1.3.5 PROFILE KK-04-00

This line stretches in a west-east direction along the northern rim of the Krško basin, starting from the left bank of the Sava river (near the town of Krško) towards the Stari Grad village. On the profile, all the lithological units, that have been determined on the regional profiles KK-1/99; KK-2/99 and KK-3/99, can also be recognized.

The Ottnangian unit is clearly transgressively deposited over the Mesozoic basement. Its thickness is not uniform, it is the highest in a small depression in the western part of the profile, where it reaches 200 meters. Badenian limestone is also transgressively deposited over Ottnangian sediments and it expresses almost uniform character and thickness. Upwards, there follow Badenian-Sarmatian calcarenite and marl, Pannonian marl, Lower Pontian sandy marl and Upper Pontian sand. They all express relative concordance of layers and constant thickness.

All listed horizons are slightly folded. They express a gentle syncline in the middle part of the profile, and an anticline in its eastern part. In the easternmost part of the profile, the strata have steeper dip towards the east, what could be also caused by normal faulting, that otherwise exist on the eastern slopes of the Libna hill. However, faulted horizons on the seismic line can not be mapped for sure. The only discontinuity that could be regarded as a faulted one is in the Badenian limestone at the western end of the profile. It appears as a sub vertical normal fault with down warped eastern side. It disappears in overlaying Pannonian marls.

s.p. 375-450
In the area of expected Libna fault, there is a problem of surface ground (waste disposal) that produces a blind zone (stations 375 to 450). Around this zone, the dip of the layers is changing from apparent horizontal (west part of the profile) to eastward dipping (east part of the profile).
s.p. 175
In the course of interpretation of the high resolution seismic profiles, acquired in 2008, some additional minor disturbances were reconsidered at s.p. 175, indicating a possible normal fault with downthrown E block.

2.1.3.6 PROFILE KK-05A-00

In most of the profile it is difficult to identify reflectors. This may be related to the presence of noise from a paper factory located near the Sava River. In the Southern part (s.p. 350), some gently South-east dipping reflectors can be identified (WS, 2008). Common interpretation is presented with KK-05B-00.

2.1.3.7 PROFILE KK-05B-00

Together with KK-05A-00 these two lines could be considered as one single profile that consists of the two, slightly translated segments. They both cut transversally the Krško syncline axis and crosscut its core. The line KK-5B/00 is extended to the south, and it reaches the DRN-1/89 borehole, what enabled correlation of seismic horizons with lithostratigraphical units determined by drilling.

On the profile, all previously described lithostratigraphic units are well expressed. Ottnangian sediments exhibit slightly increased thickness in the syncline core that can be result of syn-sedimentary deposition or of secondary folding in the syncline core. Above laying sequences, i.e. the Badenian limestone, Badenian–Sarmatian calcarenite and marl, Pannonian marl, and Lower Pontian marl and sand exhibit almost uniform shape and thickness. Upper Pontian sand indicates, however, a syn-sedimentary filling of the syncline core that is expressed by some overlapping horizons.

Listed horizons reveal the main core of the Krško syncline that is slightly asymmetric with steeper southern limb. Regarding brittle deformations, seismic horizons imaged on this line do not show any expressions of faulting.

s.p. 300 - 350
Disturbance of Badenian reflector is observed between 800 and 1000 m depth (WS 2008). Continuous reflectors are observed above the structures.

s.p. 475
A fault with subsided N block is observed at the depth of 600 - 800 m (WS 2008). Disturbance of the Badenian (B) reflector is noted. A flexure is observed above 600 m.

2.1.3.8 PROFILE P-83/59

On analogue single fold profiles P-83/59, P-84/59 and P-85/59 it was possible to interpret only two horizons (Figure 5b): the top of Badenian limestone (horizon B) and the pre-Tertiary basement (horizon C). Possibilities for interpretation of faults are very limited on these profiles. We found these profiles applicable only for identification of the Krško syncline axis.

s.p. 4 Krško syncline axis

2.1.3.9 PROFILE P-84/59

See 2.1.3.8
s.p. 6 Krško syncline axis

2.1.3.10 PROFILE P-85/59

See 2.1.3.8.
s.p. 15 Krško syncline axis
(No. 16 is missing in the numeration!)

2.1.3.11 PROFILE KK-HR01-99

The profile crosses the Artiče fault, the prominent structure imaged in the regional line KK-03/99. The high-resolution line spreads from station 614 to 694 of the KK-03/99 line. Near

surface data show the up-warping of the sedimentary strata of Pontian marl and sand close to the Plio-Quaternary filling of the subsiding central part of the basin. The poor quality of the data in the zone between two well defined traces of the fault at stations 425 and 575 is attributed to the presence of near surface alluvial loose sand or silt with peat of Holocene age. The very low seismic velocities that characterize these sediments produced a bad signal to noise ratio. Only poor continuity of the reflection data is recognizable, and it is not possible to reconstruct the exact geometry of the structure, across the entire zone of faulting. On the other hand, the borehole data (boreholes SP-1/83 to SP-4/83) suggest a continuous stretching of Pliocene and Plio-Quaternary strata across the inferred fault with only a slight flexuring.

It should also be mentioned that the profile runs along the Sromljica creek valley that is determined by a N-S, oriented fault, as there are other numerous other creek valleys at the southern slopes of the Mt. Orlica. Therefore, disturbances of seismic signals might be also caused by this supposedly vertical normal fault.

2.1.3.12 PROFILE KK-HR02-99

This line controls the surface extension of tectonic structures revealed by the western part of seismic profile KK-01-99 between station points 1282 and 1336 (Swan et al., 2004, Figure 4-12). The Holocene filling (colluvium) is resolved in the internal structure and stratification, appearing undisturbed, with layers sub-parallel to the surface, and deposited over an unconformity that represents the erosional surface of folded Pleistocene and Pliocene strata. The surface outcropping of the possible faults recognized on regional line KK-01-99 can be excluded. Some limited deformation of the reflecting markers at the very eastern end of the line are considered to be influenced by noise and by low coverage, not caused by tectonic disturbances.

2.1.3.13 PROFILE KK-HR03-99

This line images a near-surface layer of gravel along profile KK-01-99 2 km Southeast of the Krško NPP between stations 579 and 641 (Figure 4-13). The energy generated by the source is strongly absorbed by gravel and not transmitted to deeper targets. Also the base of the Holocene is only faintly recognized. It is not possible to demonstrate any upward continuation of deep faults based on this line.

2.1.3.14 PROFILE KK-HR04-99

This line, starting from the Sava riverbanks towards the north and crossing the line KK-HR03/99, shows better than line KK-HR03/99 the deposition patterns of gravel and sands over Pontian strata of this area. The interface at the base of Quaternary can be followed without uncertainty even if the reflecting amplitudes are abruptly reduced where thick gravel layers are distinctly visible near the surface, moving from the margin of the basin, where the gravel lenses are pinched out, towards the centre of the syncline. The base of Quaternary is not dissected by Neogene faults.

A syncline is identified, reaching 0,15s.

2.1.3.15 PROFILES S1 AND S2

There is a problem of acquisition (shot gun). The energy remains near the seismic source, it does not penetrate at depth and does not propagate at far offsets. Shot gun used in acquisition of these two profiles is not an appropriate seismic source in given field conditions (5-8 m thick layer of dry gravel near the surface).Larger depth penetration can not be achieved with such source. Therefore only reflected waves recorded before 0,4 s are valid. Reprocessing will not provide any improvement.
The seismic coverage is only 12, therefore the signal/noise ratio is too low.
For S2, the occurrence of a high energy superficial layer precludes the interpretation of the shallower layers (WS 2008).

2.1.3.16 PROFILES P1 AND P2

The penetration is greater than S1 and S2, but the shallower part is completely lost due to very low frequency content. This may be due to acquisition conditions (reverberations in surface layers, too strong source) as A. Gosar suggests or to processing (NMO stretching for near-surface reflectors) as A. Bitri suggests. In the latter case, reprocessing may partially help.

2.1.3.17 PROFILES NEK1 AND NEK2 (N-S AND W-E HIGH RESOLUTION PROFILES)

NEK1: A South-dipping reflector is identified on NEK 1 between 0,1 and 0,2 s, it is discontinuous and vertical offset are identified at stations 40, 80 and 120. All Northern blocks are up.
NEK2: An east-dipping reflector is identified on NEK2 between 0,1s and 0,2s but it can not be followed along the whole profile.

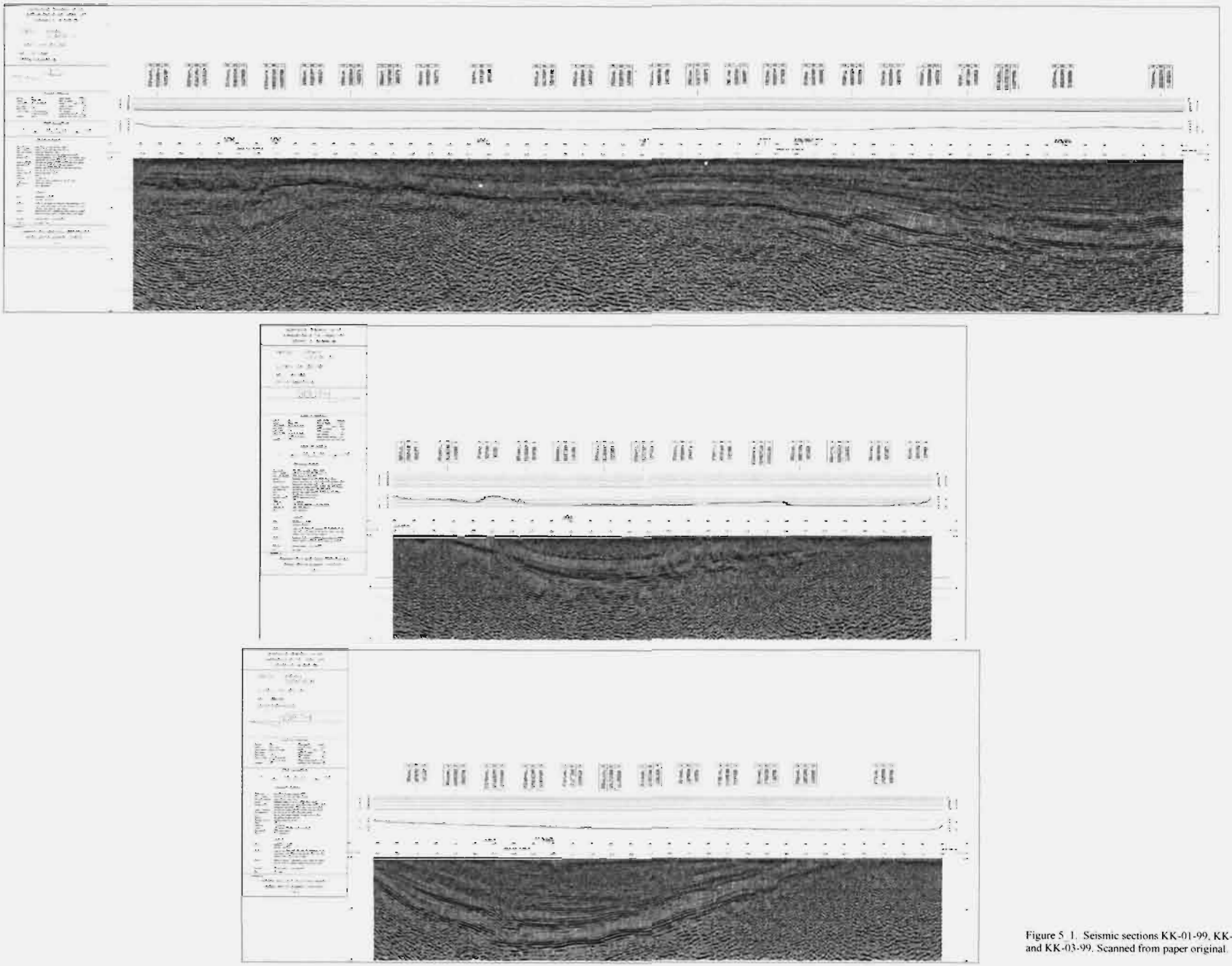

Figure 5. 1. Seismic sections KK-01-99, KK-02-99 and KK-03-99. Scanned from paper original.

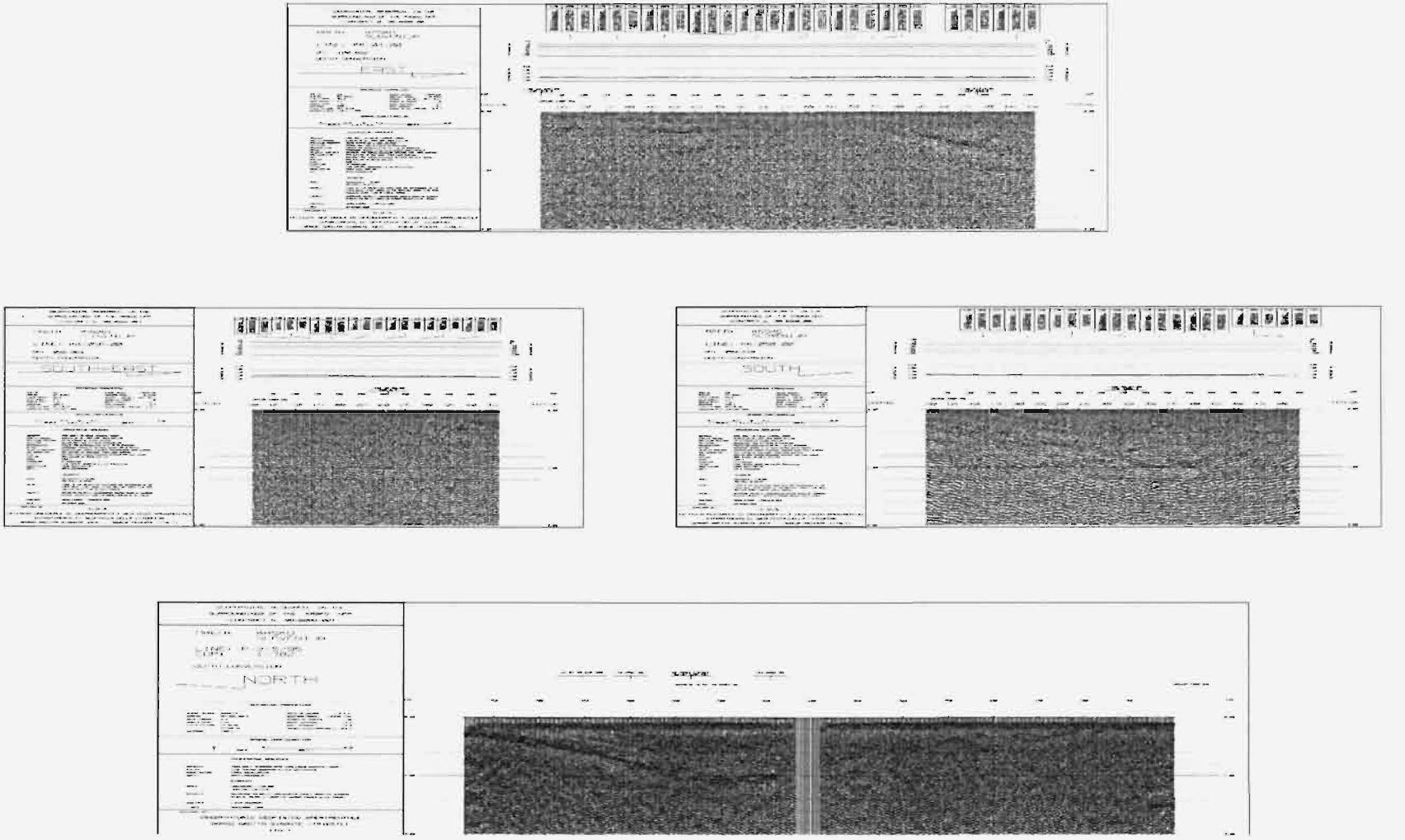

Figure 5_2. Seismic sections KK-04-00, KK-05A-00, KK-05B-00 and KK-03-99 and P-3-S/95. Scanned from paper original.

2.2 NEWLY ACQUIRED HR SEISMIC REFLECTION DATA

2.2.1 INTRODUCTION

Thirteen high resolution seismic reflection sections in total length of 15.5 km were investigated in two campaigns (Figure 6). In the first stage, four seismic reflection sections in total length of 5.4 km (08K-1, 08K-2, 08K-3 and 08K-4) were acquired. Previously unknown structural deformations were observed in these sections but coherent interpretation was not possible. Namely, some of the structures observed in individual seismic sections could not be recognized in other sections and connected in a coherent way without any additional information. For that reason 6 new sections were planned to embrace all deformation and to determine their position and extent. In the field, the planned sections were further split so finally 9 new sections were acquired in the field in 2009 in full length of 10.1 km (08K-5, 08K-6, 08K-7, 08K-8, 08K-8A, 08K-9, 08K-10A, 08K-10B, 08K-10C). In both campaigns, the field acquisition was made by Geoexpert Ltd. (Switzerland) and the data were processed by CGGVERITAS (Tunis).

Interpretation took place in three stages. At the first meeting *(Geophysical interpretation workshop III)* held in November 2008 at GeoZS, Ljubljana seismic sections 08K-1, 08K-2, 08K-3 and 08K-4 were interpreted. In May 2010 *Geophysical interpretation workshop IV* took place in Orleans. Sections 08K-5, 08K-6,08K-7, 08K-8, 08K-8A, 08K-9, 08K-10A, 08K-10B and 08K-10C were interpreted then. The interpretation was made on time sections.

Due to significant mismatch in depth sections, also sections 08K-1, 08K-2, 08K-3 and 08K-4, were re-addressed and interpreted as time sections at the Orleans meeting (originally they were interpreted as depth sections). The decision was made to make the depth conversion only when time sections interpretation is unified. This depth conversion is presented graphically in Figures 19_1 and 19_2. No structural re-interpretation was needed for sections 1 to 4, yet in several cases only marker seismohorizons were shifted vertically to obtain consistent depth interpretation across the investigated field.

Interpretation was done collaboratively by Adnan Bitri, Andrej Gosar, Olivier Serrano, Igor Rižnar, Stephane Baize, Jure Atanackov and Miloš Bavec, using SeisVision software.

Colors used for interpretation of seismohorizons:

- Red: base of Badenian
- Blue: horizon B (near top of Badenian)
- Magenta: an obvious reflector within Pannonian/Pontian succession

Due to the lack of adequate deep-drilling data, definition and correlation of seismohorizons was not an easy task. In fact, only the "blue" seismohorizon was correlated with PHARE horizon B (Badenian Lithothamnian limestone) (Persoglia, ed., 2000). However, it has to be noted that correlation is not fully reliable because the nearby PHARE sections KK-04-00 and KK-05-00 are of lower quality than the newly acquired sections.

Observed features were projected to the surface vertically from the topmost observation and logged by corresponding CDP numbers, meaning that observed structures e.g. reverse faults were not extrapolated to the surface according to the dip but vertically, where they were observed, and equipped by CDP numbers to identify their position.

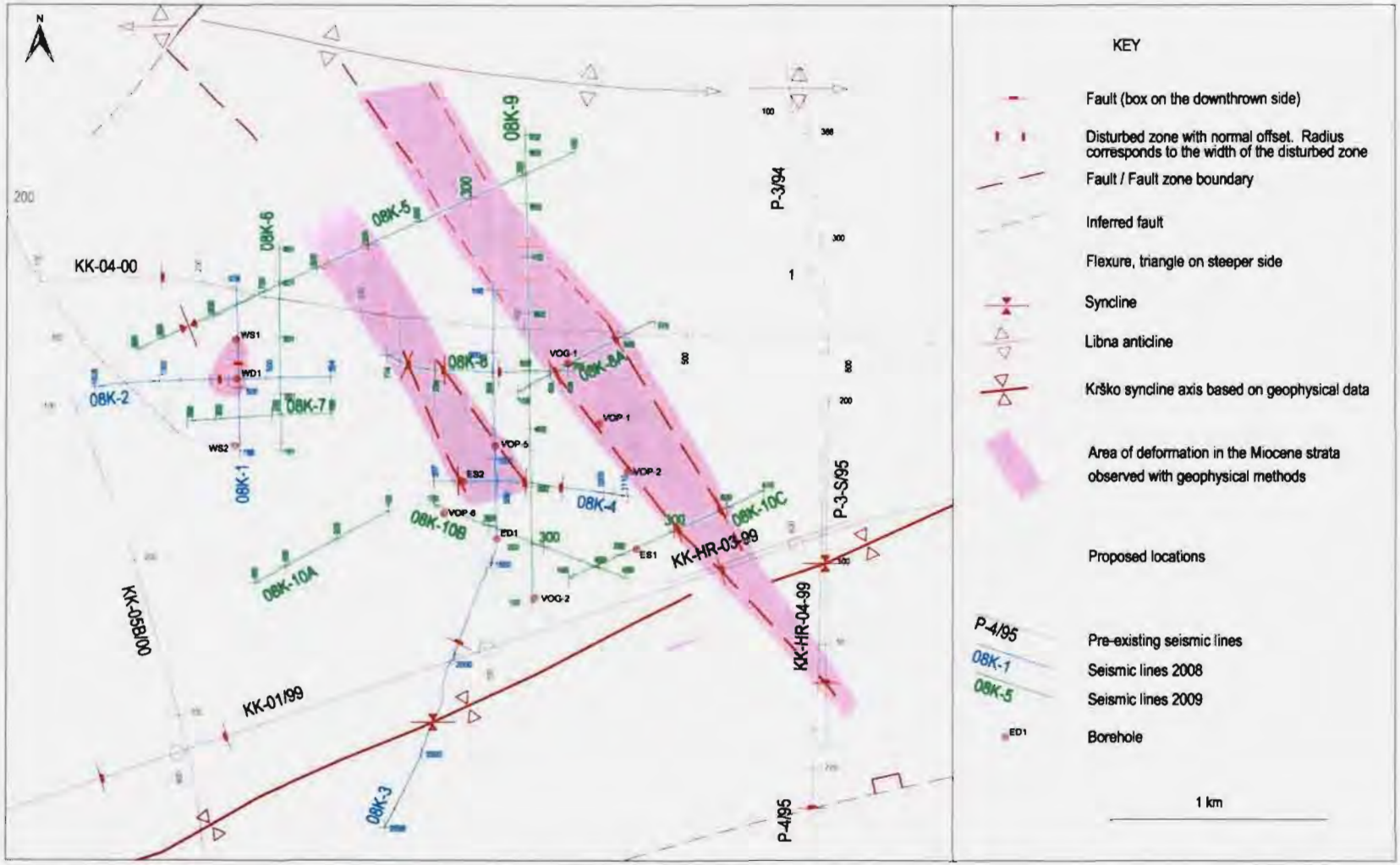

Figure 6. Observations of deformation on newly acquired seismic profiles and on relevant older profiles are indicated with respect to the potential NPP sites.

2.2.2 DESCRIPTION AND INTERPRETATION

2.2.2.1 SECTION 08K-1 (FIGURE 7)

DESCRIPTION
Reflectors do not appear clearly above 250 ms, so we can not interpret this part of the section. Generally, seismic reflectors are dipping towards the South.

In the Northern part, seismic reflectors are curved, a shallow synform is noted.

In the Southern part, seismic reflectors are straight and dip slightly towards the South.

Between CDP numbers 595 and 650 (roughly around 400 m - distance is measured from the S end of the line) and between 250 and 500 ms TWT (roughly), there is an almost 50 meters wide subvertical zone where seismic reflectors are blurred. An inflection line is noted that dips steeply toward the North.

Two flexures appear; one at CDP 517 (310 m at 300 ms) and the other at approx. CDP 620 - 725 (410 - 510 m at 460 ms).

INTERPRETATION
The blurred zone and related phenomena described above are attributed to structural elements with local extent (see overall interpretation).

2.2.2.2 SECTION 08K-2 (FIGURE 8)

DESCRIPTION
Above 220 ms TWT in the W section and above 270 ms in the E section of the section, reflectors do not appear clearly, so we cannot interpret this part of the section.

Seismic reflectors are gently dipping towards the East.

In the middle of the section (between CDP 670 and CDP 770), some seismic reflectors are blurred. At 530 ms TWT the blurred zone is 50 m wide and at 320 ms TWT it is around 80 m wide.

In the Western part of the section, at app. 960 m distance (between CDP 1100 and 1250), an antiform is observed with the hinge at 260 ms.

At CDP 1050 (840 m distance) a hinge is observed at 430 ms.

A vertical disturbance of reflectors is observed at CDP 1100 (890 m distance) but no offset is visible/interpretable.

INTERPRETATION
The perturbed zone between CDP 670 and CDP 770, may correspond to the one identified in section 1 although not the same synformal deformation are observed. The extent of deformation is local (see overall interpretation).

2.2.2.3 SECTION 08K-3 (FIGURE 9)

DESCRIPTION
Above 250 ms TWT, reflectors do not appear clearly, so we cannot interpret this part of the section.
North of the Sava River, seismic reflectors are dipping app. 30° towards the South. Seismic reflectors are not very clear in this part, which may be due to processing and dip of seismic reflectors in this part of the section. South of the river the reflectors are subhorizontal (dipping slightly due South).

Anomalies at CDP 1470 (1250 m distance; just North of the Sava River) may be attributed to acquisition technique. Distance is measured from the N end of the line.

Just South of the Sava River, between CDPs 1835 and 2045 (1600 and 1800 m), there is a 100 meters wide zone where seismic reflectors are blurred. A clear offset is observed at CDP 1940 (1700 m) at 850 ms TWT (top Badenian; PHARE horizon: "B").

In the Southern part of the section, around CDP 2300 (2050 m), a blurred zone appears. However, a clear reflector at 860 ms TWT does not seem to be affected there.

Between CDPs 2500 and 2660 (2250 and 2400 m), a wide blurred zone appears and is prolonged Northward until CDP 2300 (2150 m) at 860 ms TWT.

A gentle flexure is noted at CDP 1070 (850 m), at around 870 ms TWT in the Badenian horizon "B"). Above 650 ms TWT a flexure is not noted.

INTERPRETATION
The disturbance between CDPs 1835 and 2045 (1600 and 1800 m distance) is interpreted as a fault with slightly downthrown Northern block.

The deformation diminishes at 850 ms TWT toward the surface. It is not noted above 650 ms. Its relation to the deformation observed at depth in the P-3-S/95 section (CDP 120) was discussed yet no direct connection was interpreted. No disturbance is observed in the KK01/99 section near the lines intersection.

2.2.2.4 SECTION 08K-4 (FIGURE 10)

DESCRIPTION
Above 180 ms TWT, reflectors do not appear clearly, so we cannot interpret this part of the section.

Seismic reflectors generally dip gently towards the East.

Reflectors are offset along a line that dips toward the East and is projected to the surface at around CDP 310 (100 m). The offset of about 5 – 8 ms is uniform along the line. The eastern block is downthrown. Distance is measured from the W end of the line.

A blurred zone between CDPs 613 and 663 (400 and 450 m) appears at 370 – 630 ms TWT. The zone is related to a vertical disturbance of reflectors below 370 ms TWT. The western block is downthrown.

INTERPRETATION
A structure consisting of two branches is observed. The western branch is more pronounced and can be followed up to the interpretable depth (180 ms TWT). The eastern branch has less pronounced offsets. An interpretation of this structure might be a negative flower structure; however its continuance was not recognized in any of neighboring sections.

2.2.2.5 SECTION 08K-5 (FIGURE 11)

DESCRIPTION

The area above 100 ms is not interpretable due to low frequency noise. Also not interpretable is the area below Badenian (below red).

Axis of a syncline is observed within the Badenian at 795 CDP (1850 m) and at 850 CDP (1148 m) on the magenta reflector. Distance is measured from the NE end of the line.
It is a local syncline observed only in this seismic section, so the exact strike of its axis and its extent is not known.

A flexure is observed between 585 CDP (1260 m) at time 141 ms and 500 CDP (1948 m) at 200 ms. No clear offset is present at either side of the flexure.

From 394 CDP (764 m) to 100 CDP (NE end), the section is not interpretable because no seismohorizons are interpretable/visible in this part as there is only noise visible in the section.
INTERPRETATION

Although the axial plane of the syncline seems to be tilted it does not necessarily be the case. The tilt may be apparent due to sedimentary features. On the map, the axis of the syncline is marked at 850 CDP (1948 m).

Interpretation of the flexure: Bending of the syncline produced a flexure-like structure, related to a supposed Sarmatian fault. The Sarmatian fault itself cannot be observed at the section.

2.2.2.6 SECTION 08K-6 (FIGURE 12)

DESCRIPTION
The area above 120 ms is not interpretable due to low frequency noise. Also not interpretable is the area below 600 ms.

Southward dipping reflectors appear on the section without any deformation.

INTERPRETATION
Section clearly shows the N limb of the Krško syncline. No deformation was interpreted.

2.2.2.7 SECTION 08K-7 (FIGURE 13)

DESCRIPTION
The area above 120 ms is not interpretable due to low frequency noise. Also not interpretable is the area below 600 ms.
Only subhorizontal reflectors of relatively poor quality are visible without any disturbances.

INTERPRETATION
No deformation is interpreted.

2.2.2.8 SECTION 08K-8 (FIGURE 14)

DESCRIPTION
The area above 200 ms is not interpretable due to low frequency noise. Also not interpretable is the area below 700 ms.

Seismohorizons are gently dipping to the E. A gentle synform with axis at 398 CDP (746 m distance) is observed. Distance is measured from the W end of the line.

Three disturbed zones are observed.
A subvertical disturbed zones at 153 CDP (100 m) and 210 ms TWT can be traced down until 610 ms.

Another disturbed zone is traced from 220 CDP (274 m) and 230 ms down to 172 CDP (149 m) and 560 ms.

A subvertical disturbed zone is observed at 315 CDP (525 m) between 430 ms TWT and goes up to 245 ms TWT. Above 245 ms it is not interpretable.

INTERPRETATION
Between the two disturbed zones in the W part (traced at top between 153 CDP (100 m) and 220 CDP (274 m)) a slight graben-like feature is observed. Deformation/displacement is weak and can not be quantified.

The easternmost structure is interpreted as a normal fault with downthrown eastern block. The displacement at time section is 10 ms (TWT) which is around 10 m.

Above 245, 220 and 210 ms respectively, the deformation cannot be traced upward due to artifacts (may be due to lack of distinct layering/reflectors).

2.2.2.9 SECTION 08K-8A (FIGURE 15)

DESCRIPTION

The area above 200 ms is not interpretable due to low frequency noise. Also not interpretable is the area below 550 ms.
Slightly westward dipping seismohorizons are observed. Poor expression of seismohorizons does not allow attribution to those identified in other seismic sections.

Two disturbed zones are observed; western branch from 180 CDP (196 m) at 190 ms to 240 CDP (353 m) at 600 ms and the eastern branch between 303 CDP (519 m) at 330 ms and 282 CDP (463 m) at 510 ms is measured from the SW end of the line.

INTERPRETATION
Poor expression of seismohorizons may be due to signal damping over the abandoned landfill in this area (Petkovšek (ed), 2009).

An abrupt change in dip is observed across the western branch. A normal fault with subsided western block is observed across the eastern branch. Both branches of deformation are attributed to the Libna fault zone.

2.2.2.10 SECTION 08K-9 (FIGURE 16)

DESCRIPTION

The area above 100 to 120 ms is not interpretable due to low frequency noise. Also not interpretable is the area below Badenian (below red seismohorizon).

The area between 788 CDP (1809 m) to 940 CDP (N end of the line) is not interpretable. Distance is measured from the S end of the line.

Below the bottom of Badenian (red reflector), parallel seismohorizons are well visible in the central part of the section without a distinct unconformity with the Badenian.

In the Southern part of the section the reflectors are subhorizontal from 200 CDP to 102 CDP (S end of the line).

To the North of 200 CDP the strata are inclined (representing the Northern limb of the Krško syncline).

Between 660 CDP and 720 CDP there is a gentle flexure best visible between the bottom Badenian and 130 ms (up to the blind zone). Deformation is more pronounced in Badenian than in Sarmatian.

INTERPRETATION
The position of the flexure corresponds to the Libna fault zone. No clear offset of reflectors is observed.

2.2.2.11 SECTION 08K-10A (FIGURE 17)

DESCRIPTION
The area above 160 ms is not interpretable due to low frequency noise. Also not interpretable is the area below 950 ms.
Subhorizontal seismohorizons of poor expression are observed. No deformation is observed.

INTERPRETATION
No deformation is observed. Despite relatively poor quality, it is evident that no deformation is present.

2.2.2.12 SECTION 08K-10B (FIGURE 18)

DESCRIPTION
The area above 100 ms is not interpretable due to low frequency noise. Also not interpretable is the area below 900 ms.

Subhorizontal reflectors are slightly inclined at the W part (from 235 CDP (364 m) to 100 CDP (NW end of the line). Distance is measured from the NW end of the line.

No visible deformation.

INTERPRETATION

No deformation is interpreted.

2.2.2.13 SECTION 08K-10C (FIGURE 19)

DESCRIPTION
The area above 90 to 100 ms is not interpretable due to low frequency noise. Also not interpretable is the area below 1000 ms.

Subhorizontal seismohorizons are present throughout the section.

Two disturbed zones are observed. E branch intersects the base of Badenian at 335 CDP (623 m distance) and 846 ms. Deformation is observable upward until 390 CDP (769 m) and 260 ms. The W disturbed zone is observed from the Sarmatian at 325 CDP (596 m) and 730 ms upward until 306 CDP (546 m) and 280 ms Distance is measured from the SW end of the line.

INTERPRETATION
The two disturbed zone are interpreted to be two branches of one fault with a collapsed central part. Position corresponds to the trace of the Libna fault zone.

2.2.3 OVERALL INTERPRETATION

All the deformation can only be traced within the Miocene succession up to the blind zone, or they diminish within the Miocene succession. Further continuation towards the surface (and inside Q and PlQ sediments) can not be confirmed or disproved at this stage for those deformation that reach the blind zone (between 90 and 270 ms TWT).

Western location
Deformation observed near intersection of 08K-1 and 08K-2 was localized by surrounding sections 08K-5, 08K-6 and 08K-7. Deformation can not be traced anywhere beyond the intersection of 08K-1 and 08K-2 and is thus treated of low importance and local extent. The geometry and quality of the mentioned profiles is of high quality thus ambiguity regarding potential further extent of the deformation is minimal. This also excludes connection with minor deformation observed at 175 CDP on KK-04-00.

Eastern location
Libna fault zone is interpreted between the crest of Libna Mt and Sava River. The fault was observed in P-3-4/95, the same deformation was recognized in KK-01-99, 08K-10C and 08K-8A lines. To the NW the fault line can not be traced due to poor data quality across the KK-04-00 and 08K-5 lines. At the Mt. Libna crest, the fault is located by surface mapping and 2D electric tomography (this report). NE limit of the fault zone is relatively reliable only between 08K-10C and 08K-8A lines.

A (most probable) negative flower structure is observed on 08K-4 and shown as a gentle flexure on seismohorizon B on 08K-3 section. It can not be traced due South or East. No deformation is observed either in 08K-10B or 08K-9. However, the structure can be traced due NW, where it is recognized in 08K-8 and may potentially also be linked to gentle flexures observed on 08K-5 and also in KK-04-00 (not above seismohorizon B). In KK-04-00 the structure is very weakly expressed and was never described before.
This structure is interpreted as a strike-slip fault zone parallel to the Libna fault. It is relatively poorly expressed and limited due South but may extend further towards the NW.

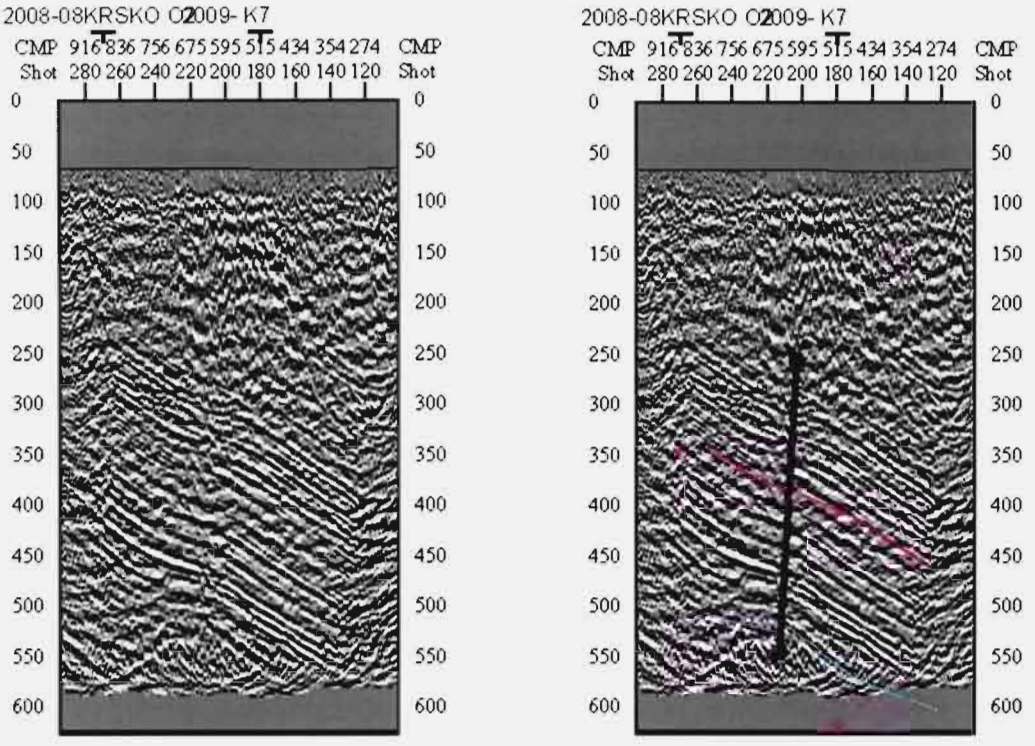

Figure 7. HR reflection seismic section 08K-1. North is to the left.

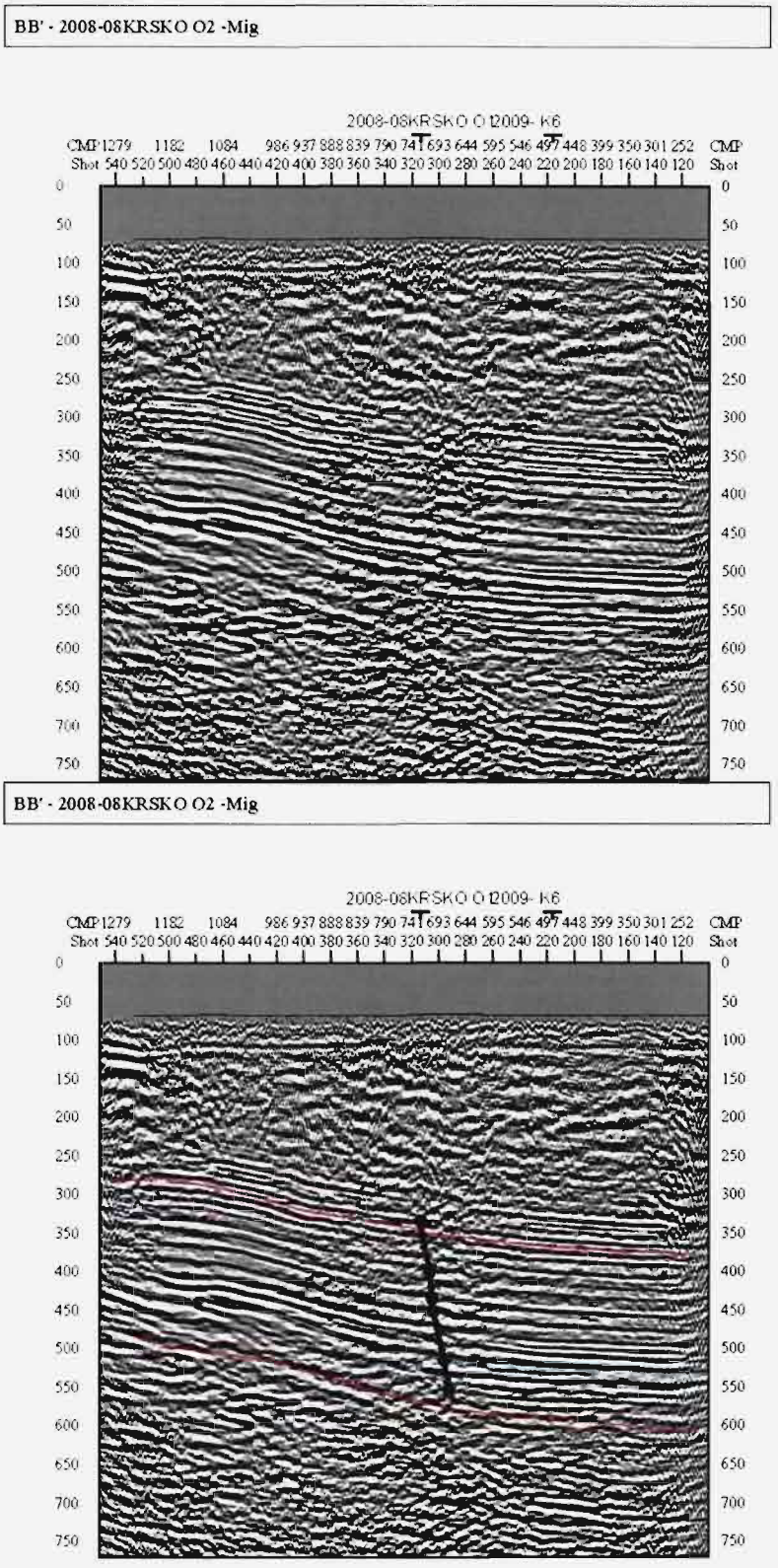

Figure 8. HR reflection seismic section 08K-2. West is to the left.

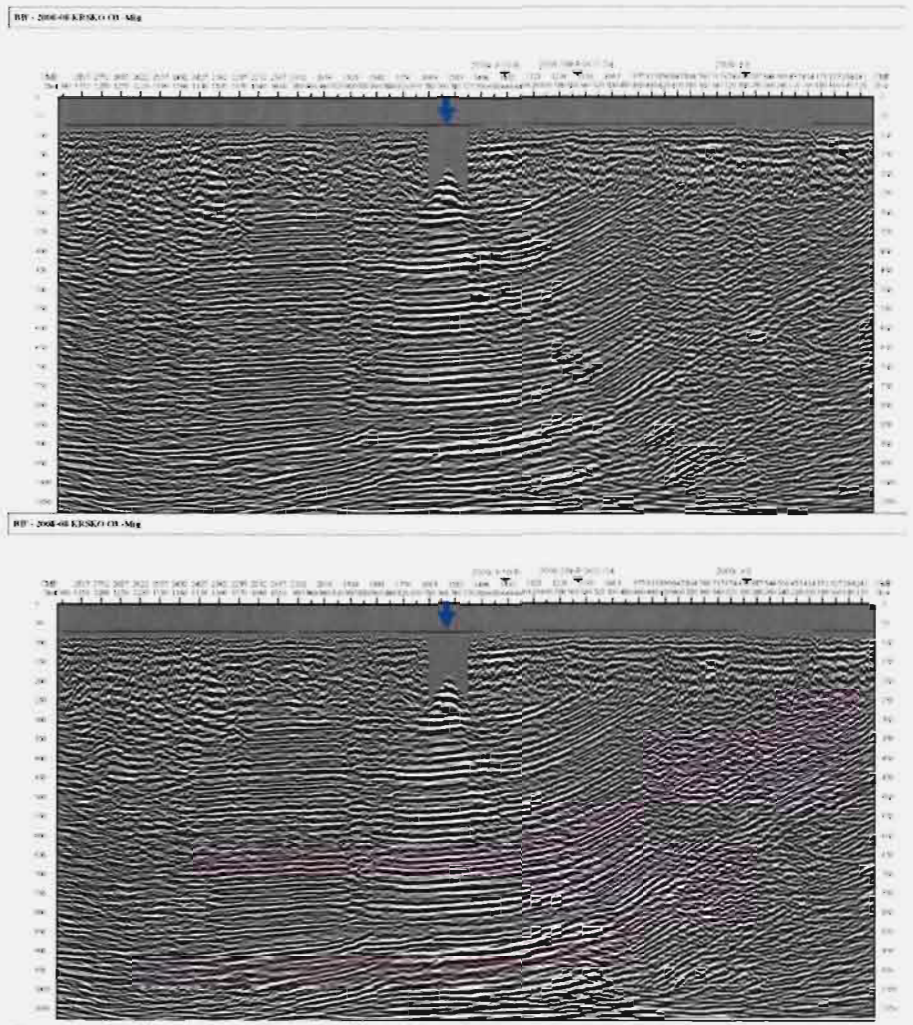

Figure 9. HR reflection seismic section 08K-3. North is to the right. Blue arrow indicates the Sava river..

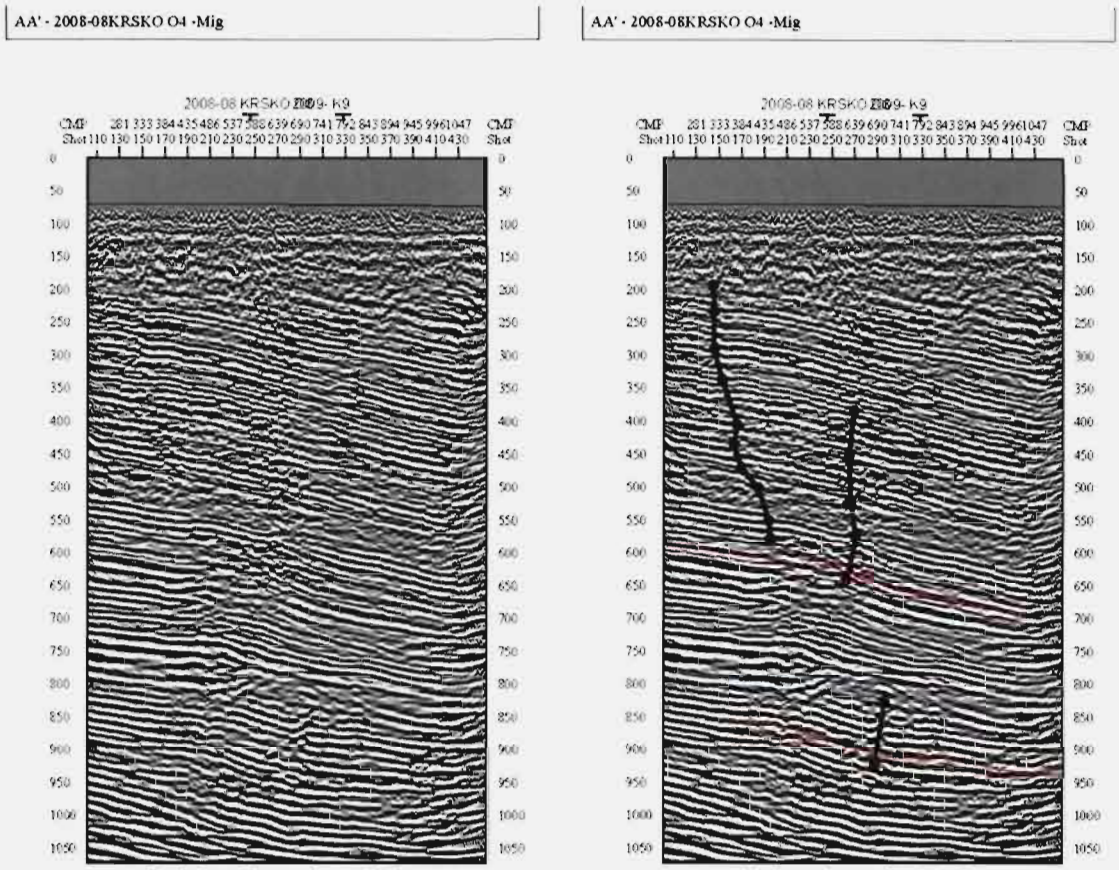

Figure 10. HR reflection seismic section 08K-4. West is to the left

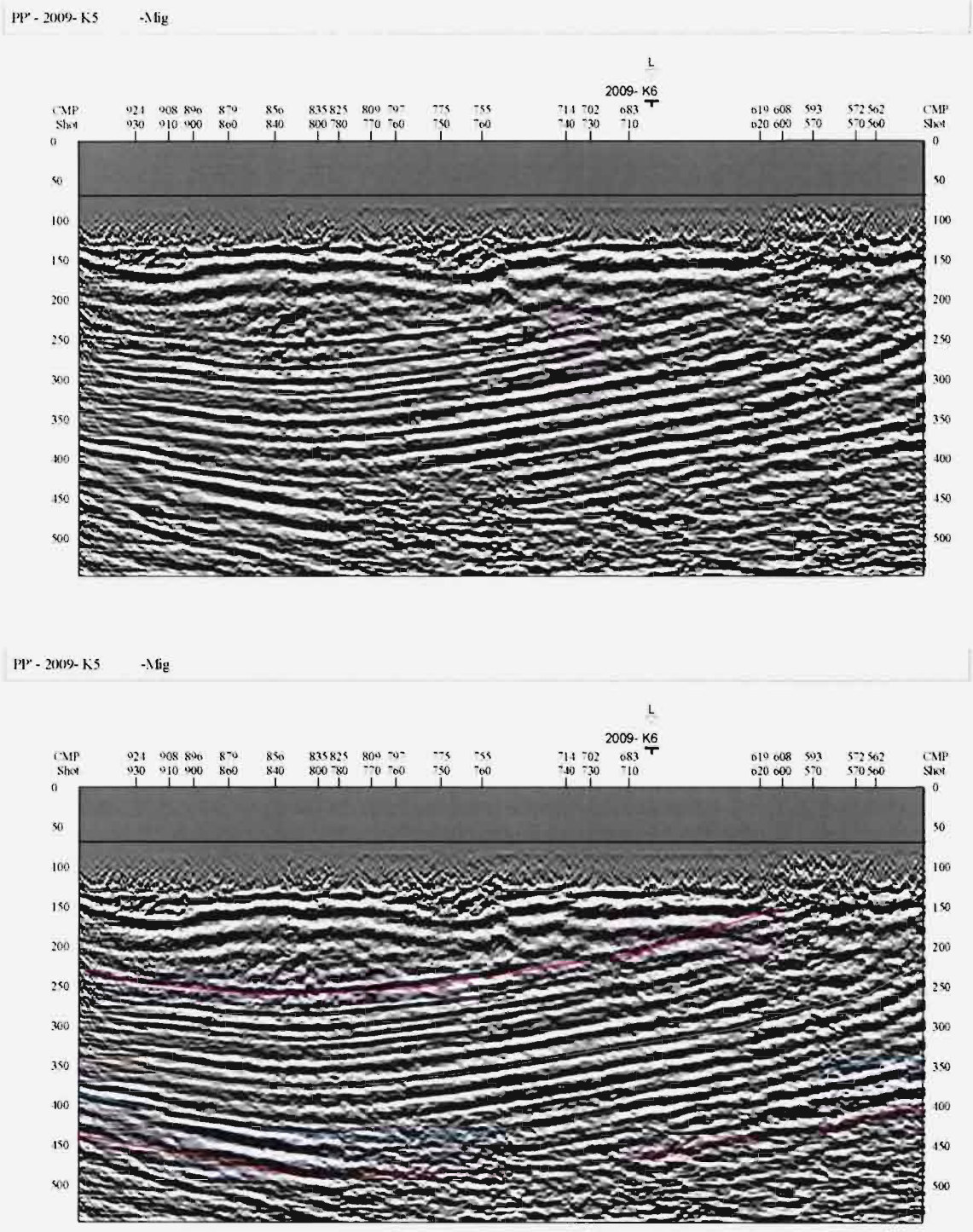

Figure 11. HR reflection seismic section 08K-5. NE is to the right.

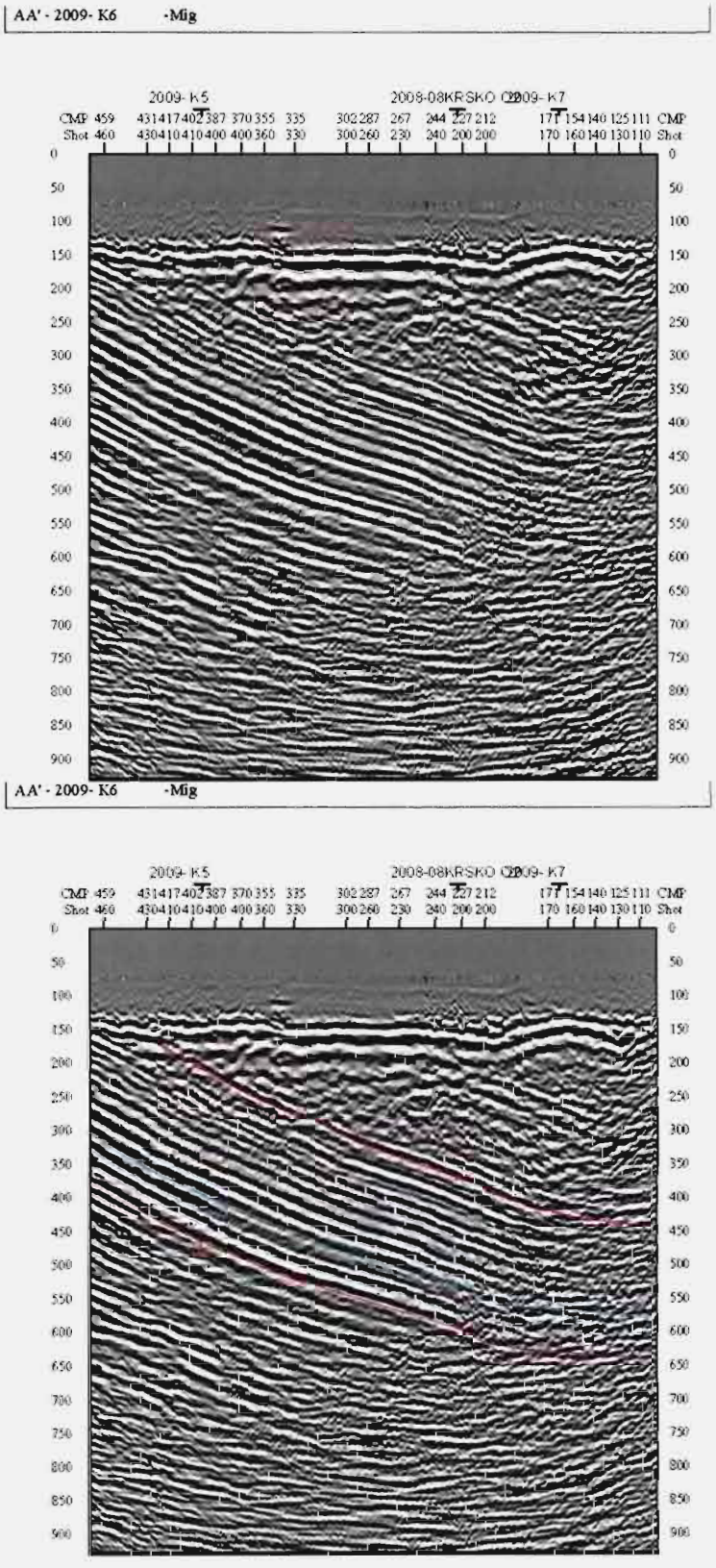

Figure 12. HR reflection seismic section 08K-6. S is to the right.

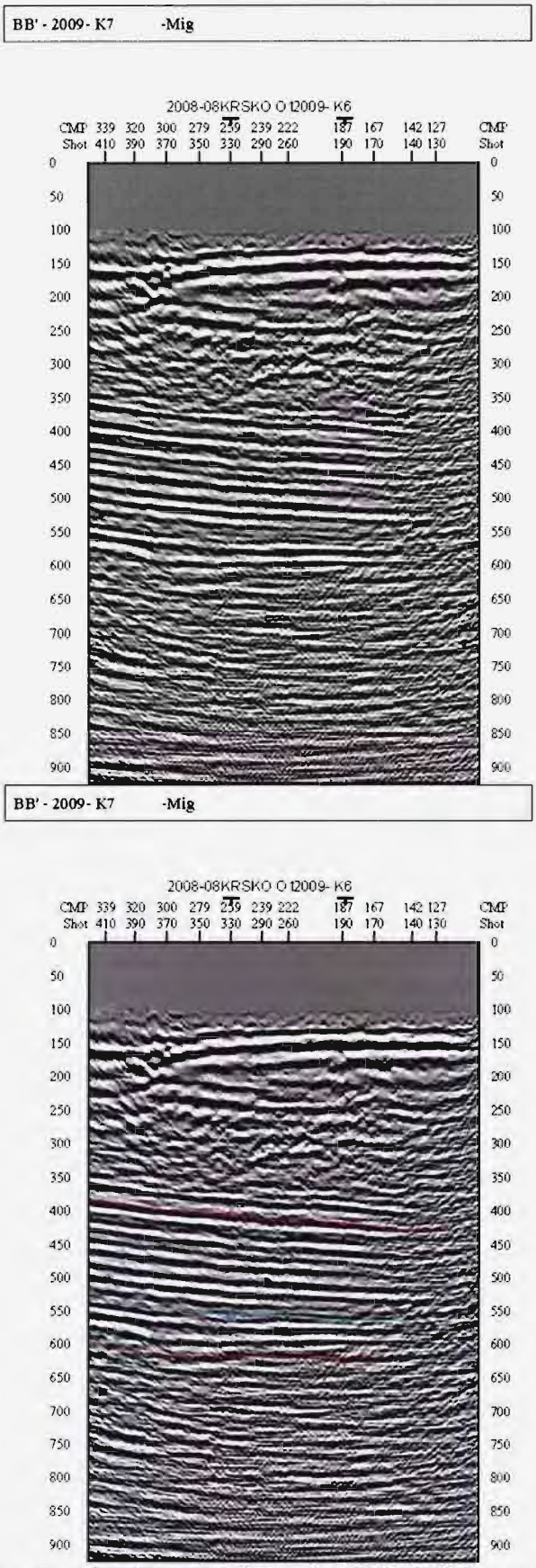

Figure 13. reflection seismic section 08K-7. E is to the right.

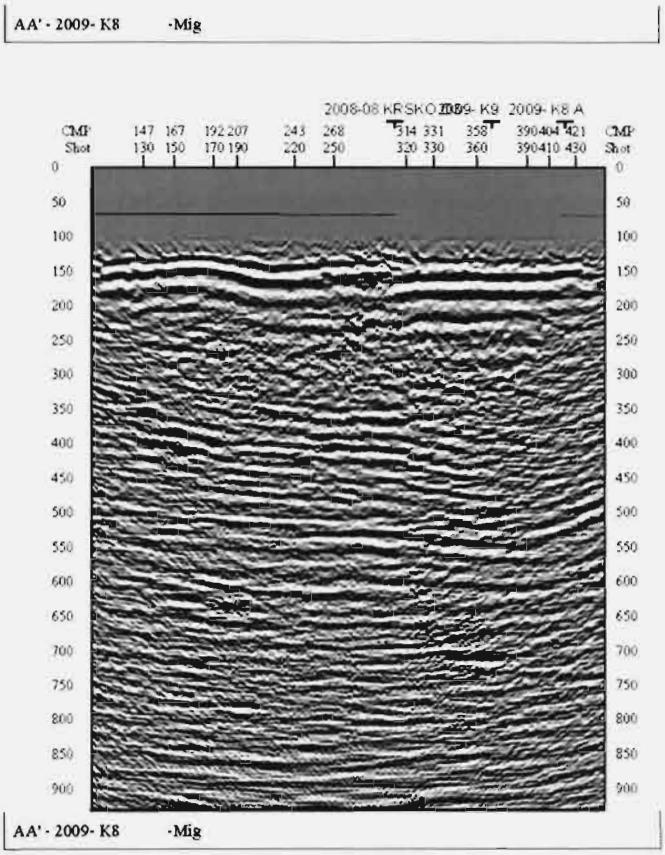

Figure 14. HR reflection seismic section 08K-8. E is to the right.

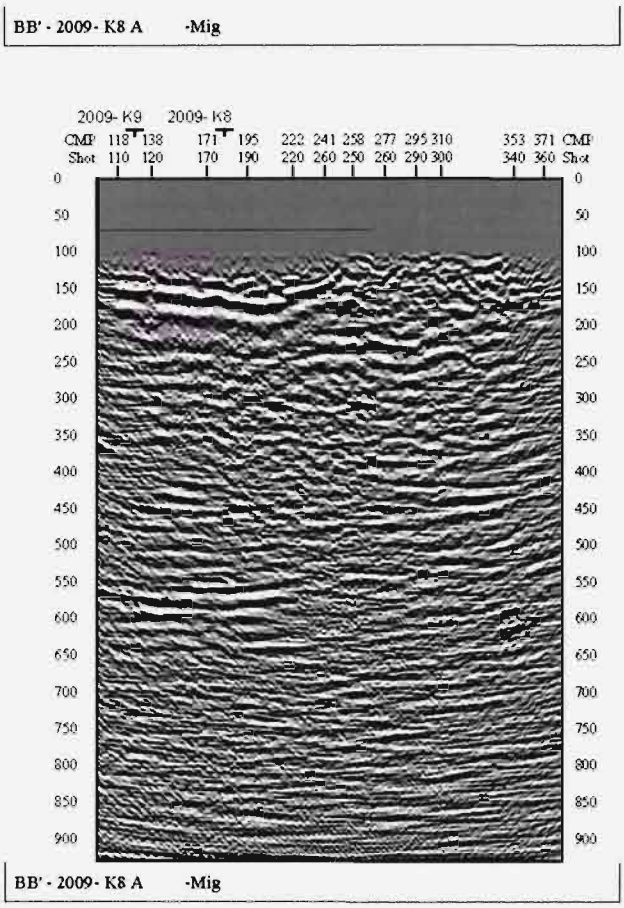

Figure 15. HR reflection seismic section 08K-8A. NE is to the right.

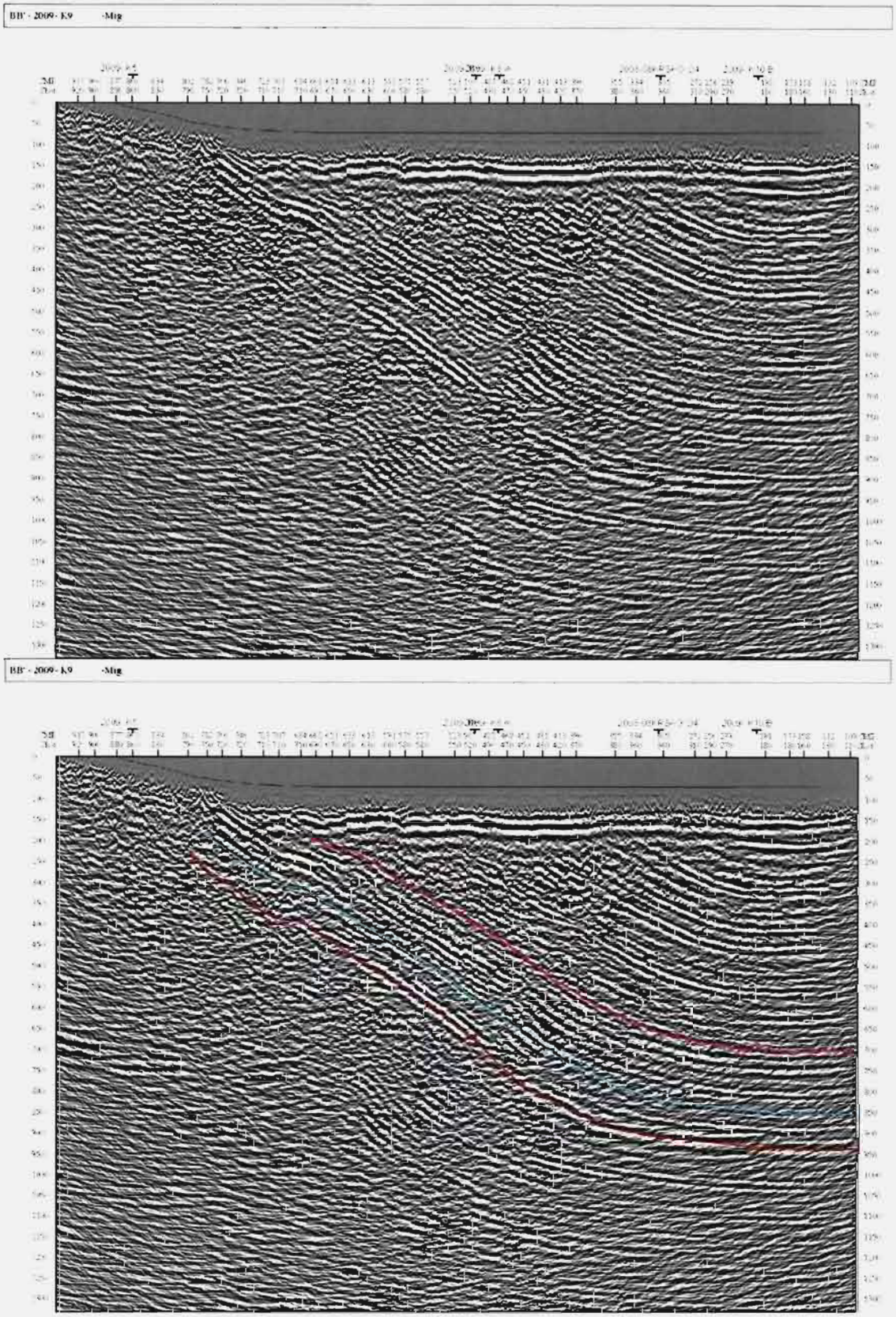

Figure 16. HR reflection seismic section 08K-9. S is to the right.

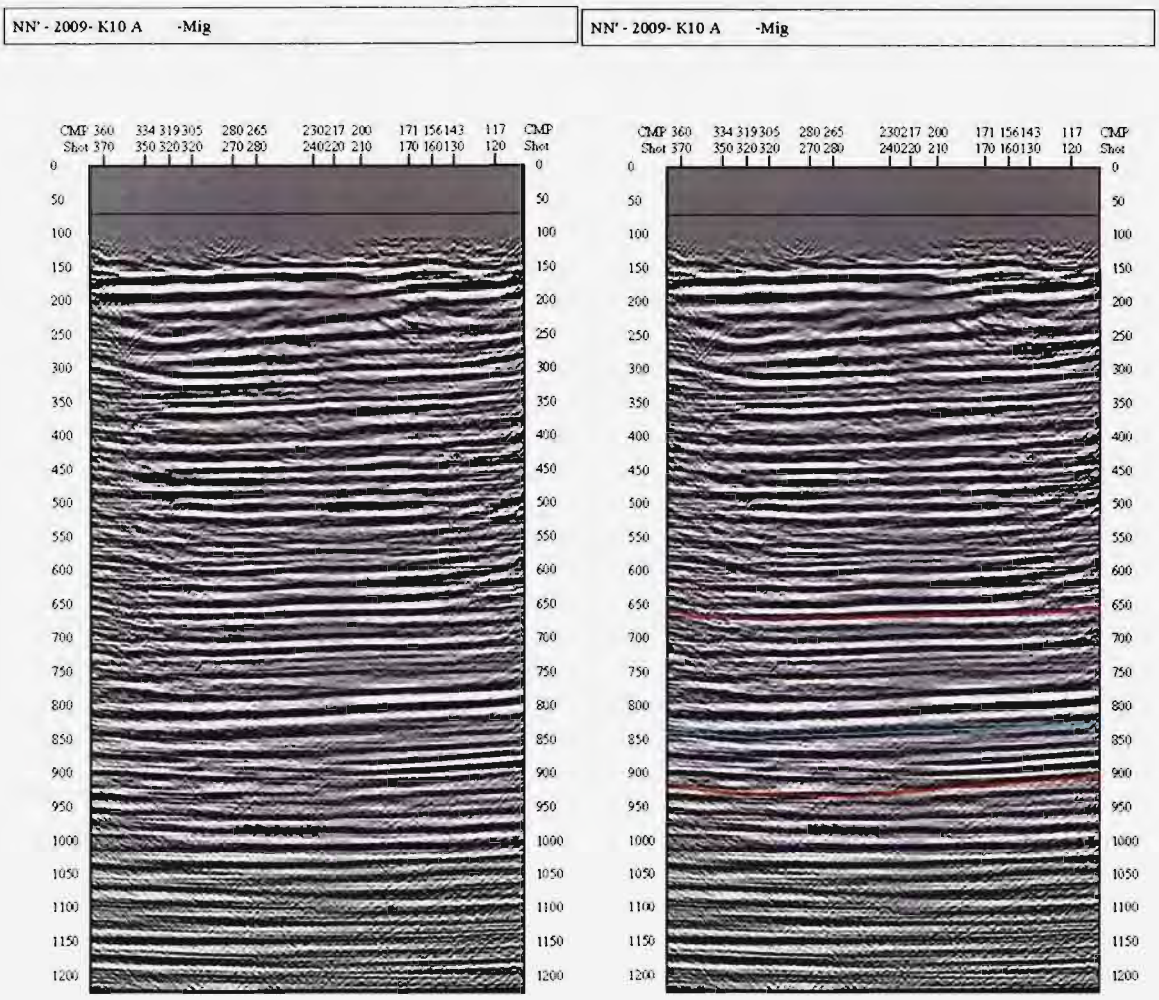

Figure 17. HR reflection seismic section 08K-10A. NE is to the right.

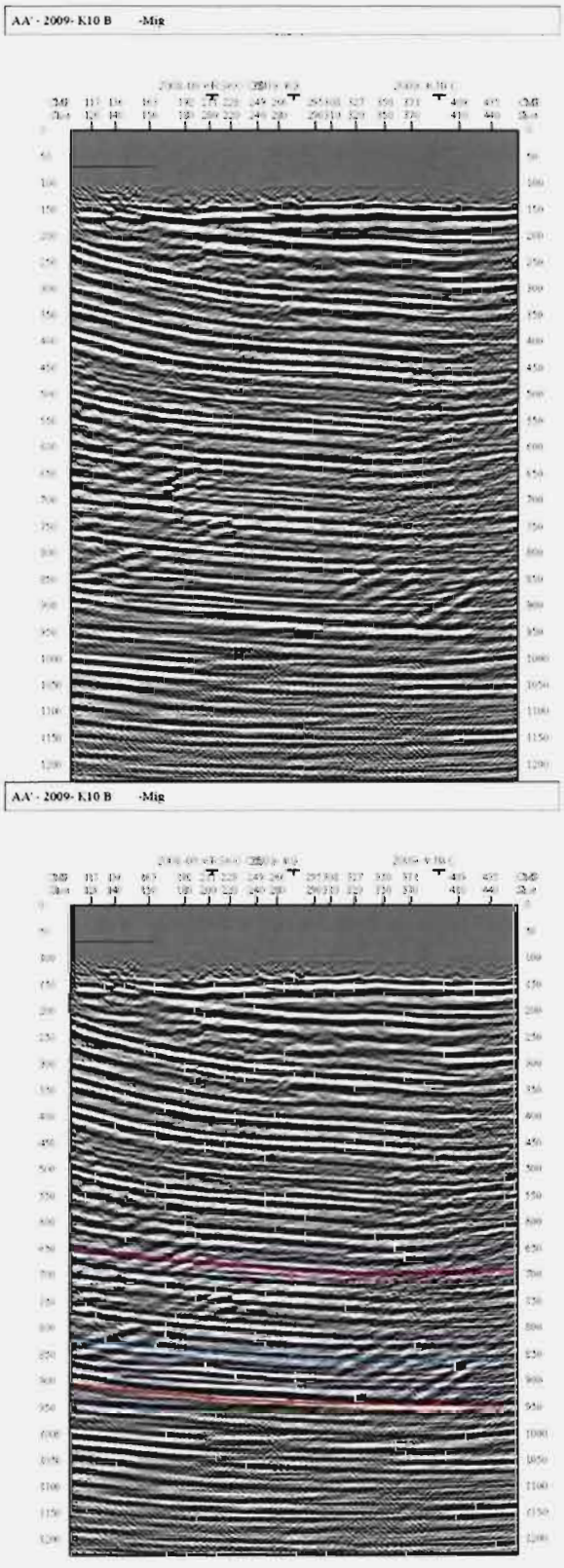

Figure 18. HR reflection seismic section 08K-10B. SE is to the right.

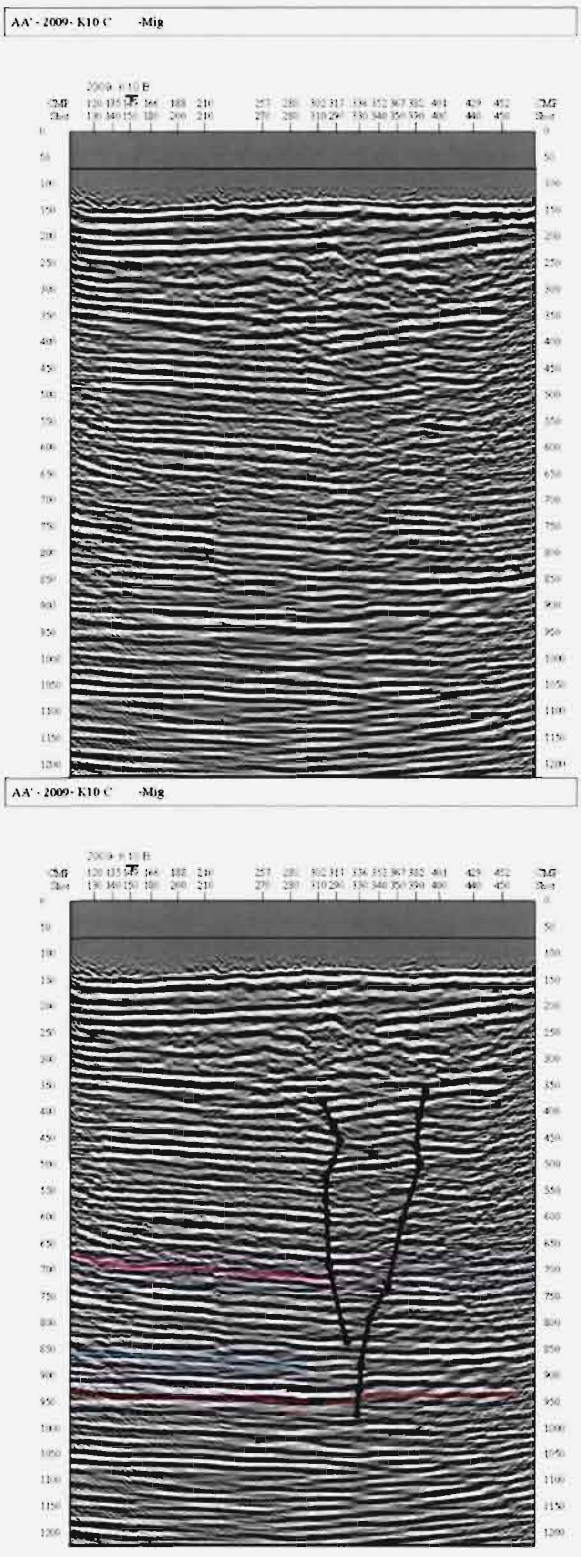

Figure 19. HR reflection seismic section 08K-10C. NE is to the right.

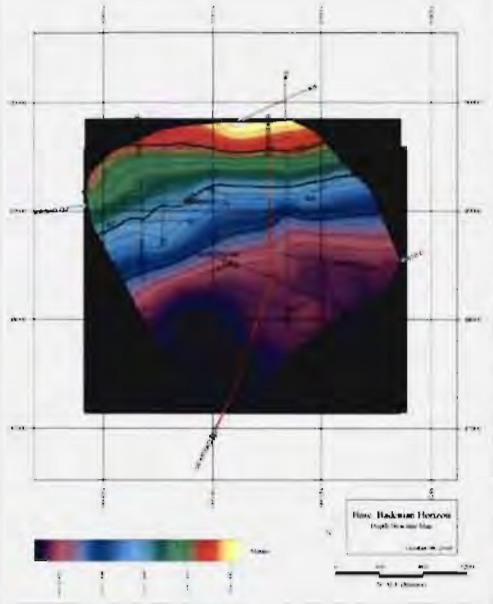

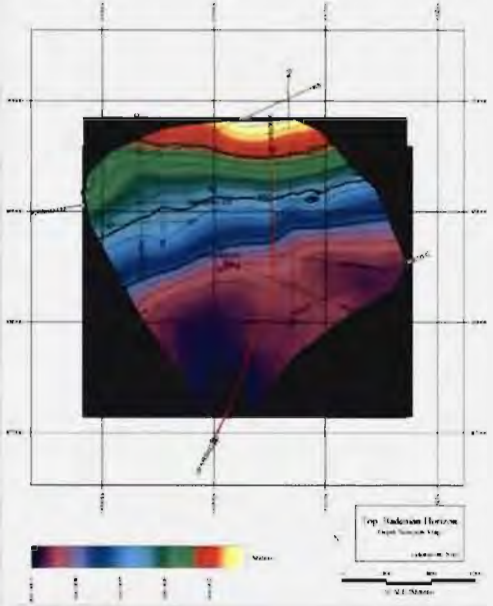

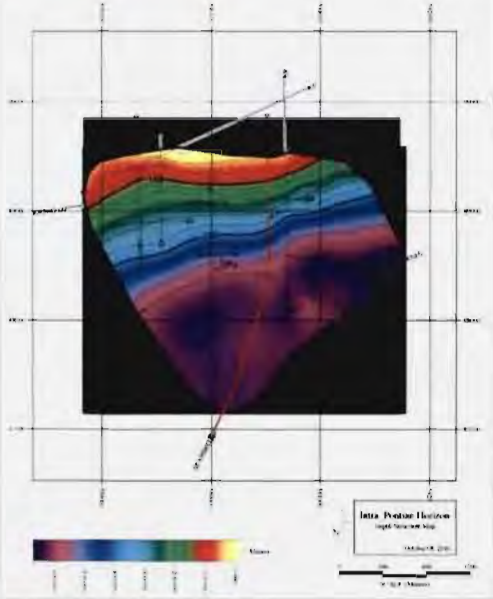

Figure 19_1. Depth interpreted seismohorizons. Top left: Base Badenian; Top right: Top Badenian; bottom: Intra Pontian.

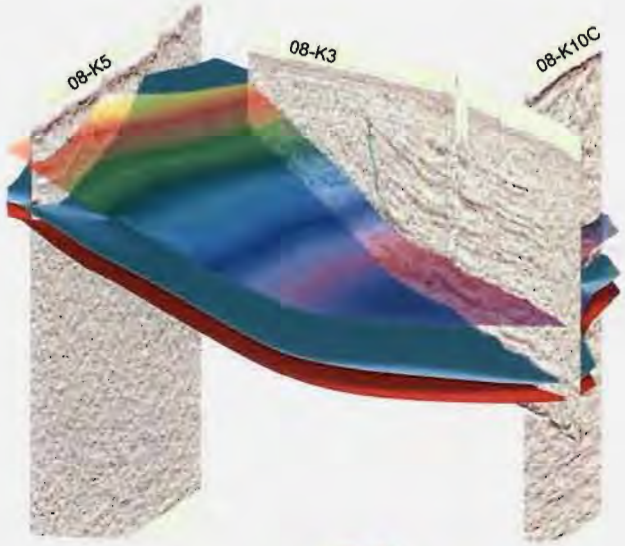

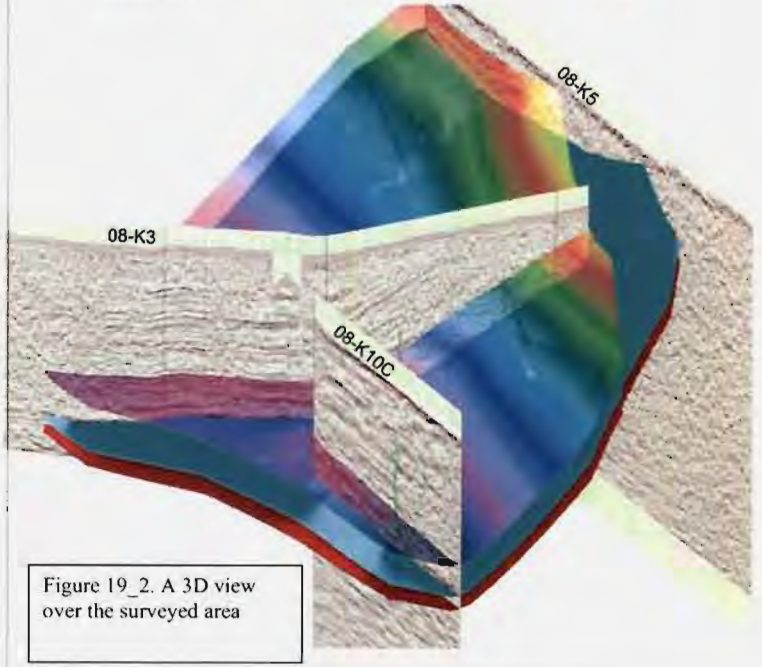

Figure 19_2. A 3D view over the surveyed area

3 GEODESY

Three independent geodetic surveys were performed in field and results were analyzed.

1. GNSS geodynamic net Krško measurement
2. Leveling
3. Libna terrestrial network

All work was done by FGG. The reports are finalized and were externally reviewed.

Repeated leveling along the railroad following the northern rim of the Krško basin (Koler, 2010) prove that there is no statistically significant displacement observed within the level of confidence and on well stabilized benchmarks.

The results of Libna terrestrial network and the GNSS measurements are not applicable at this stage and will have to be re-addressed in the future. Abandoning the GNSS results for furher consideration is due to the fact that results are all within the unceiratinty of the method thus no statistically significant displacement was observed. Results of the Libna terrestrial network were on the other hand uninterpretable so monumentation of measuring points was rechecked by a geologist (Rižnar, 2009a). This inspection questioned stability of measuring points so results were not used.

4 TECTONIC MODEL

4.1 INTRODUCTION

A Simplified tectonic map (Figure 4) is elaborated for the construction of the tectonic model. The tectonic map is based upon the detailed geologic mapping data, geophysical data, trenching and primarily on results of preliminary studies.
A reduced lithologic presentation is used for the tectonic map in order to emphasize the most recent generation of the structures. Mesozoic, Neogene, Plioquaternary and Quaternary lithostratigraphic units are shown on the map. The mapped structures are divided into three groups according to their age and importance (length and offset): Principal Neogene fault, secondary Neogene fault (both affecting the Neogene deposits) and other faults that do not affect Neogene deposits. Less important Paleogene structures are omitted. In the Krško basin, where the structures are detected by geophysical methods, the Mesozoic ones were not observed (detected) at all.

Three major groups of structures are present in the Krško Basin area. The oldest (»Dinaric«) ones exhibit predominantly NW – SE strike, include large folds (several km) and related faults. Dinaric structures observed in the Mesozoic formations and buried by the Neogene deposits are considered of Paleogene age. Some of these Paleogene faults were also reactivated later in the Neogene. The second group of structures (Balaton structures) are observed in the Neogene (and older) rocks. They mostly exhibit the NE – SW (ENE – WSW) strike and correspond to the strike of the Zagreb and Sv. Nedelja faults (and the Mid-Hungarian Zone).

In order to simplify the description of evidences, some simplifications are adopted in this text. Five formations of mostly turbidite character, including Biancone limestone, in the time range from Middle-Upper Jurassic to Uppermost Cretaceous were referred to as "the basinal deposits". The term platform carbonates is used for the Upper Triassic to Lower Jurassic dolomite and limestone including the Dachstein limestone and the dark micrite mudstone and oolitic limestone.

The applied numeration refers to the recent geologic (and tectonic) map. A hybrid citation system is used for the references that appear in the 2003 PSHA (Swan et al., 2004), for easier comparison.

4.2 TECTONIC MAP - DESCRIPTION OF STRUCTURES

Description and annotation of structures refer to the tectonic map of the Krško basin in 1:25,000 scale (Figure 4) for structures in the extended site vicinity perimeter (Krško basin). Structures beyond this perimeter are presented on, and refer to the original near regional tectonic map of the 2003 PSHA (Swan et al., 2004) study that is based on 1:100.000 geological map (Figure 20). Structures that are presented only on the small scale map are clearly referred to it ("Figure 20").

4.2.1 FOLDS

Rudnica anticline (a)
The anticline is named after Rudnica Mountain in the vicinity of the anticline axis. Triassic carbonate rocks are exposed in the core of the anticline, and the limbs are overlain by the Neogene (Oligocene to Miocene) clastic deposits. The anticline axis appears to be dissected and partly displaced to the Southeast by the NW-SE-oriented right-lateral strike-slip Buča fault (Figure. 20).

Planina syncline (b)
The Planina syncline is named after the Planina village and represents the Southward continuance of the Rudnica anticline. The Neogene deposits are exposed in the syncline core. In the western part of the syncline, the youngest Neogene deposits are of Sarmatian age, and in the eastern part of Pontian age. Such an arrangement suggests that the syncline axis plunges to the E.
Planina syncline axis is apparently displaced by the right lateral strike-slip Žalec (Figure. 20), Žegar (Figure. 20), and Buča (Figure. 20) faults as in the case of the Rudnica anticline.

Litija anticline (Figure. 20)
Litija anticline is named after the Litija town. Paleozoic rocks are exposed in the western section of the anticline. Prevailingly Mesozoic carbonate to clastic rocks crop out in the middle, and Neogene clastic sediments are present in the eastern section of the anticline. Such an arrangement indicates eastward plunging of the fold axis. A part of the Southern limb of the Litija anticline is thrusted Southward onto the Senovo syncline. The Kum thrust, represents a Southalpine thrust front. A detachment plane in the Southalpine overthrust structure to the E, is present in the Northern limb of the Litija anticline according to Placer (1999a [68]).

Senovo syncline (Figure. 20)
The syncline is named after the Senovo town, and involves Neogene deposits of Oligocene to Pontian age. As this complex syncline consists of a series of secondary folds, it should be referred to as a synclinorium in fact. In the central part, the area between the Vetrnik and Orlica Mts., the main syncline axis branches into two synclines to the W. To the E the syncline is simple with undisturbed core. To the W, Senovo syncline can be associated with a small Neogene basin, the so-called Krmelj depression. The fold axis is E-W trending. The area between the Senovo syncline and the Krmelj depression may represent an older NW-SE trending Dinaric anticline.

Orlica anticline (m)

Orlica anticline is named after the Orlica Mountain. Triassic, Jurassic and Cretaceous sediments are exposed in its core. The Southern limb of the anticline forming the Northern margin of the Krško Basin is overlain by the Neogene (Badenian to Pontian) deposits. Neogene deposits are exposed along its hinge only in the far eastern part; thus it plunges in this direction (Figure. 20).

The Mesozoic strata are deformed by a series of Dinaric NW – SE trending folds. However, these fold axes plunge toward the South to Southeast (Poljak et al., 1995 [90]; Poljak, 1999; 2000a,b [82, 83]), forming the Northern limb of a Neogene Krško syncline (g). The Orlica anticline core is also highly disrupted by tension faults that trend perpendicular to the fold axis, i.e., in N-S to NW-SE direction. A small scale pre-Pannonian syncline with a NW-SE trending axis is observed in the Southern limb of the Orlica anticline in the upper Dramlja creek valley. It is developed in the Badenian and Sarmatian deposits. The genesis of this fold is not quite clear.

To the W, the Orlica anticline is superimposed to the NW trending Dinaric Sremič anticline (B).

Libna anticline (i) and Črna Mlaka syncline (h)

Libna anticline is a secondary E – W oriented post-Badenian fold in the Northern limb of the Krško syncline (g), approximately 2 km N of the Krško NPP. The Southern limb of the Libna anticline is well documented with increasing Southerly dip of the Badenian strata from the crest towards the South, where the dip reaches its maximum of 80°. Only one NE oriented dip has been observed in the E part of the anticline's Northern flank. The fold axis is plunging towards the E where the Badenian limestone is overlaid by the Pannonian (to Sarmatian) carbonate silt. The boundary does not appear to be disrupted. Libna anticline is a tight similar fold. To the E it gradually becomes open, meaning that the shortening decreases very fast in this direction. In 1,5 km distance, the 80° dip declines to only 12° (Poljak et al., 1996b [92]; Poljak, 1997a [78]). The Libna Anticline is covered by gently tilted and faulted Plioquaternary sediments (Poljak, 1997a [78]; GeoZS, 2006a). The NNE gently (15°) tilted Plioquaternary strata are reconstructed in the N limb of the Libna Anticline (Placer, 1997 in: Poljak, ed., 1997 [78]), while to the S only 10° tilt can be calculated between the Plioquaternary base at the top of the Libna Mt. and from the boreholes E of the NPP. Some minor NW trending faults dissect the Badenian limestone in the Libna anticline (Placer, 1997 in: Poljak, ed., 1997 [78]).

N of the Libna anticline there is a less pronounced Črna Mlaka syncline. It is imaged in the N part of the P-3-4/95 seismic line together with the Libna anticline, as well as in a set of the three parallel geoelectric lines (EP-1/94, DOP-l-1/96 and LIBNA-1/97), located E of the P-3-4/95 seismic line (Poljak, 1997a [78]).

The R2-1/96 trench has been dug across the supposedly tectonically induced Quaternary slope at Marot village in the eastern continuance of the Libna anticline. Noncarbonate sandy gravel (Plioquaternary) was found in the trench below the 3,2 m of pseudogley. No tectonically disturbed sedimentary structures were observed due to intensive gleyisation of the sediment (Poljak et al, 1996b [92]).

The »Reverse Libna fault« in the N limb of the Libna anticline, proposed by Kuščer (1993 [50]) and Verbič (1995 [126]) was not confirmed in detailed mapping campaigns (Poljak et al., 1996b [92]; Poljak, 1997a [78]). Placer (in: Poljak, Ed., 1997 [78]) is proving the absence

of the fault, with the morphology of undisturbed Plioquaternary strata in the N limb of the Libna anticline.
North verging reverse fault is observed in the P-3-4/95 seismic section (Poljak, 1994 [75]) in the N limb of the Črna Mlaka syncline, but the fault has not been detected at the surface in any of the mapping campaigns.
Prelogović (1996 [96]) identified two, South-verging reverse faults (faults F2 and F3, Figure 4-2) in the Southern flank of the anticline, but these faults were not identified by Gosar (1998 [30]) nor by Persoglia (ed., 2000 [60], Figure. 4-3). However, a North-verging fault with several tens of meters of reverse displacement is detected in the P-3/95 seismic section by Gosar (1996 [29]), but the fault was not confirmed by the group of experts at the WS 2008.
Minor dislocations in Badenian limestone are observed in the P-3-4/95 seismic section (WS, 2008) in the E continuance of the Libna anticline's S limb. The disruptions can be associated also to the offsets at s.p. 525 (Fault 1I cf. Persoglia, ed., 2000, Figure 4-6; WS II 2008) observed in the KK-01/99 seismic section. In this case, the sense of the displacement would fit the geophysical data, and the trend of the fault with downthrown W block would be parallel to the Libna fault (19).
Continuance of the pre-Plioquaternary Libna anticline and the Črna Mlaka syncline across the Orlica fault (2) is constructed according to the Badenian strata dip. The fold axes are displaced in the left lateral sense by app. 100 m (Poljak, 1997a [78]). No Plioquaternary folding is observed in the NW block of the Orlica fault.
Placer (in: Poljak, 1997a [78]) proposed the most comprehensive kinematic explanation of the Libna anticline and the associated structures. Libna anticline is an extremely amplified deformation along the Orlica fault (2). Placer also claims that his kinematic model requires an approximately E – W trending fault in the basement, along which the limestone beds in the S limb of the Libna anticline are bent into a subvertical position (80°).

Krško syncline (g)
Convergent dip of the Neogene strata along the Krško Basin margins suggested the existence of the ENE - WSW trending syncline between Mt. Orlica and Marija Gorica Hills in the E, (Pleničar & Ramovš, 1954 [72]; Šikić et al., 1979 [115]). To the W, the Krško Basin was considered a tectonic graben activated along the E – W faults in Badenian, reactivated in Pontian, and still active in Pleistocene and Holocene (Pleničar & Premru, 1977 [71]). Synclinal structure of the Neogene strata in E part of the Krško Basin was obvious from the seismic sections recorded in 1959 (*cf.* Brezigar, 1993 [9]; Djurasek, 1996 [22]). Šikić et al., (1979 [115]) considered Brezina - Veliko Trgovišće syncline as the NE continuance of Krško syncline.

Krško syncline involves Neogene to Quaternary sediments. The oldest Neogene deposits are of Lower Miocene (Ottnangian) age. Three sub-basins are suggested according to Bouguer gravity anomalies. The two eastern sub-basins are well imaged in seismic line KK-01/99 (Swan et al., 2004, Figure. 4-6). As described by Persoglia (ed., 2000 [60]), the top of Mesozoic rocks are at a depth of more than 2,000 m in the easternmost sub-basin, and at about 1,900 m in the western one imaged in the KK-01/99 seismic section. The top of the Mesozoic rocks rises to about 1,000 m depth across a broad saddle between the two sub-basins. The sub-basins differ by thick middle and lower Miocene sequences in the western subbasin (Globoko Basin), and thick upper Pliocene and Quaternary deposits in the eastern one.
Folding of the Krško syncline started in Pontian as Neogene strata from Badenian to Pontian exhibit relatively uniform thickness across the syncline. The upper part of the Pontian

seismohorizons is pinching out towards the syncline flanks and marks the starting point of the folding (Rižnar, 2005). The inclination of the Plioquaternary and Mid-Pleistocene terrace remnants towards the pre-Quaternary Krško syncline axis in both limbs of the Krško syncline proves the post-Mid-Pleistocene folding of the syncline (Kuščer, 1993 [50];Verbič, 1995 [126]).

The trace of the Krško syncline axis is defined on basis of 7 seismic sections (KK-02/99, P-85/59, KK-05B-00, P-3-4/95, P-86/59, KK-03/99 and P-83/59 *cf* Brezigar et al., 1993 [9]; Persoglia (ed), 2000 [60]; Swan et al., 2004). Between Globoko and Brege villages (2 km SSW of the NPP) the Syncline's trend is roughly N70°E. However, between the KK-05B-00 and P-85/59 seismic lines, its course deviates to N100°E. Further to the SW the axis trace continues in the N50°E direction. As gravimetric data strongly support the course of the syncline axis defined by the seismic lines (*cf* Kranjc et al, 1990 [48]; Brezigar et al., 1993 [9]), its eastward continuance (E of the KK 02/99 seismic line) is defined solely according to gravimetric data.

It is not clear yet whether the anomaly in the course of the syncline axis is a consequence of tectonic activity (plicative or disjunctive deformation) or maybe due to misallocated old seismic section (P-85/59). However, an approximately 700 m right lateral offset is required to compensate the apparent deviation in of the syncline's course if only faulting was anticipated. A set of faults is observed in the KK01/99 section between s.p. 800 and 850 there at depth, but no connection to other structures is interpreted so far.

Šikić et al., (1979 [115]) presented the Krško syncline to be dissected by a **Libna - Šentlenart - Dobova - Zaprešič line.** The line was interpreted as a normal fault of the Quaternary age with downthrown SW block. The fault was marked as active up to the Mid-Pleistocene and therefore covered by Sava alluvial deposits. Brezigar (1993 [9]) considered this fault as "proved with very high degree of confidence". Some contradictory data are cited in the text and the ultimate proof seems the appearance of the fault in Kuščer's (1993 [50]) geomorphologic map, but the fault is not even debated in Kuščer's text. However subsequent studies did not confirm the fault as such..

Geodetic data indicate subsidence of the Krško Basin relative to its rims. Subsidence is larger along the syncline axis and gradually diminishes towards the basin rims. The data indicate a rate of < 1 mm/year for the past 100 years; however, the rate is below the limit of the survey resolution (Swan et al., 2004, Section 4.3.5; Koler, 2008).

Marija Gorica anticline (Figure 20)

Marija Gorica anticline (named after the Marija Gorica Hills in Croatia) is situated along the South-eastern flank of the Krško syncline. Paleozoic clastic rocks covered by Neogene sediments are exposed in its core. Thus it may represent a tectonic block uplifted during the Paleogene or even in the Mesozoic (Swan et al., 2004). To the NE the anticline plunges under the Plio-Quaternary sediments of the large Hrvatsko Zagorje depression. According to Tomljenović and Csontos (2001 [120]), The Northern flank of the Marija Gorica anticline is thrusted to the North.

Brdovec syncline (Figure 20)

Brdovec syncline, named after the Brdovec village, is located between the Marija Gorica anticline and Mt. Medvednica. On the surface it is entirely covered by Plio-Quaternary deposits. As a consequence of North-verging thrusting of the Mt. Medvednica the syncline is overturned in its NE section according to Šikić and others (1979 [115]). According to gravity data the Brdovec syncline as well as the Marija Gorica anticline terminate at the Sava valley

to the SE, as it separates the Marija Gorica hills and the Mt. Medvednica from the Gorjanci Mountains.

Gorjanci Mountains anticlinorium (Figure 20)
This large structure is situated at the Southern margin of the Sava folds. Although Gorjanci Mountains were formerly interpreted as a horst (Pleničar and Premru, 1977 [71]), they may also represent a Southernmost fold of the Sava fold belt, or to be more precise, a large anticlinorium. The Gorjanci Mts. are built of Paleozoic and Mesozoic carbonate and clastic rocks. The Neogene deposits only cover the Northern and the Southern slopes. Paleozoic and Mesozoic strata are folded, faulted, and thrusted following the Dinaric (NW - SE) trend. Unlike the Mesozoic and Paleozoic rocks, the Neogene strata on the slopes dip North to the Krško syncline and South to the Karlovac depression. Neogene strata on the Northern slopes of the Gorjanci Mts. also exhibit gentle secondary folding probably related to Balaton faults.

Anovec syncline (n)
A Syncline named after Anovec village is located between the Krško Hills and the Orlica Mountain. The NW-SE trending syncline is built up of Badenian limestone, with Cretaceous basinal deposits in its core (Swan et al., 2004). Unusual (NW) trend of the syncline axis resembles the pre-Pannonian fold in the upper part of the Dramlja creek (see Orlica anticline section).

Sušica syncline and Bočje anticline (Figure 20)
The folds described in the 2003 PSHA (Swan et al., 2004) were not confirmed in the course of remapping and additional mapping, as some new paleontological evidences aroused. The E - W trending small-scale folds (not presented on the map) still are a fact though (Rižnar, In: GeoZS, 2006b).

Leskovec folded area (j)
Due to North-westerly instead of expected Southerly tilted Plioquaternary surface NW of Leskovec (Kuščer, 1993;Verbič, 1995 [126]), gentle E – W trending *en echelon* folds are interpreted due to left strike-slip activity of the Orlica fault (2) (Poljak et al., 1996b [92]). Trenching revealed that the Plioquaternary deposits in Northern limbs of the two anticlinal folds exhibit Northward tilted sedimentary structures. A lens of clay in the paleosol was found tilted to the North by 8° and a gradation observed in the sand was tilted by 10° to the North in the Northern limb of the anticlinal fold as well (Poljak, 1997b [79]).
We interpret the deformation as *en echelon* folds due to sinistral strike - slip activity of the Orlica fault at depth.

Mraševo folded area (k)
Mraševo area is located NE of Kostanjevica and app. 5 km S of the NPP, at the Southern rim of the Krško Basin. Relatively elevated area is built of the Neogene (Badenian to Pannonian) deposits, covered by the Plioquaternary gravel and pseudogley. The Mraševo area is surrounded by the Upper Pleistocene Sava river deposits to the W, N and NE, and bound by the Krka River to the S.

According to the 1 : 100.000 basic geologic map, Novo mesto sheet (Pleničar et al., 1976 [73] and Zagreb sheet (Šikić et al., (1979 [115]) as well as Poljak et al. (1995 [90]), the area represents an uplifted block bounded by faults.
Detailed geologic mapping of this area (Rižnar, 1998 [108]) and remapping (Rižnar, In: GeoZS, 2006b) did not confirm these faults, with possible exception of the segmented Gornja Pirošica – Izvir fault (34). Different altitudes of the base of the Plioquaternary deposits at the Mraševo area, though, led us to infer on gently folded boundary between the Plioquaternary and Neogene deposits (Rižnar, 1998 [108]). The existence of the folds was only inferred as well as their trend. The area might represent a pendant of the Leskovec folded area (j).

Prilipe syncline (l)
Folds with the generally E - W oriented axes were mapped in the Čatež area in the Neogene deposits, but only the Southernmost one E of the Prilipe is well documented on the basis of the lithologic boundary and sufficient number of dips. Remapping confirmed the E - W orientation of the syncline (Rižnar, in: GeoZS, 2006b).
The folds may be formed as a consequence of the deformation in the shear zone between the eventual E continuance of Poštena vas fault (10) and the Prilipe fault (12)

Koritno syncline (q)
Koritno syncline is a large fold in Badenian limestone, with the NW trending axis. The fold is situated between the two Balaton (NE trending) faults. Folds of the same trend are known Between the Čatež tectonic zone (11) and the Jesenice fault (15). The folds may have been formed between the Riedel type faults due to strike-slip activity of the Balaton faults.

Ribnica folded area (r)
North-east trending small scale Neogene folds are present between the Jesenice (14) and Ribnica (15) faults. The vicinity of the folds (e.g. Koritno syncline) of more or less the same age but quite another trend, is partly in contradiction, but as the youngest deposits are of Badenian age, the temporal subsequence of the folds is anticipated.

Krško Hills anticline (s)
From the morphological point of view, this large and complex E - W trending structure represents the E continuance of the Orlica Mountain range. It could be interpreted as a part of the Orlica anticline as well. The anticlinal structure of the Krško Hills is expressed only in a general sense. Neogene sediments on the Northern and Southern slopes of the Krško Hills have a generally anticlinal form; however, in the central part of the Krško Hills, consisting of the Mesozoic rocks, older NW-SE-oriented Dinaric folds are preserved.
The anticlinal structure is expressed clearly North of the Raka village, where Triassic dolomite outcrops to the surface. Dips in the Triassic dolomite exhibit a Dinaric style of deformation (Poljak, 2001 [84]), however, Cretaceous beds overlying the dolomite are folded in general E - W direction. In addition, an E - W trending South verging thrust is observed. within Cretaceous deposits along the Northern part of the Lokavec creek valley. It was formed simultaneously with the other Neogene structures of this area. According to the geologic maps, some parts of the western Krško Hills are also thrusted to the North. The Southern limb of the anticlinorium is covered by Neogene sediments (Ottnangian to Pontian)

gently dipping to the South and Southeast and make a Northern limb of the Krško syncline (g).

The entire anticline is dissected by faults. The dominant ones are older Dinaric faults (Zagorje (Figure 20) and Hrastnik (Figure 4, Figure 20) showing evidence of reactivation in the Neogene as right–lateral strike-slip faults.

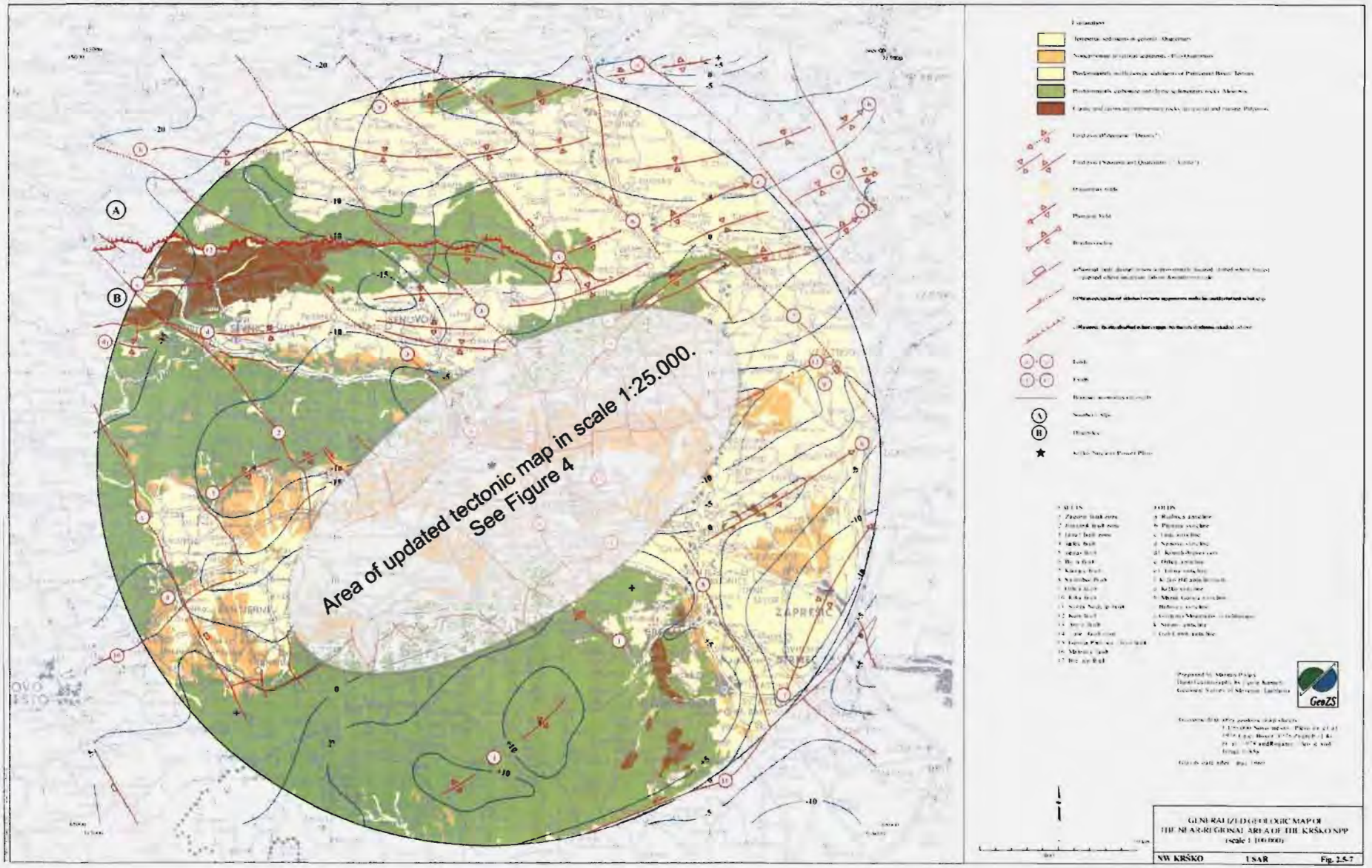

Figure 20 Generalized geological map of the near regional area from 2003 PSHA (Swan et al., 2004). Tectonic map of the Krško basin was updated since and is presented here separately as Figure 4

4.2.2 FAULTS AND FLEXURES

4.2.2.1 FAULTS AND FLEXURES BEYOND THE LIMITS OF THE SITE VICINITY AREA

Zagorje fault zone (Figure 20)

According to its strike and age, the fault belongs to a group of Dinaric structures partly reactivated in the Neogene.

According to Placer (1995 [65]), the fault represents a zone of right lateral strike-slip faults of Neogene age that manifest clearly in the Zagorje coal mine in the Laško syncline. According to other interpretations, the zone is represented by a single fault. Buser (1978 [11]) named it the Kum fault; Pleničar and Premru (1977 [71]) named it the Škocjan fault. The Southern section of this fault zone coincides with the western limit of the Krško Basin as defined by gravity data. If the fault crosscuts the entire Sava folds region from the Sava fault in the Northwest to the Gorjanci Mountains in the Southeast its total length is app. 60 km. However, this is an idealized presentation because on geologic maps (Buser, 1978 [11]; Pleničar et al., 1976 [73]) the fault is not marked as a single line in its entire length. In the Krško Hills, segments of several kilometers can be connected only conditionally. The Southern continuance of the fault beneath the Krško plain to the Gorjanci Mountains is inferred on the basis of gravity data.

Hrastnik fault zone (Figure 20)

According to Buser (1979 [12]) and Placer (1995 [65]), this fault is related to a group of Dinaric faults mapped in the Hrastnik coal mine in the Laško syncline. Buser (1979 [12]) simplifies it as a single fault that extends to the Krško hills, where it represents a significant fault boundary in the Mesozoic deposits. Within the Southern Krško hills, sub-parallel trending Lokavec fault system (17) and Senuša fault (18) approximately 2 and 4 km respectively E of the Hrastnik fault appear to have been reactivated as strike-slip faults in the Neogene.

The total length of the Hrastnik fault from the Sava fault in the N to the Northern margin of the Krško Basin is about 40 km (Poljak, 2000a [82]). However, this is a generalized presentation, as the fault is presented in segments only several kilometers long on the geologic maps (Buser, 1978 [11]; Pleničar et al., 1976 [73]). Only the Southernmost section of the fault South of the Kum thrust is considered in this study. Southward continuance of this fault under the Quaternary sediments of the Krško Basin to the Gorjanci Mountains is uncertain, but as it is not observed in the Kostanjevica area, it is supposed to end at one of the Balaton faults in the Krško basin. For the details regarding the southernmost section of the fault see also Lokavec fault system (17)

The seismicity within the Krško hills is concentrated along the Southern part of the Hrastnik fault in the area where the Hrastnik fault probably steps over into the Lokavec fault system (17).

The parameters for the Hrastnik fault are partly adopted from the 2003 PSHA:
The full length of the fault is 27,8 km.
Two segments are considered:
1) from Kum thrust to Raka: 19,8 km
2) from Raka to the continuance of the Dobe – Rakovnik fault (3): 8 km.

Letuš fault zone (Figure 20)
According to Placer (1995 [65]), this is another NW trending Dinaric fault dissecting the Sava folds. Locally, the fault displaces the Neogene coal-bearing beds of the Laško and Senovo synclines. This fault may extend through the Sava canyon from Brestanica to Krško, based on a fractured zone in the Upper Triassic dolomite (Poljak et al., 1996 [91]). This zone appears to be disrupted by NE-SW-trending faults. Southward, the inferred fault of the same trend is covered by Tertiary and Quaternary sediments.

Žalec fault (Figure 20)
Žalec fault is mapped across the Sava folds region from the Sava fault to the Orlica fault (2) (Buser, 1979 [12]). The fault coincides with a saddle in the gravity data within the Senovo syncline. This section of the fault, approximately 40 km long, disrupts the Paleozoic, Mesozoic, and Tertiary rocks. On geologic maps (Buser, 1978 [11]; Aničić & Juriša, 1985a [3]), it is presented in segments several kilometers long. On the 1 : 100.000 scale geologic map covering the South-western part of the Orlica Mountain range (Šikić et al., 1978 [114]), it is not marked at all.

Žegar fault (Figure 20)
As described by Buser (1979 [12]), this is another Dinaric fault that crossing the entire Sava folds. It displaces the eastern part of the Trojane anticline (North-east of the investigated area). Aničić and Juriša (1985a [3]) mapped the South-eastern continuance of this fault and named it Pilštanj fault. Here, the fault trace is associated with the Bistrica River valley and the eastern rim of the Vetrnik Mountains. The fault exhibits apparent normal character.

Buča fault (Figure 20)
This fault, North of Bizeljsko town was first described by Aničić and Juriša (1985a [3]). It is a right-lateral strike-slip Dinaric fault named after the Buča River N of the Orlica anticline It displaces a part of the Rudnica anticline and the Planina syncline As mapped, this fault continues to the Orlica Mt., but its South-eastern continuance to the Krško Basin is not clear. Its South-eastern extension to the Krško Basin might represent the Bukovje fault (27).

Klanjec fault (Figure 20)
According to the 1 : 100.000 basic geologic map, the Rogatec sheet (Aničić and Juriša, 1985a [3]), this fault extends across the eastern part of the Orlica Mountain range in a NW-SE direction a few km E of the Bizeljska vas village. It may continue South-eastward to the area represented by the 1 : 100000 basic geologic map sheet Zagreb (Šikić et al., 1978 [114]), where it is characterized as a normal fault displacing the Krško syncline axis Based on the gravity data, the fault may continue further to the SE to the Marija Gorica anticline, representing the eastern boundary of the Krško syncline.

Samobor fault (Figure 20)
On the 1 : 100.000 scale geologic maps, the fault is marked along the Sava River from Brežice to Zagreb (Šikić et al., 1979 [115]). According to the authors, the age of this fault is pre-Quaternary. In published literature, this fault is referred to as the Sava fault (e.g., Prelogović et al., 1998 [97]; Tomljenović and Csontos, 2001 [120]), as in earlier PSHA

studies for the Krško NPP (Fajfar and Lapajne, 1994 [24]). However, to avoid the confusion with the regional Sava fault mapped in the Northern Slovenia, this fault is referred to herein as the Samobor fault after the Samobor town in Croatia. Prelogović et al. (1998 [97]), describe the fault as bordering the Southern margin of the Pannonian Basin in Croatia and indicate that it is associated with seismicity. Tomljenović and Csontos (2001 [120]) represent the fault as a NW trending structure approximately 45 km South-east from the North-eastern margin of the Gorjanci Mountains near Brežice. Šumanovac et al., 2009 interpret the Sava fault all the way to Brežice as well, but do not consider it as a Southern margin of Pannonian basin. The geometry and continuity of this fault within the near region of the Krško NPP are uncertain. The formerly inferred segment between Brežice and Krško is not imaged in the KK-01/99 seismic section.
Correlation to the fault observed at s.p. ~ 620 in the KK-01/99 seismic section, however, cannot be precluded. The segment between Bregana and Samobor towns, denoted as two parallel faults by Šikić et al. (1978 [114]), is covered by the Quaternary deposits. According to these authors, both segments terminate to the South at the Sveta Nedelja fault (Figure 20/ fault No.11) along the Southern margin of the Gorjanci Mountains. The location and the extent of the Samobor fault are uncertain. The fault trace shown in the Figure 20 (fault No. 8) is based on the interpretation of gravity data and consists of a single trace, with a general NNW-SSE trend, separating the Gorjanci anticlinorium to the west from the Marija Gorica and Brdovec synclines to the east.

The tectonic model doesn't support the importance of the Samobor fault as the Sv. Nedelja and Zagreb faults are considered a major structure in the Mid-Hungarian Zone. Nevertheless, if the Samobor fault is active, it should be segmented by the Balaton faults. As no new evidence is gathered regarding the Samobor fault it is kept as a seismic source with the same parameters as in the 2003 PSHA (Swan et al., 2004), but assigned only 0,1 weight.

Sveta Nedelja fault (Figure 20)
The Sveta Nedelja fault is located along the Southern margin of the Gorjanci Mts. It is a transversal Dinaric fault by the origin and represents the continuance of the microplate boundary between the Tisza unit and the Dinarides (cf. Brueckl et al., 2008). According to Šikić et al. (1978) the fault has a normal character, while Tomljenović and Csontos (2000) show it as a NE striking basin-margin fault along the Karlovac Basin with a partial South verging thrusting. The seismicity in the fault area clearly indicates its sinistral strike-slip character.
According to the tectonic interpretation of the Alp 07 deep seismic profile (Šumanovac et al., 2009) the fault is bound to the SW by the Southern Marginal Fault of the Pannonian Basin. In our study Žužemberk fault is considered as the marginal fault's surface expression. To the North, the Sv. Nedelja fault is bound by the Sava* fault. The full length of the fault is 50 km .
Sv. Nedelja fault is considered as an active fault

Zagreb Fault
Zagreb fault is not in the 25 km radius and is thus not portrayed on the figure of the extended site vicinity. It is located along the Southern foothills of the Mt. Medvednica. Together with the Sv. Nedelja fault it represents the surface expression of the core of the Mid-Hungarian Zone. According to tectonic interpretation of the Alp 07 deep seismic profile (Šumanovac et al., 2009) Zagreb Fault is bound by the Sava* fault to the SW and Drava fault to the NE. The total length of the 78 km long fault is divided in two segments bound by the Kašina fault.

Southern segment between Sava* and Kašina faults is 24 km long and the Northern one between Kašina and Drava faults, 54 km. The fault between Sava* and Drava faults in the Figure 21 is not Kašina fault and probably merges with the Sava* fault as there is no evidence of Sava trough NW of Mt. Medvednica (see also Bavec, ed., 2010).

*Sava fault in Croatia is not to be mistaken with the Sava fault in Slovenia. In Croatia, Sava fault represents the Southwestern margin of the Sava tectonic through indicated also in the tectonic interpretation of the Alp 07 deep seismic profile.

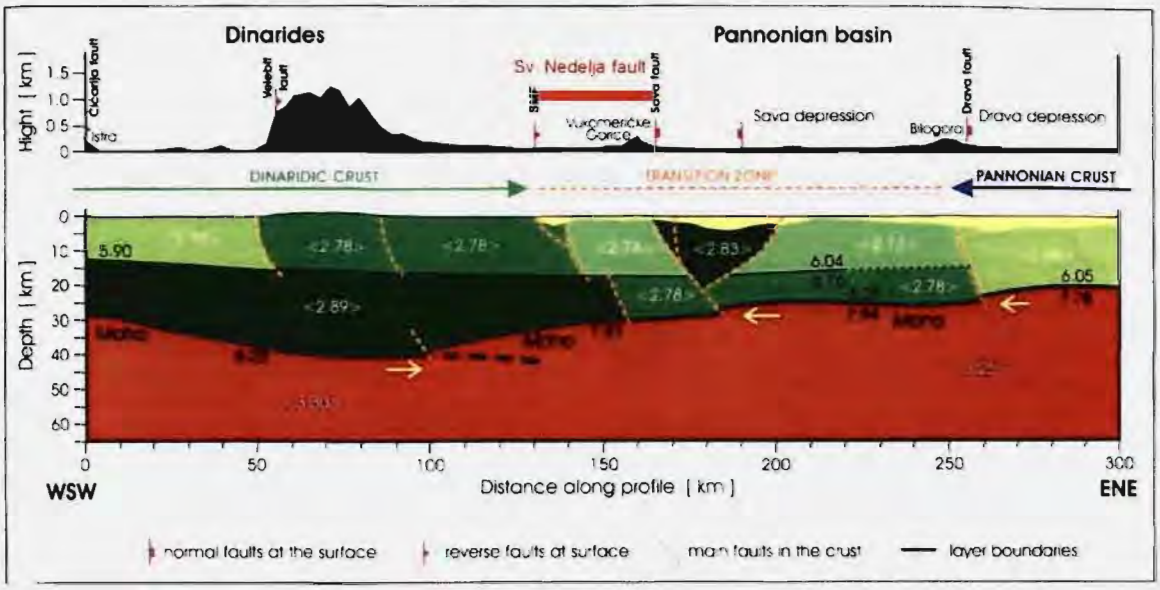

Figure 21. Sv. Nedelja fault boundaries using tectonic interpretation of the Alp 07 deep seismic profile (Šumanovac et al., 2009).

4.2.2.2 FAULTS AND FLEXURES IN THE EXTENDED SITE VICINITY AREA

Faults described in this chapter are those that affect Neogene deposits, crosscut the Dinaric (Paleogene) structures or according to their trend belong to the **Balaton** system of NE trending faults. Annotations refer to the updated tectonic map of the extended site vicinity area (Figure 4).

Grič fault (1)

The fault was mapped for the first time in the 1996 (Poljak et al., 1996b [92]). It is characterized by a broad fractured zone and numerous small scale folds observed in the Cretaceous basinal deposits. Another parallel fault has been mapped in the vicinity, bounding the two cretaceous basinal formations. The fault was inferred on the basis of irregular position of the beds and small scale folds of different trend.

The Grič fault is not observed in the Neogene deposits as it is covered by the Plioquaternary sediments to the SW. Its probable North-eastern continuance across the Sava River is not excluded. The Northernmost structure observed in the KK-02/99 seismic section is ascribed to the Grič fault.

The inferred full length between the Lokavec fault and the Sava River is app. 7 km.

Last observed activity is post-Badenian.

Orlica fault (2)

Orlica fault is a northernmost post-Badenian NE – SW trending (Balaton) fault. It has been mapped NE of Videm along the Potočnica Creek valley. On the Basic geologic map 1 : 100.000 sheet Zagreb (Šikić et al, 1978 [114]) it is shown only as far as Pleterje village as a covered fault.

Placer (1999a [68]) shows the fault on a generalized map as a Northernmost Balaton fault extending along the entire length of the Orlica Mountain range and to the W along the entire length of the Krško basin. Krka fault (Figure 20), as described below, corresponds to the western section of the fault shown by Placer (1999a [68]), but the real SW continuance of the Orlica fault is not certain.

In the recent mapping campaign the Orlica fault was mapped N of the Zdole village where the fault was inferred to continue to the NE into the Močnik gorge (Poljak et al., 1996b [92]), but in the remapping campaign (Poljak, 1997a [78]) it was realized that the fault trace changes its course to the E, North of the Zdole village. In the next mapping campaigns (Poljak, 1999 [81]; Poljak, 2000b [83]) it was shown that Orlica fault turns into an E – W trending reverse fault. This section of the fault is dissected by minor NW – SE trending inferred faults of the apparent left strike-slip character. Southeast of the Sromlje village, the Orlica fault turns into a NE – SW trending fault again (Poljak, compiled geol.map in: Swan et al., 2004).

A NE continuance of the Orlica fault along the Badenian (limestone) / Pannonian (carbonate silt) boundary is proposed as well. Pannonian deposits end up along a very straight line E of the Sromlje village. The fact would not be so surprising if the strike of the Badenian strata along the boundary trace was stable (uniform), which is not the case. Badenian/Pannonian boundary is in fact transgressive, but might be tectonically predisposed by the Orlica fault. The easternmost fault section E of Sromlje village would in that case be of pre-Pannonian age; meaning that in this section Orlica fault is a buried fault (M Poljak, personal communication, 2008).

A deviation of the Orlica fault between the Zdole and Sromlje villages is also followed by a change in a general strike of Neogene/Mesozoic boundary and a fault between the Aptian-Cenomanian/Turonian-Campanian Cretaceous formations.

SW section of the Orlica fault (SW of Sava River) is uncertain as it is covered by the Quaternary and Plioquaternary sediments. The fault trace was inferred along the very straight Plioquaternary terrace section SW of Leskovec (Pleničar et al., 1976 [73]). Kuščer (1993 [50]) inferred subsided NW block along the supposed fault trace due to the eastward tilted Plioquaternary surface SW of Leskovec. Poljak (1997a [78]; 1997b [79]) inferred gently folded Plioquaternary sediments (the Leskovec folded area (j)) with E – W oriented axes SE of the Leskovec village and ascribed them to a post-Plioquaternary sinistral strike-slip of the Orlica fault.

Several fault planes are interpreted in the KK-01/99 and KK-02/99 seismic sections, supposedly belonging to the Orlica fault (Persoglia ed., 2000 [60]). A team of experts revaluated the geophysical and geological data (WS, 2008) and interpreted two faults in the N section of the KK-02/99 seismic line. In the process of building the tectonic model (WS II, 2008), a Southern fault (observed at s.p.250 - 275 in the KK-02/99 seismic section) was interpreted as the Orlica fault, and the Northern one (s.p.225 in KK-02/99 seismic section) as an inferred fault parallel to the Orlica fault. Evidences supporting such an interpretation are the existence of a Grič fault (1), the NE trending fault app. 600 m W of a speedway stadium at Leskovec (Poljak et al., 1996b [92]) and its possible North-eastern continuance, an apparently normal fault of the same trend with subsided S block separating Cretaceous and Triassic rocks North of Videm.

Regarding the flower structure in the W part of the KK-01/99 seismic section (s.p. 1250 - 1350) it is interpreted to belong to the Lokavec fault system (17) or the S section of the Hrastnik fault, respectively. It is assumed therefore, that the Orlica fault actually doesn't propagate across the Lokavec fault system to the SW. A stepover structure is possible though as the Lokavec fault system is deformed.

Last activity: Supposed Quaternary.

Evidences observed:

Orlica fault - NE section

- Fractured Badenian limestone was observed along the Potočnica creek. Left strike-slip character was recognized on basis of analyzed fractures (Poljak, 1994 [74]).
- Sudden change in strike and dip of the Badenian strata was observed at the Stara vas village across the Orlica fault trace (Poljak et al., 1996 [92]; Poljak, 1997a [78]).
- The pre-Plioquaternary Libna anticline (h) and Črna Mlaka syncline (i) axes are dislocated by ~100 m in a left lateral sense across the Orlica fault (Poljak, 1997b [79]).
- There is no proved post-Plioquaternary fold in the NW block of the Orlica fault (Poljak, 1997a [78]).
- Plioquaternary sediments are dislocated across the Orlica fault NE of Krško, suggesting an apparent right lateral displacement or normal fault with subsided NW block respectively (Poljak, 1997a [78]), but no evidence for dislocation of the Badenian / Mesozoic boundary is observed at the same location. The Plioquaternary deposits there might be colluvial (Poljak, personal communication, 2008)!
- According to the geophysical (GPR and geoelectric sounding) and other geologic (mapping) data, the basement of the Mid-Pleistocene terrace remnant in the SE block of the Orlica fault at the Stara vas village is uplifted by app. 5 m regarding the other two terrace remnants in the NW block (Poljak, 1997a [78]).
- Seismic refraction between the two Mid-Pleistocene terrace remnants at Stara vas detected a fractured zone in the Badenian limestone (Živanović et al., 1998 [149]; Živanović, 1999 [148]; Poljak, 1997a [78]).
- No evidence of the Orlica fault in the N part of the P-3-4/95 seismic profile could be detected N of Zdole village due to a poor signal/noise ratio (WS, 2008).

Orlica fault - SW section (W of Krško):

- North-east instead of a South dipping Plioquaternary surface is observed E of the Leskovec village by Kuščer (1993 [50]).
  Gentle E – W trending *en echelon* folds (j) are interpreted EW of the Leskovec village on basis of different altitude of the base of Plioquaternary deposits, and equally trending undulation of the relief (Poljak et al., 1996b [92]). The folds are ascribed to the post-Plioquaternary activity of the Orlica fault. Trenching in the Leskovec folded area (j) revealed that the Plioquaternary deposits in Northern limbs of the two anticlinal folds exhibit Northward tilted sedimentary structures. A lens of clay in the paleosol was found tilted to the North by 8° and a gradation observed in the sand was tilted by 10° to the North in the northern limb of anticlinal fold as well (Poljak, 1997b [79]). Apart from the morphological indicators these two sedimentary features are the only geologic proof of the folds existance. Howevwer, a tilted gradation of the sand layer in the Plioquaternary gravel is rather expected as cross-stratification is a normal

depositional feature in fluvial deposits and as such doesnt prove the strataare actually inclined. The inclined lens of clay in the soil is though more convincing if it can »survive« the pedogenesis. So, the evidence supporting the existance of the folds are rather weak.

- No reflectors could be identified due to a poor signal/noise ratio in the N part of the KK-05A-00 seismic section where Orlica fault trace is expected, (WS, 2008).
- Two North dipping fault planes were identified in the N part of the KK-02/99 seismic section, one between stations 250 and 275 at depth of 400 m and another at the s.p. 200 at the depth of 200 m, both with subsided Southern block. A flexure between the faults is observed, between s.p. 225 and 250 at the depth of 400 m and 200 m respectively in the KK-02/99 seismic section (WS, 2008).
- A flower structure, suggesting a strike-slip fault was interpreted in the W part of the KK01/99 seismic section (Persoglia (ed.), 2000; WS, 2008). Persoglia (ed., 2000) excludes surfacing of these structures according to the KK-HR-02/99 seismic section.

The full length for the Orlica fault is adopted from the previous PSHA (Swan et al., 2004), except for its westernmost section between the Hrastnik (Lokavec) and Žužemberk faults (see Figure 20). The westernmost section of the Orlica fault was the least certain, and it is discarded in the new model as it is interpreted to terminate at the Hrastnik (Lokavec) fault.

The fault's full length is 40 km. It is segmented by a stepover structure. Two segments are considered:

- NE segment between the Sromljica and Krapinske Toplice in length of 24 km
- SW segment between the Močnik and Hrastnik (Lokavec) faults in length of 16 km

Last activity: suspected post-Plio-Quaternary

Rakovnik - Dobe fault (3)

The Rakovnik - Dobe fault is a NE trending fault E of the Kostanjevica town. It cuts the stratigraphic boundary between the Triassic dolomite and the Upper cretaceous carbonate flysch. It is not observed in the Neogene deposits, but nevertheless its trend clearly defines it as a Balaton fault. According to its fault trace it is subvertical fault with apparent sinistral strike-slip character. An anticlinal fold in the Triassic dolomite is present on the both sides of the fault, but its origin is not certain so far as it is observed only in the dolomite.
Last activity: observed only in the pre-Neogene deposits.

Mali Ban fault (4)

Mali Ban is a NE trending fault first presented in this project as well. According to Poljak (this project) it cuts the Badenian limestone W of the Kostanjevica town. North-western block is relatively subsided along the fault. Between the Mali Ban (4) and the Rakovnik - Dobe (3) faults two Riedel type faults with apparent normal character are present
Last activity: mapped post-Badenian.

Kočarija fault (5)

The Kočarija fault is also a NE trending fault. The fault trace to the SW is presented on the 1 : 100.000 geologic map Novo mesto sheet (Pleničar et al., 1976 [73]), but with incorrect

stratigraphic data. Its Neogene activity is only minor (Poljak, this project), but its pre-Badenian character is clearly normal, with relatively subsided NW block. The straight fault trace exhibits a subvertical fault plane.
Last activity: mapped post-Badenian.

Podstrm fault (6)
The fault is shown on the 1 : 100.000 geologic map, Novo mesto sheet (Pleničar et al., 1976 [73]) with a relatively subsided NE block. Its activity is presented as post-Badenian, but no offset is shown. The latest mapping results (Poljak, this project) prove only pre-Badenian activity. Due to Riedel type faults, the sinistral strike-slip character of the fault is inferred. Subvertical fault plane is inferred, based on the straight fault trace.
Last activity: observed only in the pre-Neogene deposits

Žabjek fault (7) and related faults
Žabjek fault is one of the most evident Neogene faults in the N slope of Gorjanci Mts. Pleničar et al., (1976 [73]) interpreted the boundary between the Neogene and the Cretaceous deposits between Kostanjevica and Žabjek village as a segmented fault, along which the Krško tectonic graben has been subsided. Detailed mapping revealed a single NE trending normal fault with a fault trace curved to the North in its Northern section. The absence of the Ottnangian (Lower Miocene) gravel along the fault and the Sarmatian marl in the vicinity of the fault S of the Slivje village, but above all the curvature of the fault, together with the supposed sinistral strike-slip activity of the Balaton faults, led us to infer on normal character of the Žabjek fault.
A small scale NW trending with apparent dextral strike-slip character is inferred to dissect Žabjek fault SE of Kostanjevica.

Evidences observed:

- Carbonate silt outcrops along the boundary with the Mesozoic deposits instead of Neogene basal conglomerate (Rižnar, 1999[109]).
- At Kolarica (app. 500 m SW of Žabjek) a set of fractures was observed in the marl of the Veliki Trn formation (110/50, 20/m). Only 300 m to the NE, a similar set of fractures has been observed in the old trail (now only a ditch, few m deep) in the Neogene carbonate sandy silt (120/45, 30/m) (Rižnar, 1999[109]).
- The fault was only traced from Žabjek to SW of Slinovce first (Rižnar, 1999 [109]), and later all the way to Nova gora hilloc (Rižnar, in: GeoZS, 2006b), where it seems displaced for app. 150 m in an apparent right lateral sense along the NW - SE trending line. As there was no outcrops in the area the line was thought to represent an erosional boundary between the Cretaceous and Neogene deposits at first (Rižnar, 1999[109]), but the intensive landsliding lead us to believe that the area NW and W of Nova gora hilloc is not built of Cenomanian - Turonian pelagic carbonate and marl (Krško formation), but rather of the Neogene carbonate silt (*cf.* Rižnar, 2005) as landslides are more frequent in such lithology.

Last activity: post-Sarmatian.

Studena fault (8)
The Studena fault is presented on the 1 : 100.000 geologic map, Novo mesto sheet (Pleničar et al., 1976 [73]) as a photogeologic fault. Studena creek springs from the fault zone. A fault

plane (340/80) is observed E of the Studena spring, but no offset was detected in the W section of the fault. In the E section, the fault exhibits a normal character with subsided N block. Its continuance into the Neogene deposits is not certain.
Last activity: observed only in the pre-Neogene deposits, suspected post-Sarmatian.

Oštrc fault (9)
Oštrc fault, named after Oštrc village is shown on the 1 : 100.000 scale Basic geologic map of SFRJ, sheet Novo mesto (Pleničar et al., 1976 [73]) as a fotogeologically observed fault representing tectonic boundary between the Lower Cretaceous platform carbonates and the Upper Triassic dolomite.
During the latest mapping campaign, it was shown that the fault represents a tectonic boundary between the Dachstein limestone and relatively uplifted Upper Triassic dolomite NE of Oštrc village. The fault continues to the NE where predominantly reverse character of the fault is observed. as the Aptian - Cenomanian Flishoid formation is relatively uplifted along the fault trace. The fault can be traced all the way to the Sušica creek SE of Podbočje village. The Neogene/Mesozoic boundary is covered by the alluvial deposits, along the right bank of the creek, but dips in Badenian limestone are not uniform, so the fault was probably still active in Badenian. No dislocation of the Plioquaternary/Neogene boundary was observed in the Dobrava area (Rižnar, in: GeoZS, 2006b).
Last activity: post-Badenian.

Poštena vas fault (10) and related parallel folds
The fault is shown on the Basic geologic map of SFRJ 1 : 100.000 sheet Zagreb (Šikić et al., 1978 [114]) as an inferred normal fault. In fact two sub-parallel NE trending faults were inferred as margins of a small scale tectonic graben. Detailed mapping confirmed the existence of the Northern fault and revealed the anticline in the NW and a syncline in its SE block. The fault zone is observed in a small quarry 200 m SW of the Poštena vas village (Verbič & Rižnar, 1997 [131]; Rižnar, 2005). The NE-trending Poštena vas fault exhibits an apparent minimum 500 m of right-slip displacement of the Neogene/Mesozoic boundary. As the fault plane has a dip of 60ş to the NW and is situated between the synclinal and anticlinal folds, a reverse character is proposed. The most of the displacement is therefore attributed to the NE verging reverse motion, but the observed sub horizontal trending fault plane undulation reveals the strike-slip character of the fault as well.

Evidences observed:

- The NW - SE trending Poštena vas fault is situated between the post-Sarmatian syncline and anticline proved by the course of the Neogene/Mesozoic boundary and a number of observed strata dips in Neogene deposits (Verbič & Rižnar, 1997[131]; Rižnar, 1998 [108]; Rižnar, 2005; Rižnar in; GeoZS, 2006b).
- A fault zone (315/60) where a undulated fault plane was observed with slickenside indicating also a strike-slip character of the fault in a small abandoned quarry 200 m SW of Poštena vas village,
- The E continuance of the Poštena vas fault is observed between Hrastek and Črneča vas villages where complex reverse fault with uplifted N block is apparent (*cf.* Rižnar in: GeoZS, 2006b).
- At the Črneča vas village a sinistral strike-slip is observed along the fault.

- SE of the Črneča vas, the fault is traced to the Črešnjevec pri Oštrcu village where it represents a tectonic boundary between the Triassic dolomite in the SE block and the relatively subsided limestone in the NW one. The fault trace turns S there (*cf.* Rižnar, in: GeoZS, 2006b) forming a horse splay.

Last activity: post-Sarmatian.

Čatež zone (11), and parallel faults in the Neogene deposits

Čatež fault, as it was presented in the 2003 PSHA (Swan et al., 2004), is discarded. The remapping (Rižnar, 2006) showed that the zone has a Balaton trend. The relevant part of this tectonic zone is composed of three NE trending faults in the Badenian and Sarmatian deposits South of Mrzlava vas. The faults are 250 to 400 m apart and are defined upon the inconsistencies in the dips of the strata across the faults and morphologic criteria. Offsets of the Badenian/Sarmatian boundaries has not been observed, but are only inferred. Due to their weak definition, only one of the faults (the one in the middle) is presented in the tectonic model as the Čatež fault. None of these three post-Sarmatian faults propagate far to the SW. To the NE, only the South-easternmost of the three post-Sarmatian faults is inferred to continue all the way to the boundary with the Quaternary deposits. We have got no information regarding the continuance of these faults below the Quaternary deposits, and the fault has not been observed in the KK-03/99 seismic section.

As the Čatež tectonic zone is a complex structure, and has been addressed in the previous PSHA (Swan et al., 2004) study, the extended description of the zone is given here.
Šikić et al. (1978 [114]) and Premru (1982) considered the Triassic dolomite and a part of the Jurassic deposits fringing the dolomite in the NE Gorjanci Mts. as a (Goli Cirnik) nappe, thrusted upon the Cretaceous flyschoid deposits from the NE, but the detailed mapping did not confirm this thesis (Verbič & Rižnar, 1997 [131]; Rižnar, 2005). The Čatež zone was introduced in order to emphasize the actual absence of the decollement *sensu* Šikić et al. (1978 [114]). It is in fact a zone of vertical tight folds North of the NE trending reverse fault along which the Triassic dolomite is uplifted SE of the Mrzlava vas village. This reverse fault is the core of the Čatež tectonic zone and is covered by the Ottnangian and younger deposits. The original age of the Čatež tectonic zone is therefore pre-Ottnangian (Lower Miocene). This zone (and the reverse fault between the Triassic dolomite, and the Jurassic and Cretaceous basinal deposits) is cut by the Malence fault (30) in the Sarmatian, and a few other minor faults, one of them exhibiting an apparent dextral strike-slip character. The three NE trending parallel faults, just a few hundred m South of the core of the Čatež tectonic zone also exhibit a post-Sarmatian age, but the Malence fault is not observed S of these three faults.
West of the Malence fault, the tight folds in the Cretaceous flyschoid deposits are bent to the North in the area of at least 2 by 3 km. Bending of the fold axes indicate the pre-Sarmatian sinistral strike-slip activity of the zone.

Other less relevant features concerning justification of the Čatež tectonic zone is that the strike of the Triassic dolomite bedding and the reverse fault along the dolomite make app. 30°, while to the E the folds and lithostratigraphic boundaries in the basinal deposits are parallel to the strike of the dolomite. This, among other indications is why we consider the Čatež tectonic zone not to continue along the boundary between the Triassic dolomite and basinal deposits, to the S (see tectonic map), but rather parallel to the Poštena vas fault (10). As the Čatež fault was not observed there, due to homogenous lithology and sporadic outcrops, it is not marked SE of the Gornja Pirošica – Izvir fault (34).

The Čatež tectonic zone is a set of NW trending faults, and as such has the capacity of the sinistral strike-slip character. However, following the trend of the Brežice structure observed in the KK03/00 seismic section, and approaching the Southern limb of the Krško syncline, we interpret that the fault zone is adopting an E – W direction and thus exhibits a reverse character there. The interpretation is supported also by the seismicity.
A cluster of seismic events at depth of 5 to 10 km are observed in the Čatež tectonic zone area, but due to relatively high frequency of Balaton faults there, the seismicity can not be attributed to any single fault. For this reason the whole cluster of seismicity is treated as a single seismic source (see Appendix 3 - Seismic source models). The length of the cluster (10 km) is taken as seismic source length. Its depth was taken from the catalogue (Živčić et al., 2010) as the shallowest and the deepest event (5 to 10 km). Also the dip is taken from fault plane solution (60°).

Evidences observed:

- There is a constant ~ 30° angle between the strike of the dolomite strata and the trace of the Čatež zone defined by fold axes trend (Rižnar, 2005). This fact makes the zone superimposed to Dinaric Goli Cirnik anticline (f).
- Deformed basinal deposits ($J_{2,3}$ - K_2) are observed in the erosional window at Čatež as well as some poor outcrops of the T dolomite, suggesting a continuance of the Čatež tectonic zone beneath the Neogene deposits there and confirming its Balaton orientation.
- NW - SE trending Malence fault (16) active during Sarmatian, dissected a pre-Ottnangian (Northern) part of the Čatež tectonic zone. At that time, the Malence fault was active as a normal fault with downthrown E block (Verbič & Rižnar, 1997 [131]).
- A reverse fault, representing the oldest part of the Čatež tectonic zone is displaced for app. 100 m along another NW - SE trending fault W of Mrzlava vas (Verbič & Rižnar, 1997 [131]; Rižnar, in: GeoZS, 2006b).
- SW continuance of the Čatež tectonic zone has not been observed due to monotonous lithology.
- Sub-vertical faults have been observed S of the Mrzlava vas in the Badenian and Sarmatian limestone. The existence of the faults between the Sobenja vas and Mrzlava vas villages is not questionable, but their exact character has not been proved but rather inferred upon the field data.

Last activity: post-Sarmatian.

Goli Cirnik fault (12)

Goli Cirnik fault, named after the Goli Cirnik hill, is mapped in the recent remapping campaign for the first time. The fault is a NE trending structure, But its post-Neogene activity can not be assesses, as it is only traced in the Mesozoic rocks. According to its straight fault trace, it is inferred as a subvertical fault with supposed sinistral strike-slip character.
Well expressed Riedel type faults with relatively subsided western blocks are observed in the South-western section of the fault. the Riedel type faults have sigmoidal fault traces and lead us to infer on the sinistral strike-slip character of the Goli Cirnik fault.
Last activity: observed only in the pre-Neogene deposits.

Koritno fault (13)

The Koritno fault is a NE trending fault. Badenian deposits are dissected along the fault. The South-eastern block is relatively subsided. Due to a small NW oriented fold in the NE section of the fault, the sinistral strike-slip character is inferred as well.
Last activity: post-Badenian.

Ribnica fault (14)
The Ribnica fault is also a NE trending Balaton fault . It has a straight fault trace, and cuts off the Neogene deposits. Due to the Riedel type faults the sinistral strike -slip character is inferred, but in the SW section also normal component with subsided SE block is observed.
Last activity: post-Badenian.

Jesenice fault (15)
The Jesenice fault is the Southernmost observed Balaton fault presented on the map. Poljak (this project) shows a small scale offset proving the sinistral strike-slip character of the fault. Small scale folds in the Badenian limestone parallel to the Ribnica and Jesenice faults versus other orthogonally oriented folds in the same deposits are not clear, but may prove subsequence of the transpressional and transtensional regime.
Last activity: post-Badenian.

Artiče fault (16)
According to its E – W to SW-NE trend, Artiče fault was considered as one of the Alpine structures. In earlier studies (e.g., Šikić et al., 1978 [114]; Poljak et al., 1985 [89]) the fault was described as a normal fault. The Artiče fault is recognized from both geophysical data (Persoglia, 2000 [60]; Section 4.3.1), geologic mapping and inferred from the boreholes data from the Globoko mine area (Poljak et al., 1985 [89]; Poljak, 1999 [81]). Interpretation of numerous boreholes drilled in the Globoko area, in the framework of coal exploration, shows that the fault was active during the deposition of the coal-bearing beds of the Pontian age. Increased thicknesses of the beds South of the fault (Poljak, 1999 [81]), suggests synsedimentary activity.
The fault is best imaged in seismic lines KK-03-99 and KK-HR01-99 (Persoglia, ed.,2000 [60]; Figures 4-8 and 4-11) approximately 2 km west of Globoko. At this location the seismic profiles clearly show a North-dipping reverse fault that displaces the Mesozoic/Neogene boundary at depth and extends up through the entire Neogene section toward the surface as a zone of deformation between s.p. 640 and 685 (line KK-03/99). Stratigraphic and morphologic observations at this location suggest latest Pleistocene (Würm) or Holocene surface deformation (Swan et al., 2004; Verbič, 2005).
Total length of the Artiče fault is uncertain. Persoglia ed., 2000[60]) infers the fault trace from seismic line KK-03/99 across the P-84/59 to the P-3/95 line near the Sava River Southeast of NPP Krško to a distance of approximately 5 km. The fault is interpreted in lines P-84/59 and P-3/95. As noted in Persoglia ed., 2000 [60]), deformation appears to decrease to the West, and is absent West of the P-3/95 line. Based on surface mapping, Placer (in: Poljak 1997a [78]) infers the western continuance of the fault along the Southern flank of Libna Mountain North of the Krško NPP. A similar post-Pliocene fault was considered on Basic geological map (Šikić et al., 1978 [114]). However, there is no evidence for the offset of this fault, larger than the resolution of the P-3/95 seismic section, being app. 10 - 15 m there. The latest set of HRS seismic profiles (2008 and 2009; this report) do not confirm the existence of the Artiče flexure nor fault along the Libna Mt. foothills. Minor deformations observed at the foothills of

the Libna Mt. belong to Libna and Stara vas faults. Quaternary activity of the Artiče fault is inferred upon morphologic anomalies observed in the Sromljica alluvium at Dečno selo (Verbič, 2005).
Artiče fault may be a part of a zone of reverse faults continuing eastward into Croatia (Figure 4-16). A North-dipping reverse fault is imaged in the N-S seismic reflection profile in Hrvatsko Zagorje basin to the East (Tomljenović and Csontos, 2001 [120]). The authors consider this fault to be related to the Late Pontian to recent shortening, showing it as a 30-km-long reverse fault extending from near Krško to the eastern end of the Hrvatsko Zagorje basin (Figure 4-16). Detailed mapping performed in Krško Basin indicates that the surface trace of the Artiče fault is fragmented and its connection to the reverse faults reported by Tomljenović and Csontos is uncertain.

Evidences observed:

- Approximately 800 m wide flexure is imaged, from the constructed contour maps drawn on the basis of the reinterpreted borehole logs data (Poljak, 1999 [81]).
- Presumably Pleistocene to Holocene lymnic and fluvial fine-grained sediments (silt, clay and sand) are interchanging with paleosol horizons, proposed as Dobrava alloformation by Verbič, (1995 [126]; 2005) South of the flexure, while only several m thick layer of noncarbonate gravel is found N of the flexure.
- Despite other interpretations, vertical displacement of the base of the Plioquaternary across the Artiče flexure is approximately 120 m (Poljak, 1999 [81], Swan et al., 2004).
- A 300 to 400 m of apparent left lateral displacement of the Artiče flexure along Sromljica fault (21) is interpreted according to the shift of the flexure from the contour maps based on the borehole logs data (Poljak, 1999 [81]).
- The evidence of Artiče flexure is fading W from the Sromljica fault according to analysis of borehole logs (Poljak, 1999 [81]). Westward continuance of the flexure is only followed as far as Močnik alluvium (Poljak, 1999 [81]).
- Apparent dextral displacement of the flexure along Gabrnica fault (22) is inferred on field mapping and boreholes data, following the Pontian/ Plioquaternary boundary, but the contour maps do not allow reliable interpretation there (Poljak, 1999 [81]).
- The eastward continuance of the flexure between Gabrnica (22) and Trsnjak (23) faults (creeks) is observed in the field as a subtle increase in the basement and the upper surface dip of the of the Plioquaternary gravel as well as the paleosol (upper surface) covering the gravel, from sub-horizontal up to 5° to the S (Poljak, 2000b [83]).
- Artiče flexure is imaged in the KK-03/99 and KK-HR-01-99 seismic sections (Persoglia ed., 2000 [60]; WS 2008). An observed steep S verging reverse fault is interpreted as **Artiče fault**.
- W continuance of the Artiče flexure along the Mt. Libna Southern slope was suggested by Placer (in: Poljak, 1997a [78]), but no field or any other evidence was given so far to support the hypothesis.
- Some minor displacements are observed in the Badenian horizons in the E continuance of the Libna anticline in the P-3-4/95 seismic section (at s.p. ~340 of the P-3-S/95 seismic section) where the W continuance of Artiče flexure might be expected (WS 2008; WS II, 2008). On the other hand, the continuance of the Artiče flexure or fault would be expected more to the South, and not near the hinge of an anticline.
- Artiče fault was interpreted as a continuance of the reverse faults from Hrvatsko Zagorje (Tomljenović & Csontos, 2001 [120]), but the field evidence has shown that

Artiče fault is segmented and its intensity fades to the E as well as to the W (Poljak, 2000b [83]; Swan et al., 2004).

- Morphometric analysis (this project, 2008) showed an amplified recent uplift exactly in the Globoko area in the E – W morpho-structural cross section in the hanging wall along the Artiče fault. The intensity of the uplift fades to the E as well as to the W.
- USA model (in: Swan et al., 2004) and Verbič (2005) suggested westward continuance of Artiče fault S of the NPP, based on the increased slope in the Quaternary deposits SW of the Leskovec, but revaluation of the seismic data did not confirm the existence of the S branch of the Artiče fault (WS, 2008).
- Verbič (2005) is explaining the flexure's Holocene activity with the subtle change in the slope along the Sromljica alluvial plane.
- The latest HRS profiles across the southern flank of the Libna anticline did not confirm the continuance of the Artiče flexure nor fault to the West along the southern flank of the Libna anticline

The main issue concerning the Artiče fault is its continuance to the Orlica fault and its trace and character to the NE. From the DEM, the trace of the fault is adopting NE (Balaton) trend and consequentially probably also sinistral strike-slip character. The curvature of the fault trace to the E appears where it approaches the Krško syncline axis. This is why we think that the E - W trending section of the Artiče fault and the Krško syncline are related. Therefore it seems reasonable that the structures would stay parallel. Due to the 30° angle between the Libna anticline and the Krško syncline axes, the continuance of the Artiče fault along the Libna anticline does not seem probable.
Two alternatives are kept in the study as far as the western continuance of the Artiče structure is concerned. The more radical alternative considers the continuance of the Artiče fault all the way to the Orlica fault along the Libna anticline. Total length of the fault is 24,3 km, taken from the 2003 PSHA (Swan et al., 2004), but only 0,2 weight is assigned to this option. As this option is not confirmed by the latest HRS profiles between the Sava River and Libna foothills, reducing the weight of the option may be appropriate (in the future).
The more probable alternative is that the full length of the fault is 12 km between the Močnik fault 1 (20) and the NW trending fault along the Sotla alluvial plane. The 0,8 probability is assigned to this alternative as a most proved one.
The segment between the Sromljica (22) and the Močnik 1 (20) faults is considered as a rupture length for two reasons. The the two faults appeared as the deepest ones in the KK-01/99 seismic section and as such they are considered as the ones that might act as the most probable barier (taking into account that the potential of the fault is related to their length and depth). Other faults apear to be even shallower than Artiče fault, and thus less likely to act as a segment barrier. Apart from this fact the evidence of the Artiče fault's activity is in general observed only between the Sromljica (22) and Močnik 1 (20) faults

Last activity: post-Plioquaternary, suspected recently active.

Lokavec fault system (17) – Southern section of the Hrastnik fault
Lokavec fault system is composed of the 3 faults roughly parallel to the regional NW trending Dinaric Hrastnik fault (Figure 7). The faults are mapped in the Badenian and Cretaceous deposits, but to the South they are covered by the Quaternary alluvium. Vertically displaced Cretaceous beds are observed along the northernmost fault in the N section of the Lokavec

Creek valley, and horizontally displaced the Neogene deposits in the Southern part. Relatively subsided E block is observed in the Badenian deposits along the middle fault of the Lokavec fault system, and just tectonized Badenian rocks are found along the N section of the southernmost fault. The three faults are connected to the three fault planes, observed in the large flower structure in the W section of the KK-01/99 profile. The fault system is extended to the northernmost evidence of the Balaton fault (the continuance of the Rakovnik – Dobe fault (3)).

An original Dinaric reverse or normal fault observed in the Mesozoic deposits was obviously reactivated during the Neogene as an apparent dextral strike-slip fault in the Badenian deposits in the case of the northernmost fault of the Lokavec fault system. It could be inferred that the Lokavec fault system was also active during or after the Plio-Quaternary. The area E of the Northern fault is characterized by Plio-quaternary deposits, which are absent West of the fault system. This means that: a) the western terrain represented a highland supposedly caused by faulting during the deposition of Plio-Quaternary sediments, or b) Plio-Quaternary sediments were deposited on both sides of the fault and were subsequently eroded from the western block due to the relative uplifting (vertical faulting) of the western terrain. Relatively subsided E block is inferred. However, both hypotheses are relevant only if relatively flat basement of the Plio-Quaternary deposits is supposed.

There is an evident cluster of seismic events along the Northern section of the Lokavec fault system, located around the fault trace bend. The fault plane solution in the cluster shows a North verging reverse fault, which may be due to the curvature of the otherwise right-lateral strike-slip fault.
The Lokavec fault system is considered as a Southernmost section of the Hrastnik fault addressed in the 2003 PSHA (Swan et al., 2004) as an active fault. The grouped seismicity along the Lokavec fault system and the post-Badenian activity of the Hrastnik fault are the reasons to keep the Lokavec fault system (as the Southernmost section of the Hrastnik fault) as the seismogenic fault.
The full length of the Lokavec fault system is 8 km between the Raka village and the extension of the Dobe - Rakovnik fault (3).

Evidences observed:

- Badenian/Ottnangian boundary is displaced for app.100 m in the right lateral sense along the Northern fault of the system. NW - SE trending fault zone is observed in Badenian limestone (Poljak, 2001[84]).
- The faults are covered by alluvial deposits to the S and their fault trace there, shown on the 1 25.000 compiled geologic map (Swan et al., 2004), has no other confirmation.

Last activity: post-Badenian, suspected post-Plio-Quaternary.

Senuša fault (18)
Senuša fault exhibits almost the same characteristics as Lokavec fault (17). Quaternary activity is inferred on different elevations of Plio-Quaternary sediments on each side of the fault. Plio-Quaternary sediments to the West are found at a higher elevation then those on the east. This condition suggests either a highly differentiated relief during deposition of the above-mentioned sediments, or post-sedimentary differentiation (tectonic) of the relief. However, the difference in elevations of these sediments also could be caused by a strike-slip displacement along the fault.

Last activity: suspected post-Plio-Quaternary.

Libna fault (19)

NW – SE trending fault across Mt. Libna was first defined as a covered normal fault with subsided NE block on the Basic geologic map 1 : 100.000 sheet Zagreb (Šikić et al., 1978 [114]). Placer (in: Poljak, 1997, [78]) described several parallel fault planes of the same trend in the S limb of Libna anticline. The fault dissecting the Plioquaternary sediments is named Libna fault and is not to be mistaken with the disproved reverse Libna fault in the N limb of the Libna anticline (Placer in: Poljak, 1997, [78]) defined by Verbič (1995 [126]).

The fault boundary between Plioquaternary gravel and Badenian limestone at the crest of Mt. Libna is suggesting that the Libna fault, along with the Libna anticline, might have been active during the deposition of the Plioquaternary gravel already. The fact, that not all the fault planes from the observed NW – SE trending Libna fault zone dissect the Plioquaternary boundary, implies that the Libna fault was formed together with the Libna anticline before the deposition of the Plioquaternary sediments and that only one fault plane of the Libna fault have been reactivated later (Placer in: Poljak, 1997, [78]). A probable continuance of the fault is interpreted in the S1 (Brenčič, ed., 2006) and KK-01/99 seismic sections as well as in the P-3-4/95 seismic section (this report). Libna fault is imaged as a subvertical E dipping normal listric fault in the KK01/99 seismic section (Persoglia ed., 2000 [60]) probably defining western border of the Globoko sub-basin. Paleoseismological survey (trench) has been performed app. 1 km NE of the NPP to investigate the eventual Quaternary activity of the fault (see Appendix 1).

In the latest set of HRS profiles measured in 2008 and 2009, between the Sava River and Libna syncline Libna fault was confirmed and interpreted as a strike-slip fault (this report).

Evidences observed:

- Repeated remapping in 2006 revealed a single 150 – 300 m wide fault zone (GeoZS, 2006a) instead of multiple discrete faults proposed by Placer (in: Poljak, 1997, [78]). One of its western fault planes exhibits normal character with subsided NE block and cuts off the Plioquaternary sediments on the top of Mt. Libna (Placer in: Poljak, 1997, [78]). The offset may be between 20 to several tens of meters but the mode of deposition of Pl,Q or "Pl,Q-like" deposits on both walls of the fault is not clear. Sediments may belong to different river terraces (*cf.* Bavec, 2003).
- The anomalies related to the SE continuance of Libna fault were interpreted in extreme N part of the N – S trending S1 seismic section (GeoZS, 2006a), but the seismic line is discarded by the team of experts (WS 2008) as not relevant due to poor quality of the data.
- Horizontal laminae were observed in the core of the VOG-1 borehole drilled in the fault zone in the Upper Miocene deposits. Considering prevailing South-eastward dip of the strata, observed in the in the construction pit for the NPP, the subhorizontal laminae imply presence of a structure E of the borehole (GeoZS, 2006a).
- Some plicative deformation are interpreted in the Badenian strata in the KK-04-00 seismic section, where the supposed SE continuance of Libna fault is crossing the seismic line (Persoglia ed., 2000 [60]).
- Another argument for the SE continuance of the Libna fault is a normal fault observed at s.p. 625 with subsided N(E) block, interpreted in the KK-01/99 seismic section (WS, 2008). Interpretation of the individual seismohorizons offsets is inconsistent (Persoglia, (ed.) 2000 [60]) though.

- The uppermost part of the KK-HR-03-99 seismic section does not allow interpretation of the supposed SE continuance of the Libna fault observed in the KK-01/99 section due to low signal/noise ratio..
- Holocene sand was geophysically interpreted to be under the Holocene gravel in the KK-HR-03-99 seismic section (Persoglia ed., 2000 [60]), but VOG-1 borehole data (~700 m W from the fault intersection with the KK-01/99 line) showed that there is more than 100 m of the Plioquaternary deposits under approximately 10 m of Holocene ones.
- Subhorizontal slickenside and scour marks are observed in the Miocene deposits just beneath the Quaternary gravel in the trench in the Libna fault zone (see Appendix 1 - Trench report).
- New seismic lines (this project) have proven univocally the existence and geometry of the Libna fault.
- Geophysical survey on Mt Libna located the line of main deformation (this project).

The Libna fault was mapped as a normal fault, due to the difference in the altitudes of the Plioquaternary deposits on the crest of the Mt. Libna, but the trenching across the fault revealed its strike-slip character. In the tectonic model, the Libna fault is acting as a CCW rotating fault due to the sinistral strike-slip activity of the Balaton faults that constrain it.
To the NW it is limited by the Orlica fault, and to the SE by the supposed line connecting the normal faults observed in the P3-4/95, KK-05/00 and KK-02/99 seismic sections. An 80° dip is adopted for the fault from the KK-01/99 seismic section. The length of the fault is thus app. 5 km. The Libna fault is not segmented.
As such, the Libna fault is considered a structure along which different ammount of plicative deformation has been compensated in the proces of Libna anticline folding (see chapter 4.2.1). Libna fault is considered structurally unimportant as it is a fault in the Libna anticline being a second order structure along the Orlica fault.

Last activity: post-Plio-Quaternary.

Močnik fault 1 (20) and Močnik fault 2 (21)
A NW trending normal fault with downthrown W block along the upper Močnik creek was inferred by Šikić et al. (1978 [114]) on basis of anomalous course of the Pannonian/Plioquaternary boundary.
According to a detailed mapping, Močnik fault 1 (20) is an inferred NE trending fault based on an unreliable displacement of the Pannonian/Pontian boundary across a 50 m wide alluvium and the outcrops being 250 m apart (Poljak et al, 1996b [92]). Interchanging of the sand and carbonate silt appear between the Pontian sand and the Pannonian carbonate silt E of the fault, that additionally complicates positioning of the boundary in the field. The fault trace is covered by the Late Pleistocene to Holocene alluvial and colluvial deposits in its entire length. Considerable anomaly in the course of the well traceable lithologic boundaries (Mesozoic / Neogene as well as Badenian limestone / Pannonian-Sarmatian carbonate silt, and base of Plioquaternary gravel) is obvious in the junction area of the Orlica and Močnik fault traces between the Zdole and Zg. Pohanca villages (see geologic map), but no disjunctive deformation could be proved in the field.
A steep W dipping normal fault with considerable offset in Ottnangian, Badenian and Sarmatian horizons is observed in the KK01/99 seismic line. Only minor offsets of the same character is interpreted in the Pannonian and Pontian horizons up to the erosional unconformity at app. 0,2 s (*cf.* Persoglia, (ed.), 2000).

Another anomaly ascribed to the Močnik fault 2 (21), at s.p. ~400 in the KK-01/99 seismic section was detected but the offsets are poorly interpreted (*cf.* Persoglia, (ed.), 2000). This anomaly was linked to the Močnik valley in the NNW direction without any other evidence.

Evidences observed:

- Badenian/Pannonian boundary could not proved as displaced along the fault trace according to mapping data (Poljak et al, 1996b [92]).
- No difference in altitude of the Plioquaternary basement is observed across the Močnik fault (Poljak et al, 1996b [92]).
- On the 1: 5000 map, significant differences in altitudes of the Plioquaternary deposits in the E block of the fault, even N dipping boundary is observed at Arnovo selo.

Last activity: Pannonian/Pontian in the Seismic section, suspected post-Plio-Quaternary.

Sromljica fault (22)

The NNW trending fault was introduced by Šikić et al. (1978 [114]) as an inferred normal fault with subsided E block, displacing Artiče fault (13) in the left lateral sense by 300 - 400 m. Marin et al, (1989) interpreted it as a strike-slip fault with vertical offset, and Verbič (1995 [126]) interpreted it as a wrench fault with subsided W block. Verbič also reports that the surface E of Sromljica creek is steeper than on the W side. Horizontal displacement of Pontian coal bearing beds is demonstrated based on analysis of borehole data from the Globoko area (Poljak, 1999 [81]. On the basis of the same data, the fault also horizontally displaces the Artiče fault in a left-lateral sense. The fault trace is covered by Holocene alluvium in its entire length. The inferred fault trace was linked to a well imaged W dipping normal listric fault with downthrown W block interpreted in the KK-01/99 Seismic line at s.p. 280 (*cf.* Persoglia, (ed.), 2000). The fault is considered as an antithetic normal fault in the Globoko (sub)basin of the Pontian age.

Evidences observed:

- Offset of the Artiče flexure across the Sromljica alluvium (Poljak, 1999 [81]), is supported by the offset of base of Plioquaternary deposits as much as 500 m on the distance of 800 m. Different tilt of the upper surface on each side of the fault is suggesting a wrench fault with the rotation axis parallel to Artiče flexure (16) (Poljak, 1999 [81]).
- 300 to 400 m of apparent left lateral displacement along the Sromljica fault is interpreted according to the shift of the flexure from the contour map based on the borehole logs data (Poljak, 1999 [81]).
- Probable S continuance of the fault is imaged at the s.p. ~280 in the KK-01/99 seismic section as a normal fault with downthrown W block is interpreted by Persoglia ((ed), 2000 [60]).
- A possible indication of the fault is bending of the 300 m altitude isoline of the base of Plioquaternary deposits to the N. The opposite situation is observed in the N part of Močnik fault trace. The isoline is bending the same way as the Badenian / Sarmatian-Pannonian, and Mesozoic / Neogene boundaries in the Sromlje village area.

Last activity: suspected recently active.

Gabrnica fault (23)

Gabrnica fault along lower Gabrnica Creek valley is inferred by Poljak (1999 [81]). The fault trace is covered with Holocene alluvial deposits in its entire length. The existence of the fault

is supported by the fact that it represents an E margin of a coal bearing strata in Globoko basin, hence the Pliocene activity of the fault is supposed to be as a normal fault with relatively downthrown W block. Neogene strata appear to be horizontally displaced along the fault, but Verbič (1995 [126]) suggests that the apparent horizontal displacement is due to vertical activity of the fault. This premise is supported by the fact that the Plio-Quaternary sediments are at different elevations on each side of the fault, which might be caused by differential uplifting of tectonic blocks as well, followed by erosion. In this case, the age of the fault would be Quaternary. The fact, that the premise considering relatively downthrown W block in the Pontian, and the different altitudes of the Plioquaternary gravel on each side of the fault, are apparently in collision can be explained by a small scale inversion in the Plioquaternary, due to rotation of the blocks in the transpressive regime.
The fault is linked to a poorly defined anomaly at s.p. 150 in the KK-07/99 seismic section (*cf.* Persoglia, (ed.), 2000).

Evidences observed:

- Upper and main lignite measures units exhibit an apparent left strike-slip across the Gabrnica fault with up to 100 m dislocation according to the data obtained from the boreholes in the lignite mine area (Poljak, 1999 [81]).
- Plioquaternary deposits reach the altitude of 310 m W of the Gabrnica creek, while to the E they are found only as high as 260 m. Poljak, (1999 [81]) interprets this anomaly as a fault evidence.
- No displacement of the lithologic boundaries was observed mapping the surface along the fault trace (Poljak, 1999 [81]).
- Possible S continuance of the fault is imaged at s.p. ~130 in the KK-01/99 seismic section as a normal fault with downthrown W block (Persoglia (ed), 2000 [60]).
- One of the most convincing evidences supporting the existence of a fault is a 40° difference in the strike of the bedding in the Pontian sand on both sides of the fault.

Last activity: suspected recently active.

Trsnjak fault (24)
Normal NW trending covered fault with subsided W block is shown in the Basic geologic map of SFRJ 1 : 100.000 sheet Zagreb (Šikić et al., 1978 [114]) on the basis of apparent dextral shift of the Plioquaternary/Pontian boundary W of Pišenbreg. Poljak (2000b [83]) also infers the fault with an apparent dextral offset along the Trsnjak creek valley. Plioquaternary deposits that are considerably lower on the eastern side of the Trsnjak creek indicate horizontal or vertical displacement of tectonic blocks and consequentially differential erosion. Plioquaternary sediments E of Gabrnica Creek valley belong to the Sotla River facies of Plioquaternary age (Verbič, 1995 [126]), that slightly differs from the Sava facies occupying most of the Krško basin. This suggests there was synsedimentary (Quaternary) activity of the Trsnjak fault.

Evidences observed:

- Dextral strike-slip is interpreted along the Trsnjak fault as the Plioquaternary deposits reach significantly higher in the SW block than in the NE one (Poljak, 2000b [83]).

Last activity: suspected post-Plio-Quaternary.

Dramlja fault (25)
A NW trending photogeologic fault with downthrown E block was shown along Dramlja creek valley by Šikić et al. (1978 [114]).The same fault is inferred by Poljak (2000b [83]) as

well, but only along the Southern, NW trending section of the valley. The fault is covered by Holocene alluvial deposits and separates areas with different altitude of Plioquaternary sediments (Poljak, 2000b [83]), suggesting its Quaternary activity. Normal fault with downthrown W block is apparent due to lower base of the Plioquaternary deposits in the W block of the fault.. The fault is located at the Northeastern edge of the Krško basin and is considered as an antithetic normal fault in the Globoko basin imaged at the E section of the KK01/99 seismic line.

Evidences observed:

- Plioquaternary deposits (as well as their base) are app. 15 m higher on the E side of the Trsnjak creek than on the W side (Poljak, 2000b [83]).
- Pl,Q gravel is observed in the escarpment in the W block of the Dramlja fault while the Pontian marl is cropping out under the same (Pl,Q) gravel in the E block, suggesting downthrown W block (Poljak, 2000b [83]).

Last activity: post-Plio-Quaternary.

Sušica fault (26)

Sušica is a NNE trending Neogene fault along the Sušica Creek valley. It is covered by Holocene alluvial sediments. Mesozoic Deposits as well as Badenian and Sarmatian deposits are displaced along the fault, but not the Pannonian ones. Apparent dextral offset or adequate subsidence of the W block should be considered, as no structural elements were observed in outcrops.

Evidences observed:

- Offset in Mesozoic and Neogene deposits is mapped by Poljak, (2000b [83]).

Last activity: pre-Pontian.

Bukovje fault (27)

The Bukovje fault, along with the Sušica fault, represents the eastern and western boundaries of an uplifted tectonic block of Mesozoic rocks on the Southern slopes of the Orlica Mountain range. Mesozoic rocks west of the Bukovje fault are uplifted relative to the Neogene sediments east of the fault (Poljak, 2000b [83]).
Last activity: post-Sarmatian.

Bizeljsko fault (28)

According to the geologic map sheet Rogatec (scale1:100,000; Aničić and Juriša, 1985a [3]), this fault lies along the entire Southern slope of the Orlica Mountain range. Detailed geologic mapping of this area at a scale of 1:5,000 (Poljak, 1999 [81]) indicates that the fault is a North-verging, NE trending reverse fault. It is exposed in the Mesozoic rocks and covered by the Neogene ones. The fault is restricted to the tectonic block bordered by the NW trending Sušica (26) and Bukovje (27) faults. Bizeljsko fault is considered to be formed in a compressional regime during an initial stage of the Krško basin forming prior to deposition of Badenian sediments. The fault is disrupted by a series of small scale NW trending faults of Neogene and post-Neogene age.
Last activity: pre-Neogene.

Orehovec - Kostanjevica fault (29) and parallel faults in its vicinity

The fault was defined on the 1 : 100.000 scale Basic geologic map of SFRJ (Pleničar et al., 1976[73]) as a covered fault without a defined character. The fault was shown as dissected by a NNW - SSE trending photogeologic fault. According to the latest detailed mapping data, the NNE trending fault bounds the uplifted dolomite of the Mt. Opatova gora to the E and the Cretaceous basinal deposits covered by Neogene ones to the W. The fault was traced from the Studena creek SE of Kostanjevica, to the steep slope app. 1 km S of the Orehovec village. Several fault planes (270/70-90) were observed only at its Southernmost section.

Orehovec - Kostanjevica fault is considered as one of the three sub-parallel faults forming an E boundary of the releasing band (small scale pull apart basin) due to a left lateral strike-slip activity in the area. Subsequent CCW rotation of the faults was proposed due to left strike-slip activity (Swan et al., 2004; Rižnar, 2005).

Last activity: post-Badenian.

Malence fault (30) and parallel faults in the area

Malence fault, defined as a photogeologic fault by Šikić et al. (1978 [114]) is considered as a Paleogene structure (Swan et al., 2004) dividing the collapsed anticline crest, characterized by North-dipping dolomite, from the South-western limb, and the anticline, which has a constant dip to the Southwest. Verbič and Rižnar (1997 [131]) described it as a post-Badenian fault having normal or apparent normal character. The fault was reactivated initially during the Neogene as a N-S-trending synsedimentary normal fault of Sarmatian age having down-to-the-east displacement. NE trending axes of folds observed in the Cretaceous basinal deposits change their trend to NW in the vicinity of the Malence fault, suggesting its CCW rotation and consequential right lateral strike-slip (Rižnar, 2005) considering the overall sinistral strike-slip character of the Mid-Hungarian zone. Possible deformation of the middle Pleistocene terrace near Velike Malence suggests that the fault may have been reactivated as a right-lateral strike-slip fault, at least locally, (Swan et al., 2004).

Evidences observed:

- A fault zone (70/70) is observed at the Mrzlava vas village (Verbič and Rižnar, 1997 [131]). The fault is dividing Cretaceous and Neogene deposits along the E slope of the Globočec valley.
- Thickness of the Badenian limestone is considerably reduced in the W block of the fault.

Last activity: Sarmatian.

Ključe - Črneča vas fault (31)

Only a short section of this fault is shown in the 1:100.000 basic geologic map sheet Novo mesto (Pleničar & Premru, 1977 [71]) between the Balaton faults. The reverse fault with SW vergence is defined by a tectonized boundary between the Upper Triassic dolomite covered by the Upper Cretaceous Krško formation in the hanging wall, and the dark micrite limestone (Upper Triassic to Lower Jurassic) in its footwall at the Ključe village. The fault zone **(50/70)** is observed in the outcrops at the Ključe village and at the S part of the valley, app. 300 m SE from the Ključe village (Rižnar, 1999[109]). Between the Oštrc and Črneča vas villages it is characterized by the Upper Triassic dolomite in its footwall and coarse grained breccia of presumably Albian-Cenomanian age. The fault plane **(30/60)** is observed there (Rižnar in: GeoZS, 2006b).

The Ključe – Črneča vas fault is deformed and dissected by the Balaton faults at the Ključe village, NE of Oštrc and at Črneča vas, to the SE in segments of 1 - 2 km long. To the SE,

Ključe - Črneča vas, the fault was mapped 400 m SW from Vrbje village along Sušica creek, where the Upper Triassic dolomite is thrusted upon the limestone **(90/60)** the same way as at Ključe village (Rižnar, in: GeoZS, 2006b).

Krško fault (32)

The Krško fault is a very gently SE dipping (20 - 30°) reverse fault observed on the both sides of the Sava River near Krško town. To the N and to the S it is cut off by the NW trending normal faults. The origin of the fault is not certain.
Last activity: pre-Badenian.

Gornja Pirošica-Izvir fault (33)

Šikić et al. (1978 [114]) show a NW-trending photogeologic fault in the Triassic dolomite SE of Izvir village, and a covered and partly observed fault between the Izvir and Pirošica villages. Another fault, characterized as active up to the Middle Pleistocene is shown parallel to it as well.
According to its trend, the Gornja Pirošica – Izvir fault is probably one of the Dinaric faults, but it is obviously dissected as its trace is deformed along the NE trending (Balaton) faults. Detailed mapping and remapping of this structure showed that there is a fault zone S of the Izvir village. A deep straight gorge is cut in the Triassic dolomite there. However, the fault is dissected as the straight gorge abruptly changes its course approximately 800 m SW of the Globočice village at the junction with the Čatež tectonic zone (11) and the inferred continuance of the Poštena vas fault (10). NW of Krška vas village, the Gornja Pirošica - Izvir fault was only inferred because a complex Čatež tectonic zone (11) continues across the inferred fault trace there. No offset of any structure could have been proved along the Gornja Pirošica - Izvir fault trace. At the D. Pirošica village, the fault defined by Šikić et al (1978 [114]) turned out to be a normal lithologic boundary between the Aptian-Cenomanian basal breccia and overlying fine grained red and grey clastites (Rižnar in: GeoZS, 2006b).
Kuščer (1993 [50]) shows a possible post-Plio-Quaternary fault in NW continuance of the Gornja Pirošica-Izvir fault, projecting it into the Krško Basin. Verbič and Rižnar (1997 [131]) identified an apparent down-to-the-east step in the Middle-Pleistocene terrace, consistent with the apparent displacement of the Plio-Quaternary sediments (Swan et al., 2004, Section 4.3.3). The continuance of the fault under the Krško basin may correlate with the fault imaged in the KK-01-99 seismic section at s.p. 875. As the fault is dissected by the NE trending Balaton faults, it is very unlikely, that its trace would reach the KK-01/99 seismic line undisturbed.
Last activity: pre-Neogene where mapped.

Brežice structure (34)

"Brežice fault" as a NNW - SSE trending normal fault along the W margin of the Brežice terrace (Šikić et al., 1978 [114]) was disproved by Kuščer (1993 [50]), and this fault is not to be mistaken by the E- W trending Brežice fault from the 2003 PSHA (Swan et al., 2004).

The controversy of the "new" Brežice fault has been discussed in Swan et al., 2004 (Rev. 1, p. 35). Brežice – Koprivnica fault (zone) was proposed by Prelogović (1996 [96]) based on his interpretation of the P-3-4/95 seismic section, where numerous N verging reverse faults were interpreted in the S limb of the Krško syncline, and South verging reverse faults were interpreted in the N part of the seismic section (N limb of the Krško syncline). The

discrepancies among different interpretations (Gosar, 1998 [30]; Djurasek, 1996[22]) of the same seismic sections and later interpretations of the KK-02/99 and KK03/99 seismic sections (Persoglia ed., 2000) did not support Prelogović's argumentation. Brežice fault in Croatian 2004 model is in fact the extrapolation of Brežice – Koprivnica fault interpreted in seismic sections in Hrvatsko Zagorje basin (Tomljenović & Csontos, 2001[120]) 40 km to the E. Recent activity of the Brežice – Koprivnica fault in Hrvatsko Zagorje Basin was again interpreted by Prelogović (1998 [97]) based on morphology and association of seismicity and fault plane solutions consistent with the reverse displacements. Northward tilt of the Brežice terrace was associated with the »blind« Brežice thrust (Gosar, 1998 [30]).
Verbič (2005) explained Brežice fault as a complex extensive reverse structure in the S limb of the Krško syncline (g) with the main (northern) branch situated 500 - 1000 m S of the Krško syncline axis. The main branch was inferred to decline to the SW and turn into a sinistral strike-slip fault app. 2 km NW of Kostanjevica. Southern branch was located at Šentlenart. Backthrust faults were inferred as well: one between Brežice and Čatež and the other app. 500 m S of the main branch. Morphologic and borehole data were used in the interpretation. After revision of arguments we partly agree with this interpretation yet we dispute the parts of interpretation that infer Quaternary deformation related to this structure.

Revision of the geophysical data gave the following result. A significant bulge is observed in the Southern limb of the Krško syncline between s.p. 475 and 500 of the KK-03/99 seismic section. The bulge includes three consecutive flexures in the Badenian seismohorizons, fading towards the surface. Two southernmost flexures are shown on the tectonic map. According to the KK-03/99 seismic section, the Brežice flexure is a North verging structure. Very weak evidence of similar structures as in the KK03/99 seismic section was observed in the old P-84/59 seismic section. Although it was decided not to use the old seismic sections for other purposes than to locate the Krško syncline, the observations are conditionally included into the data set. The connection of the described features is parallel to the Krško syncline. To the East, the disturbance of the Badenian reflector is observed in the P-3-4/95 (s.p.740) and KK05-00 (s.p. 475) and KK-02/99 (s.p. 450) seismic lines. All the disturbances are of the same character (subsided northern block).
Considering the connection of the selected disturbancies observed in the seismic section into a single line and connecting it to one of the Balaton faults in the Kostanjevica area may seem a simple solution and has been debated during one of the workshops. But as the seismic sections are 3 to 5 km apart, it is difficult to connect them undoubtfully into one single structure, especially because there are at least 5 Balaton faults in the Kostanjevica area are less than 1 km apart. Therefore, connecting the most obvious deformation into one single line (Brežice flexure), leads to a very radical model driven solution. Structures observed in the southern limb of the Krško syncline in the KK-03/99 seismic section may a well correspond to the folds (t) observed in the P-3-4/95 seismic section and continue to the Žabjek (7), Studena (8) and Oštrc (9) faults. The disturbancies at s.p. 740 (P-3-4/95) just S of the Krško syncline axis, the disturbance at s.p. 475 (KK-05B/00) and the possible flower structure at s.p. 450 - 500 (KK02/99) are connected and may continue into one of the Balaton faults W of the Kostanjevica town. However, ascribing all these observations to one single (Brežice) structure does not seem realistic, taking into account high frequency of parallel faults in the Kostanjevica area.
Last activity: Lower Pontian reflectors are flexured in the KK-03/99 seismic section.

Stara vas fault (35)

After the acquisition of the new HR seismic profiles, a previously unknown fault was found crossing the proposed E site (Figure 4, Figure 6). A (most probable) negative flower structure is observed on 08K-4 and shown as a gentle flexure on seismohorizon B of 08K-3. It can not be traced due South or East - no deformation is observed either on 08K-10b or 08K-9. However, the structure can be traced due NW, where it is recognized on 08K-8 and may potentially also be linked to gentle flexures observed on 08K-5 and also on KK-04-00 (not above seismohorizon B). In the KK-04-00 seismic profile the structure is very weakly expressed around CDP 320 and was not described in previous interpretations.

Stara vas fault is interpreted as a strike-slip fault zone parallel to the Libna fault. It is relatively poorly expressed and limited due South but may extend further toward the NW to the Orlica fault (Figure 6). It was mapped within the Badenian limestone at Stara vas (Poljak, 1997b [79]. A fault plane was observed there with a dip 70/80 (azimuth 160°, dip 80° NWW) and slickenside dipping 30°SE.

No deformation on this structure was observed extending above Miocene strata. In addition, the deformation dies out on the site itself and is therefore treated as tectonically and seismotectonically less important.

4.3 MORPHOMETRIC ANALYSIS OF THE SITE VICINITY AND NEOTECTONIC IMPLICATIONS

4.3.1 DATASETS

The morphometric analysis is made using a Digital Elevation Models (DEM) of the region, whose analysis is coupled with geomorphologic, geologic and earth-observation data (aerial pictures). The pixel size of the Slovenian DEM is 12.5m, whereas the (briefly) analyzed Croatian DEM has a 25-m pixel. The covered surface is 1400 km^2. Morphotectonic analysis was conducted by IRSN (Baize, 2008) and is presented here in full.

4.3.2 METHODOLOGY OF ANALYSIS

We calculated from the DEM various parameters dealing with relief and drainage network. We report conclusions arising from local slope and exposition, which give regional characterization of the morphology. Topographic sections are automatically elaborated with the DEM and their analysis is combined to geological and geomorphologic data. Then, slope change can be used as a relevant indicator of vertical movements along faults or folds. A large set of parameters are calculated after extracting and ordering the drainage network (Strahler, 1957) and defining the drainage basins: the hypsometric curve and integral of drainage basins, the local drainage density and the asymmetry of drainage network.
All these parameters are commonly used in morphotectonic studies; hypsometry, asymmetry and slope indices are often considered as the most relevant parameters to point out neotectonic activity (e. g. Merrits and Hesterberg, 1994; or Burbank and Anderson, 2001 for an overview). These cited studies also clearly state that these descriptive parameters must be controlled by detailed geological knowledge. For representation we use ArcGIS 9.2 while for morphological analysis we used MorphoDEM, a routine developed by the IRSN and the University of Strasbourg.

4.3.3 MAIN MORPHOLOGIC FEATURES OF THE AREA AND THEIR RELATION TO TECTONIC STRUCTURES

The NPP is located along the Northern rim of the Sava River, inside its current alluvial plain. In Krško city, the Sava River is entering the subsiding syncline that runs in a N60-70° direction (the so-called Krško syncline), after cutting the Krško and Orlica uplifted hills (Figure 22).
According to the geological and morphological data, it is clear that the flat area surrounding the NPP (Figure 22 Sava plain) was originated by Sava River divagation during Pleistocene to historical times, before the canalization of the Sava River for NPP building. Aerial pictures and DEM show significant curvilinear scarps and lineaments that correspond to abandoned meanders (Figure 23). In this flat area, the outcropping sediments are fluvial deposits. The ages of these deposits range from Middle Pleistocene to Historical. They cover Neogene layers (up to Plio-Quaternary Globoko formation). There is a gap in sedimentary record, between 1.5 Ma (suspected age of the youngest deposits of Globoko formation) to 150 000 y (oldest deposits of the known fluvial sequence) (Verbič, 2005). The rest of the flat area of the Krško syncline is constituted of Pleistocene lacustrine to alluvial sediments (Dobrava and Krakovski plains). Figure 23 shows the "Holocene" alluvial plain where recent sediments (supposed age < 15 ky) cover Neogene and Pleistocene deposits. The sediments excavated during the Stari grad trench (this project) emphasize the youth of the deposits overlying the

Neogene basement in the plain, as their age is between 400 and 200 years old. The trench has been dug at the Northern red-dotted line of the Figure 23, and it clearly shows that the "scarp" is not a tectonic one as suggested by the figure legend, but that it is a sedimentary feature like the other scarps of the plain.

The depression of Krško, taken as a whole from Novo mesto district to its Croatian continuation, coincides geographically with the pre-Tertiary basement isolines (deduced from gravimetric and seismic data) and with the Tertiary fold axis (Gosar et al., 2005; Gosar, 2008). In addition to the main syncline axis, the revision of the existing seismic lines (this project) leads to the conclusion that other structures exist beneath the Sava-Dobrava-Krakovski plains), consisting of slight inflexion and flexures of the Neogene layers which seem to stretch along a NE-SW to ENE-WSW direction. The relief of Orlica hills is driven by tectonic features, like the Orlica anticline and the Orlica fault. This fault clearly cuts the Miocene and Pliocene deposits, and seems to offset the post-Pliocene fold axis in the Libna hill area. The highest parts of the Orlica hills coincide with the oldest series (Triassic), in the axis of the anticline. The Krško hills are the western continuation of the Orlica hills and they are also folded. To the east, in Croatia, the anticline is gently bent into an EW direction.
To the South, the Gorjanci hills are part of a WSW-ENE elongated ridge. This is structured by NE-SW to ENE-WSW folds and faults that are related to the Balaton system, expressed in Croatia by the Zagreb and Sveta Nedelja faults. This Balaton system is also known as the Mid-Hungarian Line that separates ALCAPA and Tisza units, two microplates or megablocks that show quite different constitution and that underwent differential histories during Neogene times (Bada et al., 1999; Brückl et al., 2007). In addition to the post-Badenian Balaton folds and faults, some "Dinaric" directions (NW-SE) are also mapped. The Gorjanci hills are abruptly disrupted by the Sava course and, to the East, this large anticlinorium continues by an anticline implying post-Badenian layers (Marija Gorica anticline).

According to Placer (1998), all these structures (except Medvednica Mts.) and related relief belong to the Sava folds, which form a triangular wedge pinched between the Alpine block (to the North), the Adria block (to the west) and the Tisza block including the Medvednica Mts. (to the east). A recent evaluation tends to ascribe them to the Mid-Hungarian tectonic zone (Swan et al., , 2004, Figure. 2-3).

4.3.4 GENERAL MORPHOMETRIC PARAMETERS OF THE AREA

The general morphometric parameters are graphically presented in Figure 24.
The local slope is calculated by derivation of the Krško area DEM (pixel 12.5 x 12.5 m), with the existing tools in ArcGIS. This calculation highlights the geomorphologic and lithological units:
1) Very low slopes (0-5%) for the Pleistocene and Holocene alluvial plains;
2) Low to moderate slopes (5-30%) for the Plio-Quaternary plateaus but also the surrounding hills;
3) High slopes along the main valleys incising the hills, but also for the Northern part of the Neogene plateau of Artiče. There, a clear change in slope values is associated with a lithological change, from Plio-Quaternary coarse deposits to Pontian marls.

The local slope parameter drastically emphasizes the major fault and fold lines that are suspected to have been active in Neogene times. The Orlica fault and the Artiče flexure appear more like boundaries between zones with different slope pattern, than linear features associated with a local slope increase due to local tectonic offset. The reasons for that are (1)

these structures delimitate various lithological blocks, (2) the relief has been largely incised and almost balanced, (3) the offset may be too small and resolution may be insufficient. The rapid changes in local slopes are a proxy for "roughness" evaluation. (Roughness is defined as the ratio between real and planimetric surfaces.) It seems particularly high within the Orlica fold and fault area, above all where the basement is constituted of Triassic rocks. Roughness is also high in the Northern part of the Artiče plateau which might be compared to a kind of badlands (basement of marls sharply dissected). The exposition of pixels is estimated for each pixel (12.5 x 12.5 m) of the DEM and it corresponds to the azimuth of its slope. It has a bimodal distribution around the N120-150° and N300-330° classes. These correspond to hillslopes driven by NE-SW elongation of relief, in accordance with the dominant structural direction (Orlica fault, faults of the Gorjanci hills).

The examined drainage parameters are the drainage density and the hypsometry, which are coupled in the interpretation. These 2 parameters are often used as neotectonic markers, even if they may also be controlled by other criteria. (The hypsometric parameter is, with stream slope changes and basin asymmetry, one of the most cited as a relevant index for neotectonic activity.)

The drainage density is defined as the ratio between length of drains and surface area. In our case, it is calculated from the drainage extraction of the 12.5m-DEM, for cells of 100x100 pixels.
The hypsometry is performed for 3rd and 4th order watersheds (according to the Strahler, 1957). Here we present the value of the integral of the hypsometric curve that displays the fraction of noneroded relief of the drainage basin.
Thanks to these 2 parameters, we can clearly distinguish 2 morphometric units: the Neogene plateaus that have high drainage density and low hypsometric integrals (orange to red colors on figure 25, values between 0.3-0.45) and the Mesozoic ridges that have moderate drainage density and high hypsometric integrals (pink-violet colors, values higher than 0.5). This inverse relation between the 2 parameters has been observed and related to the relative maturity of watersheds in the singular morphological context of badlands (Schumm, 1956). The higher the hypsometric integral is (and the drainage density low), the more the watershed is "immature". Despite the more complex character of Krško basin geomorphology, we interpret in the same way the observations, even if we know that the lithological variations are partly responsible: the (Orlica-Krško-Gorjanci) hills have immature watersheds, although the (Artiče) Neogene plateaus have mature watersheds. Considering the relative position of the watersheds with respect to the base level (Sava river), this would mean that the denudation behaves like a head-ward propagating incision that has still not reached the valley heads.

The variation of the morphometric parameters, examined at a regional scale, cannot be univocally associated with recent vertical displacements due to faults or folds because:

- Lithological conditions cannot be discarded as the major controlling factor of these variations,
- Recent displacement rates are expected to be lower than the vertical incision and headward erosion rates, and then can easily be overwhelmed by them.

Considering the main issues of the GG&S project ("seismotectonic model and calculation" but above all "capable fault"), we focus on the singular Artiče area and its lateral continuations. We try to describe and interpret local and specific changes as vertical offsets of thalwegs or surfaces, derivation of streams, etc...

4.3.5 FOCUS ON THE NORTHERN PART OF THE KRŠKO BASIN

In the Artiče area, the deformation of Plio-Quaternary deposits has already been demonstrated in previous studies (Poljak, 1999; Markič and Rokavec, 2002; Verbič, 2005). Even if poorly supported by geological data, the previous US seismotectonic model (Swan et al., 2002) has pointed out the possibility of the continuation of the fault beneath the site vicinity. The high resolution seismic survey performed within this project (this report) ruled out the possibility of the Artiče fault on site and at near site vicinity. The proximity to the NPP of the nearest section of the mapped Artiče flexure anyhow requires necessary detailed paleoseismological investigations. A potential site for geophysical and trenching survey is the alluvium of the Sromljica creek. In addition, Verbič (2005) reports also morphological anomalies in the Leskovec area (western rim of the Sava River), which are linked according to him to Artiče flexure/fault continuation. We thus extend the investigation a little bit to the west (Figure 25 and Figure 26). On the Croatian side, the DEM (25m of resolution) allow us finding surface indices of the possible continuation of the Artiče structure (as suggested by Tomljenović and Csontos, 2001 [120]).

4.3.5.1 MORPHOMETRIC ANALYSIS OF THE ARTIČE FLEXURE

The Artiče flexure is ENE-WSW structure, which was first deduced from borehole data Poljak, 1999). It has been correlated with the linear scarp that bounds to the North the Dobrava plain. At the Sromljica mouth (in the Dobrava plain), the scarp and the flexure are located right above a reverse offset of the buried Badenian layers, as shown on the KK 03 seismic line (at ca. TWT 1.5 s). The Artiče flexure is mapped by Poljak (1999) and is disrupted by several perpendicular faults (this report; Figure 4). It seems that this structure is critically segmented in strands of a few kilometers. We analyze this topographic anomaly thanks to transversal (streams and basin divides) and parallel profiles.

Transverse profiles and activity of the Artiče flexure

Stream elevation and slope profiles are commonly used in morphotectonic studies as an indirect approach to vertical displacements. Stream-gradient indices (SL) are also reported. SL is given by the relation SL=D.(dh/dl), where (dh/dl) is the local slope and D the distance to the basin divide. SL is a good proxy for stream power which should remain nearly constant for a graded stream in an homogenous basin and is such a useful parameter for morphotectonic studies (Burbank and Anderson, 2001) to display the anomalies. We examined elevation, slope and stream-gradient index profiles for 3 main streams cutting transversally the scarp (Figure 27). The 3 cases are clearly not completely graded streams. There is a geographic correlation between slope and stream-gradient index increase with the studied feature. For the 3 streams, the slope is decreasing (10-15% to 1-2%) from the basin divide over distances around 4000 m, and the stream-gradient index decrease from 80-150 to 40-60. Concerning the Gabrnica and Sromljica creeks, the 2 parameters then increase slightly (slope from 1 to 2-5%, SL from 30 to more than 50) when passing through the Artiče flexure and entering the Dobrava plain. Concerning the Močnik creek, the indices also increase, but first crossing the Orlica fault and the associated lithological change from limestones to marls. Then, they slightly decrease until they increase again when passing through the Artiče flexure. Each stream crosses and strongly incises the Artiče plateau. When crossing the Artiče scarp, the Gabrnica and Sromljica creeks immediately enters the Dobrava depression (z=160

m) with an almost null incision and maybe aggrading above the top surface of the plain. The case of Močnik creek seems quite different. When crossing the Artiče structure, it directly joins the current Sava plain (i.e. regional base level), which is lower (z=150 m) than the Dobrava plain surface.

An increase in slope (thereafter called knickpoint) and a change in stream gradient index may be due to several causes like, among others, tributary confluence, lithological variation or headward migration of incision due to a base level change. The first cause can here be easily ruled out. The second cause should be possible because of the contact between Plio-Quaternary coarse deposits and the Pleistocene fine sediments. However, it is discarded because of the absence of such slope change in similar context for the Senuša and Velikovaški creeks (see Figure 28, where the referred contact is underlined by the red dot). The base level change is thus the most probable cause for the gradient-index and slope changes. We support the hypothesis of a base level drop due to tectonic uplift of the Artiče plateau because of the geographical link between the 3 (slight) knickpoints and the flexure and scarp locations. This also suggests that headward erosion is not completely done and then that this movement is quite young or still active. Concerning the Močnik stream, the abrupt increases of stream-gradient index are interpreted by (1) the effect of Orlica fault and/or its lithological change (Figure 27, distance 6000 m), and (2) the probable effect of the Sava River base level that probably caused enhanced vertical incision.

Derivation of the drainage network and lateral evolution of cumulated uplift

For asymmetry parameter, we first made a quantitative estimation based on Cox (1994) method. This automatic application using DEM calculates the values with reference to the "main" stream in the sense of Strahler ordering, i.e. the highest order stream whose definition only depends on upstream topology and confluence pattern. This definition of "main" stream is here not relevant in terms of morphotectonic analysis. To analyze the topography of the Artiče area, we chose to work with the streams representative of the regional slope from the NNW to the SSE (from Orlica hills to Dobrava plain) and then perpendicular to the Artiče flexure. The outlined streams (Figure 25), which are considered as "reference streams" (RS), are underlined in bold blue. We then define the asymmetry in a qualitative way, by estimating the number and length of secondary streams (SS) on each side in the watersheds.
The Figure 29 shows an outstanding trend in the pattern of the drainage network of the Artiče plateau: from west to east, the left-side tributaries (i.e. the eastern ones) are systematically longer than the tributaries from the right-side (western ones). This pattern is observed for each watershed, from Libna basin to Dramlja basin. This deflection of the flow towards the west for each watershed is suspected to correspond to a
differential vertical movement, i.e. tilt of surface topography. This was demonstrated or suggested for some cases in low deformation rate area with active faults of poor surface expression (e.g. Cox, 1994; Carozza & Baize, 2005). We suggest that the drainage basins of the Artiče plateau underwent a differential uplift from east to west during the vertical incision of the local network, i.e. after Plio-Quaternary deposition and thus probably during the Quaternary. This would have caused a general migration of flow towards the west.
This approach cannot be conclusive concerning the pattern of tilt. Is there a general uplift increasing from west to east or is there local tilt of each watershed that should correspond to relative block displacements, where the hypothesis of tear faults bounding rotating blocks is suggested)? Even if we cannot observe an increasing elevation of the Artiče plateau towards the east, the increasing age of outcropping sediments in the same direction (if we exclude the singular Libna hill) support the hypothesis of a general tilt, perhaps completed by

local movements. This is also consistent relief of the Orlica hills towards the east, up to the Sotla River (Croatia/Slovenia border).

Lateral evolution of the Artiče flexure offset

This estimation is based on topographic profiles of basin divides, performed perpendicularly to the Artiče flexure. We also perform two profiles parallel to the Artiče flexure, one in the Dobrava plain and one in the Artiče plateau. We combine automatic topographic profiles from the DEM and geological map information. The first set of sections complement the last remark of the section *Derivation of the drainage network and lateral evolution of cumulated uplift* (Figure 30), concerning the eastward increase of outcropping formation age and uplift amount. From west to east, we observe both the increase of the cumulated topographic scarp (from almost 50 m on profile 4 to more than 100 m on profile 1) and the minimal offset of the Plio-Quaternary top around the flexure (from almost 50 m, profile 3, to 150 m, profile 1), which is in the same magnitude level than reported by Poljak (1999) from borehole data analysis in the Globoko area (located at profile 2, Figure 30).
In order to get a continuous lateral picture of the offset, we calculate the difference between the Artiče and Dobrava plateaus elevations, along the Artiče flexure. We assume that it gives approximation of the cumulative offset of the reverse displacement associated with the Artiče flexure. Considering the previous 4 sections, we underline that it is minimal assessment of the post- Plio-Pleistocene offset, above all in the eastern part of the presented section because Plio-Quaternary has there been eroded.
The Plio-Quaternary parallel section (Figure 31A) shows the position of transverse faults (e.g. Sromljica and Gabrnica faults). The plateau elevation increases drastically across the Sromljica fault and a vertical displacement on this fault is possible (distance 8000 to 6000 m, Figure 17). To the East, the elevation tends to decrease as well as the inferred offset (distance 4000 m), across the Gabrnica fault (Figure 30). However, considering that the outcropping deposits are there older (compare profiles 2 and 1 on figure 29), the cumulated offset may be larger east of the Gabrnica fault (Figure 31, full red line) that displayed on the Figure 31 (dotted red line). Eastward, the apparent vertical offset seems again to decrease (distance 1000 m). This decrease is confirmed by Croatian DEM analysis (*section Continuation in Croatia*).
To conclude this section, we suggest that vertical offset on Artiče flexure shows a triangular pattern, with a maximum value close to the Gabrnica Creek. We however cannot exclude that the offset present a "scaled" pattern accommodated by the transverse fault (which should then support the hypothesis of rotating blocks). We remind that triangular pattern of cumulated (or individual earthquake) offsets have been documented for worldwide faults (Manighetti et al., 2005) and we thus support this hypothesis.

4.3.5.2 THE LESKOVEC AREA: AN EVIDENCE OF POST PLIO-QUATERNARY DEFORMATION AT THE NORTHERN KRŠKO BASIN EDGE?

The analysis of seismic-reflection profiles suggests the occurrence of deep deformation within the Neogene deposits at the edge of the Krško hills. These are interpreted as possible buried continuation of the NE-SW Orlica fault. At the surface, east-west trending folds have been mapped into Plio-Quaternary deposits (Figure 32), right above these deep deformation features.
The DEM shows there also striking morphological features:

- A slight NE-SW topographic ridge (red crosses on Figure 32), over 2.5 km between Krško city and Velikovaški Creek, which disrupts the slope from Krško hills to the Sava plain;

- A correlative deflection of the conform-to-slope streams in a NE-SW direction.

These features are absent to the east, at the Senuša Creek.
We conclude that a possible surface deformation of Quaternary age (because affecting the current drainage network) affect a part of the Krško hills edge of the basin.

4.3.5.3 CONTINUATION IN CROATIA

We here analyze the 25m-pixel DEM of Croatian side of the Krško basin, in combination with the Zagreb and Rogatec geological maps (1/100.000).
Figure 33 reports the qualitative analysis of the drainage pattern in relation with known surface structures and lithological variations. Between Sotla and Krapina Rivers, regional slope is dipping to the S-SSE, up to the Marija Gorica anticline. Stream flows are consistent with this, from the Northern relief associated to the continuation of Orlica anticline (not shown on Figure 29). However, this pattern is disrupted when streams approach the possible continuation of Artiče flexure, where some NE-SW-elongated topographic "ridges" induce the deflection of streams and tributaries. In the Jezero-K. area, this may be due to lithological changes between Middle and Upper Miocene layers, but in the V. Trgovišće and Strmec area, this explanation is not so obvious because geological reports only Pliocene outcropping. We thus suggest that these features should be due to post- Pliocene folding or faulting.
When looking at elevation profiles of the main streams (Figure 34), we observe "knickpoints" in the Strmec area. For the Vucolnica creek, this could be due to lithological change between Upper Pliocene and Plio-Quaternary, but this explanation is not retained for the Ribnjak creek. From this, arises the question of a possible vertical displacement along the NE-SW continuation of the Artiče flexure.
Looking at the basin divide profile that should give the cumulated offset, this does not appear obvious and a maximum offset of 20 meters could be retained.
To conclude this section, there is a possible surface continuation of the Artiče flexure in Croatia with post-Plio-Quaternary activity. However, this seems attenuated in cumulated vertical offset and is dying out after 5 km from the Slovenian-Croatian border. This is consistent with the seismic reflection data from Tomljenović and Csontos (2001).

4.3.6 DISCUSSION AND CONCLUSION

We report the following facts:

- Relief is driven by 2 almost parallel tectonic features (Orlica anticline and Krško syncline). In between, 2 WSW-ENE structures (Orlica fault and Artiče flexure) affect the fold limbs.
- We divide the relief between (1) the Orlica and Krško hills, (2) the Artiče plateau, (3) the Krško Syncline plain.
- The Orlica hills and the Artiče plateau exhibit older deposits towards the East, and the Orlica hills elevation increases in the same sense.
- Regional slope, following this Neogene fold limb, control an incised drainage network into the Artiče plateau. This network is dramatically asymmetric, suggesting a higher uplift to the East during the period of drainage incision (Quaternary).
- Crosscutting the Artiče slope (located above Artiče flexure and reverse fault), each stream shows a weakly increasing slope.

These facts are all together consistent and they strongly support a Quaternary uplift of the whole Northern limb of the Artiče flexure. This has already been demonstrated for Pliocene deposits (cf Poljak, 1999). The slight increasing of the stream slope suggests that at least part of this uplift may be due to local displacement along the Artiče flexure during Quaternary.

Moreover, from the lateral evolution of uplift (according to geological maps and DEM data), arises the issue of a lateral attenuation of displacement along the Artiče flexure, from a maximum close to Globoko mine towards the west (beneath the Holocene Sava plain) and the east (Croatia). There, the offset may also exist, but it is lower and seems to die out after a course of almost 6 km. The total length of the structure should reach 15 km. The available maps suggest that this is segmented at the surface (Poljak, 1999) and works performed within this project support this interpretation.

.

This lateral attenuation could be a good point for the site selection. However, the recent works by Manighetti et al. (2005) suggests that this pattern could also be the consequence of a laterally growing fault. In their worldwide synthesis, it is indeed shown that cumulative slip profiles (as well as seismic slip profiles for individual earthquakes) have a triangular shape, with maximum slip at fault initiation zone and lateral decrease of slip towards the propagating tips. The Artiče structure is suspected to be the surface expression of the Southern limit of a large-scale block uplifting (up to the Orlica hills). The rate of uplifting is low, at a maximum of 150 m during the last 5 Ma (maximum age of Plio-Quaternary base surface) or 1.5 Ma (minimum age of Plio- Quaternary top surface according to Verbič, 2005) (i.e. 0.03 to 0.1 mm/a).

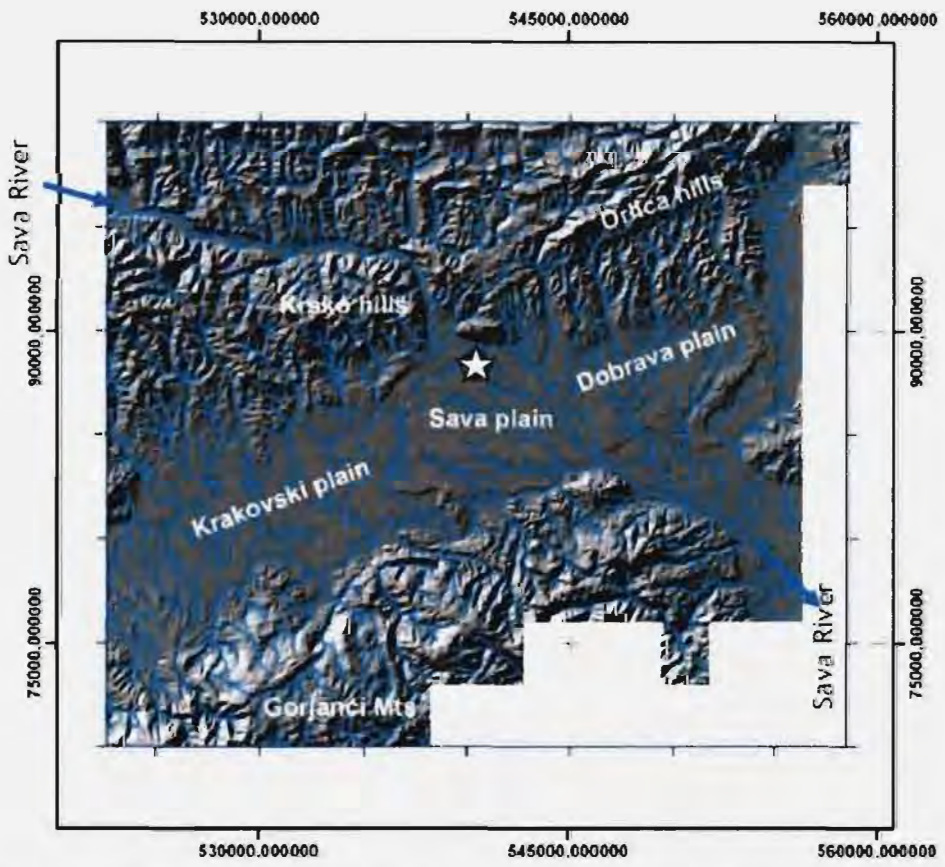

Figure 22: The site in its morphological contexts. The existing NPP is located along the Northern rim of the Sava River, inside its current alluvial plain. 12.5m-DEM and the numerically-deduced drainage network. For geological context see Figure 3. Coordinates are given in meters and refer to the Slovenian projection (MGI: Transverse Mercator projection, Bessel-1841 spheroid).

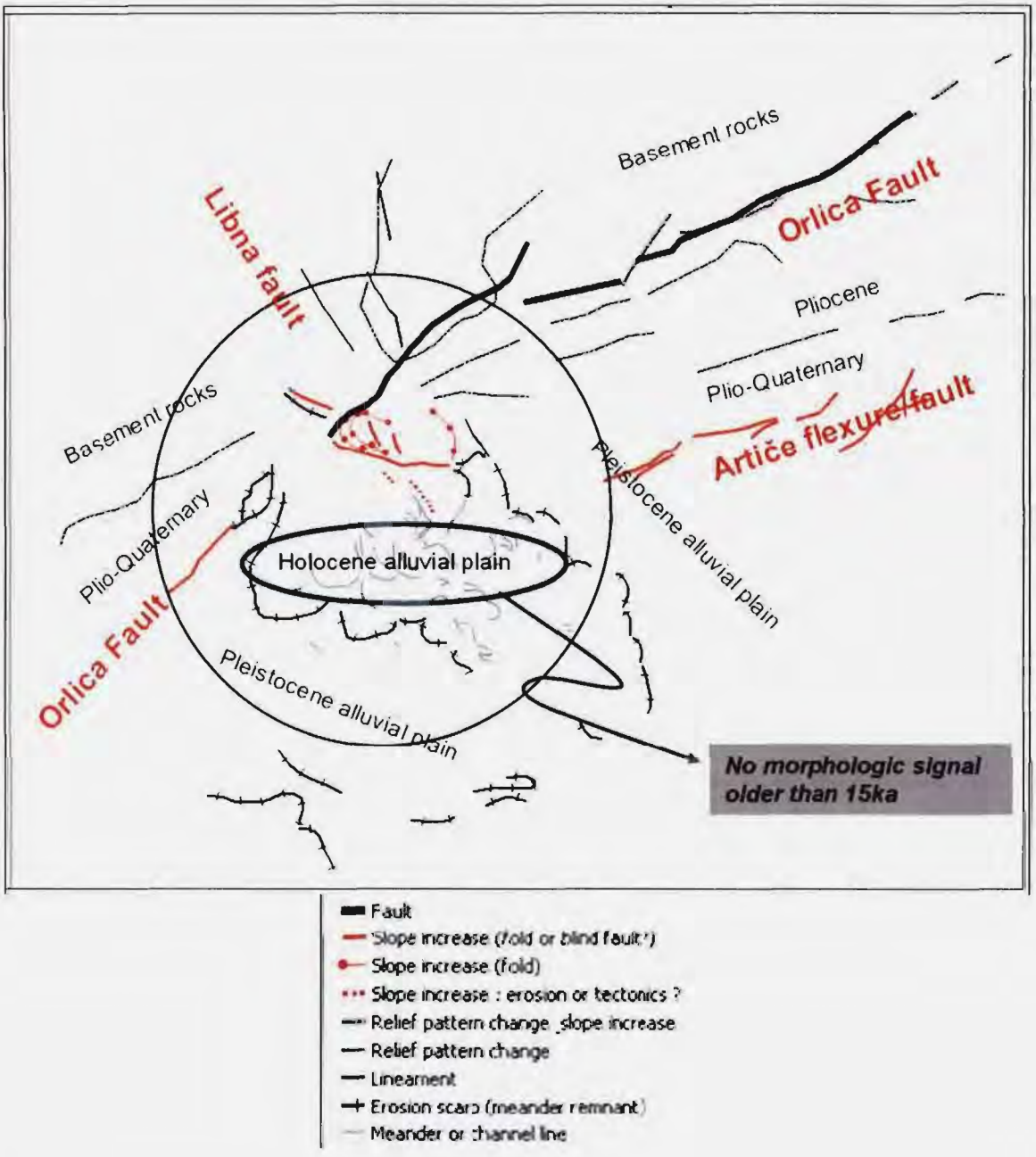

Figure 23: Synthetic analysis of lineaments from the 12m-DEM and aerial pictures. The circle represents the site vicinity area (5 km around the NPP site). Tectonic features are represented in bold black and red. Others are either sedimentary features (due to river shifting and channel incision) or lithological variations (between Plio-Quaternary and Pliocene for example). In the so-called Holocene alluvial plain of the Sava river, the shifting of its course caused erosion of pre-Holocene deposits and deposition of Holocene to Historical alluvial sediments over thicknesses of few meters, as shown in the Stari grad trench.

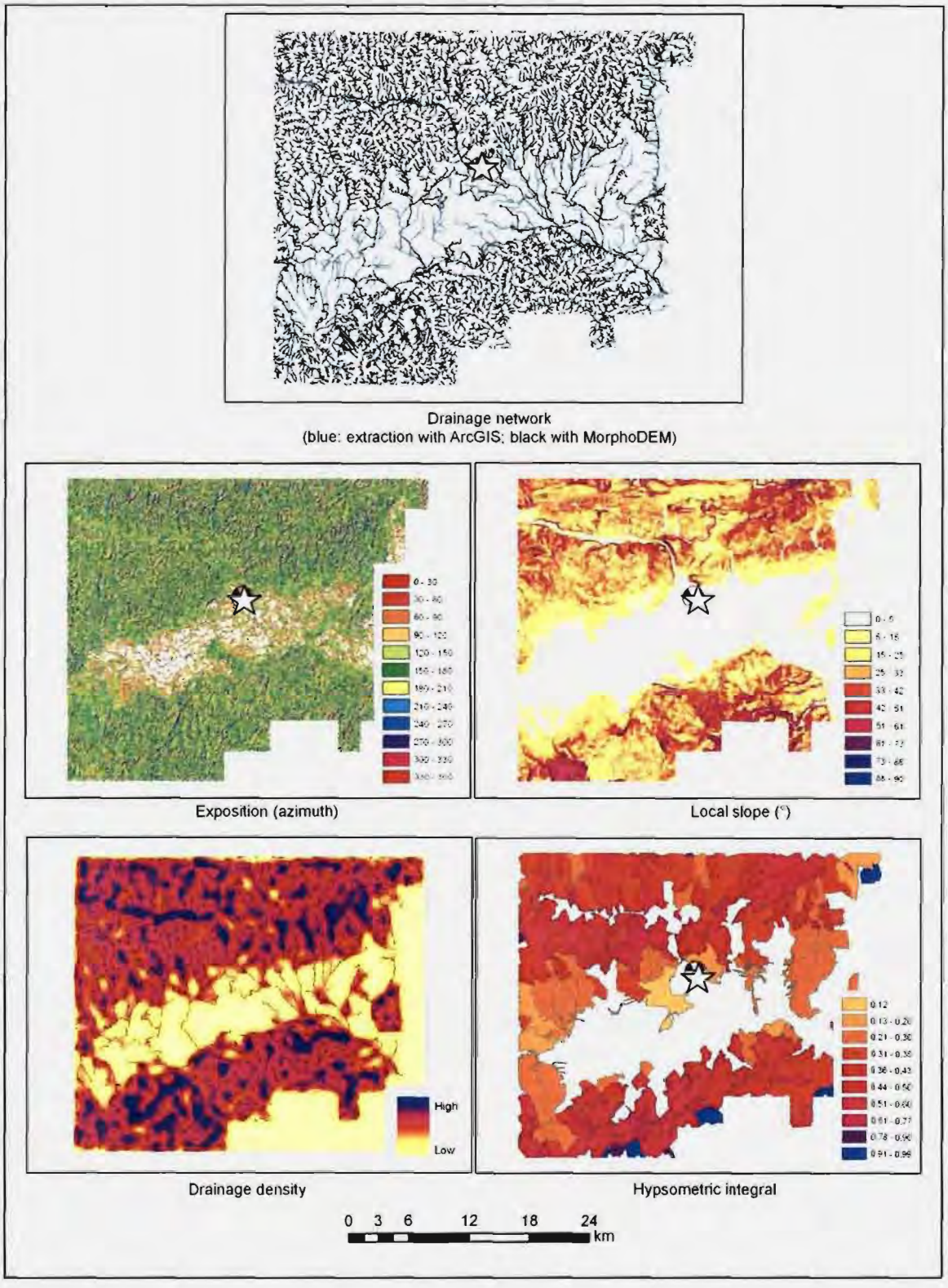

Figure 24: Maps of various morphometric parameters in the NPP site region. See text for explanation.

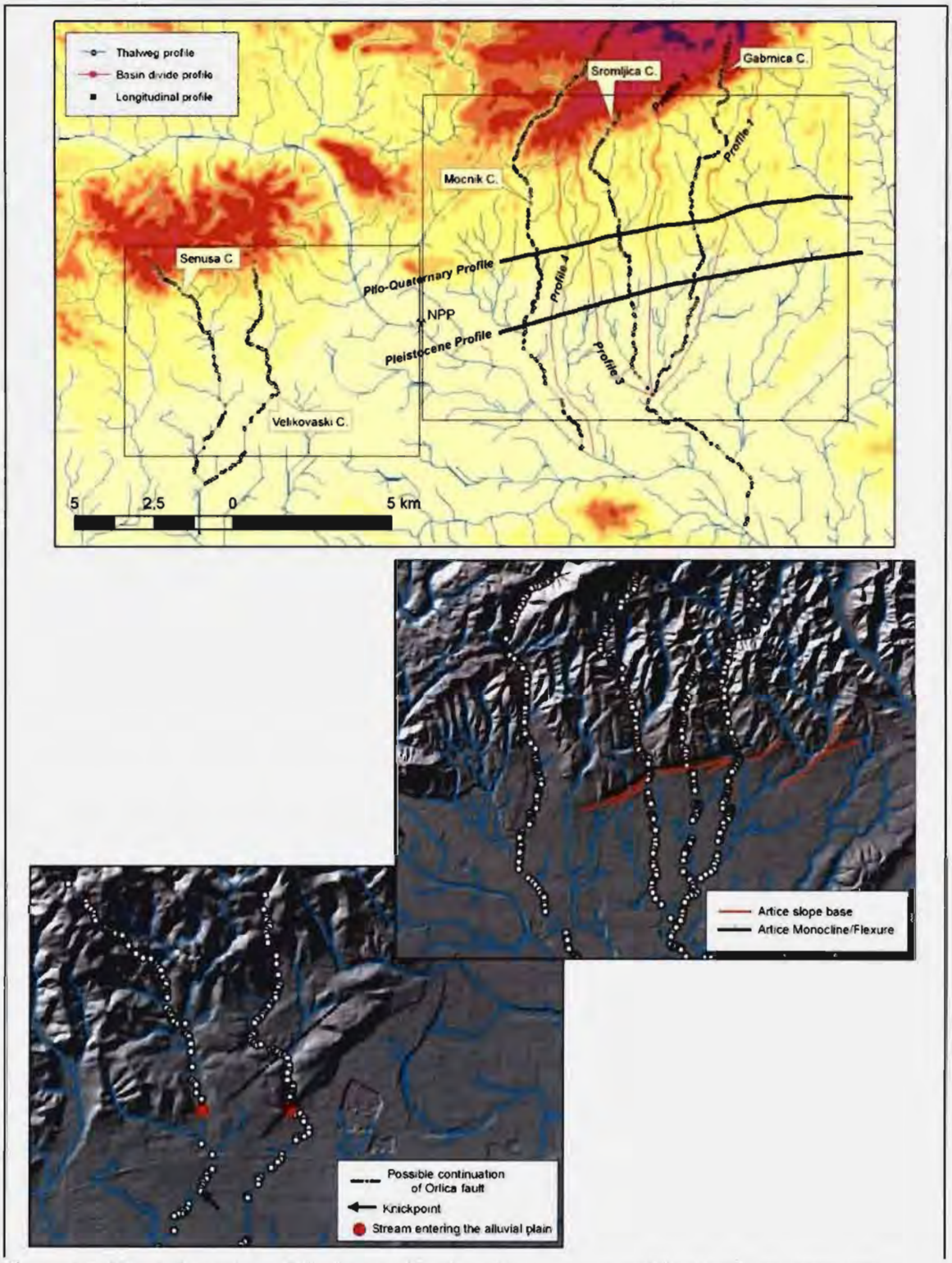

Figure 25 (Top): Location of the longitudinal and transverse profiles (with respect to the studied structures (Orlica and Artiče fault/flexure). Transverse profiles are basin divide profiles and thalweg profiles (extraction from the DEM). Longitudinal profiles consist of topographic section deduced from the DEM, parallel to the Artiče flexure.

Figure 26 (Bottom): Focus on the studied cases, with the location of the expected tectonic structures and morphologic key features (see Figure 30 and Figure 31).

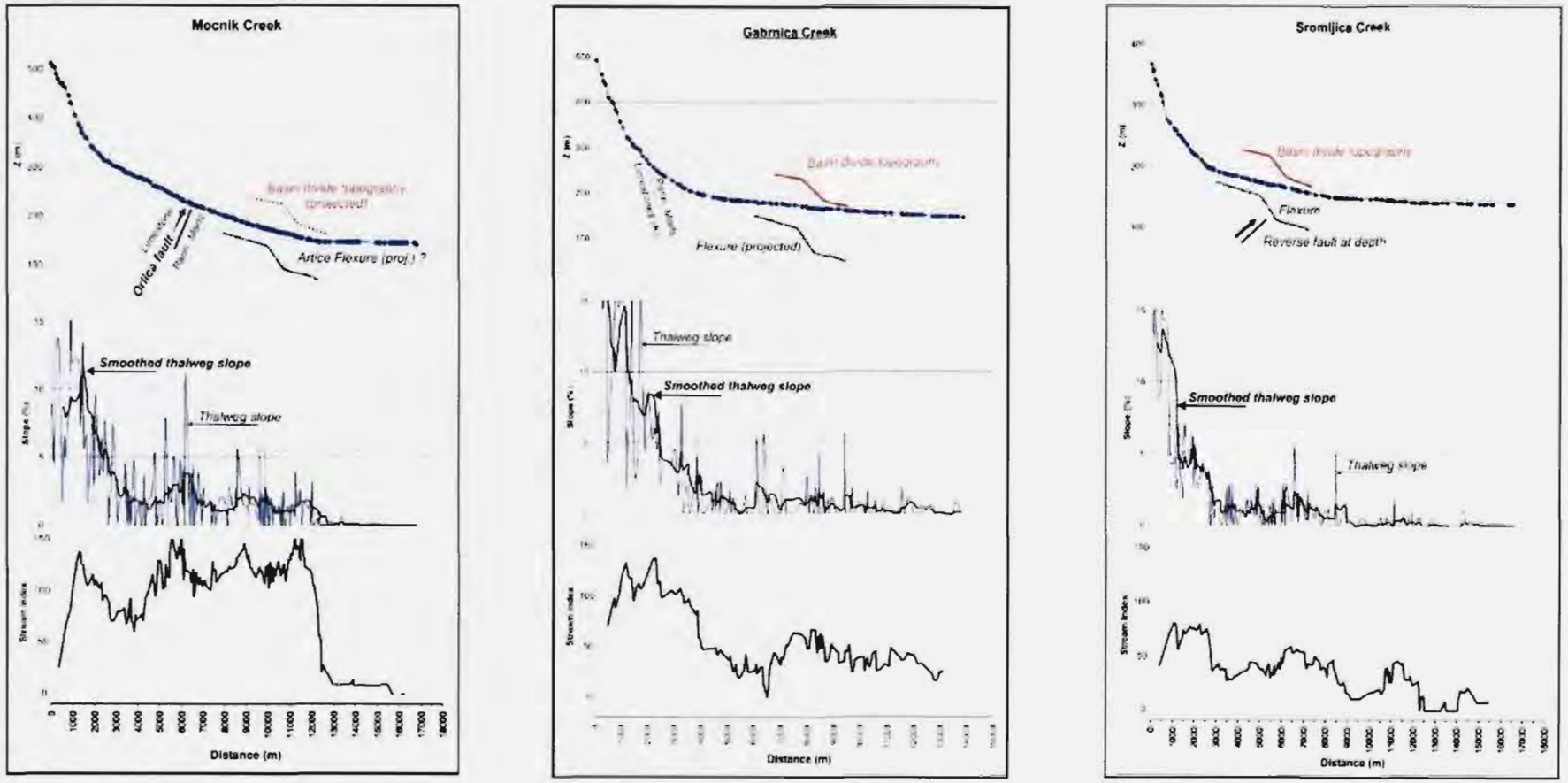

Figure 27: Transverse elevation profiles of the 3 main streams crossing the Artiče flexure, from west to east: Močnik, Gabrnica and Sromljica creeks. Location of key topographic and geologic features along the elevation profiles, to the top. The slope and stream-gradient index profiles are also presented: they allow locating the main morphologic anomalies, when slope or stream-gradient indices increase downstream.

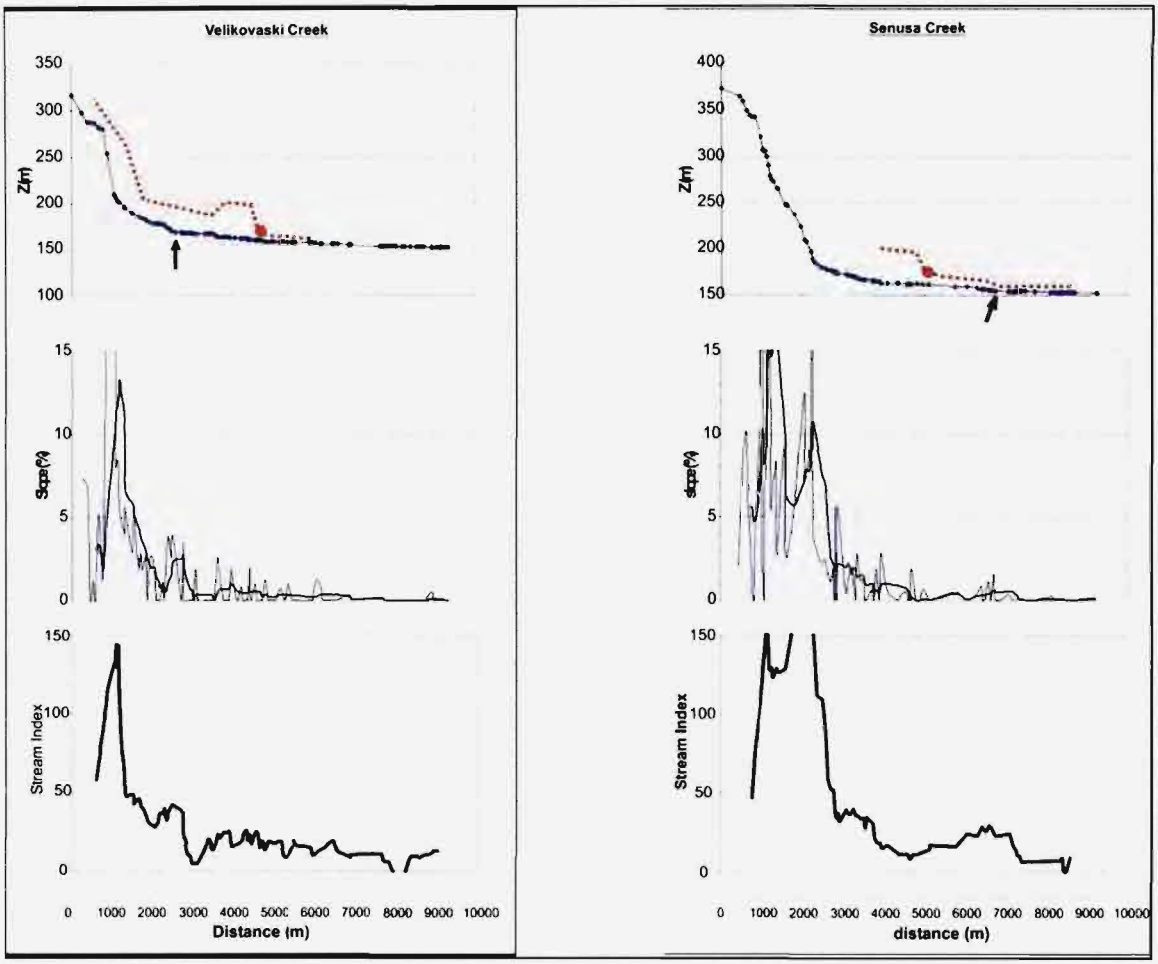

Figure 28: Transverse topographic profiles of the 2 main streams crossing the Orlica fault suspected from seismic lines, from east to west. Red dots and black arrows are located in the Figure 25.

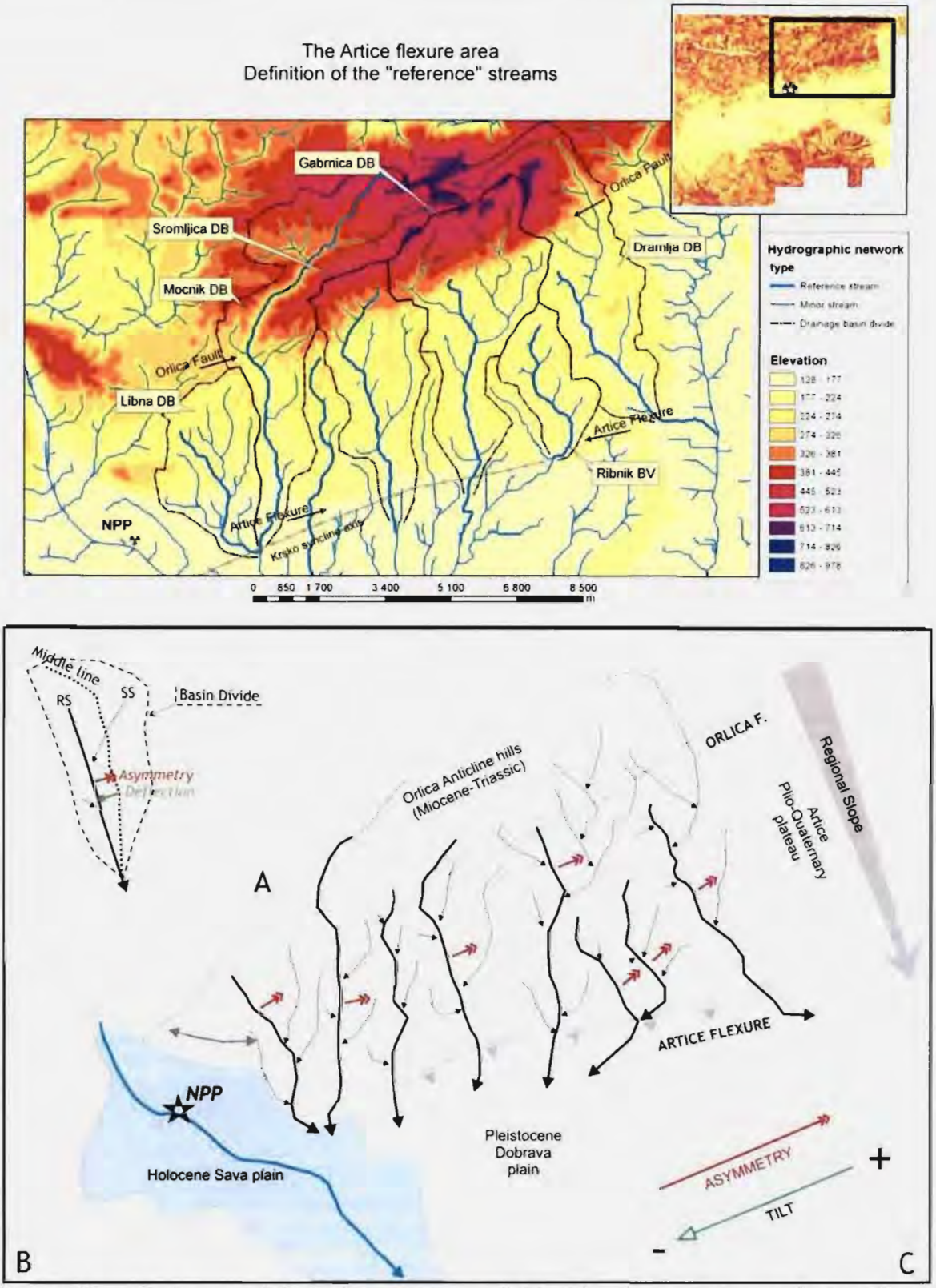

Figure 29: A- Definition of the Reference streams (RS) within the studied watersheds of the Artiče plateau, defined as the streams that are conform to the "regional" slope between Orlica hills and Dobrava plain; B- sketch map of the asymmetrical network, which shows a systematic deflection towards the west suggesting a differential uplift increasing to the east.

Figure 30 : Simplified morpho-geologic profiles across the Artiče flexure, from eastern slope of Gabrnica Creek (profile 1) to eastern slope of Mocnik Creek (profile 4). Elevation is taken from the DEM and geology from the 1/25.000 map (see Figure 4). The Artiče fault projection on profiles comes from the KK-03 seismic line, performed in the Sromljica creek, between profiles 2 and 3).

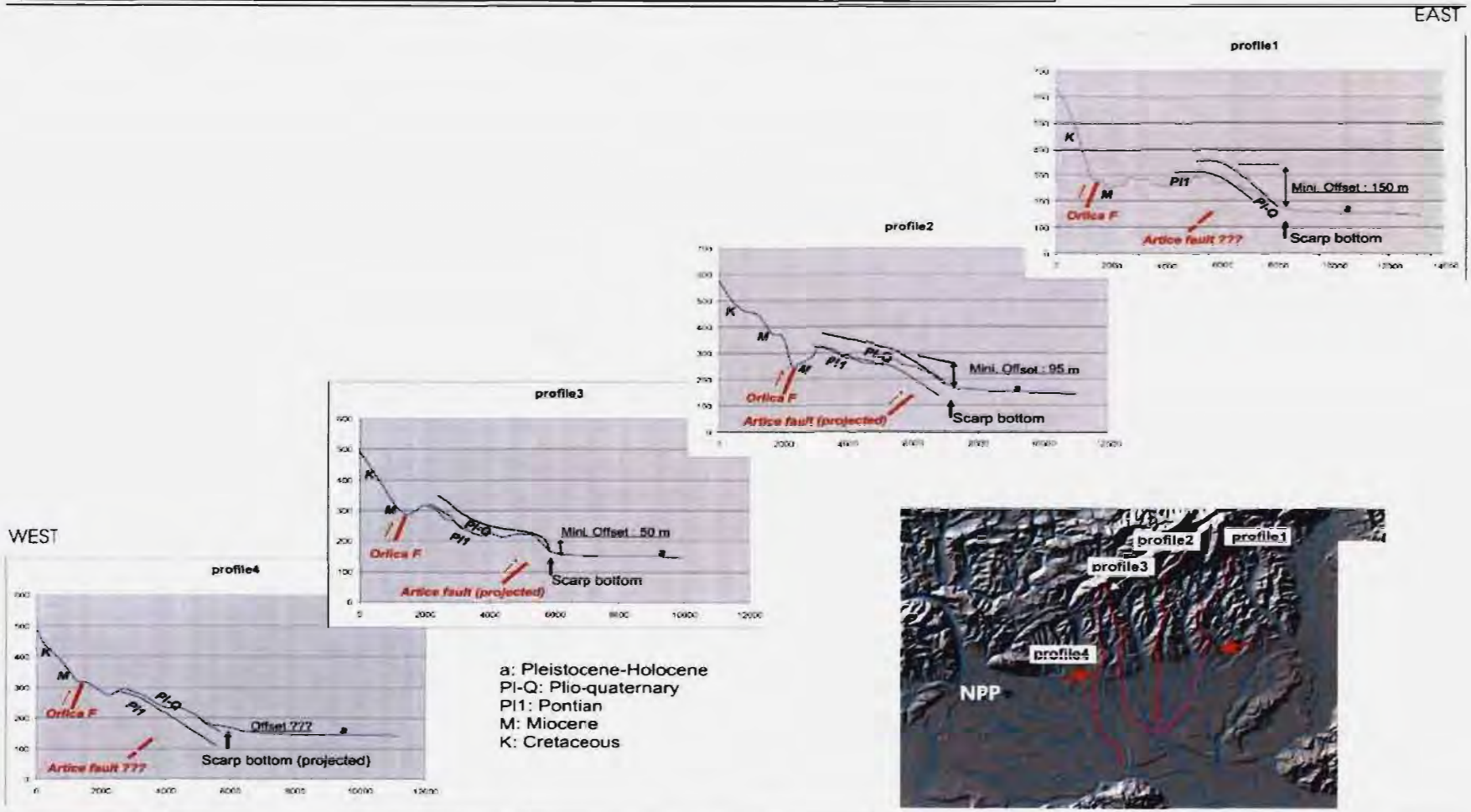

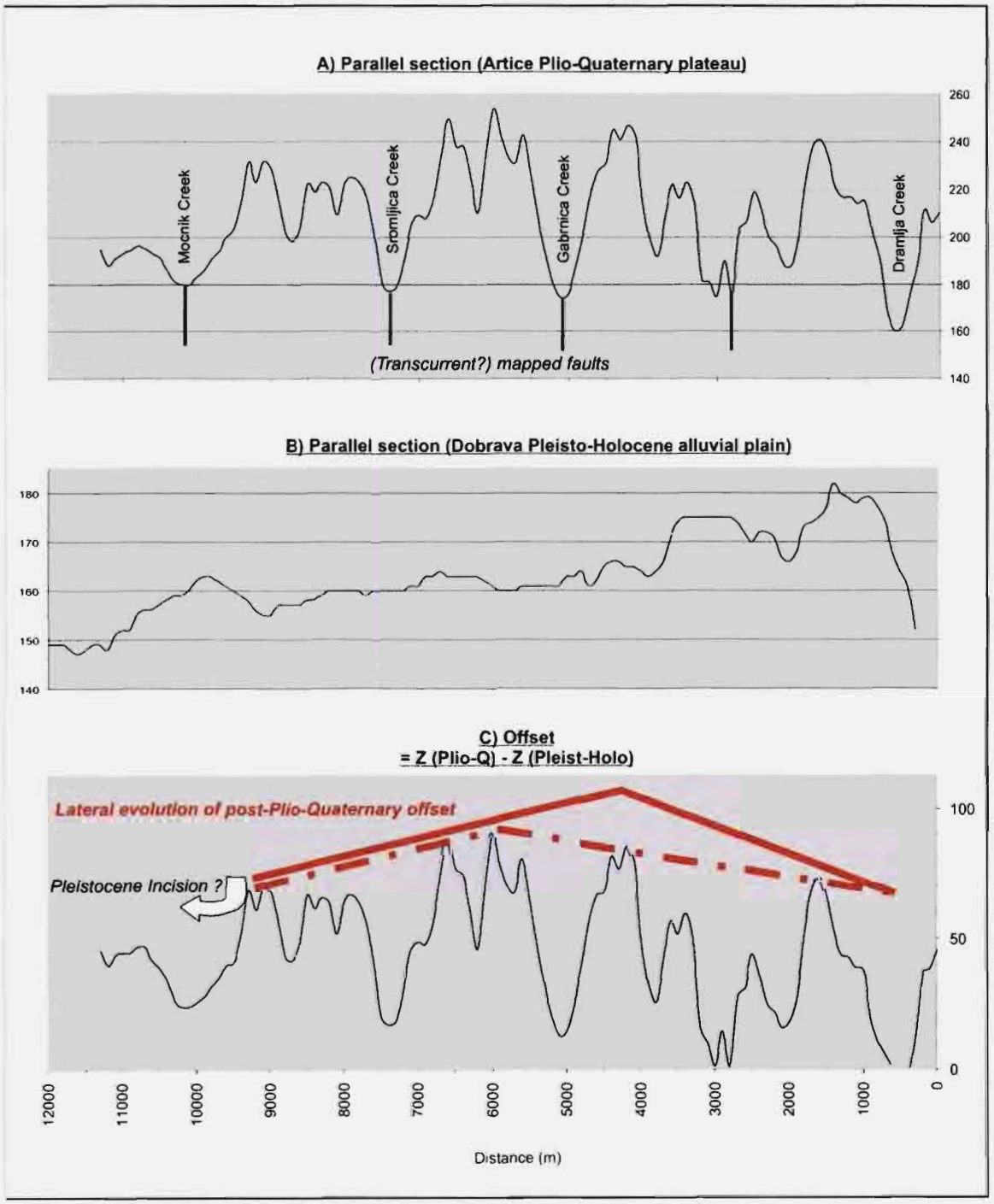

Figure 31: Longitudinal elevation profiles, according to the DEM (profiles A and B), and difference between the Plio-Quaternary plateau profile (Artiče plateau) and the Pleisto-Holocene profile (Dobrava plateau) (profile C). This is taken as an approximation of the offset of the Plio-Quaternary deposits by the Artiče flexure. 2 options are presented for the envelop curve: the full red line takes into account the geology (older formations to the east) and the dotted one does not.

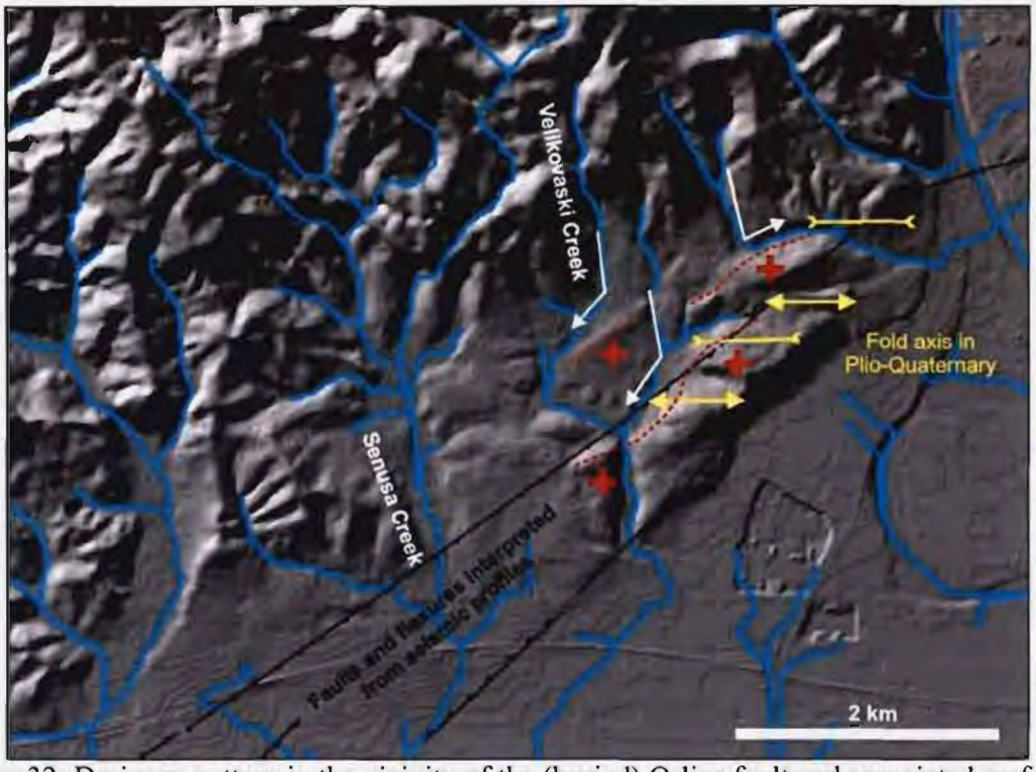

Figure 32: Drainage pattern in the vicinity of the (buried) Orlica fault and associated surface deformation. Red crosses represent "uplifted" and NE-elongated sectors. White arrows symbolize deflection of streams.

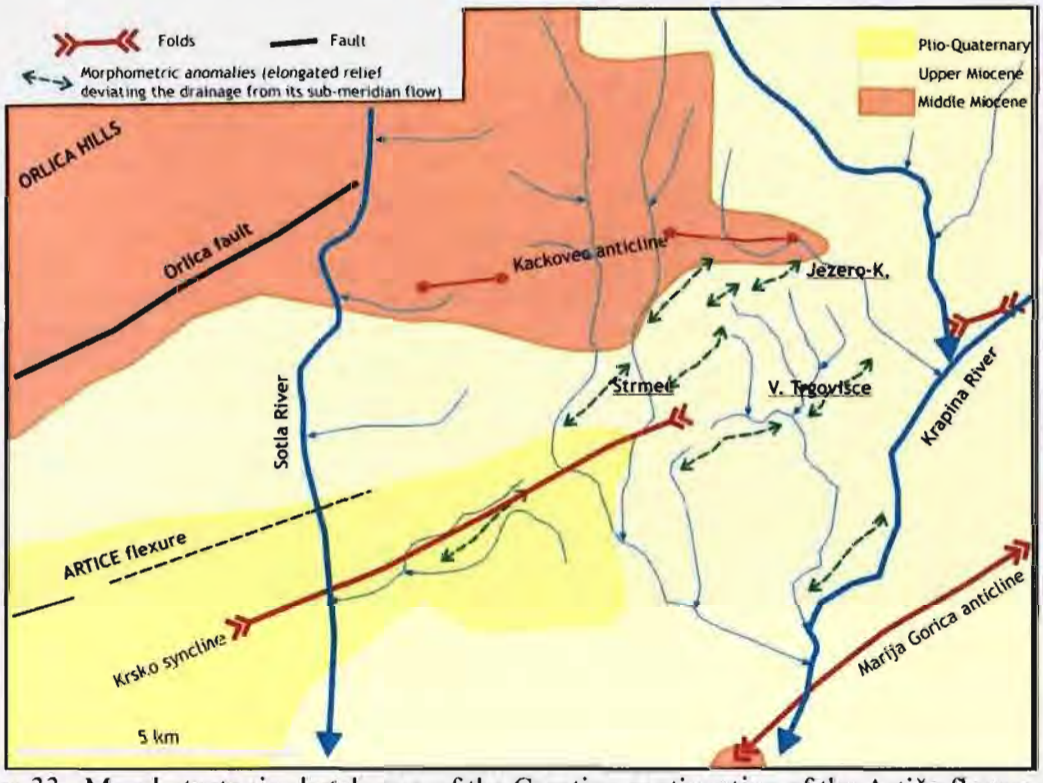

Figure 33 : Morphotectonic sketch map of the Croatian continuation of the Artiče flexure, deduced from the DEM and the geological maps from Rogatec and Zagreb (1/100.000).

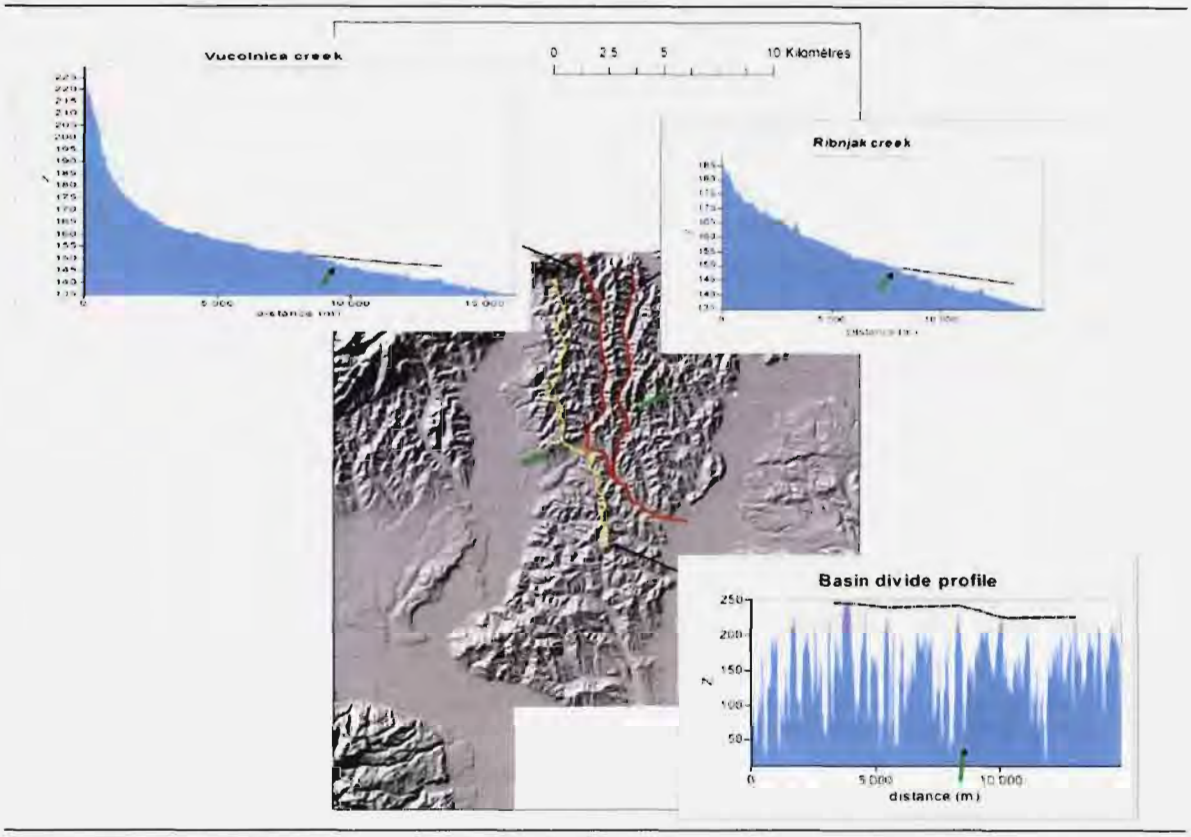

Figure 34: Stream elevation profiles of the 2 main streams crossing the potential continuation of the Artiče flexure in Croatia. A basin divide profile is also presented. These come from automatic extraction from the 25m-pixel Croatian DEM. Black arrows represent the possible location of Artiče flexure (on map and elevation profiles).

4.4 INTERPRETATION OF THE TECTONIC MODEL

Annotations in this section refer to the tectonic map of the Krško basin (Figure 4) and to the interpretative tectonic model of the extended site vicinity area (Figure 35). The tectonic model is based on the tectonic map and the concept of new model by Rižnar (2008).

Tectonic setting

The modeled area is situated in the North-western margin of the sinistral strike-slip Mid-Hungarian zone, adjacent to the South-eastern margin of the Sava tectonic wedge characterized by the E-W oriented Sava folds (Swan et al., 2004, Figure 2-3).

The principal structures in the Mid-Hungarian zone are the NE trending (Balaton) strike-slip faults. The core (leading) structure of the sinistral strike-slip-zone is the Sveta Nedelja fault along the Southern margin of the Gorjanci Mts. and Zagreb fault (not shown in the model) along the Southern margin of Mt. Medvednica. The Sv. Nedelja fault is a transversal Dinaric fault by the origin and represents the continuance of the Zagreb fault, the latter being microplate boundary between the Tisza unit and the Dinarides (Brueckl et al., 2008).(Sv. Nedelja fault itself is not a microplate boundary!). The Orlica fault is the North-westernmost of the Balaton faults exhibiting the post-Badenian sinistral strike-slip activity and thus considered as an external margin of the Mid-Hungarian strike-slip zone. The frequency of the Balaton faults increases from Orlica fault towards the South-east.

Main features

The Krško syncline is the most prominent plicative structure in the marginal part of the Mid-Hungarian zone. According to the seismic sections data combined with the gravity maps its axis has a North-eastern trend in the central part of the Krško basin, and turns into E - W oriented fold to the W, approaching the SW continuance of the Orlica fault. However, the central and the eastern part of the Krško syncline is not parallel to the Balaton faults. Instead it makes approximately 30° angle with them. Taking into account the sinistral strike-slip character of the Balaton faults, the Krško syncline may represent a "fault-flank depression" between (or related to) the Orlica and Artiče faults to the N, and the set of sub-parallel Balaton faults S of the syncline, observed in the Gorjanci Mts. (Figure 36; *cf.* Woodcock & Schubert, 1994, Figure. 12.15).

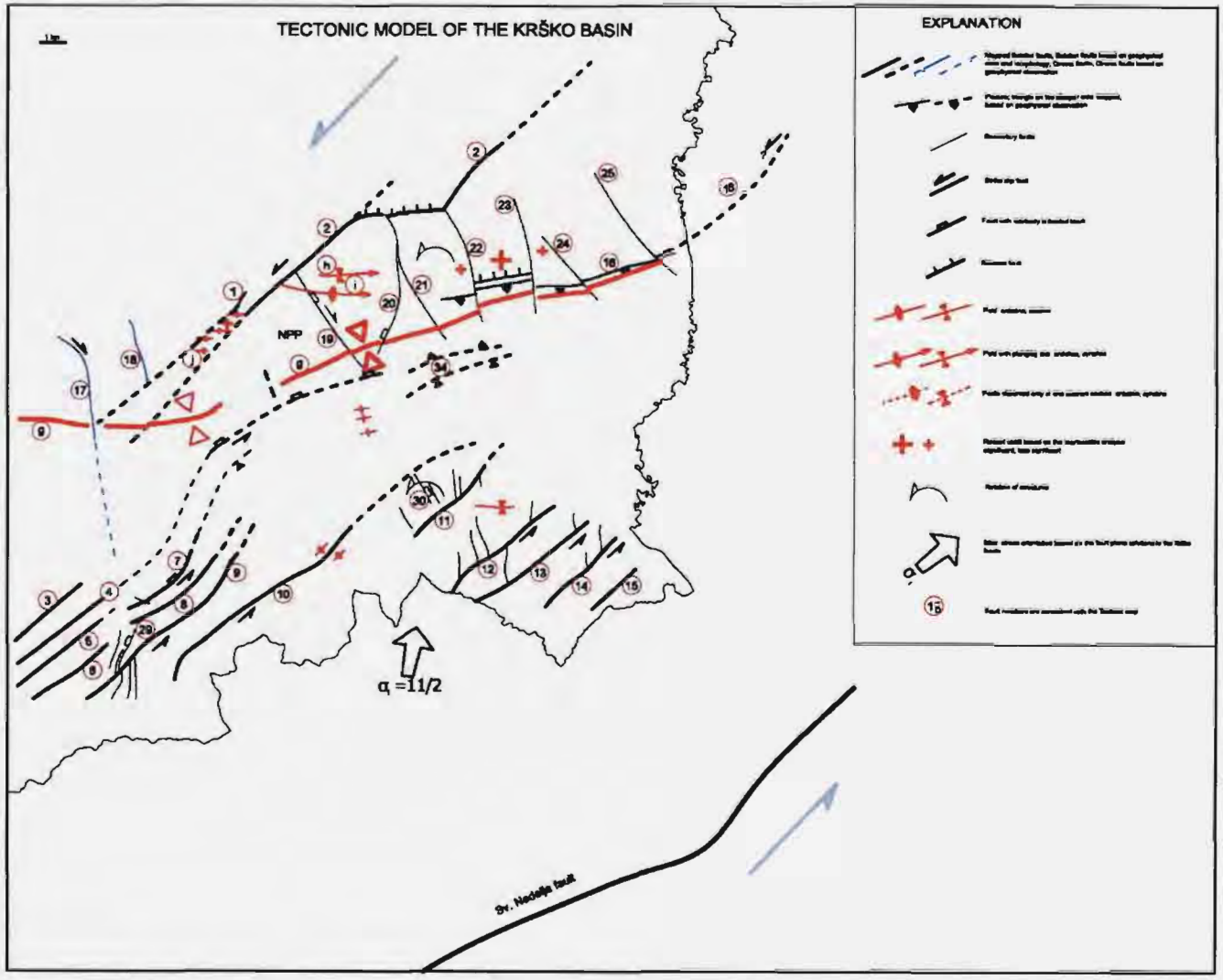

Figure 35. Tectonic model of the extended site vicinity area. For denomination of structures see Figure 4.

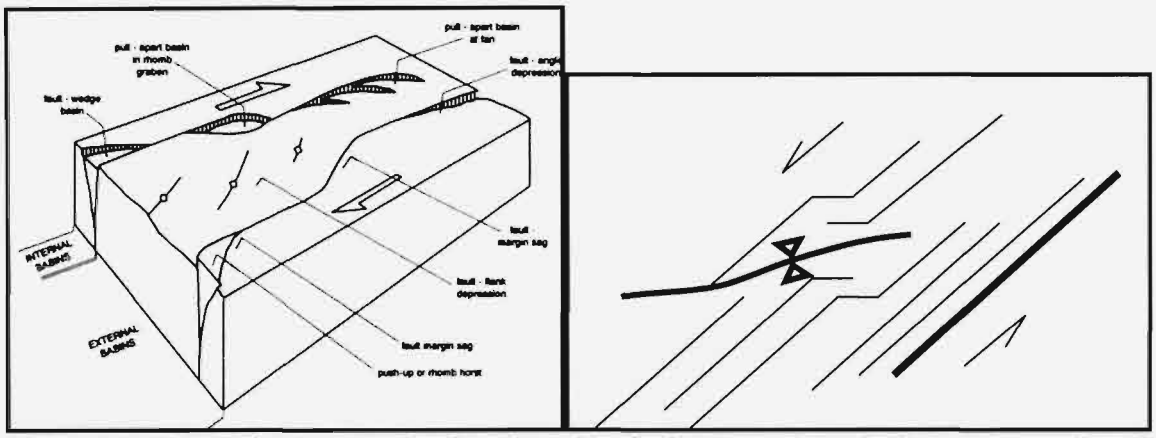

Figure 36. The textbook example of modes of basin formation in and adjacent to a strike-slip fault zone (Woodcock & Schubert, 1994) (left) and adoption to the model of the Krško basin (right).

The restraining bend between the Orlica fault and the Artiče structure

The NE part of the Orlica fault exhibits a stepover structure, as it deviates from its Balaton course into an E - W trending South verging reverse fault, and then continues again in the NE direction. The Artiče structure (19) also exhibits an E - W trend between the Močnik fault (20 and 21) and the Sotla River, but toward the NE, the structure trace adopts the Balaton course. The Artiče structure includes also a S verging reverse fault observed in the KK-03/99 seismic line. The deformation along the Artiče flexure is dying out in the NE direction as well (see section 4.3.5.3. Continuation in Croatia). The Artiče structure has the reverse character forming a flexure only in its E - W trending section (like the Orlica fault). The area between the Artiče and Orlica faults is a restraining bend (Figure 37).

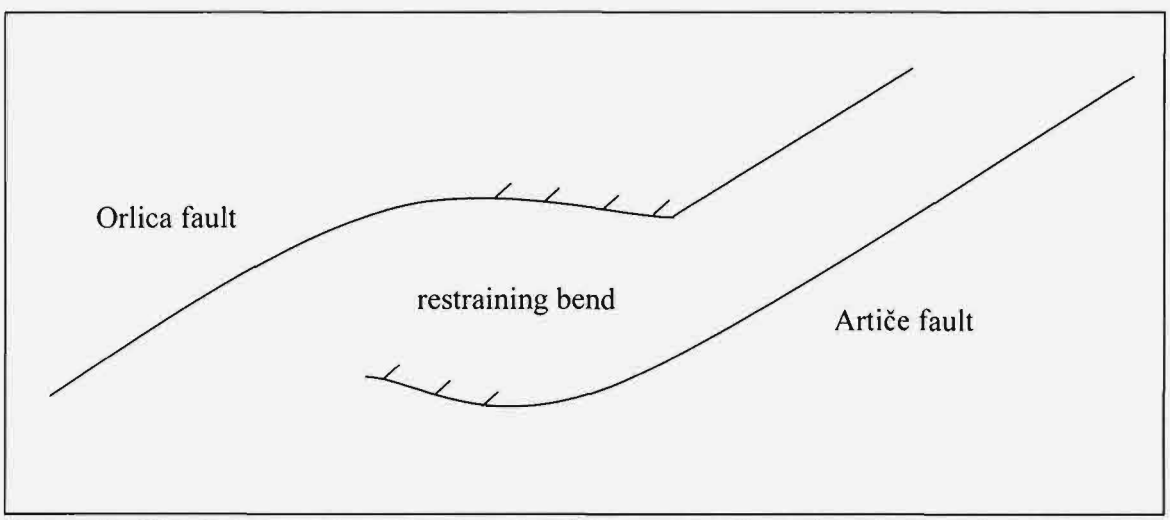

Figure 37. The restraining bend between the Orlica and Artiče faults. Not to scale.

The restraining bend is dissected by the N - S to NW - SE trending faults (faults 19 to 25). To the North, these faults stop at the Orlica fault, while toward the South their extent beyond the Southernmost evidences at KK-01/99 seismic section is unknown. However, we understand that these faults stop at one of the Balaton faults to the South.

Uplifting is observed N of the Artiče flexure in the centre of the Globoko sub-basin, which indicates the ongoing inversion of the Globoko basin. The normal faults in the area of the

uplift (e.g. Sromljica (22) and Gabrnica (23) faults) are adopting the reverse character, but above all, they tend to rotate in the CCW direction and act as a Riedel type dextral strike-slip faults (sub-horizontal slickensides were observed in the Libna fault zone).
Despite the fact that all of the N – S to NW – SE trending faults in the restraining band do affect the Plioquaternary deposits, they will not be considered as seismic sources. They are too short thus negligible. Only the Libna fault (19) will be considered as a seismic source due to its vicinity to the NPP and relatively large suspected offset of the Plioquaternary deposits.

Libna anticline and Libna fault
As Placer (in: Poljak, ed., 1997 [78]) explained, the Libna anticline represents a local structure along the Orlica fault. A part of the fold, clenched between the Orlica and Libna faults is folded into a tight fold with steep Southern limb, but in a short distance toward the E, the fold is gradually becoming a gentle anticline. Libna fault was formed or reactivated to compensate the differential folding.

Small scale folds in the Leskovec area (j)
The E - W oriented small scale folds in the Leskovec area represent the uplifted area. Considering the orientation of the folds, the folding and consequential uplift is associated to an inferred SW section of the Orlica fault or to the area between the Orlica and Grič (1) faults due to the sinistral strike-slip activity of the fault in the depth.

The W section of the Krško syncline (g) and the Lokavec fault (17)
The course of the Krško syncline is adopting an E - W trend to the W according to the gravimetric data (*cf.* Figure 36), while toward the E it was bent into the NE trending fold. This implies, that the Orlica and Grič faults are not active (cease to exist?) SE of the Lokavec fault and that the Southern part of the Lokavec fault (Southern part of the Hrastnik fault (Figure 4, Figure 35) takes over the strain there. It consecutively implies the Dinaric (NW trending)s Lokavec fault being an active structure although it does not penetrate the Pleistocene deposits (Persoglia, ed., 2000).
The Lokavec fault doesn't appear in the Kostanjevica area, meaning that it terminates along one of the Balaton faults observed E of Kostanjevica.

Southern limb of the Krško syncline
The Southern limb of the Krško syncline is symmetrical to the Northern one. The anomalies observed in the seismic sections in the Southern limb of the Krško syncline exhibit flexures related to suspected flower structures (see description of geophysical data). These structures are ascribed to the Balaton faults, observed in the Gorjanci Mts.

Due to a relatively high frequency of the faults there, the immediate connection between observations in seismic sections and structures mapped is not possible. We interpret that the flexures in the eastern part of the S limb of the Krško syncline, observed in the KK-03/99 and the old P-84/59 seismic sections are connected to the folds observed in the S part of the P-3-4/95 seismic section thus indicating a possible connection to Studena (8) and Oštrc (9) faults. Faults observed in the P-3-4/95, KK005/00 and KK002/99 seismic sections are connected and ascribed to the Mali Ban fault (4).

Gorjanci Mountains area

The continuance of the Poštena vas fault (10) is inferred along the Krka River upon morphologic criteria.

North to North-West trending faults are mapped between all the Balaton faults SE of the Poštena vas fault (10). The CCW rotation of the Riedel type faults S of the Poštena vas fault is reflected in their sigmoidal traces, and in bending of the folds in the Cretaceous deposits in the W block of the Malence fault (Rižnar, 2005).

5 LIBNA FAULT

5.1 PALEOSEISMOLOGICAL TRENCH AT STARI GRAD

5.1.1 INTRODUCTION

As a part of initial share of supplies within the project *Geotechnical, Geological and Seismological (GG&S) Evaluations for the New Nuclear Power Plant at The Krško Site (NPP Krško II)* a paleoseismological trench was conducted across the trace of the Libna fault in order to determine the fault's possible recent activity / capability of surface or near-surface rupturing.

The geophysical preliminaries were performed by R. Stopar and M. Car (Geoinženiring d.o.o). Trench preparation, logging, interpretation and report write-up was done collaboratively by S. Baize (IRSN), M. Bavec and D. Skaberne (GeoZS). Field work and logging was assisted by J. Jež (GeoZS) and students from the Department of Geology, NTF, University of Ljubljana. A separate trenching report (Bavec, ed., 2008) includes all appendices (geophysical preliminaries, dating) that are summarized here. Trench details are also addressed in the IRSN geology report (Baize, 2008).

5.1.2 TECHNICAL DETAILS

The trench was excavated by excavator and logged between Jan 28th and Feb 1st 2008 following the preliminary geophysical survey. It was placed along the WSW-ENE trending axis between endpoints X=540755.8827; Y=89216.0701 and X=540761.8850; Y=89208.1520 (Gauss-Krueger coordinate system). The position of the trench was chosen according on the presumed trace of the Libna fault, which was established with the various methods (geological mapping, seismic lines...). Possible recent activity would be proven with displaced and deformed Holocene gravels covering Miocene basement. The significant thickness of the Holocene gravels would cause technical problems during excavation (ground water, possible collapse of the trench wall) so the trenching was performed in the location with relatively thin sheet of gravels.
The axis was moved approximately 10 m NW from the axis of the geophysical preliminaries to enable fieldwork. The trench consisted of the main trench in total length of 52 m at surface and a perpendicular secondary trench in length of 15 meters (Figure 1). Surface width was 6 m. The depth of the trench was 3.7 meters to the NE and 2.3 meters to the SW (Figure 2). This change in depth is due to the slope of the surface. The bottom of the trench was excavated between 40 and 60 cm below the erosional surface between Holocene and Miocene lithologic units and was almost horizontal.

After detailed cleanup the South-eastern wall was equipped for logging in length of 28 m covering the whole height. The slope of the wall was kept at 45 – 90 ° depending on cohesion of the sediment. Before logging the South wall of the trench was marked by measuring grid with cells, 2 m long (lines A, B, C, D, E, F, G, H, I, J, K, L, M, N) and 1m high (lines 1, 2, 3) (Figure 4). The wall was photographed in sections on axes of vertical grid lines. Mosaic photography was constructed from these sections. The wall was logged in scale 1:20 in full length and height. Observations and some logs were also made on other walls and on the trench floor.

The trench was flooded by groundwater thus app. 4l/s of water was constantly pumped into the nearby stream.

Figure 38. Trench site at Stari grad.

Above: Location sketch with trench site indicated in yellow.
Left: Survey site in detail. Gauss - Krueger coordinate system.

Figure 39. The view over the trench toward the WSW.

Loose gravel in the walls together with significant inflow of groundwater (4 l/s) caused problems with the stability of trench walls (Figure 40). After the preliminary overview a decision was made to keep the Southern wall as vertical as possible throughout the survey while other walls including the secondary trench were cleaned and surveyed provisionally.

Figure 40. Groundwater inflow (app. 4 l/s) affected stability of trench wall.

5.1.3 GEOLOGICAL BACKGROUND

5.1.3.1 GENERAL LITHOLOGY AND STRATIGRAPHY

At Stari Grad trench site the stratigraphy is relatively simple. Atop the sedimentary sequence lie the Holocene fluvial gravels, sands and silts. Along the trench, its thickness varies between 2 and 3.5 meters. Below the Holocene unit, there is the Miocene basement, consisting of massive semi-consolidated silt or clay-silt. The near–horizontal surface between the two units is erosional (Figure 41).
The dip of Miocene layers towards the SE is inferred from regional geology (Brenčič ed., 2006), however a shell-rich layer was observed in the trench dipping toward SSW (198/22).

5.1.3.2 THE LIBNA FAULT

NW – SE trending fault across Mt. Libna dissecting Plio-Quaternary sediments is named Libna. It was first defined as a buried normal fault with subsided NE block on the Basic geologic map 1 : 100.000 sheet Zagreb (Šikić et al., 1978). Placer (in: Poljak et al., 1997) described several parallel fault (planes) of the same trend in the Southern limb of Libna anticline. The fault continuation underneath the Holocene alluvial plain was long unknown. Therefore the last PSHA (Swan et al., 2004) did not pay special attention to this fault. In 2006, during the preliminary geological survey for siting the LILW repository in the vicinity of the existing NPP (Brenčič, ed., 2006), anomalies related to the SE continuance of Libna fault were interpreted in extreme N part of the N – S trending seismic section S1 (This section was during the course of this project evaluated as non reliable due to due to poor quality of the data by the team of experts). Furthermore, horizontal laminae were observed in the core of the VOG-1 borehole drilled in the fault zone in the Upper Miocene deposits (Brenčič, ed., 2006). Considering prevailing South-eastward dip of the strata, observed in the in the construction pit for the NPP, the subhorizontal laminae imply presence of structural deformation. Repeated remapping in 2006 revealed a single 150 – 300 m wide fault zone (Brenčič, ed., 2006) instead of multiple discrete faults proposed by Placer (in: Poljak, 1997, [78]). One of its western fault planes exhibits normal character with subsided NE block and cuts off the Plioquaternary sediments on the top of Mt. Libna (Placer in: Poljak, 1997, [78]). Libna fault is imaged as an E dipping normal listric fault in the KK-01/99 seismic section (Persoglia (ed), 2000). During the course of this project we realized that such interpretation overestimates the faults importance (see tectonic model report). After the fault was recognized in the S-1 seismic section (Car, 2006; Brenčič ed., 2006) its continuation was also looked for on other seismic sections. During this project we estimated that certain anomaly is also noted on the P-3-4/95 seismic section. The fault was observed in P-3-4/95, the same deformation was recognized in KK-01-99, 08K-10C and 08K-8A lines. To the NW the fault line can not be traced due to poor data quality across KK-04A-00 and 08K-5 lines. At the Libna Mt. crest, the fault is located by surface mapping and 2D electric tomography (this report). NE limit of the fault zone is relatively reliable only between 08K-10C and 08K-8A lines.

This fault is not to be mistaken with the disproved E-W trending reverse fault in the Northern limb of the Libna anticline, also formerly called 'Libna fault' (Placer in: Poljak et al., 1997; Verbič, 1995).

The location of fault trace between Plio-Quaternary gravels and Badenian limestone at the crest of Mt. Libna suggests that the Libna fault, along with the Libna anticline, might have

been active during the deposition of the Plio-Quaternary gravels (see tectonic map for geographic explanation). The fact, that not all the faults (fault planes) from the observed NW – SE trending set dissect the lower Plio-Quaternary boundary, implies, that folding of the Libna anticline and the faults formed at that time must have only been active before the deposition of Plio-Quaternary sediments, and that only Libna fault has been active (reactivated?) after (Placer in: Poljak, 1997).

At this stage of the project, we interpret the Libna fault as a fault with relatively subsided NE block with characteristics of both, a normal, and a strike-slip fault. No sedimentary deformation or topographic expression in post-Plio-Quaternary sediments is known to be related to the Libna fault. No direct observations of recent activity are known (e.g. notable displacement in the Holocene alluvial plain).

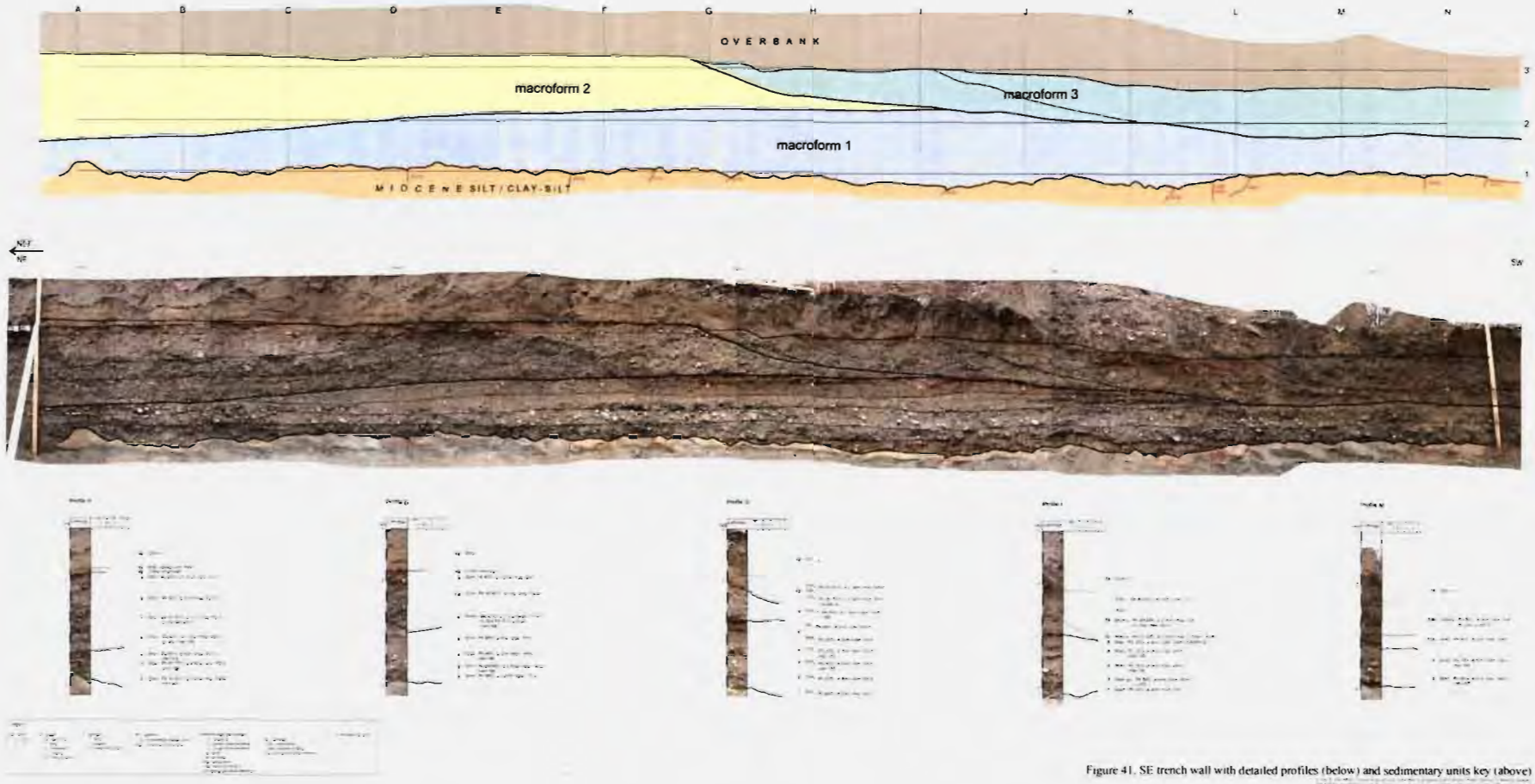

Figure 41. SE trench wall with detailed profiles (below) and sedimentary units key (above)

5.1.4 PRELIMINARY GEOPHYSICAL SURVEY

Preliminary geophysical survey (Appendix 1) was made in the Holocene (historical) alluvial plain, a few hundred meters South of the Libna foothill. The line (200 m long) crossed the whole width of the Libna fault zone in order a) to evaluate thickness of Holocene sediments prior to excavation and more importantly b) to identify potential major deformation at the base of the Holocene fluvial infill. The location of geophysical survey is indicated on Figure 38.

Three methods were foreseen for the survey: refraction seismic survey, active MASW and GPR (ground penetrating radar). However, only refraction seismic survey and MASW were executed (Figure 42), due to elevated water table within the Holocene gravels that obstructed the GPR signal to such an extent that measurements were not possible.

Figure 42. "Landstreamer" acquisition setup for seismic survey across the Libna fault zone

A rough estimate of Holocene infill thickness was attempted by compiling the results of both methods. There were no clear evidence of deformation, yet it was noted that between the points S02 and S05 and especially between S02 and S03 (Figure 43) the Miocene surface is less even if compared to the rest of the profile. For that reason, the decision was made to focus further actions to this part of the fault zone.

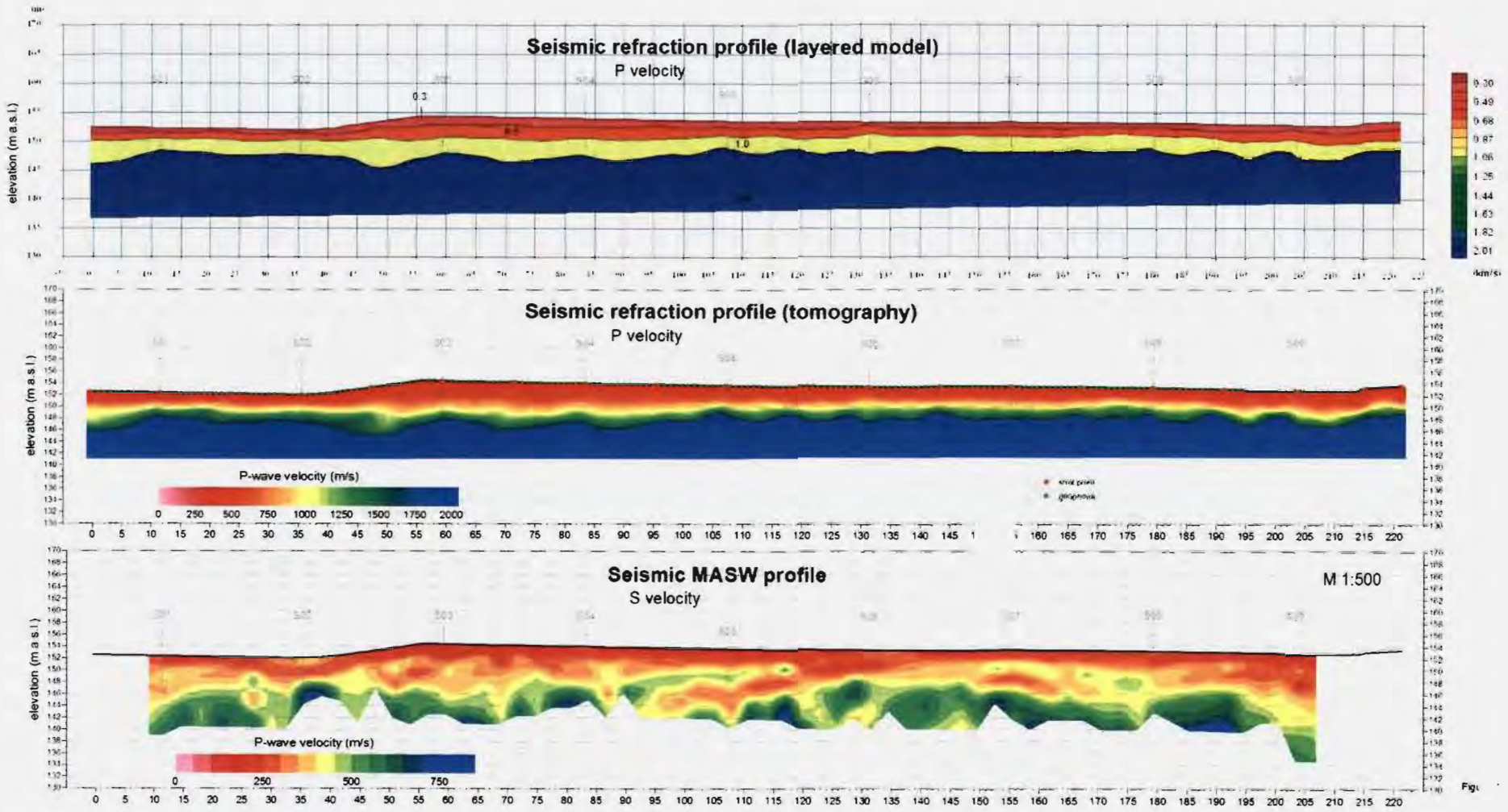

Figure 43: Refraction seismic, and MASW cross sections across the trace of the Libna fault at Stari grad. The direction (right-hand) of the profiles is N69°

5.1.5 TRENCH LOG

The wall was logged in scale 1:20 in a length of 28 m and up to 3 m height. Main mapped units are outlined on the mosaic photography (Figure 41). Description of main sedimentary units is represented here in respect to five vertical profiles drawn about 6 m apart. Description is based on macroscopic observations.

5.1.5.1 DESCRIPTION AND INTERPRETATION OF MAIN SEDIMENTARY UNITS

5.1.5.1.1 General description

The **Miocene base** consists of semi-consolidated silt or clay-silt.

The Miocene sediments are overlain by about 3.5 m thick **unconsolidated Holocene sediments** of fluvial origin. They consist of up to 2.2 m thick **braided-stream deposits** that are overlain by about 1.5 m thick **overbank fine sandy silt**. These sediments were divided into 14 lithological units (Figure 41). Carbonate rocks (mostly limestone) prevail in composition of the pebbles, indicating provenience of the Sava River. The channel deposits are divided into three sedimentary macroforms that are at their bases bounded by erosional surfaces.

5.1.5.1.2 Sedimentary log

Miocene (Pannonian) silt and clay-silt

This layer is very homogeneous. It is very rare to find an evidence of stratification within these grey marls. When found, this is highlighted by an accumulation of shells. At one such spot the in the trench a dip toward SSW (198/22) was observed. The current top surface of this unit is erosional. Together with the facies of upper layers, it is clear that the erosion is of fluvial origin. The most prominent features are the scour marks (25 to 100 cm of amplitude; 10-25 cm of height) (Figure 44. Due to the relative position of steep and gentle slopes, they indicate a clear North-eastward flow.

Figure 44: Example of scour cast at the erosional surface of the Miocene silt and clay-silt / erosional base of the Holocene fluvial sediments. The flow sense to the left (i.e. NE) in fluvial gravels is indicated both by the steeper slope location in the scour cast and the imbrication of flat pebbles.

Holocene braided-stream deposits

The Holocene unit is divided into three sedimentary macroforms (1,2,3) and the overlaying overbank deposits that are further subdivided into lithological units (LU). Denominations and descriptions refer to the Figure 41.

Holocene Macroform 1

The first erosive macroform overlies the Miocene basement and can be divided into five lithological units.

1. Brownish grey massive sandy gravel (SGm). Pebbles occupy 60 % of the sediments. Mean size of pebbles is 2 cm, max. size is 7 cm. The unit is preserved in the depression between G and L. Its max. thickness is up to 30 cm.
2. Grey mostly massive sandy gravel with some indistinct planar cross-bedded at the SE (SGm-(p)). Pebbles occupy 50 % of the sediment, Mean size of pebbles is 3-4 cm, max. size is 30 cm. Imbrication ←NE was observed. The thickness of the unit is about 25 cm.
3. Grey massive sandy gravel (SGm). Pebbles occupy 50 % (70% in places) of the sediment. Mean size of pebbles 4-5 cm, max. size is 20 cm. Imbrication ←NE was observed. The thickness of the unit is about 30 cm.
4. Grey massive sandy gravel (SGm). Pebbles occupy 40-60 % of the sediment. Mean size of pebbles is 3 cm, max. size is 15 cm. Imbrication ←NE was observed. The mean thickness is about 30 cm.
5. Grey and reddish massive sandy gravel (SGm). Pebbles occupy 60 % of the sediment. Mean size of pebbles is 2 cm, max. size 10 is cm. In central part of the trench coarsening upward to massive gravel (Gm) was observed. There pebbles with mean size of 3 cm and max. size 15 cm occupy 80 % of the sediment. The mean thickness is about 35 cm.

Interpretation: The first sedimentary macroform is interpreted as a bar complex composed of five longitudinal bars (lithological units), formed by a braided-style stream, flowing in the direction to the NE (imbrication).

Holocene Macroform 2

The second macroform overlies an erosional surface dipping in the direction to NE and cutting into the first macroform. It is thickening towards the NE, from about 115 cm to about 155 cm (where the lithological units n°5 and n° 4 are respectively entirely and partly eroded). This macroform can be divided into four lithological units in the NE part. Bedding was observed at the NE part of the trench and is getting less distinct (vanishes) toward the SW.

6. Grey massive and trough cross-bedded sandy gravel (SGm). Pebbles occupy 50 % of the sediment. Mean size of pebbles is 2-3 cm, max. size is 15 cm. Imbrication ←NE was observed. Within this unit lenses up to 1m long and up to 15 cm thick of massive gravel (Gm) exist. In these lenses pebbles of mean size around 2 cm occupy 80 % of the sediment. In the NE part of the section we observed transition to planar cross-bedded gravel (Gp) with pebbles occupying 80 % of the sediment. Mean size of pebbles in this sub-unit is 1-2 cm, max. size is 10 cm. Imbrication ←NE was observed

and planar cross-bedding dipping to NE. The mean thickness of the whole unit 6 is about 40 cm.

7. Grey massive sandy gravel (SGm). Pebbles occupy 50-60% of the sediment. Mean size of pebbles is 3 cm, max. size is 15 cm. In the upper part, lenses are observed up to 1m long and up to 15 cm thick, consisting of massive gravel (Gm). In these lenses pebbles occupy 80 % of the sediment, their mean size 2 is cm. The mean thickness of the whole unit is about 35 cm.
8. Grey massive sandy gravel (SGm). Pebbles occupy 40-50 % of the sediment, their mean size is 2 cm and max. size is 12 cm. The mean thickness of the unit 8 is about 60 cm.
9. Brownish grey massive sandy gravel (SGm). Pebbles occupy 40 % of the sediment, their mean size is 1-2 cm and max. size is 6 cm. The thickness of the unit is about 15 cm.

Interpretation: The second sedimentary macroform is interpreted as bar complex composed from longitudinal and (maybe) some diagonal bars, formed by a braided-stream flowing in the NE direction (imbrication and planar cross-bedding).

Holocene Macroform 3

The third macroform overlies the second macroform to the NE and the first macroform to the SW, because of the dip of its basal erosional surface. It is mainly composed of coarse-grained gravely sediments, but some fine-grained silty sediments are enclosed.

10. Dark grey nearly black organic rich sandy silt (OrSSi) with charcoal fragments overlies the second macroform. Toward the SW sediment in this layer coarsens and passes to silty sand. The layer's thickness is 5 cm, however it pinches out (or was eroded) in SW part of the section.
11. Grey horizontally laminated fine silty sand (fSiShl) with laminae of coarse sand and thin beds and lenses of sandy gravel up (lenses up to 2 cm thick) form a thin lenticular sand body that is up to 15 cm thick in NE part of the section and it pinches out to SW. Alternative interpretation of this layer could be that it is a part of the overbank sedimentary unit that overlies it.
12. Grey massive and in SW part indistinct planar cross-bedded sandy gravel (SGm-p). Pebbles occupy 50-60 % of the sediment, their mean size is 2-3 cm and max. size is 10 cm. The cross-bedding is dipping to the NE. This lithologic unit overlies the master erosion surface dipping to the SW, and is cutting into sediments of both the second and the first macroform. It encloses smaller lenses of sandy silt (SSi) as well as erosion and accretion surfaces of the lower order, all dipping to the SW.
13. Grey, partly reddish grey massive and planar cross-bedded sandy gravel (SGm-p). Pebbles occupy 40-60 % of the sediment. Pebbles mean size is 2-3 cm and max. size is 7 cm. It overlies erosion surface dipping to the SW, thus cutting off the 12. lithologic unit and cutting into sediments of the second and the first macroform. This lithologic unit can be divided into two parts (13a and 13b) toward the SW, where it is separated by indistinct erosion or lateral accretion surface. Along the erosion surface the 13a, the unit includes lenses of sandy silt up to 1.3 m long and some rib up clasts of sandy silt, up to 55 cm across. There are also lenses of gravel with pebbles (mean size 1-2 cm; up to 5 cm across) occupying 80 % of the sediment, that gently dip toward the SW.

Pebbles are coated by black Mn oxides in some of those lenses. The sandy gravel is cross-bedded in places. The cross-beds are dipping to SW.

Interpretation: The third macroform is interpreted as channel complex deposited by lateral accretion to the west - South-west. The stream was flowing in a Southward direction .
Between 1st-2nd macroforms and 3rd macroform, the stream thus changed its course by about 90°. It was then flowing to the South, cutting a channel into the older sediments.

Overbank sediments of LU10 and LU11 were deposited before the channel was filed by LU12. LU11 filled a small depression on the second macroform.

Holocene overbank deposits

The uppermost lithologic unit, covering the whole section, is the unit consisting of fine - grained overbank deposits.

14. Grey mostly massive, partly horizontally laminated sandy silt (SSim-(l)) on which a thin veneer of recent soil is formed. The unit is about 1.5 m thick.

Interpretation: This lithological unit is interpreted as overbank sediment deposited by more distant stream running on a flood plain formed by older channel deposits.

5.1.5.1.3 Age of sediments

For the Holocene unit the age was determined by two independent absolute dating methods in three labs (see table 1 for results and Figure 41 for sampling sites). The organic remains of adequate size were treated at commercial ^{14}C lab (Appendix 2), while the small size samples needed more sophisticated approach and were treated separately (Appendix 3). Two samples for OSL age-determination were also analyzed (Appendix 4). Results are listed in table below.

^{14}C (Beta Analytic; Darden Hood)

SAMPLE	REMARK	RESULT
SG1	Peat from the gravel unit. Position provisional due to wall collapse - between B1 and B2	sample destroyed
SG5	Wood from the 5cm clay/silt layer below the upper sand unit. Outside gridded part. App 150 cm left (NE) from A.	170±40 (^{14}C yr)
SG9	Charcoal from the N wall. Upper sand unit.	190±40 (^{14}C yr)

^{14}C (Laboratoire de Mesure du Carbone 14; JP.Dumoulin, C.Moreau)

SAMPLE	REMARK	RESULT
SG4	Wood from the 5cm clay/silt layer below the upper sand unit. Outside gridded part. App 3,9 cm left (NE) from A.	225±30 (^{14}C yr)
SG6	Charcoal from the lower gravel unit. Very small sample. 30 cm left and 20 cm down of B3.	8125±30 (^{14}C yr)
SG7	Peat from the »lower« gravel unit. 75 cm left and 35 cm up from C2.	395±30 (^{14}C yr)

OSL (Institut für Geologie, Universität Bern; Frank Preusser)

SAMPLE	REMARK	AGE
SG2	Upper sand/slit layer. 65cm up and 20 cm right of D3	920 ± 1560 yr
SG3	Collapsed sand/silt clast. 30 cm left and 30 cm up of K2	850 ± 190 yr

Table 1. Absolute age dating results of Holocene sediments from the Stari grad trench. Sampling sites are indicated on Figure 41.

Due to methodological limitations we accept the results for SG5, SG9, SG4 and SG 7 as most reliable. We estimate that the age of SG6 was most probably overestimated due to reworking. Due to very low ages of the sediment, the OSL method did not provide results of sufficient quality and should be in this case neglected. We thus interpret the age of the Holocene unit to be around 200 years b.p. for the uppermost layer and around 400 years for the lower layers.

For the Miocene unit the age was determined by paleontological analyses of ostracode fauna (Appendix 5). Its stratigraphic age was determined to be at the transition between the Lower, and Mid-Pannonian - C/D *Hungarocypris* zone (stratigraphic division after Piller et al. 2007). In absolute age this is roughly around 10,5 million years b.p. which would in global stratigraphic division correspond to the Lower Tortonian.

5.1.6 STRUCTURAL AND NEOTECTONIC OBSERVATIONS AT THE MIOCENE / HOLOCENE BOUNDARY

All along the trench, we found evidences of fracturing within the Miocene unit. Eleven fractures were prominent enough to enable univocal observation and dip measurement (Figures 41, 45). Because of the absence of clear stratification in the marls, we could not infer the amount of potential displacements and we only found once evidence of slip.

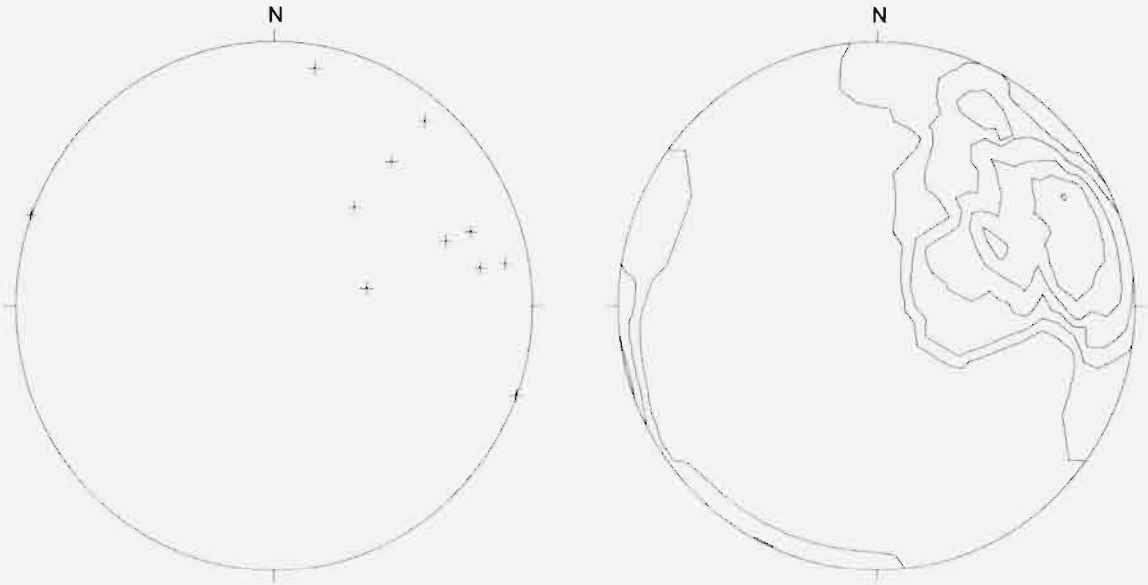

Figure 45. Stereographic projection of fracture poles Equal area, upper hemisphere projection. Left: dip measurements, right: density plot.

Although the number of measurements is too low for statistical treatment, a rough estimate of prevailing strike is possible and does support the hypothesis of direct relation of deformation to the trace of Libna fault zone (NNW-SSE).

The fractures do not exhibit any displacements within the Holocene deposits neither displacement of the Miocene upper erosional surface with an exception of one system. The feature that was observed at the far SW part of the SE wall (the far right deformation shown on Figure 41) may allow an interpretation as being a result of tectonic displacement, not only within the Miocene sediments but also of the Miocene/Holocene boundary. Namely, the irregularity in the erosional surface is oriented opposite to expected scour cast orientation (against the interpreted stream direction). In addition, the erosional surface exhibits a sharp step (5-8 cm high, Figure 46) right above this fracture in Miocene sediments. The system of fractures is prominent enough to be followed across the trench floor to its Northern wall. There, 70 cm Southwest from the NW wall, the general pattern of the faults suggests an apparent right-lateral kinematics on N150° planes (Figures 47 and 48). The strike-slip motion on these faults is confirmed by the gently North dipping striae on some lustrated planes (Figure 49). This general pattern in the Marls is consistent with the expected trace of the mapped Libna fault.

Along a part of this Miocene/Holocene step, we found that the Miocene marls are "striated" along fault, as we can observe linear "negative" imprints with individual lengths of 10-15 cm (Figure 46). These linear features could be interpreted as grooves made by pebbles. This would mean that the Pleistocene/Holocene gravels could have been displaced along the marls

after their deposition, during an offset of the fault. These imprints have a slight plunge to the South (10-15°), which is slightly steeper if compared to the few observed striae in the Miocene sediments (2° to 5°),

Such imprints due to sliding of clasts along a soft rock are known as trailed material indicators (Doblas, 1998) or tapering grooves (Petit and Laville, 1987). We could not observe the tapering shape of the lineation, in order to infer the sense of slip.

The texture of the overlying sediments, as well as the low amplitude of potential displacements, may explain the absence of fracturing or shearing. The Pleistocene gravels have here a large amount of sandy/clay matrix. This "non-shearing" behavior is known for similar conditions (lithology, saturated or soft sediments), even for larger offsets

There is however, a plausible interpretation of these features that does not include tectonic displacement along the fault after deposition of the Holocene gravel. Since the deformation were found at the far end of the trench, we had a chance of removing in full the Holocene sedimentary sequence at the SW trench wall and see the irregularity also in ground plan (Figure 50). Following its trace in length of app 3 m, it became clear that the step (offset?) in the erosional surface diminishes from 5 - 8 cm to none. The fractured zone below the gravel infill has served as groundwater conductor which is well visible at its upper surface (Figures 46 and 50). From this we infer that it is possible that only groundwater flow caused the selective erosion along deformed thus softened sediment. In that interpretation, deformation continuation since deposition of Holocene sediments is not necessary to explain our observations. No visible deformation in gravel above such erosional feature (a collapse) can have identical explanation as lack of visible deformation in the same material when tectonically deformed.

Figure 46. A sharp step in the Miocene / Holocene erosional boundary before and after the full cleanup of the ground plan.

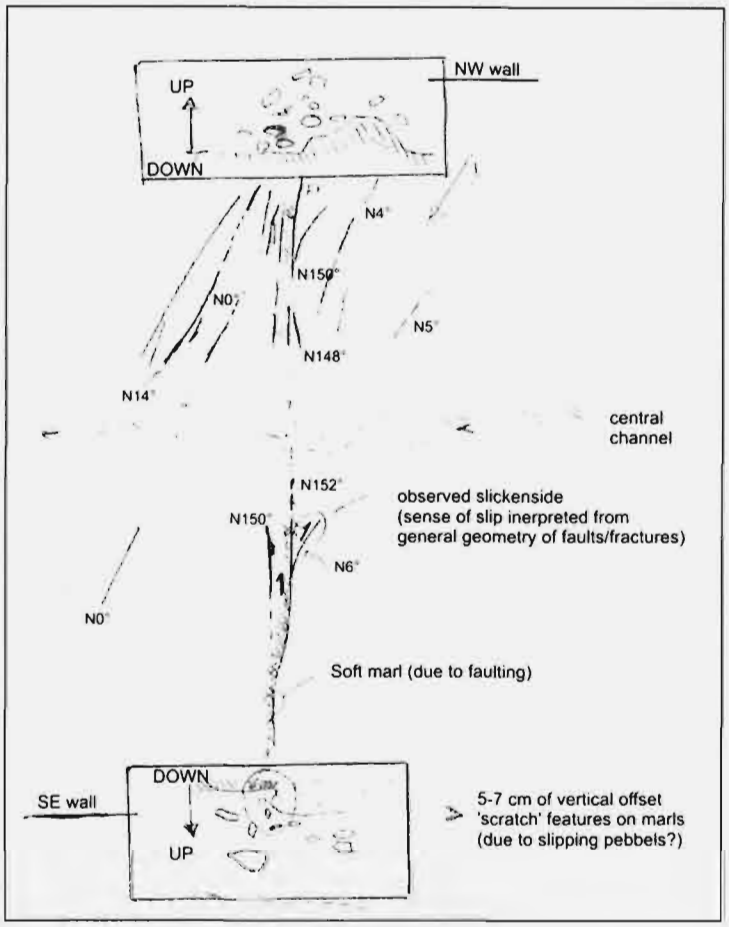

Figure 47: Sketch map of the N150° fault zone in the Miocene sediments. The 2 insets represent the schematic section of the walls at the location of the observed step in the Miocene/Holocene boundary.

Figure 48. Continuation of the N150° system of fractures to the NW trench wall

Figure 49: Lustrated fault plane and low dip slickenside, within the Pannonian marls. After removing sediments of the fault's opposite block.

Figure 50. The irregularity in Miocene /Holocene erosional Boundary after removal of Holocene fluvial sequence from the NW trench wall.

5.1.6.1 STRUCTURAL INTERPRETATION

These tenuous observations are not conclusive concerning the recent activity of the Libna fault. Faulting within the Miocene sedimentary sequence is a fact, however its continuation into the Holocene fluvial sediments is highly ambiguous. We believe that given the amount of information that we obtained from this survey, two interpretations are equally plausible:

1. The step in the Miocene / Holocene boundary is an erosional feature formed due to enhanced erosion along the faulted and fractured Miocene substratum.
2. The step in the Miocene / Holocene boundary is an offset along one of the fault planes within the Libna fault zone.

5.1.7 CONCLUSIONS FROM THE STARI GRAD TRENCH

The aim of the paleoseismological trench was to determine possible recent activity of the Libna fault by finding either:

- tectonic displacement within the Holocene fluvial cover or,
- tectonic displacement of the boundary between the Holocene fluvial cover and its Miocene silt / clay - silt substratum.

The results are ambiguous.

Tectonic displacement within the Holocene fluvial sedimentary sequence was not observed. However, the fluvial gravel is only up to 400 years old, so minor displacements may have been overlooked. With a slip rate of 0.1 mm/a (order of magnitude), one can only expect 4 cm of displacement if the Libna fault was active. In addition, such coarse grained and loose sediments may compensate for significant displacements by internal restructuring of the sediment.

Tectonic displacement was also not conclusively observed at the boundary between the Holocene fluvial cover and its Miocene silt / clay - silt substratum. However, at the far SW side of the trench a series of evidences were observed that may equivalently lead to two opposite interpretations. The first interpretation does not include any tectonic displacement after deposition of the Holocene gravel (in historic times). The second interpretation, on the other hand, infers post depositional tectonics.

In order to narrow down the ambiguities it was proposed to GEN Energija d.o.o. that further paleoseismological survey should be performed in the Libna hill or at its foothills where older sediments could have recorded more cumulated deformation if it exists. The proposed survey was accepted and is described in the following chapter.

5.2 LOCATING PALEOSEISMOLOGICAL TRENCHES ON THE LIBNA MOUNTAIN

5.2.1 INTRODUCTION

After the results of the Stari Grad trench were realized as potentially ambiguous, a proposal was accepted by the client to broaden the Libna fault paleoseismological survey on the Libna Mt. The work was agreed upon with the Annex No. 1 to the main contract.
The survey on Mt. Libna was proposed in three steps, of which two were conducted by the time of finalization of this report and with which we were able to select the best sites for the third step – paleoseismological trenching.

1. Sedimentary test pits were made across the Libna Mt. to investigate the feasibility of successful paleoseismological trenching.
2. The trace of the Libna fault zone was surveyed by three geophysical methods (electrical resistivity mapping, GPR, 2D resistivity tomography) in order to identify maximum of potential deformation in the subsoil.

Phase 3 (trenching on Libna) was postponed into early phase 2 of the project.

Partial reports are presented as Appendices 6, 7 and 8. .

5.2.2 SEDIMENTARY TEST PITS ON LIBNA

Seven test pits were excavated in order to asses a possibility for potential GPR measurements on previously defined locations in the Libna fault zone (Figure 51). Two locations were defined in the area where the Libna fault trace crosses a narrow terrace along the Southern slope of the Mt. Libna. Three test pits were planned across the infill of the two morphologically expressed fault zones that belong to the Libna fault and two were planned below the escarpment near the top of the Mt. Libna where the potential post-Plioquaternary offset is supposed to be the most prominent.

The summary of the full report that contains all logs and photographs of pits (Appendix 6; Rižnar, 2009) is presented here. Presented here is only a part of graphics that illustrates the area that was in step 2 (geophysics) selected as most suitable for trenching in step 3.

Test pit L-1/09
The L-1/09 reached karstified white Badenian limestone at the bottom of the pit in the depth of 3,5 m. The limestone is covered by fat inorganic reddish marmorised clay without any pebbles. At least 1.5 m of clay is observed in the pit. The clay is covered by 20 cm thick layer of gravel with silty to clayey matrix. The gravel layer is tilted to the North by 20°. The boundary between the gravel and the clay is blurred. The gravel is covered by inorganic marmorised clayey silt with low plasticity. The silt contains occasional noncarbonate pebbles, limonite nodules and coatings. The uppermost layer is 170 – 230 cm thick in the test pit. The age of the gravel is probably Plioquaternary.

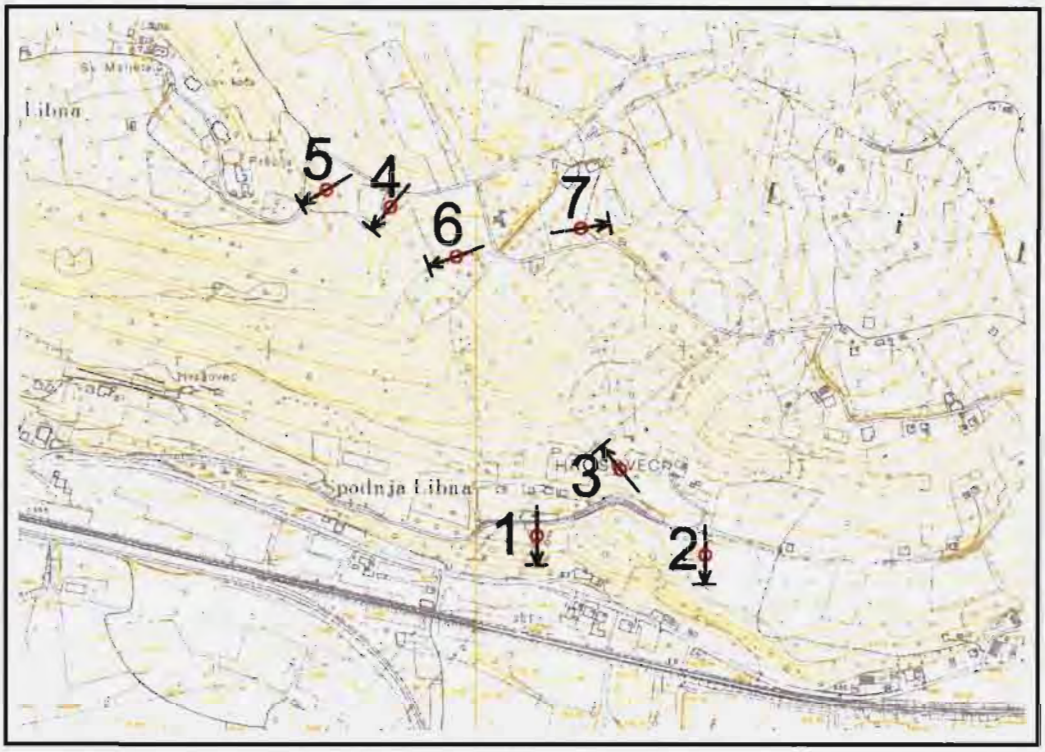

Figure 51. Location and orientation of the test pits on Mt. Libna

Test pit L-2/09

Almost identical situation is observed in the test pit L-2-09. The same fat reddish marmorised clay without any pebbles is deposited upon the karstified white Badenian limestone. Towards the surface, t he reddish clay is gradually becoming silty and lean with occasional noncarbonate pebbles. The upper "layer" in the pit is the same as in the test pit L-1/09, marmorised clayey silt with limonite nodules and occasional noncarbonate pebbles. Except for the missing gravel layer, the test pits L-2-09 and L-1-09 are identical. The inclination of the boundary between the reddish clay and the overlying silt could not be observed due to blurred transition between the clay and the silt.

Test pit L-3/09

Test pit L-3/09 was located on the edge of a relatively flat valley representing one of the fault zones of the Libna fault. Badenian limestone was found in the depth of 380 cm. Brown silty clay with occasional noncarbonate pebbles was observed on the limestone. Between 300 and 270 cm, a layer of a clayey silt with organic matter and fragments of bricks was observed. Marmorised clayey silt with occasional pebbles, limonite coatings and nodules is observed on top of the layer with organic matter. The uppermost layer is clayey silt with fragments of

Badenian limestone and occasional noncarbonate weathered pebbles. The approximately 20 cm thick layer between 2.70 and 3.00 m is interrupted in the South-western wall of the test pit, but the boundaries are not sharp. However, the landowner explained that a landslide was triggered in 1954 in the test pit area, so the darker layer is most probably the pre-slide surface, covered by a colluvium.

Test pit L-4/09

A succession of a fat marmorised reddish inorganic silty clay with limonite coatings, and a completely weathered gravel was observed in the test pit L-4/09 (Figure 52). The underlying clay is without any pebbles, and similar as the one found in the test pits L-1/09 and L-2/09 on a top of the karstified Badenian limestone. The boundary between the clay and the weathered gravel is not sharp and neither flat, but rather irregular. The gravel is completely weathered. Only the quartz, some chert and quartz sandstone pebbles are still recognizable. Other pebbles are weathered into silt, clay and sand. The uppermost part of the gravel is 20 cm thick, where the quartz and chert pebbles are concentrated (Figure 53). The uppermost part of the gravel contains also less silty matrix. The uppermost 50 cm is recent soil, silt with noncarbonate pebbles

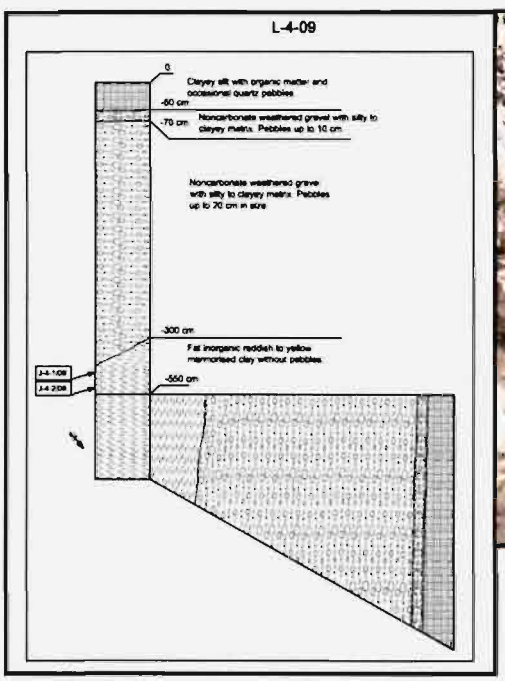

Figure 52. Test pit L-4/09

Figure 53. The uppermost part of the gravel and soil above in the test pit L-4/09.

Test pit L-5/09

Test pit L-5/09 (Figure 54) was located in the colluvial slope in the zone of presumably the most prominent branch of the Libna fault. The test pit was 5.5 m deep. Fragments of the Badenian limestone up to 15 cm in size were observed in the uppermost 20 cm of the soil (Figure 55). Only reddish marmorised silty clay with limonite coatings and large blocks of the Badenian limestone was observed throughout the rest of the test pit. Some streaks of greenish lean clayey silt were observed and sampled in the clay, but no pebbles. A lump of darker clayey silt, probably containing organic matter is found 1.5 m below the surface. It is not clear

whether the limestone at the bottom of the pit represents a large colluvial block or intensely karstified basement.

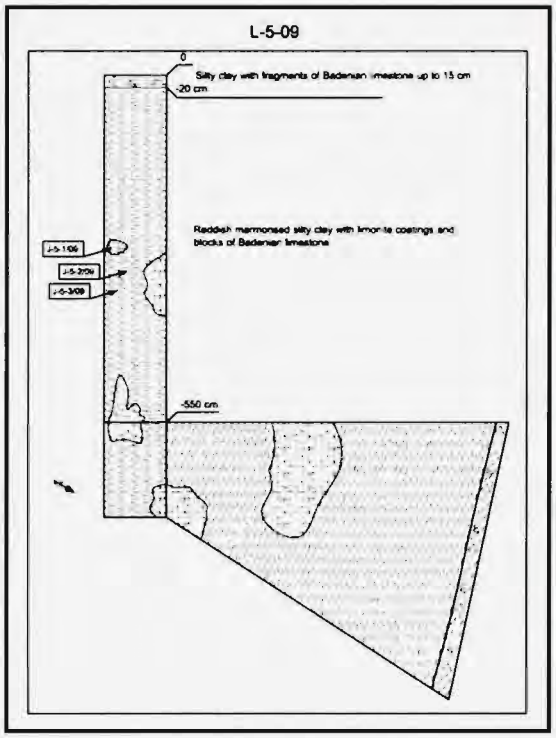

Figure 54. Test pit L-5/09

Figure 55. Test pit L-5/09

Test pit L-6/09

Test pit L-6/09 (Figure 56) had similar position like the L-3/06 test pit. The L-6/09 test pit was located in a relatively flat valley, a morphological feature related to the South-westernmost branch of the Libna fault. The pit was 4.5 m deep and did not reach the Badenian limestone basement. The same reddish silty clay with limonite coatings was observed in the deeper part of the pit. Between 1.8 and 2.4 m, a layer of completely weathered gravel was observed (Figure 57). A layer of gravel is formed in a flat channel parallel to the valley (see Figure 51). The gravel is covered By a marmorised clayey silt with occasional weathered noncarbonate pebbles up to 10 cm in size.

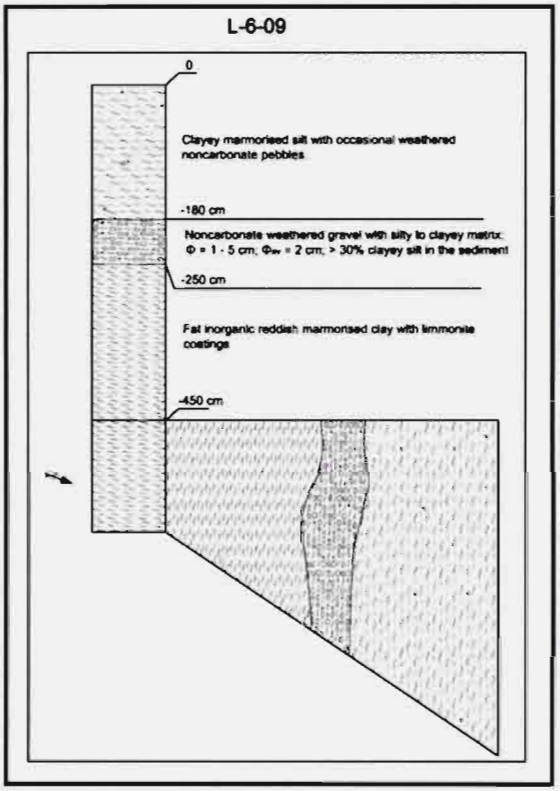

Figure 56. Test pit L-6/09

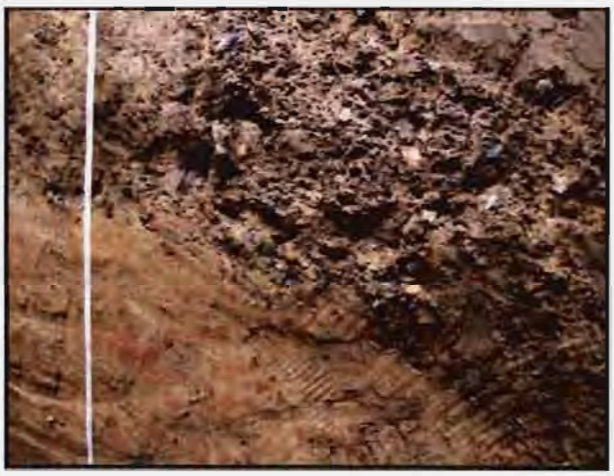

Figure 57. Marmorised silty clay is covered by weathered gravel with silty and clayey matrix in the test pit L-6/09.

Test pit L-7/09

Test pit L-7/09 was located in the same valley as the L-3/09 but approximately 250 m due North (Figure 51). Only reddish clay with colluvial blocks of Badenian limestone were observed in the test pit. Limestone blocks were up to 1 m in size. The clay contained organic matter from the open sewage above the test pit location. No pebbles were observed in the silty clay nor any other sedimentary feature.

5.2.3 GROUND PENETRATING RADAR AND RESISTIVITY SURVEY ON MT. LIBNA

Intensive GPR sounding and resistivity mapping at several areas at Mt. Libna was conducted for recognition of shallow deformation in Miocene and/or Plioquaternary sediments due to Libna fault. The full report (Mušič, 2009) is appended to this report as Appendix 7.
All roads crossing Libna fault zone in east-west direction were surveyed by GPR profiles (Figure 58; profiles GPR pr_1 - 5). Besides roads, several areas inside of the territory of Libna fault zone were selected for resistivity mapping (Figure 58; Areas 1 – 9). For revealing sharp lateral changes in resistivity of top 3 m thick horizon resistivity mapping applying »twin probes array« was used. This probe geometry was designed for »enhancing« contrasts in horizontal direction. Acquisition was conducted in dense grid with 2 m separation between parallel profiles and 1 m distance between measuring points along profiles, what should assure expected quality of survey. Resistivity maps were smoothed by low pass filter in window dimension 1x1 what gives softer appearance of otherwise only slightly sharper anomalies observed in raw data. The same areas were resurveyed with parallel GPR profiles with 10 m profile separation for independent data source and more reliable interpretation. Because of exclusively linear low resistivity anomalies, we consulted all existing infrastructural maps. Deep modern trenches for subsurface infrastructural installations can sometimes significantly reduce apparent resistivity over much larger space than the physical geometry of infrastructures is. Quite impressive collection of infrastructural maps for surveyed area and its near surroundings doesn't show any spatial correlation with observed resistivity anomalies. GPR echoes from infrastructures were depicted on GPR profiles and eliminated from interpretation.

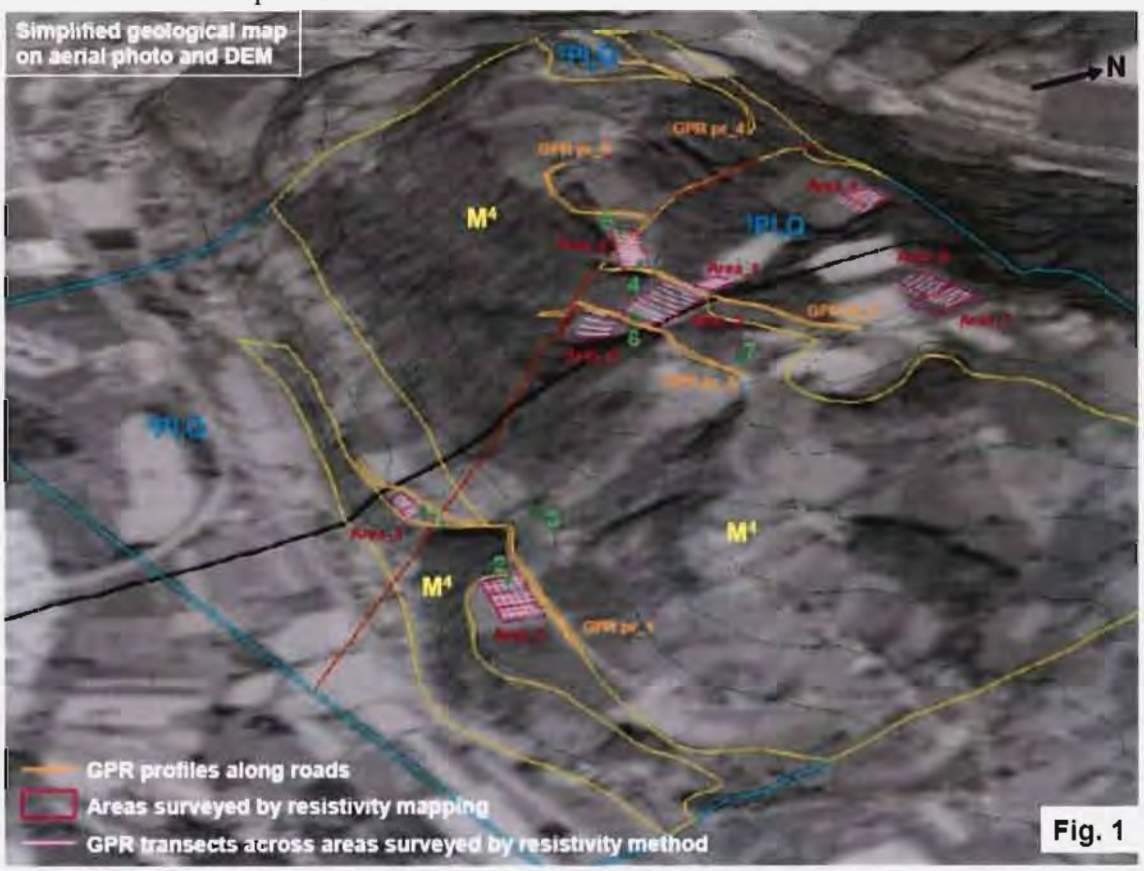

Figure 58. Site map of geoelectric resistivity mapping and GPR surveying on Mt. Libna.

5.2.3.1 RESISTIVITY SURVEY

The name The twin probes array arises from the two identical pairs of electrode probes (C1P1 in C2P2). One pair of the current and potential electrodes (C1P1) is practically infinitely distant from the other matching pair (C2P2). This condition is met in the field by a at least 30-fold distance between mobile probes (C1P1). Such a mutual distance between both twin probes prevents the orientation of the measuring twin probe from having much of an influence on the measured values. In order to detect relatively small lateral differences in resistivity, it is important that they are situated in the vicinity of a high gradient electrical field during measurements. This means that they would need to be in the direct vicinity of the measuring twin probe; in practice this denotes a high lateral resolution for structures with high resistivity shallowly beneath the surface.

This method is applied exclusively for geoelectric mapping as the values of the apparent resistivity are recorded to the same depth, which is determined by the distance between the mobile twin probes (C1P1). At a distance of 1 m, and with optimal humidity of the soil, the depth range measures app. 3 m. In addition to the distances between the mobile twin probes in the depth range, the seepage of the soil also has significant impact. The depth range is usually less when there is a high level of humidity in the upper soil layer; this is because most of the electrical current flows in the direction of higher electrical conductivity shallowly beneath the surface. Geoelectric mapping was executed in a grid of 2 x 1 m and the measured values were interpolated by bicubic interpolation to a grid of 1 x 1 m. The measured electrical resistance is converted into resistivity by the simple equation $\rho = \pi Ra$, whereby ρ is the apparent resistivity, R is the measured resistance and a is the distance between the mobile twin probes. The results from this calculation are presented in figures. 4, 5, 6, 7 and 8 of the full report (Appendix 7- Mušič, 2009) where directions of the most obvious aligning of lateral changes in resistivity are indicated. In some areas (Area 7, for instance) correlation between grayscales contrast on aerial photos and measured variability in resistivity is evident. It can not be excluded that some differences appear as consequence of moisture distribution as a consequence of modern land use, infrastructural objects etc. Therefore, all available maps of infrastructural installations were consulted for more reliable interpretation and no spatial correlation with resistivity anomalies was observed.

Possible noise sources for resistivity mapping:
External sources:
- Shallow low resistivity medium:
- Infrastructural ditches
- Sharp lateral changes in resistivity as consequence of topography and/or sediment composition (different moisture capacity)
- Efficiency of modern land use on moisture distribution

Results of resistivity mapping are represented in resistivity span exclusively chosen for every single area separately in the way that lateral resistivity changes are enhanced and clearly visible. The selected span is indicated for every surveyed area (1-9) separately on the maps. On the basis of test pits description the situation for upper 3-4 m is quite unique with dominant clay sequence with or without intercalations of thin layers of pebbles and/or Badenian limestone blocks in some areas superimposed above Badenian limestone.

Area 1 and 2 (Figure 58): Background resistivity at the Area 1 is slightly lower than at Area 2. In both areas Badenian limestone was encountered at depth 200 and 330 cm respectively.

Higher resistivity values at Area 2 can be at least partly consequence of "noncarbonated weathered gravel" which appear in test pit 1 at depth 230 cm. Resistivity mapping at Area 2 with otherwise unique resistivity distribution, revealed sharp resistivity boundary at the most western part.

Areas 3, 4, 5 and 6 (Figure 58): Several more than less parallel low resistivity anomalies occur in the Area 3. The resistivity span is between 148 and 182 ohm.m. No surface indications for these significant anomalies were observed. In the test pit no. 6, at the depth of 180 cm "noncarbonate weathered gravel" appears. Linear, low resistivity anomalies across the Area 3 in the direction Northwest - Southeast, can be interpreted as consequence of interruptions in this gravel horizon. Towards the west resistivity readings are higher what suggests the efficiency of colluvium with Badenian limestone blocks and/or limestone bedrock closer to the surface. Low resistivity at the Area 6 (166-210 ohm.m) can be also result of water saturation on contact between limestone and prevailing clay sediments to the east.

Areas 7, 8 and 9 (Figure 58): In Areas 7 and 8 in general, significantly higher resistivity values were measured than on other areas. The whole resistivity span for Areas 7 and 8 and Area 9 is 345-464 ohm.m and 207-361 ohm.m respectively. High resistivity background is consequence of limestone bedrock closer to the surface. The origin of sharp linear low resistivity anomaly in the direction North-South at the Area 7 is unknown.

5.2.3.2 GROUND PENETRATING RADAR SURVEY

Measurements were carried out using the classic reflection measuring technique, where there is a short distance between the transmitter and the receiver. By altering the position of the monostatic transmitter-receiver, traces of a connection profile with a particular density are built up along the profile. The resolution classifies the capacity to divide two nearby forms before they seem like one to the viewer. First and foremost, it is the central frequency antenna that classifies it, while at the same time having a strong influence on the relative dielectric constant, or the dielectric material in which the measurements are being executed. The resolution is mostly dependent upon the wavelength. The wavelength of electromagnetic waves from a 200 MHz antenna, as was used in the georadar investigations at Mt-. Libna, measures 1.5 m in the air. In materials with a relative dielectric constant of 15, this wavelength decreases to 0.52 m.

At the evaluated average dielectric constant (15), the wavelength of a 200 MHz antenna in this ground measures approximately 0.5 m. Essentially this means that horizontal layers thicker than 0.15 m can be reliably discernible on the GPR profiles. The higher the permittivity of the surface material, the slower the propagation of electromagnetic waves; at the same time, the sheaves of the elliptic cone determining the ratio between the depth and resolution will be narrower. The measured parameter in georadar measurements is double the time a wave travels and it is expressed in nanoseconds (10-9s). By knowing the dielectric constant, and thus also the speed of expansion of the EM fluctuation in the investigated media, the times of the reflections may be calculated into units of length, or rather depth sections. For more reliable interpretation of GPR profiles all different noise sources have to be recognized and eliminated prior to interpretation.

Noise sources:
External sources:
- High voltage power lines
- Subsurface infrastructural objects
- Strong contrast in dielectric permittivity between road construction material and clay sediments (....multiples)
- Significant signal attenuation with depth in wet conditions
Internal sources:
- Low frequency "ringing"
- "Snowy" appearance because of close maximum depth range of 200 MHz antenna EM signal effective penetration.

Basic processing procedure incorporated following processing steps for reducing noise:

XFl ipProfile / 0 / 0 / 0 / 0 / / 0 / 0 / 0 / 0
remove header gain / 0 / 0 / 0 / 0 / / 0 / 0 / 1 / 14434
cor rect max. phase / 15,5 / 18,5 / 16,7291 / 0 / / -1 / 1 / 1 / 0
move starttime / -16,72481 / 0 / 0 / 0 / / 0 / 1 / 1 / 0
background removal / 0 / 163,125 / 0 / 288,66 / / 0 / 0 / 0 / 0
manual gain (y) / 4,413792 / 61,10345 / 0 / 0 / / 0 / 0 / 1 / 14434
subtracting average / 500 / 0 / 163,125 / 0 / / 0 / 0 / 1 / 14434
average xy-filter / 3 / 2,0736 / 0 / 164,125 / / 0 / 0 / 1 / 14434
Kirchhoff migration / 50 / 0,08 / 0 / 163,125 / / 1 / 0 / 1 / 14434
bandpassfrequency / 50 / 150 / 250 / 350 / / 0 / 1 / 1 / 14434
manual gain (y) / 2,344827 / 11,86207 / 0 / 0 / / 0 / 0 / 1 / 14434
Traceinterpol-3DFile / 0,02 / 285 / 0 / 0 / / 0 / 0 / 0 / 0

GPR echoes were classified into few groups on the basis of signal characteristics (see Appendix 7, Mušič, 2009):

1. Limestone close to the surface (compact limestone)
2. Limestone bedrock
3. Limestone bedrock and colluvium with limestone blocks
4. Signal attenuation (wet clay?)
5. Sharp limestone boundary
6. Echoes from inclined strata

5.2.3.3 CONCLUSIONS FROM GEOELECTRIC MAPPING AND GPR SURVEY ON MT. LIBNA

It is evident that resistivity span for any of surveyed area doesn't prove significant resistivity anomalies. It is also true that probe configuration used for this resistivity survey is sensitive for changes in top soil water content and therefore results represents also general map of moisture distribution. We couldn't recognize any of surface evidences which can possibly control moisture distribution and consequently affect resistivity measurements. Topographically all areas are flat with certain inclination but without clear linear micromorphological surface features in the direction of low resistivity anomalies. At the area 7, for instance, sharp resistivity boundary can be correlated with darker stripe on aerial photos what is clear indication for high water saturation but without any surface indications.

The most prominent (potential) deformation observed is at the Area B (Figure 59).
In GPR profile GPR pr_3 sharp vertical boundary between limestone bedrock and presumably clay/colluvium sediments to the east, can be clearly traced (see Appendix 7, Mušič, 2009). GPR profiles over limestone bedrock here show chaotic echoes and only some sequences of echoes from inclined strata what suggests more than less fragmented limestone bedrock. It can be natural appearance of Badenian limestone, but tectonic influence can't be excluded only on the basis of GPR survey. Anyhow, this area and its near surroundings should be, according to our results, resurveyed by geoelectrical pseudosections for more reliable interpretation (Figure 59).

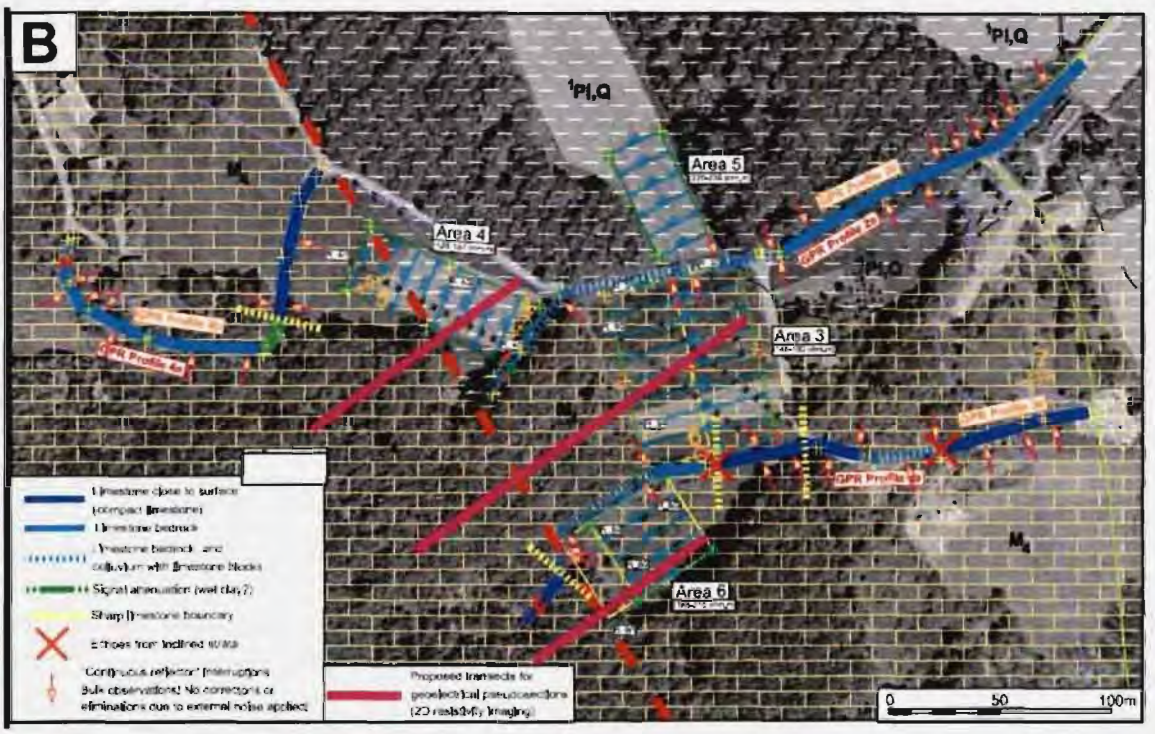

Figure 59. The area of most prominent potential deformation along the Libna fault [redacted] as shown by geoelectric resistivity mapping and GPR surveys combined. In purple t[redacted] proposal for 2D resistivity tomography is presented that was later slightly adapted to field conditions and is described in the following chapter.

5.2.4 ELECTRICAL RESISTIVITY TOMOGRAPHY ON THE LIBNA FAULT AREA

5.2.4.1 DESCRIPTION

Following 1) sedimentary investigations by test pits and 2) combined geoelectrical mapping and GPR survey it was proposed to the client (and accepted) to perform additional 2D resistivity tomography (ERT) along selected sections in order to narrow down the ambiguity regarding localization and extent of potential deformation caused by the Libna fault. More specifically, the tomography had 2 main objectives:

- Highlight any sustained-vertical discontinuities which may correspond to active faults in the colluvial cover based on the Badenian limestone formation;
- Confirm the location of the westernmost fault of bundle Libna and to characterize it.

To answer these objectives, it was decided to perform 3 ERT sections of about 200m long intersecting the Libna fault where deformation was observed as potentially most prominent by previous works (proposal presented on Figure 59; actual sections presented on figure 60).The electrical device recommended for achieving these two goals is the dipole-dipole, as this method is most suited to the detection of sub-vertical discontinuities. The geometry of the system has also been chosen to meet these 2 objectives (Figure 61):

- dipoles of 1.5m with n = 1 to n = 8 for an investigation depth of about 3m, with a vertical resolution of 25 to 50cm in order to detect possible vertical shifts affecting colluviums;
- dipoles of 3m with n = 4 to n = 8 for an investigation depth of about 7m;
- dipoles of 6m with n = 4 to n = 8 for an investigation depth of about 13m in order to achieve the Badenian limestones. According to geological estimations, the roof of the limestone should be at least 10m deep.

Figure 60. Location of ERT lines (lines 1 to 3), principal structures observed on ERT and proposed trench sites

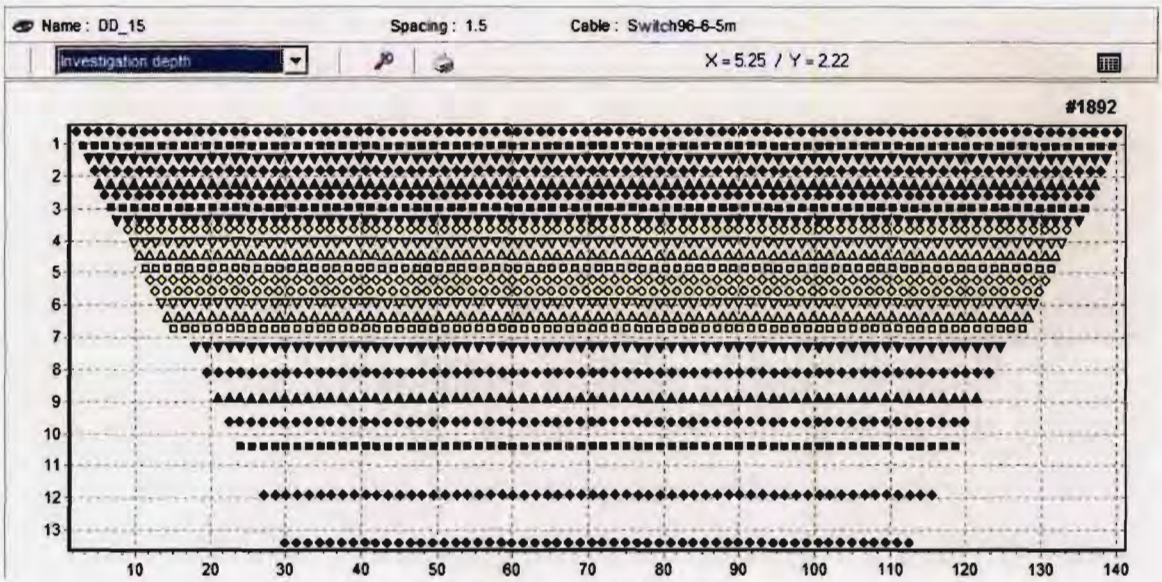

Figure 61. Geometry of the ERT survey

The position (X, Y) and leveling (Z) of 3 lines were made by GPS and a theodolite (see Appendix 8, Mušič, 2010).

Equipment used

- 1 Syscal Pro 96 (IRIS Instruments)
- 6 cables 96 channels
- 96 stainless steel electrodes
- 1 GPS
- 1 theodolite
- Software (Prosys, electre pro,X2IPI,res2dinv)

5.2.4.2 RESULTS

General structure

A major sub-vertical discontinuity (F1) is highlighted in the SW part of the 3 lines (Figure 62, Figure 63). It probably corresponds to the westernmost fault of the Libna zone. In the absence of well-characterized marker horizon, it is difficult to estimate the throw of this fault. However given the resistivity contrast between the SW compartment (resistant) and the NE compartment (conductive), it is likely that the NE compartment collapsed.

Given the morphology of geoelectrical horizons revealed, it would be in the presence of an anticlinal structure in the SW compartment (particularly visible on the line 2) and a synclinal structure in the NE compartment (or central compartment).

A second major discontinuity (F2) is also suspected in the NE end of the 3 lines. It is poorly characterized because it is located at the end of the profiles but it appears to confirm the collapse of the central compartment. It could correspond to the fault of the Eastern Libna fault area (more precisely the eastern edge of the divergence of Libna SW fault area).
Within the compartment collapsed, the electrically resistant bedrock (resistivity> 700 ohm.m) lies at a depth of about 9 m which is identical on the 3 lines. This horizon may correspond to

the sound limestones. In the SW compartment these sound limestones may be sub-outcropping.

Structure in the central compartment

In the central compartment, the vertical distribution of geoelectrical horizons is upwards as follows (Figure 62):

- An electrically resistant bedrock R1 (resistivity> 700ohm.m) corresponding to the sound limestone of the Badenian formation;
- An electrically conductive Horizon C1 (resistivity <30ohm.m), with a thickness of 3 to 5m relatively constant over the 3 profiles. The conductive unit may correspond to the zone of weathering of limestone (decalcification clays);
- A high resistant area R2 (50 <resistivity <500 ohm.m) with a thickness of about 1.5 to 2m continuously present in the central compartment and on each profile;
- A conductive horizon C2 (resistivity <30ohm.m) with a thickness of about 0.75 to 1.5m present throughout the central compartment and on 3 profiles;
- A surficial layer of quite variable resistivity (30 to 500ohm.m) and with a thickness of between 1 and 2m.

Within this compartment, several discontinuities (D) were identified through sub-vertical shifts of the horizons C1, C2 and R2. The numbers of discontinuities are 5 on line 1, 5 on line 2 and 6 on line 3. They are slightly marked within the electrically resistant bedrock (R1), probably due to a lower resolution at this depth and they do not affect the surficial horizon. The vertical throws generated by these discontinuities are very small (1 to 1.5m maximum).

5.2.5 CONCLUSION AND PROPOSITION OF TRENCH SITES

Trench sites 1 and 2 (Figure 60, Figure 63) are located perpendicular to a structure interpreted as the F1 fault zone. This fault zone is represented on the three ERT profiles by a strong contrast from high resistivity values to the West, to low resistivity values to the East (Figure 62). This anomaly is interpreted as the abnormal transition zone between Badenian limestone and Plio-Quaternary deposits. ERT profiles allowed also suspecting internal deformation into the Plio-Quaternary formation that could be associated to deformation associated with the F1 fault zone. According to the interpretation of ERT profiles, the trench site 1 is the most favorable for trenching, but it appears that crossing the F1 structure could be impossible due to both the relief and vegetation. Then, the trench site 2 is proposed as a complement in order to be sure to cross the F1 structure.

Trench site 3 is located on a more ambiguous structure observed on each ERT (Figure 63). This structure appears as a vertical discontinuity interpreted as a possible F2 fault. As it is not possible to exclude the existence of such a structure, a smaller trench is proposed on this site.

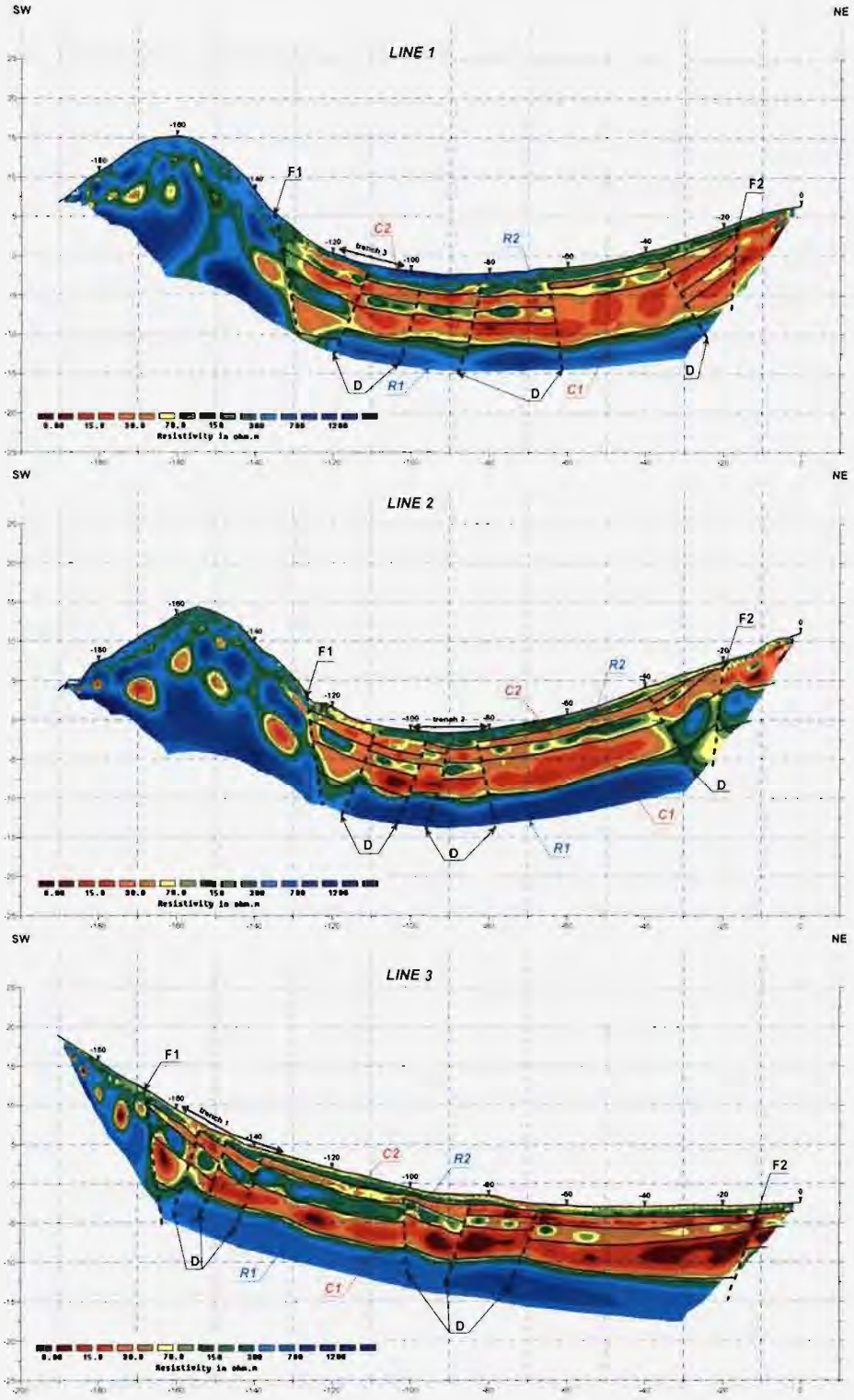

Figure 62. Definition of layers and observations of potential structural deformation along ERT sections 1 to 3.

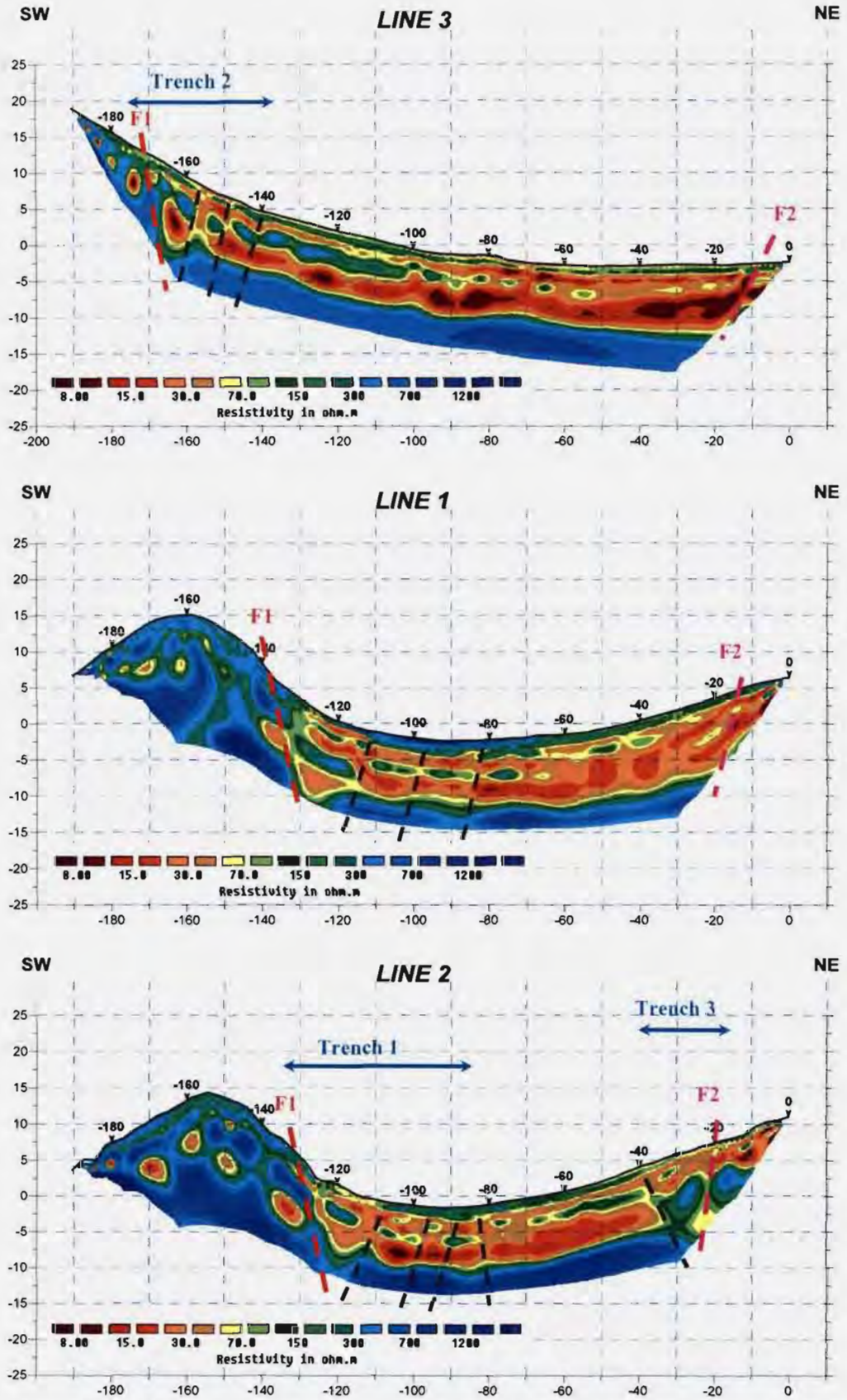

Figure 63: ERT sections with localization of F1 (red) and F2 (pink); deformation within Plio-Quaternary deposits (black) and localization of trenches

6 SITE GEOLOGY

6.1 GEOLOGICAL STRUCTURE OF THE EAST SITE

E site is completely covered with **Quaternary gravely-sandy sediments (Q_2)** of Holocene age. They are composed primarily of carbonate gravel and sand. More precise composition is evident from chapter "Lithological logging of the cores of the boreholes" (see below) and in the report about the initial field investigations for potential LILW deposit Vrbina (Brenčič (ed.), 2006; Petkovšek (ed), 2009). In the construction of the thickness of Quaternary gravely-sandy sediments, we used boreholes made within the scope of this project, and also other available data. The thickness of Holocene sediments increases from North to South and reaches a maximum thickness of 10,5 m. Geoelectric investigations (Car & Stopar, 2008) have shown that the thickness of Quaternary sediments is actually highly variable; however, the density of data for the production of a reliable map of thicknesses is still insufficient.
Previous geoelectrical investigations (Car & Stopar, 2008) raised up the question of the geological structure in the Southern - central area of the E site, which show that there are markedly silty-sandy or even clayed Quaternary sediments present there. This area actually overlaps with a part of the fly ash landfill, but we nevertheless allow for the possibility that its actual extent is greater than the one shown in the original plan, from which it was transferred into the geological map.

Lithological units below Holocene (Q_2) sediments

Southern part of the E site is covered with **Plio-Quaternary sediments (Pl,Q).** Plio-Quaternary sediments disconformaly overlay the Miocene (Upper Pontian) sediments. They consist predominantly of polymict quartz silty (muddy) sandy gravel with intercalations of sandy gravel, pebbly sand, pebbly silty sand, sand, pebbly clayey silt and clayey silt. For detail sedimentological analysis see chapter 6.3. Lithological logging of the cores of the boreholes" and Appendix 9 (Trajanova et al., 2009).
As regards the current knowledge of the Plio-Quaternary sediments, we can state that the paleorelief, where the Plio-Quaternary sediments were deposited, is not uniform because of the type of sedimentation and cannot be treated as a flat plane. In addition, it cannot be adequately reconstructed because of the insufficient amount of data. It is possible that in places we could only find their relatively thin and isolated erosional remnants. Plio-Quaternary sediments were deposited synchronously with the folding of the Krško syncline and were later partially eroded.
The crucial question is the position of the pinch-out boundary line of the Plio-Quaternary sediments under the Holocene sediments. Based on the data from new boreholes (ED-1, ES-1), older ARAO boreholes (VOP-6, VOG-2) and previous geoelectric investigations (which are however to some extent doubtful and contradictable), we can conclude, that the pinch-out line runs somewhat North of borehole VOP-6, generally in the E to E-NE direction. The dip angle of the contact with the underlying Miocene sediments is around 20° to the SSE in the Northern part, further to the South the dip angle is more gentle (almost horizontal) towards the axis of the Krško syncline (Figure 64). Compared to the last known report on this matter (Petkovšek, ed., 2009) the pinch out line was shifted slightly toward the North.

Figure 64. Approximated pinch out line (black dashed) of the Plioquaternary (M/PlQ boundary) underneath the Holocene gravel cover. Plioquaternary sediments fill the central part of the Krško syncline (red dashed) South of the line.

The youngest Miocene unit on the E site is the **gray muscovite carbonate silt with intercalation of lamina and thin beds (mostly 0.5 to 5cm thick) of more clayey silt and somewhere thicker beds of sandy silt, very fine sand and very fine sand with laminas of silt of Upper Pontian age (M_7).** For detail sedimentological analysis see chapter "Lithological logging of the cores of the boreholes" and Appendix 10 (Mišič, 2009). This lithological unit was drilled below Holocene sediments in the borehole ES-2 and below Plio-Quaternary sediments in the boreholes ED-1 (at -63,60m) and ES-1 (at -80,10m). Results are summarized below and are presented in Appendix 11 (Hajek-Tadesse, 2009). This unit covers Northern part of the E site below Holocene sediments. According to geological structure of the wider area, borehole logging (dip log) and previous investigations, it is established that strata dips in the SSE direction towards the axis of the Krško syncline. At the limbs, strata dip at angle around 20°, than flattens in the broad, gentle hinge area. No older lithological units were drilled, but according to the current seismic reflection lines and previous research, next underlying lithological units represent **carbonate clays and silts** in the lower part, **muscovite-carbonate silts of Sarmatian-Pannonian-Lower Pontian (M_{5-7}) age** in the upper part; **Lithothamnian limestones and calcarenites of the Badenian age (M_4)** and the lowest **Ottnangian clastites** or **Mesozoic lithological members** (Figure 65).

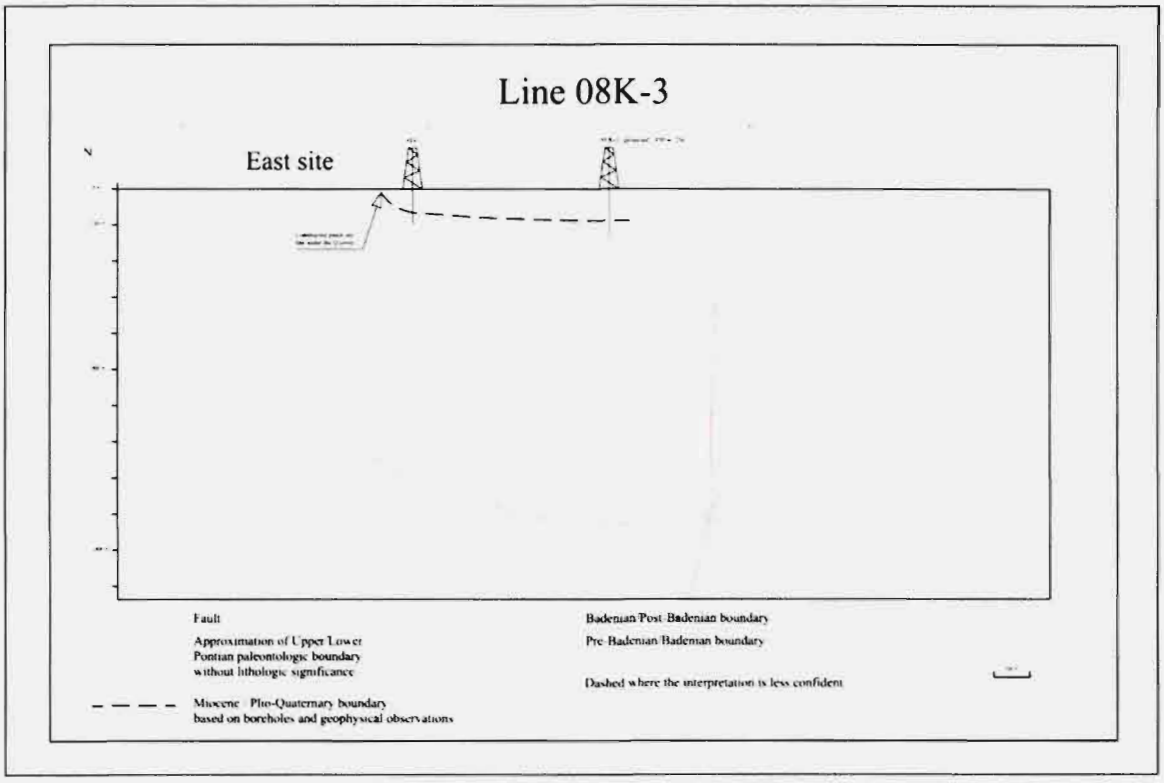

Figure 65. Schematic cross - section along the seismic line 08K-3 running N-S across the E site. Depths are informative.

In general, we find that the geological boundaries at and under the E site reflect the shape of the North limb and hinge area of the Krško syncline which generally plunges towards E-NE in the direction of the Globoko depression (Gosar et al., 2005).

East from the site, a potentially active NW – SE trending Libna fault was detected (described in detail above). The new geophysical survey also revealed that the E site is crossed by a strike-slip fault parallel to the Libna fault (see Geophysical data section). The deformation is extended toward NW to the Orlica fault (Figure 6) and was also mapped at Stara vas (Poljak, 1997b [79] for which it was called the Stara vas fault (described above). No deformation on this structure was observed extending above Miocene strata. In addition, the deformation dies out on the site itself and is therefore treated as tectonically and seismotectonically less important.

6.2 GEOLOGICAL STRUCTURE OF THE WEST SITE

Also the W site is completely covered with **Quaternary gravely-sandy sediments (Q_2)** of Holocene age. They are composed primarily of carbonate gravel and sand. More precise composition is evident from chapter "Lithological logging of the cores of the boreholes" (see below). According to boreholes WS-1, WD-1 and WS-2, the thickness ranges from 7,5 m in the Northern part, to 9 m in the Southern part of the W site.

Lithological units below Holocene (Q_2) sediments

Plio-Quaternary sediments are not present at the site, as they pinch-out under the Quaternary sediments about 400m South from the W site.

On the whole W site, below Quaternary sediments there occur **gray muscovite carbonate silt with intercalation of lamina and thin beds (mostly 0.5 to 5cm thick) of more clayey silt and somewhere thicker beds of sandy silt, very fine sand and very fine sand with laminas of silt of Upper Pontian age (M_7).** For detail sedimentological analysis see chapter "Lithological logging of the cores of the boreholes" and also Appendix 10 (Mišič. 2009). This lithological unit was drilled below Holocene sediments in all three performed boreholes (WS-1, WD-1 and WS-2). Results are summarized below and are presented in Appendix 11 (Hajek-Tadesse, 2009). According to geological structure of the wider area, borehole logging (dip log) and previous investigations, it is established that strata dips at an angle around 25° to the SSE direction towards the axis of the Krško syncline. Location is positioned in the N limb of the syncline. No older lithological units were drilled, but according to the current seismic reflection lines and previous research, next underlying lithological units represent Carbonate **clays and silts in the lower part, muscovite-carbonate silts of Sarmatian-Pannonian-Lower Pontian (M_{5-7}) age in the upper part.** The contact with the overlying M_7 lithological unit below Holocene sediments is interpreted North of the W site, and pass roughly in the W-E direction. Underlying **Lithothamnian limestones and calcarenites of the Badenian age (M_4)** crop on the Libna hill more to the North and the lowest **Ottnangian clastites** or **Mesozoic lithological members** could only be interpreted in the profiles below the W location (Figure 66).
In general, we find that the geological boundaries at and under the E site reflect the shape of the North limb the Krško syncline which generally plunges towards E-NE in the direction of the Globoko depression (Gosar et al., 2005).

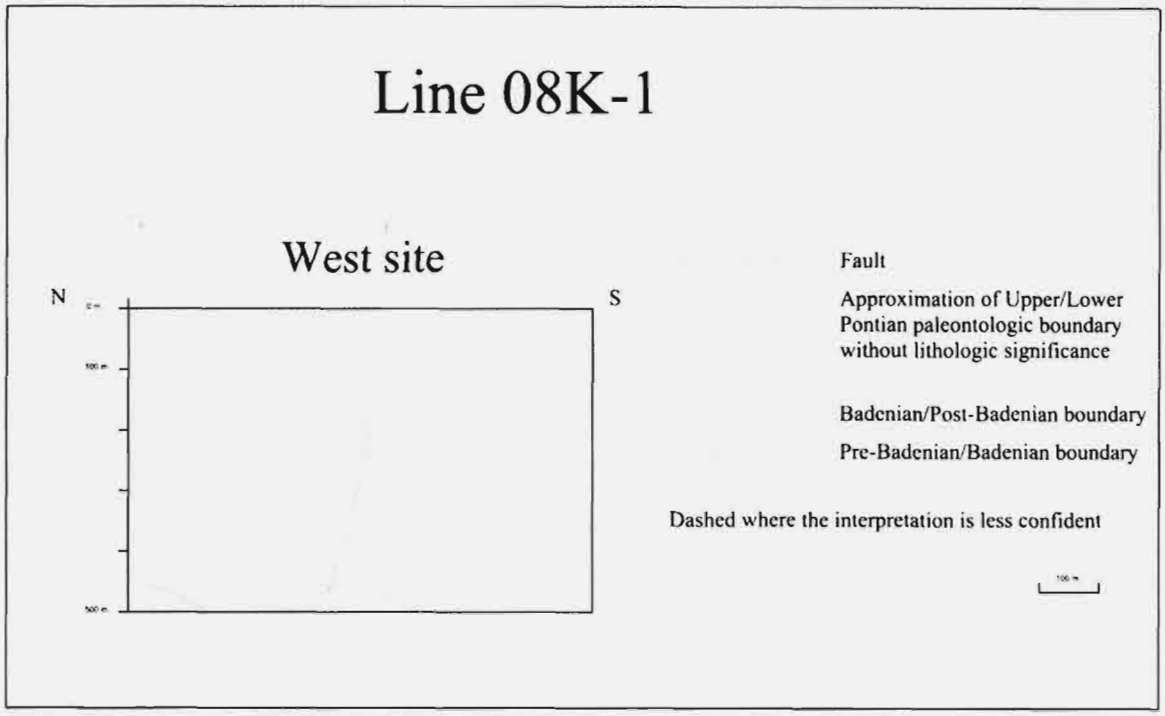

Figure 66. Schematic cross - section along the seismic line 08K-1 running N-S across the W site. Depths are informative.

6.3 LITHOLOGICAL LOGGING OF THE CORES OF THE BOREHOLES ED-1, ES-1, ES-2, WD-1, WS-1 AND WS-2

In the first phase of the project Geotechnical, Geological and Seismological (GG&S) Evaluations for the New Nuclear Power Plant at The Krško Site (NPP Krško II) two sites, located each side (east – E and west – W) of the actual nuclear power plant, along the river Sava, were evaluated. In this phase six fully cored boreholes, three in the E and three in the W side, were drilled. They are located on the youngest Holocene fluvial terrace (Vrbina Allomember sensu Verbič, 2004) of the Sava River, on which it was historically documented fluvial activity until the end of 19th century (Verbič, 2004). The three boreholes on the E side are arranged in triangle with cathetus in the E – W and SE – NW directions and hypotenuse in the ESE – WNW direction. On the W side they are arranged along a country road in the line in the N – S direction. Planed design of three boreholes on E and W side was that the middle borehole (D) is 100m deep with shallow ones (S) 50 m deep on each side.

Detailed lithological logs with data on: borehole diameter, % of core; geotechnical AC classification, lithology, macroscopic description, color, geological age; position of samples, pocket penetration tests, dilatometer, water tests and remarks are given in Appendix 12. The technical drilling report is presented in Appendix 13.

In the continuation summaries of logs for each borehole and description of the drilled lithological unites are given.

6.3.1 BOREHOLE ED-1

The coordinates of the borehole ED-1 are: x-540902.65, y-8751.06, z-154.05. The borehole ED-1 is 100m deep and was drilled from 1.7.2009 to 10.7.2009 by continuous core boring method with borehole diameters 101/76 mm. It was drilled thought the following lithological unites:

Depth (m)	Lithological unit
0.00 - 2.10	pebbly sandy silt – soil;
2.10-10.40	sandy gravel with sandy silt on the top – Quaternary (Holocene) Sava sediments;
10.40-63.60	silty sandy gravel with some intercalations of clayey silt – Plio-Quaternary sediments;
63.60-89.70	silt with some intercalations of clayey silt – Miocene (Upper Pontian) sediments;
89.70-100.0	very fine sand and very fine sand with laminas of silt – Miocene (Upper Pontian) sediments.

Detailed lithological log is given in the appendix 12 (ED-1). The samples ED-1 75,10-75,20m and ED-1 88,85-89,00m of silt belong to the Middle Pontian (details in Appendix 11).

6.3.2 BOREHOLE ES-1

The coordinates of the borehole ES-1 are: x-541543.54, y-8703.91, z-151.71. The borehole ES-1 was planned to be 50m deep, but it was prolonged to the depth 87m because of an unexpected thickness of the Plio-Quaternary sediments. It was drilled from 21.7.2009 to 4.8.2009 by continuous core boring method with borehole diameters 101/76 mm. It was drilled thought the following lithological units:

Depth (m)	Lithological units
0.00 - 0.80	sandy gravel – soil;
0.80-10.10	sandy gravel with clayey silt on the top – Quaternary (Holocene) Sava sediments;
10.40-80.10	silty sandy gravel with sandy gravel, pebbly sand and sand – Plio-quaternary sediments;
80.10-87.00	silt with some sandy silt – Miocene sediments.

Detailed lithological log is given in Appendix 12. In the samples ES-1 80,35-80,50m and ES-1 86,53-86,70m of silt no ostracode fauna was found (details in Appendix 11).

6.3.3 BOREHOLE ES-2

The coordinates of the borehole ES-2 are: x-540748.18, y-88115.90, z-152.58. The borehole ES-2 is 50m deep and was drilled from 14.7.2009 to 30.7.2009 by continuous core boring method with borehole diameters 101/76 mm. It was drilled thought the following lithological unites:

Depth (m)	Lithological units
0.00 - 0.40	pebbly sandy silt – soil;
0.40 - 8.10	gravel and sandy gravel on the top – Quaternary (Holocene) Sava sediments;
8.10-50.00	silt with some intercalations of sandy silt, very fine sand and clayey silt – Miocene (Upper Pontian) sediments.

Detailed lithological log is given in Appendix 12. The samples ES-1 9,00-9,20m and ES-1 49,80-50,00m of silt belong to the Upper Pontian (details in Appendix 11).

6.3.4 BOREHOLE WD-1

The coordinates of the borehole WD-1 are: x-539710.96, y-88589.31, z-155.39. The borehole WD-1 is 100m deep and was drilled from 15.7.2009 to 30.7.2009 by continuous core boring method with borehole diameters 116/76 mm. It was drilled thought the following lithological unites:

Depth (m)	Lithological units
0.00 - 0.50	pebbly sandy silt – soil;
0.50 - 8.50	gravel, sandy gravel and pebbly sand – Quaternary (Holocene) Sava sediments;

8.50-100.0	silt with some intercalations of clayey silt and very fine sand – Miocene (Upper Pontian) sediments.

Detailed lithological log is given in the in Appendix 12. The samples WD-1 10,00-10,20m and WD-1 99,40-99,60m of silt belong to the Middle Pontian (details in Appendix 11).

6.3.5 BOREHOLE WS-1

The coordinates of the borehole WS-1 are: x-539707.06, y-88772.57, z-155.91. The borehole WS-1 is 50m deep and was drilled from 1.7.2009 to 14.7.2009 by continuous core boring method with borehole diameters 101/76 mm. It was drilled thought the following lithological unites:

Depth (m)	Lithological units
0.00 - 0.30	sandy gravel - soil;
0.50 - 7.50	sandy gravel and silty sand on the top - Quaternary (Holocene) Sava sediments;
7.50-50.00	silt with some intercalations of clayey silt and very fine sand with laminas of silt – Miocene (Upper Pontian) sediments.

Detailed lithological log is given in the in Appendix 12. The samples WS-1 8,80-8,90m and WS-1 49,50-49,70m of silt belong to the Upper Pontian (details in Appendix 11).

6.3.6 BOREHOLE WS-2

The coordinates of the borehole WS-2 are: x-539702.99, y-88280.81, z-157.95. The borehole WS-1 is 50m deep and was drilled from 1.8.2009 to 4.8.2009 by continuous core boring method with borehole diameters 116/76 mm. It was drilled thought the following lithological unites:

Depth (m)	Lithological units
0.00 - 0.10	pebbly sandy silt - soil;
0.10 - 8.70	sandy gravel with intercalation of pebbly sandy silt and sandy silt – Quaternary (Holocene) Sava sediments;
8.70-50.00	silt with intercalations of very fine sand 33.00-35.30m – Miocene (Upper Pontian) sediments.

Detailed lithological log is given in the in Appendix 12. The samples WS-2 13,10-13,20m and WS-2 48,90-49,00m of silt belong to the Upper Pontian (details in Appendix 11)

6.3.7 DESCRIPTION OF THE DRILLED LITHOLOGICAL UNITS

The boreholes were drilled through Quaternary (Holocene) Sava sediments, Plio-Quaternary and Miocene (Upper Pontian) sediments.

6.3.8 MIOCENE (UPPER PONTIAN) SEDIMENTS

The oldest drilled lithological unit in the explored area are the Miocene (Middle and Upper Pontian) sediments. Detail paleontological report is shown in Appendix 12) These are clastic sediments, prevailing medium gray muscovite carbonate silt with intercalation of lamina and thin beds (mostly 0.5 to 5cm thick) of more clayey silt (Figures 67, 68) and somewhere thicker beds of sandy silt, very fine sand and very fine sand with laminas of silt. The thicker (more than 50cm thick) beds of:

- sandy silt was detected in the ES-1 (80.1-81.1m) and ES-2 (23.0-25.0m; 37,7-39.0m);
- very fine sand is situated in the ES-2 (39.0-40.5m), WS-2 (33.0-35.0m) and the thickest interval at the end of the ED-1 (89.7-100.0m) (Figure 69).

These sediments are slightly consolidated. But it is enough that the core holds its shape. The thickest interval (8.5 to 100.0m) of the Upper Miocene (Upper Pontian) sediments was drilled in the borehole WD-1.

In the muscovite carbonate silt, darker, mostly 1 to 3mm thick laminas of more clayey silt in a distance 2-3cm (0.5 to 5cm) were observed, always when it was drilled with borehole diameter 76mm and very often at the diameter 101mm. These laminas are predominantly uneven thick, thicker on edges of the core and thinning to the middle of the core. The laminas are mostly horizontal, slightly curved down in direction of drilling on the edges of the core (Figure 67) or convex bended in direction of drilling (Figure 68). Circle orientation marks can be observed on some parting plains (Figures 68, 70). Grain size analyses presented by fraction of sand (S), silt (Si) and clay (Cl) are shown in the Table 2 and Figure 77. From 22 analyzed samples there are 16 determined as silt, 5 as sandy silt and 1 as very fine sand. They have average composition: S 19,6%; Si 76,6%, Cl 3,8%. Average mineral composition of bulk samples are given in weight %; quartz 26%, muscovite/illite 24%, dolomite 19%, chlorite 12%, plagioclases 9%, calcite 6%, pyrophyllite and hornblende 2%. Average composition of clay fraction is illite 5%, Ca-montmorillonite 3% and chlorite 2%. Detailed mineralogical report is shown in Appendix 10.

From our experience of drilling borehole VOG-3 (Petkovšek, ed., 2009) we assumed that this lamination was produced by drilling (Figures 67, 68). Our assumption was proven as correct by changing the borehole diameter from 76 to 101mm in the borehole ES-2 in the depth 20.0 m (Figure 71). After that the borehole diameter was changed to 116mm in the boreholes WD-1 and WS-2. In cores from these boreholes drilled with 116mm diameter the muscovite carbonate silt is homogeneous, mostly massive, without lamination. In the massive intervals bioturbation structures were observed (Figure 72). Macro fossils, above all bivalves (Figure 73) and gastropods were found in the deferent depths. Shells are mostly fragmented, but somewhere they are whole.

Tectonic structures were found in the muscovite carbonate silt in the core of the borehole ES-2 in the depth interval from 29.9 to 35.0m. The most pronounced is older, nearly vertical (85°) one (Figure 74); less pronounced is younger one with the dip angel of 30°. These tectonic structures were produced by oblique-slip movements.

The Miocene (Upper Pontian) muscovite carbonate silt is overlain by Plio-Quaternary or Quaternary fluvial sediments. Along disconformity the muscovite carbonate silt, sandy silt and very fine sand were oxidized and are colored brown (Figure 75).

No	Borehole	Depth		Age	Cl < 0,002mm	Si 0,002-0,063mm	S 0,063-2,00mm
1	ED1	28,75	28,85	Pl/Q	18,7	69,4	11,9
2	ED1	57,35	57,50	Pl/Q	12,5	56,9	30,6
3	ED1	69,85	70,00	M	2,5	87,3	10,2
4	ED1	80,00	80,20	M	1,9	71,3	26,8
5	ED1	99,00	99,15	M	2,0	40,7	57,3
6	ES1	81,50	81,60	M	2,1	76,9	21,0
7	ES2	10,00	10,30	M	3,4	84,8	11,8
8	ES2	23,30	23,50	M	2,0	57,9	40,1
9	ES2	29,40	29,60	M	2,8	83,3	13,9
10	ES2	46,00	46,20	M	2,0	59,2	38,8
11	WD1	17,70	17,85	M	4,4	77,3	18,3
12	WD1	31,25	31,40	M	4,4	83,8	11,8
13	WD1	42,30	42,50	M	5,0	85,5	9,5
14	WD1	62,30	62,45	M	1,7	54,1	44,2
15	WD1	80,50	80,65	M	7,2	90,5	2,3
16	WD1	98,00	98,15	M	6,5	92,4	1,1
17	WS1	11,15	11,30	M	2,6	66,0	31,4
18	WS1	19,25	19,50	M	4,6	90,3	5,1
19	WS1	38,70	38,90	M	5,7	89,8	4,5
20	WS1	48,80	49,00	M	7,8	90,2	2,0
21	WS2	13,10	13,20	M	5,3	81,1	13,6
22	WS2	24,60	24,80	M	2,1	61,7	36,2
23	WS2	33,10	33,20	M	4,6	82,0	13,4
24	WS2	49,70	49,80	M	3,8	77,8	18,4

Table 2: Grain size composition of mineralogical analyzed samples

6.3.9 PLIO-QUATERNARY SEDIMENTS

Plio-Quaternary sediments disconformaly overlay the Miocene (Upper Pontian) sediments (Figure 76). They consist predominantly by polymict quartz silty (muddy) sandy gravel with intercalations of sandy gravel, pebbly sand, pebbly silty sand, sand, pebbly clayey silt and clayey silt. The sediments are mostly moderately yellowish brown in color, with more reddish thither bands in places. According to older data (Verbič, 2004, Tab. 2, p. 178) the Plio-quaternary gravel consists only of noncarbonate pebbles: red siliciclastics (17%), other siliciclastic (14%), Triassic extrusives and tuffs (22%), Tertiary extrusives and tuffs (13%), cherts (22%) and quartz (12%), larger as 2cm. By logging was seen that some lithic pebbles, especially tuff ones are weathered and limestone pebbles were detected somewhere. That for macroscopic lithological and granulometrical analysis was performed in 14 samples of the Plio-quaternary silty sandy gravel (muddy gravel according to the grain size analysis; in Appendix 9) from the borehole ED-1 and ES-1. They revealed that nearly 50% of pebbles (larger as 2mm) belong to carbonate rocks. The average lithologic composition of analyzed 14

samples is: limestones (47.4%), dolomites (0.8%), gray marly mudstone (3.9%), polymict limestone sandy conglomerate to calcarenite (6.5%), sericite-quartz sandstone and siltstone (0.4%), weathered brownish and gray mudstone and sandstone (2.8%), light yellowish gray, cherty mudstone to claystone (2.4%), silicified light brownish gray mudstone (1.1%), red (to green) volcanic rock (porphyryte-andesite?) (1.5%), tuffs and tuffites (2.9%), red and gray quartz sandstone (Val Gardena Sandstone) (7.9%), cherts (different colors) (5.4%), quartz (different colors) (14.8%), limonitized fragments and limonite crusts (1.6%) and metamorphic rock fragments (0.6%). (Details are in the appendix 3). The thickest interval (10.1 to 80.10m) of the Plio-quaternary sediments was drilled in the borehole ES-1. Two grain size analysis of the Plio-quaternary muddy sediments from the borehole ED-1 are classified as silt and sandy silt with average composition 21,3% S, 63,2% Si, 15,6% Cl (Table 1, Figure 77). It is evident that these Plio-quaternary muddy sediments contain about 10% of clay more than the Miocene sediments. Average mineral composition of bulk samples are given in weight %; quartz 48%, muscovite/illite 33%, chlorite 12%, plagioclases 5% and calcite 3%. Average composition of clay fraction is illite 9%, Ca-montmorillonite 5%, chlorite 2% and kaolinite 1%. Detailed mineralogical report is shown in Appendix 10.

6.3.10 QUATERNARY SEDIMENTS

The youngest Quaternary (Holocene) sediments paraconformaly overlay Plio-quaternary or Miocene (Pliocene) sediments. They consist prevailing of sandy gravel with lesser amount of gravel, pebbly sand and sandy silt or clayey silt. The upper part of the sediments was highly oxidized and in the upper most part top soil was formed. According to Verbič (2004, Tab. 2, p. 178) the pebbles larger as 2cm of these gravels are composed mostly – 77% of carbonate rocks and subordinate – 23% of non-carbonate rocks: red siliciclastics (3.4%), other siliciclastic (7.4%), Triassic extrusives and tuffs (3.9%), Tertiary extrusives and tuffs (4.8%), cherts (2.1%) and quartz (1.4%). The greatest thickness (10.10m) of the Quaternary (Holocene) sediments was drilled in the borehole ED-1.
The Quaternary (Holocene) sediments are fluvial origin – Vrbina Allomember (Verbič, 2004) deposited by Sava River and form fluvial terraces. The coarse grained sediments are interpreted ad channel bar deposits and the finer ones are overbank deposits, deposited by braided stream.

Figure 67: Thin bed (5cm) and laminas of clayey silt in the muscovite carbonate silt. The laminas are horizontal, slightly convex bended on the edges of the core. WD-1, 16.37-16.46m.

Figure 68: Thin bed (5cm) and laminas of clayey silt in the muscovite carbonate silt. The laminas are horizontal, slightly convex bended on the edges of the core. On the convex parting plain circle orientation marks can be observed. WD-1, 17.75-17.95m.

Figure 69: Very fine sand and very fine sand with laminas of silt. They are brownish with up to 15 cm thick or oxidized reddish bands. ED-1, 90.0-95.0m.

Figure 70: On the convex parting plain circle orientation marks can be observed. ES-2, 17.95m.

Figure 71: Laminated muscovite carbonate silt in the interval 19.5-20m drilled with diameter 76mm and massive muscovite carbonate silt in the interval 20.0-20.5m drilled with diameter 101mm, ES-2.

Figure 72: Vertical bioturbation structure in the massive muscovite carbonate silt. ES-2, 10.0-10.2m.

Figure 73: Fractured bivalves shell. WD-1, 69.5m.

Figure 74: Nearly vertical (85°) tectonic structures produced by oblique-slip movements. ES-2, 33.80-34.20m.

Figure 75: Near the disconformity the muscovite carbonate silt, sandy silt and very fine sand were oxidized and are colored brown. ED-1, 65.0-66.0m.

Figure 76: The disconformity at 63.60m between the oxidized Miocene (Pliocene) muscovite carbonate silt and Plio-quaternary polymict silty sandy gravel. ED-1.

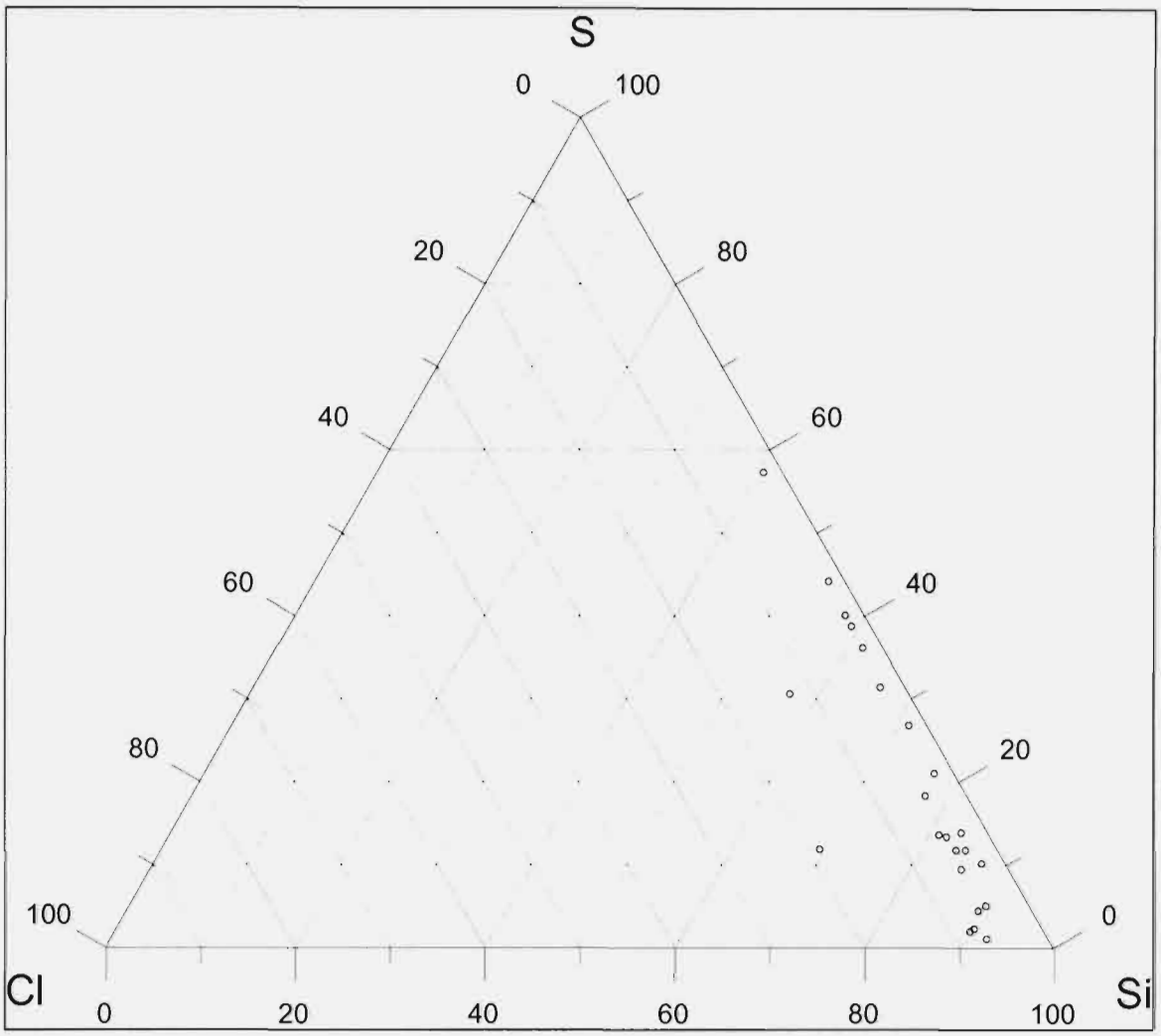

Figure 77: Grain size composition of analyzed samples

6.3.11 PALEONTOLOGICAL ANALYSES

Following samples were investigated for presence of ostracods. Original report (Hajek-Tadesse (2010) is provided in Appendix 11.

ED-1 borehole: 2 samples: 75,10-75,23 m and 88,85-89,00 m;

ES-1 borehole: 2 samples: 80,35-80,50 m and 86,53-86,70 m.

ES-2 borehole: 2 samples: 9,00-9,20m and 49,80-50,00 m;

WD-1 borehole:2 samples: 10,00-10,20 m and 99,40-99,60 m;

WS-1 borehole**:** 2 samples 8,80-8,90 m and 49,50-49,70 m;

WS-2 borehole: 2 samples: 13,10-13,20 m and 48,90-49,00 m;

We should first stress that the division of Upper Miocene into the Pannonian and Pontian stages in the Pannonian basin is no longer used (Piller et al., 2007). According to the latest research, Pontian belongs to another geodynamic space and was excluded from the Pannonian basin system.

In previous reports, particularly for the potential LILW disposal Vrbina (Brenčič, ed., 2006; Petkovšek, ed., 2009) we used the Pontian stage in the paleontological determinations and in the naming of lithostratigraphic units and it would seem unreasonable to use a different division in this report as this would cause too great confusion in the naming and primarily in communication. We therefore decided to use the old division. We appropriately translated the age determinations provided in paleontological reports so that they are comparable to the age determinations to the other recent reports.

sample	**depth (m)**	**Age** (Appendix 12)	**Age (translated)**
ED-1	75,10-75,23	Upper Pannonian (lower part)	Middle Pontian
ED-1	88,85-89,00	Upper Pannonian (lower part)	Middle Pontian
ES-1	80,35-80,50	no ostracode fauna	
ES-1	86,53-86,70	no ostracode fauna	
ES-2	9,00-9,20	Upper Pannonian	Upper Pontian
ES-2	49,80-50,00	Upper Pannonian	Upper Pontian
WD-1	10,00-10,20	Upper Pannonian	Upper Pontian
WD-1	99,40-99,60	Upper Pannonian (lower part)	Middle Pontian
WS-1	8,80-8,90	Upper Pannonian	Upper Pontian
WS-1	49,50-49,70	Upper Pannonian	Upper Pontian
WS-2	13,10-13,20	Upper Pannonian	Upper Pontian
WS-2	48,90-49,00	Upper Pannonian	Upper Pontian

Table 2. Paleontological samples from boreholes ED-1, ES-1, ES-2, WD-1, WS-1, WS-2 with their ages translated to the old division of Upper Miocene.

Paleontological results clearly correspond to the stratigraphic interpretation in the Northern limb of the Krško syncline and the dip of strata in to the SSE direction. The oldest, i.e. Middle Pontian layers are found in the lowest parts of the boreholes.

7 SEISMICITY DATA

7.1 FAULT PLANE SOLUTIONS AND THE PRINCIPAL STRESS

This chapter is a resume of a separate report of ARSO (Živčić & Ložar Stopar, 2009). There were three fault plane solutions available for the PSHA for the Krško NPP (Živčić, 1994) with two additional solutions made for the next PSHA study in 2003. With the remarkable increase in the number of seismic stations active in the area the number of the earthquakes for which the determination of the fault plane solutions is possible increased.

There are 21 FPS for the earthquakes from 2002 till 2008 in the area of about 40 km around Krško NPP (Ložar, 2008). In addition, there are four centroid moment tensor (CMT) solutions available from the databases on the internet. The authors searched Harvard (CMT, 2008), USGS (NEIC, 2008), ISC (International Seismological Center, 2008), Italian RMTS (Pondrelli et al., 2006), MedNET (2008) and ETH (2008) databases and three solutions from the ETH MTS database (ETH, 2008) and one from the Italian RMTS (Pondrelli et al., 2006) were located in the area of interest. From the total of 25 available solutions 6 are within 25 km from the NPP Krško site (Figure 78).

Most of the earthquakes are of the strike-slip type with several FPS of reverse character within the Krško basin itself.

Based on the tectonic model it can be assumed that the stress is uniform throughout the South central part of the Sava wedge. Therefore the principal stress $\sigma 1$ is determined from 9 FPS of the earthquakes in the Krško basin – Gorjanci Mts. area using the method of Gephart and Forsyth (1984). Its azimuth is 11 degrees, and its dip 2 degrees (Figure 79) with the misfit of 1.96. Dip of the least principal stress $\sigma 3$ of 10 degrees is consistent with regional strike-slip regime. This region is confined within two strike-slip faults that define the current seismotectonic model of the area. In addition, the horizontal stress field in the wider region, as determined from focal mechanisms of 23 earthquakes has also an approximately N-S-oriented maximum principal stress. However, the large smaller misfit of 4.14 of individual nodal planes suggests that the stress is not that uniform within the volume considered

Approximately N-S direction of maximum horizontal stress with some deviation toward the E can also be inferred GNSS report (Stopar & Sterle, 2010) and from the caliper analysis of the boreholes shape – the "breakout analyses" (Jeras, 2009; Appendix 14). Both results are at this stage less reliable than inversion by fault plane solutions.

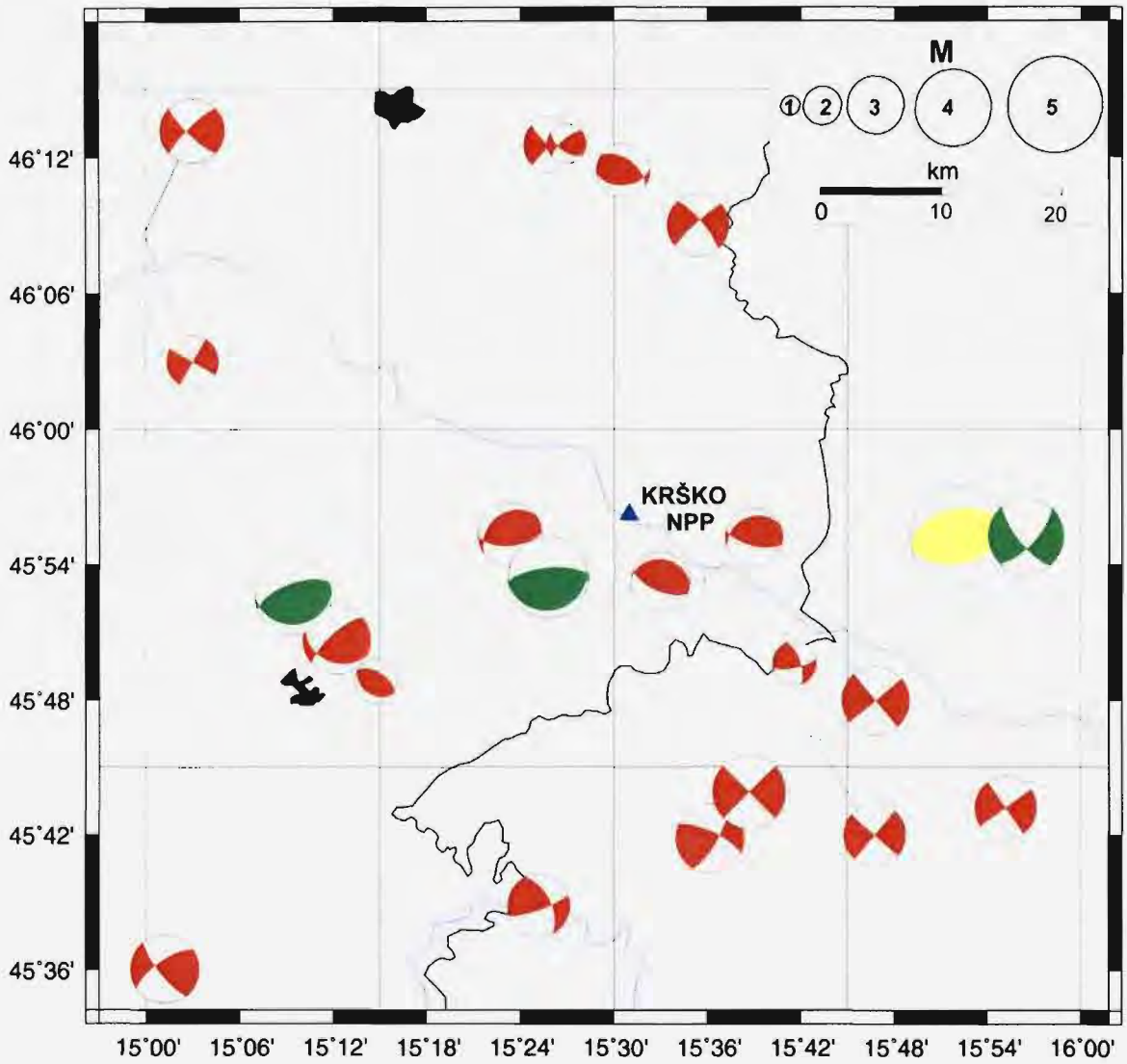

Figure 78. Fault plane solutions from Ložar (2008) and Ložar and Živčić (2007 and 2008) (red), ETH (2008) CMT solutions (green) and from Italian RMTS (Pondrelli et al., 2006) (yellow) for the earthquakes in the wider area of the Krško basin. Shaded quadrants are compressional. (from Živčić & Ložar Stopar, 2009).

7.2 CORRELATION MAP OF GEOLOGY AND SEISMICITY

The results of the relocation of local earthquakes in Krško area using double difference method (Waldhauser and Ellsworth, 2000) are combined with the fault plane solutions (Čarman & Živčić, 2009; Živčić & Ložar Stopar, 2009) and overlaid over the map with tectonic model of the Krško basin. The overlay was used to analyze the coincidence of structures with the seismic activity.

Figure 79 shows locations of the relocated earthquake epicenters for the period 1977-2008 with respect to the major tectonic features of the area. There is no clear correspondence of the seismic activity and the location of the mapped faults.

Figure 80 shows locations and fault plane solutions of the earthquakes with respect to the tectonic features. The most prominent structure is Sv. Nedelja fault whose mapped trace well corresponds both with the distribution of the earthquake hypocenters and with four fault plane solutions available. All this information is combined on the last figure.

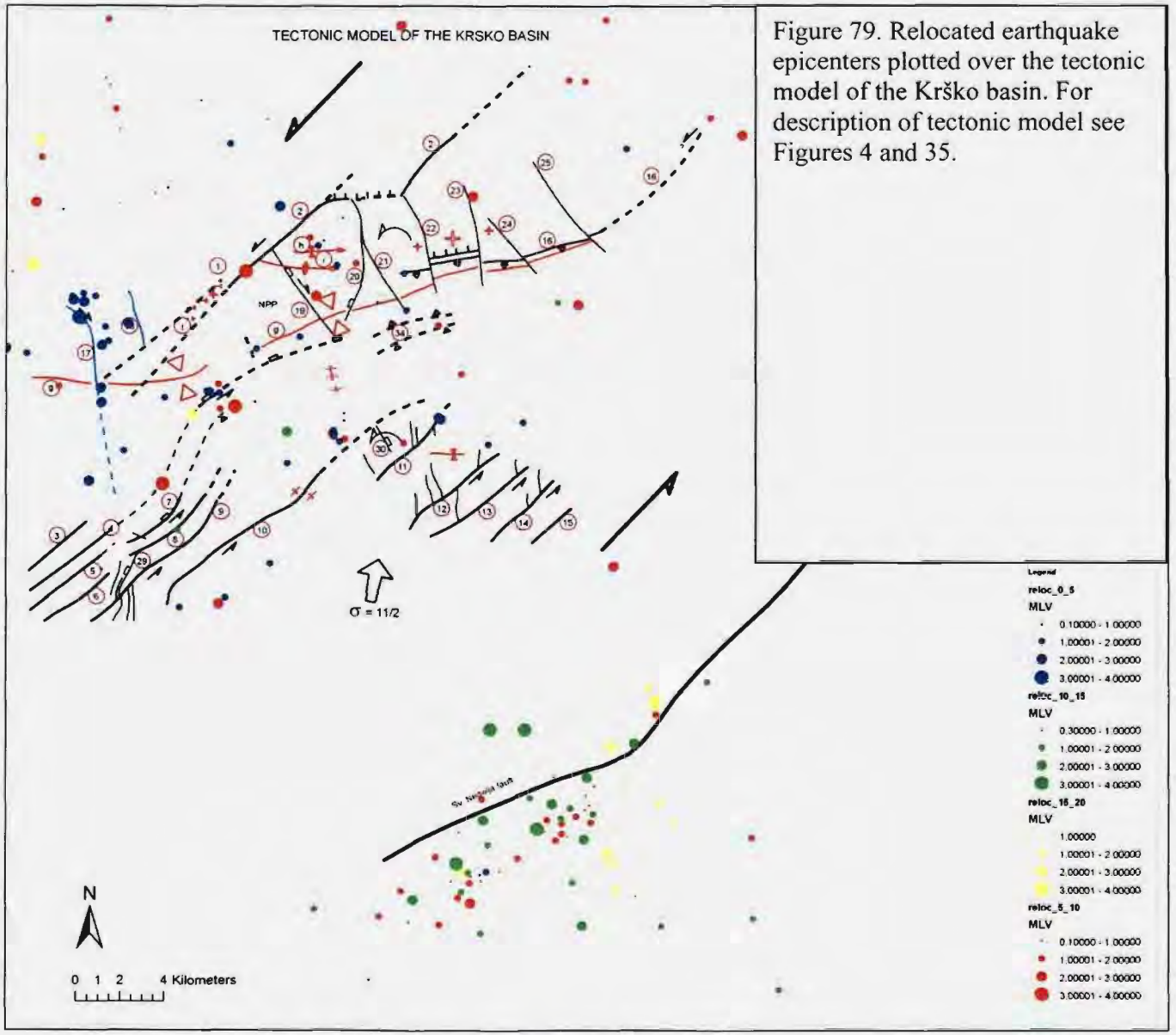

Figure 79. Relocated earthquake epicenters plotted over the tectonic model of the Krško basin. For description of tectonic model see Figures 4 and 35.

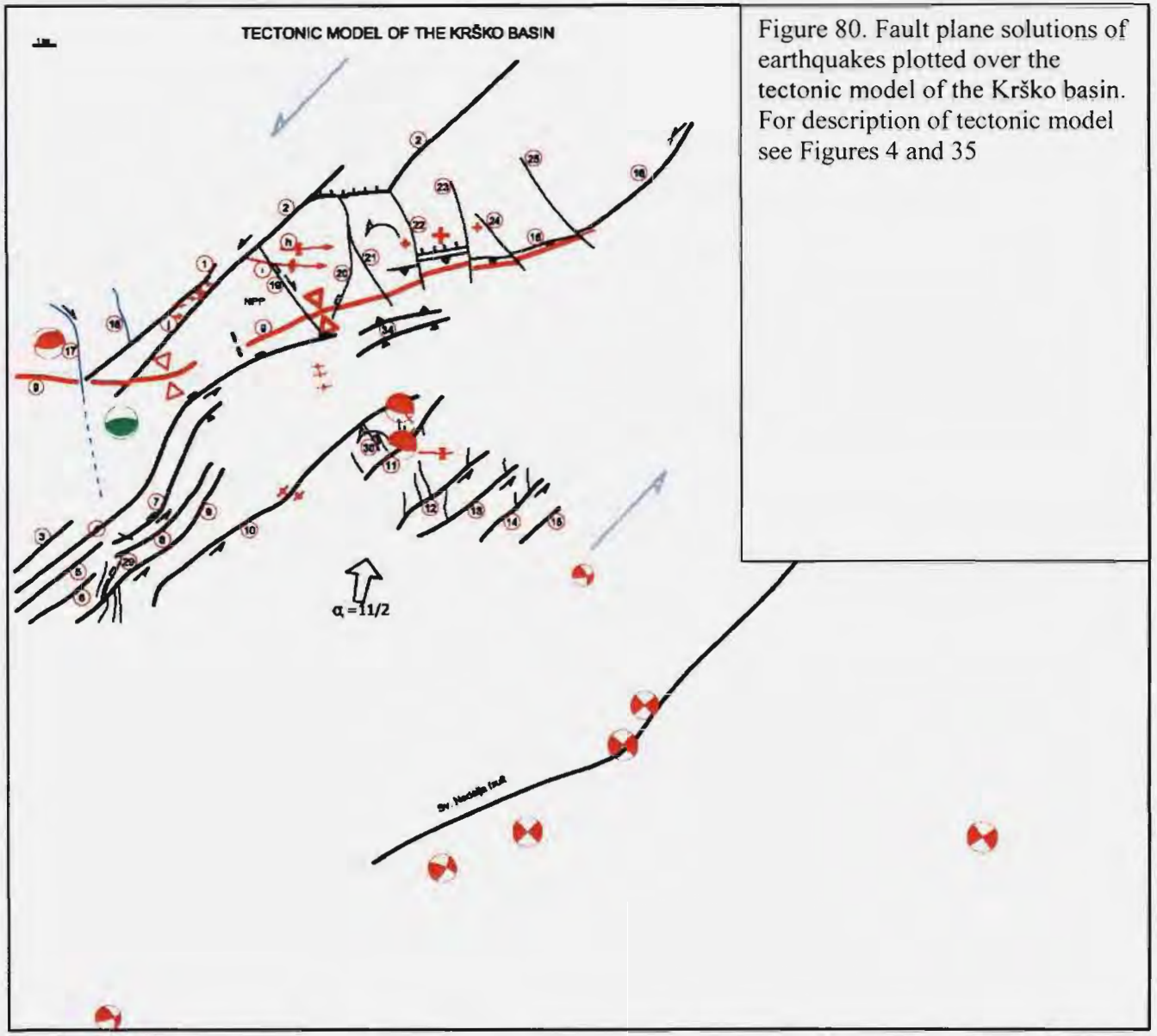

Figure 80. Fault plane solutions of earthquakes plotted over the tectonic model of the Krško basin. For description of tectonic model see Figures 4 and 35

8 SEISMOTECTONIC MODEL AT THE END OF PHASE 1 – A SUMMARY

The observed Neogene and post-Neogene deformation in the Krško basin area are a part of the NW section of the large sinistral strike-slip NE trending Mid-Hungarian zone. To the North, this zone borders with the Sava compressive wedge, characterized by the E – W trending folding and reverse faulting between the Mid-Hungarian zone, the NW trending Dinaric faults of the Idrija tectonic zone, and the Periadriatic zone in the North. The core of the Mid-Hungarian zone is the microplate boundary between the Tisza unit and the Dinarides along the Southern foothills of Mt. Medvednica and its extension along the S foothills of the Gorjanci Mts. referred to as the Zagreb and Sv. Nedelja faults respectively. The prominent deformation in the Mid-Hungarian zone are the NE trending (Balaton) faults of general sinistral strike-slip character. The NW boundary of the Mid-Hungarian zone is the Orlica fault. The Krško syncline is formed as a large oblique fold in the external part of the Mid-Hungarian zone to compensate the strain that is realized along the Balaton strike-slip faults in the internal (proximal) part of the zone. Four sets of potentially active structures can be expected in this tectonic model (Figure 4 and Figure 35).

1) The Balaton faults, as the prominent strike-slip faults. The straight sections of the Orlica fault and other Balaton faults observed in the Gorjanci Mts. fit into this group. These structures are potentially active.

2) The Balaton structures do represent the strike-slip faults, but when they are bent from their NW trend, they partly adopt the reverse character. The reverse type of such structure is found in both limbs of the Krško syncline. In the Northern limb, it is the Artiče fault and the connected flexure, together with the NE part of the Orlica fault. In the Southern limb of the syncline, the Brežice flexure and the deformation connected to the Balaton faults in the Kostanjevica area are their pendant.

3) Another type of the active structures represents the N (NE to NW) trending faults between the Balaton faults. A set of such faults is observed between the Orlica and Artiče structures. These faults are acting as CCW rotating Riedel type faults in the sinistral strike-slip zone. However, due to their position in the restraining bend between the E – W trending sections of the Orlica and Artiče faults, these submeridian faults act also as reverse faults along which the restraining bend is locally uplifted. Similar conditions are observed also South of the Krško syncline, but because the Balaton faults there are not stepping over, no restraining bends are formed. Only Riedel type faults are observed there between them.

4) In the Western part of the Krško Basin, Krško syncline is adopting an E – W direction due to the NW trending Lokavec fault, presumably active as a right lateral strike-slip fault, cutting off the SE continuance of the Orlica fault there. Because the Lokavec fault disables the sinistral strike-slip activity there, the Krško syncline could not keep its ENE direction to the W.

The maximal stress orientation based on the inversion of the fault plane solutions is 11/02. The angle between the Balaton faults and the maximal stress is 30 - 35°.

At this stage of seismotectonic model, the potential activity of structures is defined by deformation in the Plio-Quaternary deposits. This approach leads to a relatively high number of active structures in the Krško basin. It has to be noted here that results obtained and

conclusions presented in the report, are the most accurate taken into account the number and quality of available (past and obtained in the study) data. Conclusions will be included in seismic hazard assessment process and will probably lead to a rather conservative seismic loading estimate for the design. Further attempts should be made toward determining the age of the Plio-Quaternary and investigations of potential deformation in younger (Post - Plio-Quaternary) deposits should be performed, in case that uncertainty in the seismotectonic model has to be reduced.

9 REFERENCES

9.1 Referring to 2003 PSHA report

3. Aničić, B., and Juriša, M., 1985a, Osnovna geološka karta SFRJ 1:100,000, list Rogatec: Zvezni Geološki Zavod, Beograd.

9. Brezigar, A., Tomšič, B., Stopar, R., and Živanović, M., 1993, Pregled in reinterpretacija geofizikalnih raziskav v okolici ne Krško: Unpublished report submitted by the SP Geološki Zavod Ljubljana, št.dok. ŠGGS5, 32 p.

11. Buser, S., 1978, Osnovna geološka karta SFRJ 1:100,000, list Celje: Zvezni Geološki Zavod, Beograd.

12. Buser, S., 1979, Osnovna geološka karta, SFRJ 1:100,000, tolmač lista Celje: Zvezni Geološki Zavod, Beograd (in Slovene with English abstract).

22. Djurasek, S., 1996, Krško polje—interpretacija seizmičkih podataka: Unpublished report, št. dok. ŠGGS13, 7 p., Slovenian Nuclear Safety Administration.

24. Fajfar, P., and Lapajne, J. (eds.), 1994, Probabilistic assessment of seismic hazard at Krško Nuclear Power Plant (Revision 1): Unpublished report prepared by the Faculty for Civil Engineering and Geodesy (FGG) for Nuklearna Elektrarna Krško.

29. Gosar, A., 1996, Seismic reflection method in structural investigations for assessment of earthquake hazard in the Krško basin: Ph.D. Thesis, University of Ljubljana, Ljubljana, Slovenia, (in Slovenian with English Summary).

30. Gosar, A., 1998, Seismic-reflection surveys of the Krško basin structure—Implications for earthquake hazard at the Krsko nuclear power plant, SE Slovenia: Journal of Applied Geophysics, v. 39, p. 31-153.

50. Kuščer, D., 1993, Neotektonika Krške kotline: Unpublished report, št.dok. ŠGGS3.

65. Placer, L., 1995, O aktivnosti Škocjanskega preloma na območju Zagorske sinklinale: Geol. Zbor., v. 10, p. 58-61, Ljubljana (in Slovene with English abstract).

60. Persoglia, S. (ed.), 2000, Geophysical research in the surrounding of the Krsko NPP: Final Report and Annexes, Contract No. 98-0286.00 for European Commission Directorate General IA Tacis Procurement Unit.

68. Placer, L., 1999a, Contribution to the macrotectonic subdivision of the border region between Southern Alps and External Dinarides: Geologija, v. 41, p. 223-255.

71. Pleničar, M., and Premru, U., 1977, Osnovna geološka karta SFRJ 1:100,000, tolmač lista Novo Mesto: Zvezni Geološki Zavod, Beograd.

72. Pleničar, M., and Ramovš, A., 1954, Geološko kartiranje severovzhodno od Brežic: Geologija, v. 2, p. 242-253.

73. Pleničar, M., Premru, U., and Herak, M., 1976, Osnovna geološka karta SFRJ 1:100,000, list Novo Mesto: Zvezni Geološki Zavod, Beograd.

74. Poljak, M., 1984, Neotectonic investigations in the Pannonian basin based on satellite images: Adv. Space Res., v. 4, no.11, p.139-146.

75. Poljak, M., 1994, Neotektonske raziskave na območju JE Krško: Unpublished report prepared by the Inštitut za geologijo geotehniko in geofiziko (IGGG), št. dok. ŠGGS7, 22 p.

78. Poljak, M., 1997a, Geološka reambulacija hriba Libne pri Krškem in okolice: Unpublished report prepared by the Inštitut za geologijo geotehniko in geofiziko (IGGG), št. dok. ŠGGS15, 21 p.

79. Poljak, M., 1997b, Geološka reambulacija hriba Libne pri Krškem in okolice—geološki razkopi: Unpublished report prepared by the Inštitut za geologijo geotehniko in geofiziko (IGGG), št. dok. ŠGGS16, 17 p.

81. Poljak, M., 1999, Detajlno geološko kartiranje območja Globokega v merilu 1:5,000: Geološki Zavod Slovenije (GZS), Ljubljana, št. dok. ŠGGS23.

82. Poljak, M., 2000a, Structural-tectonic map of Slovenia: Geologic Survey of Slovenia (scale 1:250,000).

83. Poljak, M., 2000b, Detajlno geološko kartiranje na območju Bizeljskega v merilu 1:5,000: Geološki Zavod Slovenije (GZS), Uprava RS za jedrsko varnost, Ljubljana, št. dok. ŠGGS26, 23 p.

84. Poljak, M., 2001, Detajlno geološko kartiranje na območju Raka-Ravni v merilu 1:5,000: Geološki Zavod Slovenije, Uprava RS za jedrsko varnost, Ljubljana, št. dok. ŠGGS26, 18 p.

89. Poljak, M., Žnidarčič, M., Demšar, M., and Cajhen, J., 1985, Raziskave premoga Globoko, Izdelava strukturno geološke karte v merilu 1:10,000: Geološki zavod Ljubljana.

91. Poljak, M., Verbič, T. Gosar, A., Zivcic, M., and Ribicic, M., 1996a, Neotektonske raziskave na obmocju JE Krsko: Technical report, IGGG, Ljubljana št. dok. ŠGGS6 (Slovene with English abstract).

92. Poljak, M., Verbič, T., Rižnar, I., Toman, M., and Demšar, M., 1996b, Poročilo o detajlnem geološkem kartiranju Libne pri Krškem in okolice: Unpublished report prepared by Inštitut za geologijo geotehniko in geofiziko (IGGG), št. dok. ŠGGS14,

96. Prelogović, E., 1996, Geološka intepretacija refleksijskih seizmičnih profilov iz leta 1994 in 1995: Unpublished report, št. dok. ŠGGS12.

97. Prelogović, E., Saftić, B., Kuk, V., Velić, J., Dragaš, M., and Lučić, D., 1998, Tectonic

activity in the Croatian part of the Pannonian basin: Tectonophysics, v. 297, p. 283-293.

108. Rižnar, I., 1998, Geološka karta ozemlja med Izvirom in Starim gradom, scale 1:5000, št. dok. ŠGGS20.

109. Rižnar, I., 1999, Geološka karta okolice Kostanjevice, scale 1:5,000, št. dok. ŠGGS21.

114. Šikić, K., Basch, O., and Šimunić, A., 1978, Osnovna geološka karta, SFRJ 1:100,000, list Zagreb: Zvezni Geološki Zavod, Beograd.

115. Šikić, K., Basch, O., and Šimunić, A., 1979, Osnovna geološka karta SFRJ 1:100,000, tumač za list Zagreb: Savezni Geološki Zavod, Beograd, 81 p. (in Croatian with English abstract).

120. Tomljenović, B., and Csontos, L., 2001: Neogene-Quaternary structures in the border zone between Alps, Dinarids, and Pannonian basin (Hrvatsko zagorje and Karlovac basins, Croatia): International Journal of Earth Sciences (Geol. Rundsch), v. 90, p. 560- 578.

126. Verbič, T., 1995, Kvartarni sedimenti v vzhodnem delu Krške kotline: Unpublished report, št. dok. ŠGGS7, 248 p.

131. Verbič, T., and Rižnar, I., 1997, Geološka karta med Prilipami in Velikim Bregom: Unpublished report, št. dok. ŠGGS17, 56 p.

148. Živanović, M., 1999, Dopolnilne georadarske preiskave na delu srednjepleistocenske terase pri Stari vasi: Unpublished report by the Inštitut za Geologijo, Geotehniko in Geofiziko (IGGG), št.dok. ŠGGS19, 2 p.

149. Živanović, M., Stopar, R., Gazzano, G., and Poljak, M., 1998, Geofizikalne in geološke raziskave na treh ostankih srednjepleistocenskega zasipapri Stari vasi: Unpublished report by the Inštitut za Geologijo, Geotehniko in Geofiziko (IGGG), št.dok. ŠGGS18, 23 p.

9.2 Not referenced in 2003 PSHA report

Baize, S. 2008: Geological contribution of the SARG/BERSSIN to the GG&S project (Krško, Slovenia). Phase 1. DEI/SARG/2008-047. – Internal report, 52 pp, IRSN.

Bavec, M. 2000: Poročilo o določanju starosti kvartarnih sedimentov v Krški kotlini z metodo termoluminescence (TL) in optično stimulirane luminescence (OSL). Projektna naloga: Neotektonske raziskave na območju JE Krško. Naročnik Uprava RS za jedrsko varnost. - Tipkano poročilo. Geološki zavod Slovenije.

Bavec, M. (ed.) 2008: Paleoseismological investigations of the Libna fault. Trench in Stari Grad. – Project report for Geotechnical, Geological, and Seismological (GG&S) Evaluations for the New Nuclear Power Plant at the Krško Site (NPP Krško II); tasks 4.3.1.c, 4.3.1.c1, 4.3.1.d; 22pp, 5 appendices.

Bavec, M. 2003: Pliokvartarni sedimenti med Sevnico in Brestanico : preliminarni rezultati raziskav. V: Horvat, A. (ur.). *16. Posvetovanje slovenskih geologov : Razprave. Poročila : Treatises. Reports*, (Geološki zbornik, 17). Ljubljana: Univerza v Ljubljani, Naravoslovnotehniška fakulteta, Oddelek za geologijo, 2003, str. 5-7.

Brenčič, M. (ed.) 2006: Izvedba terenskih raziskav na potencialnih lokacijah v Republiki Sloveniji, za prostorsko umestitev odlagališča nizko in srednje radioaktivnih odpadkov (NSRAO), v postopku priprave državnega lokacijskega načrta (DLN) za odlagališče NSRAO, 2. faza – začetne terenske raziskave geosfere in hidrosfere potencialna lokacija Vrbina v občini Krško. Končno poročilo. - Konzorcij partnerjev ZAG, GeoZS, ZVV Maribor, Geoinženiring d.o.o.

Burbank D.W. and Anderson R. S. 2001: Tectonic geomorphology. Blackwell Science, 274 pages.

Car, M., Stopar, R., Giustiniani, M., Accaino, F. 2006: Izvedba terenskih raziskav na potencialnih lokacijah v Republiki Sloveniji, za prostorsko umestitev odlagališča nizko in srednje radioaktivnih odpadkov (NSRAO), v postopku priprave državnega lokacijskega načrta (DLN) za odlagališče NSRAO, 2. faza – začetne terenske raziskave geosfere in hidrosfere potencialna lokacija Vrbina v občini Krško, Sklop 3: Površinske geofizikalne raziskave. – Geoinženiring d.o.o.

Čarman M., Živčić M., 2009: Double-difference hypocenter relocation of earthquakes in the area of Krško II NPP proposed site. Report NEK 2523-08-40013/1a - Appendix 2, Seismology and geology office, ARSO, Ljubljana

Carozza J-M & Baize S. 2004: L'escarpement de faille de la Têt résulte-t-il d'une exhumation pléistocène ? C.R.Géoscience, vol. 336, pp 217-226 (abstract in english).

Cox R.T. (1994). Analysis of drainage-basin symmetry as a rapid technique to identify areas of possible Quaternary tilt-block tectonics. Geol. Soc. Am. Bull., vol. 106, pp 571-581.

Doblas, M. 1998: Slickenside kinematic indicators. - Tectonophysics, 295, 187-197

EARS (Environmental Agency of the Republic of Slovenia), 2003-2007, Digital earthquake catalogue for Slovenia from 2003 to 2007

Gephart, J.W., and Forsyth, D., 1984, An improved method for determining the regional stress tensor using earthquake focal mechanism data—application to the San Fernando earthquake sequence: Journal of Geophysical Research, v. 89, p. 9305-9320.

GeoZS, 2006a: Izvedba terenskih raziskav zna potencialnih lokacijah v RS za prostorsko umestitev odlagališča nizko in srednje radioaktivnih odpadkov (NSARAO), v postopku priprave državnega lokacijskega načrta (DLN) za odlagališče NSRAO, 2. faza.- Arhiv GeoZS, Ljubljana.

GeoZS, 2006b: Izdelava geoloških kart.-Letno poročilo za leto 2006, Arhiv GeoZS.

Gephart, J.W., and Forsyth, D., 1984, An improved method for determining the regional stress tensor using earthquake focal mechanism data—application to the San Fernando earthquake sequence: Journal of Geophysical Research, v. 89, p. 9305-9320.

Gosar A., Komac M. and Poljak M. (2005). Structural model of the pre-Tertiary basement in the Krško basin. Geologija, vol. 48/1, pp 23-32 (abstract in English).

Gosar A. (2008). Gravity modelling along seismic reflection profiles in the Krško basin (SE Slovenia). - Geologica Carphatica, vol. 59, pp 147—158.

Hajek – Tadesse, V., 2010: Determination and analysis of Ostracods fauna from the borehole samples: ED-1, WS-2, WS-1, WD-1, ES-2, ES-1of Krško area (Republic of Slovenia). – Internal report, HGI.

IAEA, 2002: Evaluation of Seismic Hazards for Nuclear Power Plants. – Safety Guide No. NS-G-3.3.

Jeras, Z. 2009: VOG-1, VOG-2, VOG-3, WD-1 in ED-1 (Breakout Analysis and In-Situ Stress Interpretation). – GeoZS internal report

Kogoj, D., Poljak, M. &Vodopivec, F., 2004: Determination of local recent movements in Slovenia. in: ŚLEDZIŃSKI, Janusz (ed.). *Proceedings of the EGU G11 symposium "Geodetic and geodynamic programmes of the CEI (Central European Initiative)", Nice, France, 25-30 April 2004*, (Reports on geodesy, No. 2(69)). Warszawa: Instytut Geodezji Wyższej i Astronomii Geodezyjnej Politechniki Warszawskiej, 133-139.

Koler, B. 2010: Report and analysis of leveling network Krško. – FGG report.

Kranjc, S., Božović, M. & Matoz, T. 1990: Končno poročilo o geoloških raziskavah na Krškem polju za potrebe podzemnega skladiščenja plina, vrtina DRN-1/89. Poročilo, Arhiv Arhiv Inštituta za geologijo, geofiziko in geoinženiring, 19 str., Ljubljana.

Lienert, B. R., 1994, HYPOCENTER 3.2 – A Computer program for locating Earthquakes Locally, Regionally and Globally, Hawaii Institute of the Geophysics and Planetology, Honolulu, 70 pp

Manighetti I., Campillo M., Sammis C., Mai P.M. and King G. (2005). Evidence for self-similar, triangular slip distributions on earthquakes: implications for earthquake and fault mechanics. J. Geophys. Res., vol. 110, B05302, doi:10.1029/2004JB003174.

Marin, M., Markič, M., Zakrajšek, S., Žuža, T., Mišič, M. & Peček, D., 1989: Spremljava in obdelava podatkov geotehničnih lastnosti hribin, strukturnih in hidrogeoloških razmer na območju rudnika Globoko, pri poizkusnem odkopavanju zaizdelavo glavnega rudarskega projekta in investicijskega programa - III. del (Arhiv GeoZS), Ljubljana.

Markič, M., & Rokavec, D., 2002: Geološka zgradba, Nekovinske mineralne surovine in lignit okolice Globokega (Krška kotlina). RMZ – Materials and Geoenvironment, 49, 2, 229-226, Ljubljana.

Merrits D. and Hesterberg T. (1994). Stream networks and long-term surface uplift in the New Madrid seismic zone. Science, vol. 265, pp 1081-1084.

Michelini, A., Živčić, M., and Suhadolc, P., 1998, Simultaneous inversion for velocity structure and hypocenters in Slovenia, Journal of Seismology, 2, 257-265.

Mišič, M. 2009: Report on mineralogical investigations of the cores from the boreholes ED-1, ES-1, ES-2,WD-1, WS-1 and WS-2 by X – ray diffraction. – Internal report, GeoZS.

Mušič, B., 2009: Report on ground penetrating radar and resistivity survey. Libna, Oct. 2009. - Internal report, Gearh d.o.o.

Mušič, B., 2010: Tehnično poročilo o opravljenem delu pri spremljavi terenske izvedbe geoelektričnih psevdosekcij na Libni (9.2.-12-2.2009, naročilnica št. 37/2010). - Internal report, Gearh d.o.o

NRC, 2007: 10 Code of Federal Regulation (CFR) Part 100 – Reactor Site Criteria.

Pavlis, G. L., 1986, Appraising earthquake hypocenter location errors: a complete, practical approach for single-event locations, Bull. Seism. Soc. Am. 76, 1699-1717.

Pavlis, G. L., 1992, Appraising relative earthquake location errors, Bull. Seism. Soc. Am. 82, 836-859.

Persoglia, S. (ed.) 2000: Geophysical research in the surroundings of the Krško NPP (Contract No. 98-0286.00). - European Commission, Directorate general IA, Tacis procurement unit.

Petit J.P. & Laville E. 1987: Morphology and microstructures of hydroplastic slickensides in sandstone. - Geol. Soc. Lond. spec. publ., Conf. Deformation of sediments and sedimentary rocks, N° 29, 107-121.

Petkovšek (ed), 2009: Implementation of supplemental field investigations on potential location Vrbina in Krško municipality and implementation of the initial field investigations on potential location Vrbina in Brežice municipality. Potential location Vrbina in the Krško municipality - Arhiv GeoZS.

Piller, W. E., Harzhauser, M. & Mandić, O. (2007): Miocene Central Paratethys stratigraphy - current status and future directions. *Stratigraphy,* vol.4., 151-168.

Poljak, M., 2004: Strukturno in stratigrafsko kartiranje južnega roba Krške kotline. In: Jelen, B. (ed),2004: Terciarna in kvartarna geodinamika na stičišču Alp, Dinaridov in Panonskega bazena. (*Tertiary and Quaternary geodynamics at the junction of the Alps, Dinarides and Pannonian Basin*). - GeoZS, Ljubljana.

Poljak, M., Verbič, T., Rižnar, I., Toman, M. & Demšar, M. 1996: Detajlno geološko kartiranje območja Libne pri Krškem in okolice. – 11 str., 19 pril., Arhiv GeoZS, Ljubljana.

Poljak, M., Placer, L., Stojanovič, B. & Rifelj, H. 1997: Geološka reambulacija hriba Libne pri Krškem in okolice. - Unpublished report prepared by the Inštitut za geologijo geotehniko in geofiziko (IGGG), št. dok. ŠGGS15, 21 p.

Premru, U.,1982: Geološka zgradba južne Slovenije. Geologija, 25/1, 95-162, Ljubljana.

Rižnar, I., 2005: Geološka zgradba mejnega področja med Zunanjimi in Notranjimi Dinaridi vzhodne Slovenije. Doktorska disertacija.- Sveučilište u Zagrebu, Zagreb.

Rižnar, I., 2007: Overview of existing geophysical data in Krško basin. – Internal report. Geološke ekspertize Igor Rižnar s.p

Rižnar, 2008: Tectonic model of the Krško basin. – Internal report. Geološke ekspertize Igor Rižnar s.p.

Rižnar, I., 2009: Report on test pits on Mt. Libna. – Internal report. Geološke ekspertize Igor Rižnar s.p.

Rižnar, I., 2009a: Comment on the Libna terrestrial network. – Internal report. Geološke ekspertize Igor Rižnar s.p

Schumm S. A. (1956). Evolution of drainage systems and slopes in badlands at Perth Amboy, New Jersey. Geol. Soc. Am. Bull., vol. 67, pp 597-646.

SED, 2007, http://www.seismo.ethz.ch/mt/armt/full_armt.html

Shearer, P., 1997, Improving local earthquake locations using the L1 norm and waveform cross correlation: application to the Whittier Narrows, California, aftershock sequence, J. Geophys. Res. 102, 8269-8283.

Snoke, J.A., Munsey, J.W., Teague, A.G. in Bollinger, G.A., 1984. A Program for Focal Mechanism Determination by the Combined Use of Polarity and SV-P Amplitude Ratio Data, Earthquake Notes, 55, No. 3, p. 15.

Stopar, B. & Sterle, O. 2009: Report and analysis of GNSS network Krško. – FGG report.

Strahler A. N. (1957). Quantitative analysis of watershed geomorphology. Trans. Am. Geophys. Union, vol. 38, pp 913-920.

Swan, H. B., Hanson, K.L., Poljak, M., Živčič, M. & Gosar, A. 2004: Revised Seismotectonic Model of the Krško Basin, Part 1, PRS-NEK 2.7.1 rev. 1. prepared for Nuclear Power Plant Krško, Vrbina 12, Krško, Slovenia; by Geomatrix Consultants, Inc, Oakland, California, USA; in cooperation with University of Ljubljana, Faculty of Civil and Geodetic Engineering Institute of Structural Engineering, Environmental Agency of the Republic of Slovenia, Office of Seismology; and Geological Survey of Slovenia.

Šumanovac, F., Orešković, J., Grad, M. and ALP 2002 working group, 2009; Crustal structure at the contact of th Dinarides and Pannonian basin based on 2-D seismic and gravity interpretation of the Alp 07 profile in the ALP 2002 experiment. Geophys. J. Int., 179, 615-633.

Trajanova, M., Bole, B. & Zakrajšek S. 2009: Poročilo o granulometrijski in litološki sestavi vzorcev proda iz vrtin ED-1 in ES-1 s Krškega polja. – Internal report, GeoZS.

Verbič, T., 1995, Kvartarni sedimenti v vzhodnem delu Krške kotline: Unpublished report, št. dok. ŠGGS7, 248 p.

Verbič, T., 2004: Quaternary stratigraphy and neotectonics of the eastern Krško basin. Part 1: Straigraphy. - Razprave IV. Razreda Sazu, vol. XLVI-1, pp 171-216 (Abstract in English).

Verbič, T., 2005: Quaternary stratigraphy and neotectonics of the eastern Krško basin. Part 2: Neotectonics. - Razprave IV. Razreda Sazu, vol. XLVI-1, pp 171-216 (Abstract in English).

Vidrih, R., (ed.), 2006, Državna mreža potresnih opazovalnic = Seismic network of Slovenia, Agencija RS za okolje, Urad za seizmologijo in geologijo, Ljubljana (in Slovenian and English).

Waldhauser, F., 2001, hypoDD – A Programe to Compute Double-Difference Hypocenter Locations, U. S. Geol. Surv. Open File Rep. 01-113, 25 p.

Waldhauser, F., and W. L. Ellsworth, 2000, A double-difference earthquake location algorithm: Method and application to the Northern Hayward fault, Bull. Seism. Soc. Am. 90, 1353-1368.

WS 2008: Workshop of the F and SLO teams for the reevaluation of the geophysical data, held at the GeoZS, in Feb. 2008.

Živčić, M., 1994, Earthquake catalogue, in Fajfar and Lapajne (eds.), Probabilistic Assessment of Seismic Hazard at Krško Nuclear Power Plant, (Revision 1): University of Ljubljana, Department of Civil Engineering.

Živčić, M., Cecić, I., Čarman, M., Jesenko, T., Ložar Stopar, M. & Pahor, J. 2010: Earthquake catalogue – final report. - Report NEK 2523-08-400013/1a - Seismology and geology office, ARSO, Ljubljana.

Živčić M. & Ložar Stopar, M. 2009:. Fault plane solutions and the principal stress. - Report NEK 2523-08-400013/1b - Appendix1b, Seismology and geology office, ARSO, Ljubljana.